2012

Systematics, diversity, and origins of upper cretaceous continental molluscan fauna in the infra- and intertrappean strata of the Deccan Plateau, central India

Marron J. Bingle-Davis
University of North Dakota

SYSTEMATICS, DIVERSITY, AND ORIGINS OF UPPER CRETACEOUS CONTINENTAL MOLLUSCAN FAUNA IN THE INFRA- AND INTERTRAPPEAN STRATA OF THE DECCAN PLATEAU, CENTRAL INDIA

by

Marron J. Bingle-Davis
Bachelor of Science, Michigan State University, 2002
Master of Science, University of North Dakota, 2005

A Dissertation
Submitted to the Graduate Faculty

of the

University of North Dakota

in partial fulfillment of the requirements

for the degree of

Doctor of Philosophy

Grand Forks, North Dakota
August
2012

This dissertation, submitted by Marron J. Bingle-Davis in partial fulfillment of the requirements for the Degree of Doctorate of Philosophy from the University of North Dakota, has been read by the Faculty Advisory Committee under whom the work has been done and is hereby approved.

Chairperson

This thesis meets the standards for appearance, conforms to the style and format requirements of the Graduate School of the University of North Dakota, and is hereby approved.

Dean of the Graduate School

July 20, 2012

Date

PERMISSION

Title	Systematics, Diversity, and Origins of Upper Cretaceous Continental Molluscan Fauna in the Infra- and Intertrappean Strata of the Deccan Plateau, Central and Western India
Department	Geology
Degree	Doctor of Philosophy

In presenting this dissertation in partial fulfillment of the requirements for a graduate degree from the University of North Dakota, I agree that permission for extensive copying for scholarly purposes may be granted by the professor who supervised my dissertation work or, in his absence, by the chairperson of the department or the dean of the Graduate School. It is understood that any copying or publication or other use of this dissertation or part thereof for financial gain shall not be allowed without my written permission. It is also understood that due recognition shall be given to me and to the University of North Dakota in any scholarly use which may be made of any material in my dissertation.

Signature Marron Bingle-Davis____________

Date June 14, 2012__________________

TABLE OF CONTENTS

LIST OF FIGURES

LIST OF TABLES

ACKNOWLEDGMENTS

I would first like to thank Dr. Joseph Hartman. He not only offered me this interesting and fulfilling project but also guided me along the way. I would also like to thank the University of North Dakota for providing Dr. Hartman and I the seed grant that allowed the field research to be completed in India. I also thank the University of North Dakota for providing student assistantship funding during the completion of my coursework. My thanks go out to Dr. Dhananjay Mohabey (Geology Survey of India), Dr. Sunil Bajpai (University of Roorkee), Dr. Henning Schölz (Museum für Naturkunde), and Dr. Ritu Sharma for providing invaluable assistance in the field and beyond. I also thank Ashley Ignatius, Jessica Haas, Kristyn Voegele, and Don McCollor for their assistance in the preparation of the bulk material. I would also like to thank my husband, Mike, for his countless help and patience during the course of my project. Finally, I would like to thank my daughter, Alice, for her unprecedented patience during the completion of this work.

To My Grandpa,

Ralph E. Patterson Jr.

He was the first to call me doctor but never got to see me become one.

ABSTRACT

The Deccan Plateau in western and central India has been a major area of interest for researchers since the 1800s. In 1840, James Sowerby described the molluscan collection sent to him by John Malcolmson. In 1860, Stephen Hislop identified new molluscan species and redescribed based on better preserved material. Although this seminal work was comprehensive, interpretations have changed since the mid 1800s. Species need to be reassigned to current and/or accurate taxa, as well as revalidated statistically. Seventeen character traits were measured on over 600 specimens from five eastern Deccan Plateau localities representing a stratigraphic and temporal sequence. Cluster analysis was utilized to observe grouping patterns among specimens including Deccan type specimens and modern related species. Three new species (*Lymnaea pokhariensis*, *Bellamya lattooformis*, and *Zootecus burji*) and four new subspecies (*Tricula conoidea conoidea*, *T. c. hislopi*, *Valvata unicarinifera unicarinifera*, and *V. u. chiknaformis*) were identified and described. Three families with their associated genera and one genus (Viviparidae to Pomatiopsidae, Viviparidae to Subulinidae, Physidae to Planorbidae, and *Viviparus* to *Bellamya*) were revised to accommodate a more accurate taxonomic and biogeographic framework. Analysis of Variance (ANOVA) was employed to look at changes in morphology through the sequence and χ^2 tests were used to observe changes in diversity and abundance. Overall, there is a dramatic decrease in species size with the onset of volcanism but morphology and diversity remain stable. Species abundance changes but the lack of pattern suggests it is not a result of the volcanism.

CHAPTER I

INTRODUCTION

The Deccan Traps have been a subject of diverse inquiry since the 1800s including studies on basalt geochemistry, flow stratigraphy, and paleobiogeography. The diverse fossil assemblage, especially the dinosaurs and other vertebrates, has been studied extensively. Despite the amount of work done on the paleontology of the Deccan Plateau, little has been accomplished in regards to the continental mollusks. James Sowerby described the collection sent from John Malcolmson in 1840. He named four new species of gastropods (one Thiaridae ["Melaniidae"], one Viviparidae ["Paludinidae"], one Lymnaeidae, and one Physidae) and one new species of bivalve (Unionidae). Since Sowerby described new species from a collection sent to him, he did not describe geologic context in a detailed manner. Stephen Hislop comprehensively collected in the region surrounding Nagpur. In 1860 he published an expansion of Sowerby's work on the continental mollusks. He described 22 new species and three new subspecies of gastropods and four new species of bivalves, renamed one species of bivalve, and redescribed two of Sowerby's species using better specimens. Hislop incorporated a geologic description with his paleontology providing the first and last extensive study of the continental mollusks of the Deccan Plateau. Although Hislop's work on the mollusks was inclusive, his knowledge of molluscan taxonomy was limited. For example, he used Viviparidae as an all-inclusive family incorporating any broadly similar morphology. Therefore, it is necessary to reevaulate his familial placements. Also, much of the nomenclature used by Hislop is antiquated and in need of revision. Sowerby and Hislop used taxonomic categories that are no longer considered valid, like "*Paludina*," "*Melania*," and the alternative spelling "*Limnea*." Until the taxonomy is reviewed later in this paper, the current usages *Viviparus*, *Thiara*, and *Lymnaea*, respectively, will be applied.

The vast eruption of lava in the Deccan Plateau potentially contributed to the extinction event at the end of Cretaceous. The eruption was periodic with periods of volcanism punctuated by periods of quiescence, allows for a unique perspective on the potential effects of this volcanism over an extended period of time. Several groups exhibit patterns of extinction during this period of eruption, including the dinosaurs and many foraminifera (Pardo and Keller, 2008). Little is known regarding the pattern of biotic change in the continental mollusks. It is important to analyze morphologic changes as well as diversity and abundance changes to achieve a comprehensive understanding of the molluscan response to volcanism.

CHAPTER II

PREVIOUS STUDIES

Since the Deccan Traps have been examined extensively since the 1800s, a review of the history of Deccan research is vital to understanding this current work. Three phases of research are discussed below, the initial studies before 1850, the work of Stephen Hislop (1853-4, 1860), and subsequent studies after 1860.

Before 1850

H. W. Voysey's studies describing the geology of central India provide the basis for subsequent work on both the Deccan trap sequence and the molluscan fossil assemblage (Figure 1). He described the hills around Nagpur as containing semi-columnar porous basalt underlying an indurated claystone underlying a nodular basalt (Voysey, 1833a). He considered the basalt to be of igneous origin under pressure of a large body of water (Voysey, 1833a). Voysey (1833b) observed fossil shells in the intertrappean indurated clay west of Nagpur that were siliceous with some specimens completely replaced by chalcedony. He considered these fossils of marine origin, which reinforced his speculation of the existence of a large body of ocean water covering peninsular India. Voysey (1833b) concluded the flattening of many of the specimens indicated the presence of heat during fossilization, which further reinforced his theory that the Deccan basalts were the result of subaqueous volcanic eruptions.

John Grant Malcolmson, a Lieutenant in the 3rd Bombay Light Cavalry, examined the geology of central India between Hyderabad and Nagpur. Although he sent his fossil specimens to London for investigation, he traced and described the trap related formations across the region. Malcolmson built his geologic interpretation on the prior work of Voysey, including Voysey's maps and identifications of specific lithologies. Malcolmson described the Deccan trap basalts as being either amygdaloidal or having a "concentric globular structure" and overlying, in many instances, a decaying granite (Malcolmson, 1836). He reported fossil shells from the intertrappean sediments near Eidlabad (part of the Sichel Hills also known as the Nirmul Range), Etchoda, Medcondah, Munoor, and between Munnoor and Thitnoor (Mekalgandy Ghat) (Malcolmson, 1836, 1840) (Figure 1). Malcolmson (1836, 1840) noted that the fossils were found in situ and as float littering the ground, and their preservation as often converted into chalcedony but sometimes unaltered shell material effervescing in acid. Malcolmson concluded that although most mollusk specimens were from various freshwater families, some were apparently marine. He suggested that a large inland sea or estuary with associated continental environments, most likely lakes due to the accumulation of shells, existed during the eruption of the Deccan flood basalts (Malcolmson, 1836, 1840). He also stressed the importance of determining whether the fossils and basalts he observed in the Sichel Hills region could be correlated, temporally and geographically, to other trap outcrops in India. This type of correlation would establish not only the size of the eruption but an age relationships as well.

James Sowerby (1840) described and illustrated the continental invertebrate fossils obtained by Malcolmson in 1832 and 1833 from the Deccan region between Hyderabad and Nagpur. The collection included mainly mollusks but also included charophytes and ostracodes. Sowerby's species descriptions represent the first published taxonomic work on the Deccan infra- and intertrappean continental mollusks. He described one species of charophyte, *Chara*

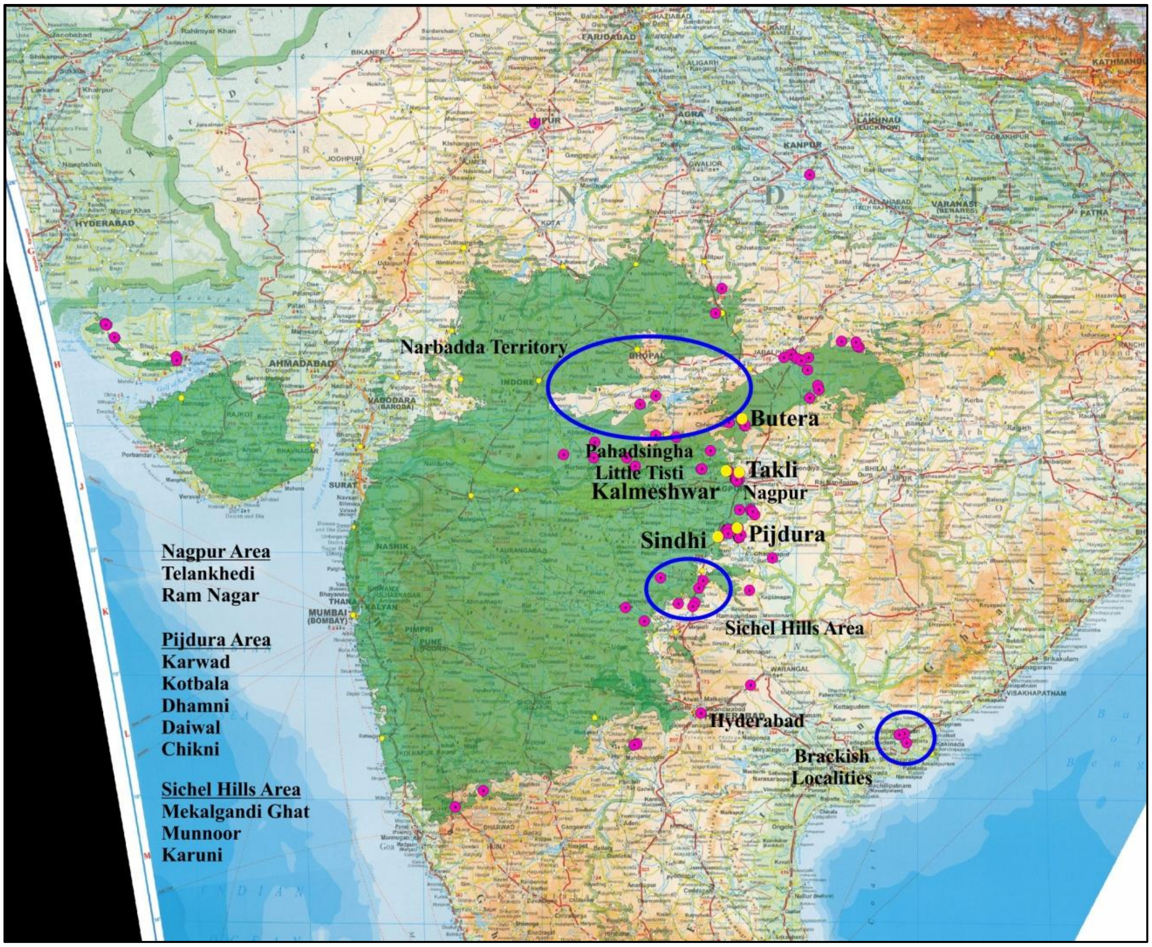

Figure 1. The Deccan (basalt) Plateau in green with all continental mollusk localities in pink. Study localities labeled and in yellow (Geology – GSI, 1998; Base Map – Gizi Map, 2005).

malcolmsonii, two species of freshwater ostracode were described, *Cypris cylindrical* and *Cypris subglobosa*, two species of unionoid bivalves, *Unio deccanensis* and *Unio tumida*, and four species of freshwater gastropods, *Thiara quadrilineata*, *Lymnaea subulata*, *Physa prinsepii*, and *Viviparus deccanensis* (Sowerby, 1840). Many of the specimens were collected from Munnoor and other localities in the Sichel Hills Region and Chickni (Sowerby, 1840).

Stephen Hislop (1853–1860)

Reverend Stephen J. Hislop began his work on the geology and paleontology of the Deccan Plateau while he was in India as a Christian missionary. He arrived in India from Scotland in 1844 and founded the Christian Mission and College in Nagpur (Smith, 1888). In 1845 he started exploring the area around Sitabaldi Hill and Kamthi (Smith, 1888). Further missionary work opened up the region outside Nagpur to Hislop after 1847, and he expanded his interests to not only documenting the physical features but also the geological history and fossil and mineral assemblages of the region (Smith, 1888). It was his collaboration with Reverend Robert Hunter that led to his fundamental contribution to the knowledge of the paleontology of the Deccan Plateau. Hislop and Hunter took a walk in 1851 to observe the surrounding geology that resulted in a large collection of fossils, minerals, and rocks (Smith, 1888). Hislop reported that he found his first fossil, a *Physa*, on Sitabaldi Hill (Hislop, 1853). This collection was later sent to London and formed the basis of several major publications including Hislop's 1860 seminal paper. Hislop and Hunter explored and collected at many localities around the Nagpur region.

Hislop (1853) published his first major work with the Royal Asiatic Society's journal on the geology of Nagpur and of western Bengal and Central India. Hislop published several more papers with his partner Hunter, with the Geological Society of London beginning in 1854. Aside from the articles written by Hislop, others used his collections to write several more. For example, Sir C. Bunbury (1861) published descriptions of the plant fossils of Nagpur that were collected by Hislop and Hunter. Even though Hislop contributed so much to the understanding of the geology and paleontology of central India, he fell to tragedy. Hislop, while working on stone circles near Takalghat in 1863, attempted to cross an unexpectedly swollen Wana River and drowned.

Hislop recognized the previous work done by Voysey and Malcolmson as the foundation of his studies and stated that his main goals were to describe the fossils found in the Nagpur region and not the reexamination of the physical features already described. Although his main focus was fossils, he described the typical sequence of beds in the Nagpur area (Figure 2). Hislop (1853) described the beginning of the section as metamorphic rocks disturbed by granite. The crystalline basement rock is overlain by either a Precambrian limestone or marble depending on the locality, which Hislop observed was often dolotomized from what he suggests was likely heat (Hislop, 1853).

The Precambrian basement is overlain by early Mesozoic sandstone and shale beds, which were deposited while India was connected to the supercontinent Gondwana. This interval is composed of a lower, middle, and upper sandstone with shale at the base. The shale contained some fossil remains including reptile (claw impressions) and earthworm trace fossils and the plant *Phyllotheca* (Hislop, 1853). The middle sandstone also contained fossil material such as plants and two species of mollusk (e.g., the corbulid *Cyrena*). Hislop considered the entire sequence conformable.

Overlying the sandstone and shale sequence is the first basaltic flow, which Hislop noted was most often vesicular. The basal trap is overlain by the intertrappean which, which Hislop identified as the freshwater formation. He described the intertrappean bed as between two centimeters and two meters thick, but the composition, color, and fossil content was variable depending on locality (Hislop, 1853). The intertrappean bed is no more than half a meter thick in the vicinity of Nagpur. The intertrappean formation contained a diverse fossil assemblage including reptiles (and/or dinosaurs), fish, insects, crustaceans, mollusks, and plants. Hislop noticed a distinct similarity between the flora of Nagpur, the flora of the intertrappean strata of

Mumbai (Bombay) and to the fruit fossils of the London clay of the Isle of Sheppey (Hislop, 1853).

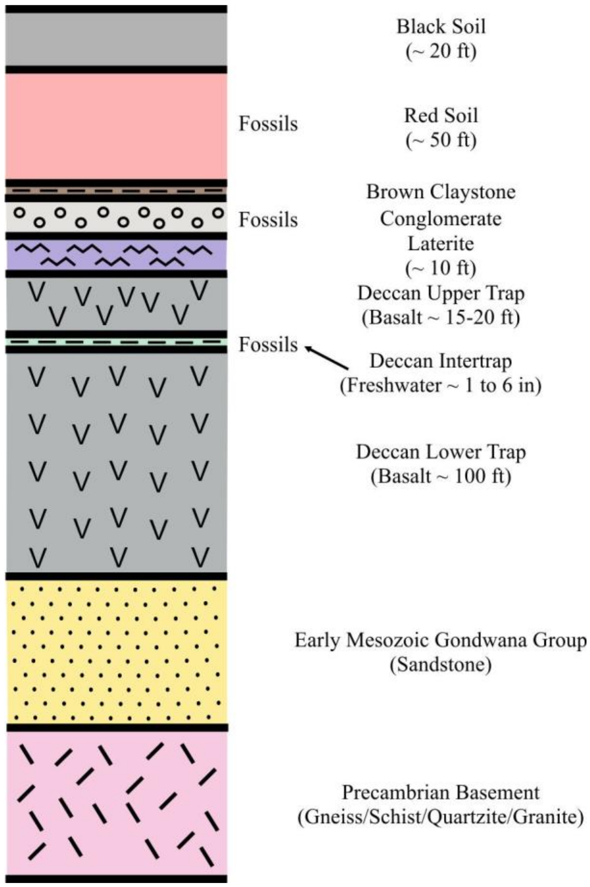

Figure 2. Typical Deccan sedimentary sequence around Nagpur as described by Hislop (1853; 1860).

Hislop (1853) noted the molluscan assemblage throughout Nagpur and the surrounding regions listing Sowerby's species and identifying any new species to the genus level only (e.g., *Thiara quadrilineata* and *Thiara* n. sp.). He named and described these new species in 1860 (Table 1). Hislop (1853) also noticed similarity between the *Unio* obtained from Chickni in the Nagpur region and those from Ellichpur in the Sichel Hills region discussed by Sowerby and Malcolmson (Figure 1).

In Nagpur, the intertrappean bed is overlain by a nodular basalt flow. Overlying the trap is an unfossiliferous laterite that extends over a large geographic area but is no more than 1.5 meters thick (Hislop, 1853). The final interval in the Nagpur Deccan sequence is a recent soil. The soil is either black or red in color and may contain, in the red soil, unaltered modern fluviatile and lacustrine shells, such as *Unio*, *Cyrena*, and *Lymnaea*.

Hislop suggested that the abundance of land plants, the presence of the continental corbulid, *Cyrena*, and the complete absence of marine species confirmed the freshwater origin of the Gondwanan interval. Similarly abundant land plants and freshwater mollusks and absence of marine species confirmed the freshwater origin of the intertrappean interval. This interpretation invalidates the alternative view held at that time that these two formations were formed under marine conditions and any freshwater species present were carried to the ocean. Hislop proposed that the freshwater system producing the intertrappean beds was extensive but shallow, which he concluded based on the maximum thickness of the intertrappean intervals. Hislop estimated the age of the intertrappean beds and associated traps were Eocene, which is contrary to the current age interpretation of Upper Cretaceous and early Paleocene.

In 1860, Hislop focused primarily on the paleontology. He described and named 27 new species and three new subspecies, added information to Sowerby's 1840 species descriptions, and discussed his interpretation of the geology of the Deccan trap sequence, with an emphasis on the nature of the body of water in which the lava extruded (Table 1) (Appendix 1). Hislop obtained his fossil collection from the Nagpur District and areas outside of the Nagpur province in all directions as far away as Jabalpur (270 km), Mekalgandi Ghat (240 km), and Rajamundry (560 km). Hislop's and Sowerby's collections were reposited in the National Museum of Natural History in London, England. Although Hislop and Sowerby did not designate type specimens, lectotypes or neotypes were assigned from the collections at the National Museum of Natural History (GS number series) (Hartman et al., 2008). Type localities are proposed in table 1.

Table 1. Type specimen information from Sowerby (1840), Hislop (1860), and Hartman et al. (2008). Taxon numbers refer to plates in Appendix 1.

Taxon Number	Species	Lectotype	Localities	Notes
01	*Thiara* [*Melania*] *quadrilineata* (Sowerby)	Plate 47, fig. 18 (GS 10421) (Sowerby, 1840)	Chikni*; Karwad (c); Pahadsingha (un); Karuni	Found with unionoids at Karuni
02	*Thiara* [*Melania*] *hunteri* (Hislop)	Plate V, fig. 1 (GS 10257) (Hislop, 1860)	Pahadsingha* (c)	Differs from *M. quadrilineata* by lack of carinae
03	*Viviparus* [*Paludina*] *normalis* (Hislop)	Plate V, fig. 2b (GS 10259) (Hislop, 1860)	Pijdura*(c); Takli(c); Karwad; Ambiakanti, Tandra, Kateru	Found in brackish localities (Kateru) as well as freshwater
04	*Viviparus* [*Paludina*] *deccanensis* (Sowerby)	Plate 47, fig. 20 (GS 10423) (Sowerby, 1840)	Munnoor*; Chikni; Takli; Karwad	Common wherever fossils found
05	*Viviparus* [*Paludina*] *wapsharei* (Hislop)	Plate V, fig. 3 (GS 10260) (Hislop, 1860)	Karwad* (c); Pijdura (r)	Differs from *V. deccanensis* by having banding and being smaller
06	*Viviparus* [*Paludina*] *acicularis* (Hislop)	Plate V, fig. 4 (GS 10261) (Hislop, 1860)	Telankhedi* (c); Butera; Chichundra, Takli, Little Tisti	Shell with or without banding; based on preservation
07	*Viviparus* [*Paludina*] *pyramis* (Hislop)	Plate V, fig. 5 (GS 10262) (Hislop, 1860)	Telankhedi* (r)	
08	*Viviparus* [*Paludina*] *subcylindracea* (Hislop)	Plate V, fig. 6 (GS 10263) (Hislop, 1860)	Telankhedi*	
09	*Viviparus* [*Paludina*] *sankeyi* (Hislop)	Plate V, fig. 7 (GS 10246) (Hislop, 1860)	Telankhedi*	
10	*Viviparus* [*Paludina*] *takliensis* (Hislop)	Plate V, fig. 8b (GS 10265) (Hislop, 1860)	Takli*	
11	*Viviparus* [*Paludina*] *soluta* (Hislop)	Plate V, fig. 9 (GS 10267) (Hislop, 1860)	Narbadda Territory* (c); Karwad (r)	
12	*Viviparus* [*Paludina*] *conoidea* (Hislop)	Plate V, fig. 10 (GS 10268) (Hislop, 1860)	Pijdura*	
13	*Viviparus* [*Paludina*] *rawesi* (Hislop)	Plate V, fig. 11b (GS 10270) (Hislop, 1860)	Takli* (c)	

Table 1 cont.

Taxon Number	Species	Lectotype	Localities	Notes
14	*Viviparus* [*Paludina*] *virapai* (Hislop)	Plate V, fig. 12a (GS 10271a) (Hislop, 1860)	Takli*	
15	*Valvata minina* (Hislop)	Plate V, fig. 13 (GS 10273) (Hislop, 1860)	Karwad* (c); Little Tisti (c); Butera (c); Karuni (c)	Much smaller than other valvatids, shell has fine striae
16	*Valvata unicarinifera* (Hislop)	Plate V, fig. 14 (GS 10274) (Hislop, 1860)	Butera*; Melanwada	More high-spired
17	*Valvata multicarinata* (Hislop)	Plate V, fig. 15a-b (GS 10274a) (Hislop, 1860)	Little Tisti* (c); near Takli	Sculptured
18	*Valvata decollata* (Hislop)	Plate V, fig. 16 (GS 10277) (Hislop, 1860)	Takli* (r)	More elongate
19	*Succinea nagpurensis* (Hislop)	Plate V, fig. 14 (GS 10278) (Hislop, 1860)	Telankhedi*(r)	One specimen
20	*Lymnaea* [*Limnea*] *oviformis* (Hislop)	Plate V, fig. 18a-b (GS 10279) (Hislop, 1860)	Pijdura*; Takli (r)	Similar to modern *Lymnaea luteola*
21	*Lymnaea* [*Limnea*] *subulata* (Sowerby)	Plate XLVII, fig. 13 (Sowerby, 1840); Neotype: Plate V, fig. 19 (GS 10280) (Hislop, 1860)	Telankhedi*; Chikni	Hislop redescribed this species based on better preserved material
22	*Lymnaea* [*Limnea*] *attenuata* (Hislop)	Plate V, fig. 20 (GS 10281) (Hislop, 1860)	Telankhedi*	More slender than other lymnaeids; Hislop doubts the validity of the species
23	*Lymnaea* [*Limnea*] *telankhediensis peracuminata* (Hislop)	Plate V, fig. 21a (GS 10282) (Hislop, 1860)	Telankhedi*(c)	More elongate
24	*Lymnaea* [*Limnea*] *telankhediensis radiolus* (Hislop)	Plate V, figure 21b (GS 10283) (Hislop, 1860)	Telankhedi*(c); Takli (c); Butera (c); Karwad (c)	More robust
25	*Lymnaea* [*Limnea*] *spina* (Hislop)	Plate V, fig. 22 (GS 10284a) (Hislop, 1860)	Telankhedi*(c); Takli (c)	Smaller than other lymnaeids
26	*Platyphysa* [*Physa*] *prinsepii* (Sowerby)	Plate XLVII, figs. 14-16 (Sowerby, 1840) (paralectotype)	Chikni*; Hyderabad	Paralectotype poorly preserved
27	*Platyphysa* [*Physa*] *prinsepii normalis* (Hislop)	Plate V, fig. 23a (GS 10285) (Hislop, 1860)	Chikni*; Takli (c); Telankhedi (c); Butera (c); Pijdura (c); Chichundra; Pangadi; Kateru	Found wherever fossils found; found in brackish sediments (Pangadi and Kateru)
28	*Platyphysa* [*Physa*] *prinsepii elongata* (Hislop)	Plate V, fig. 23b (GS 10286) (Hislop, 1860)	Chikni; Takli (c); Telankhedi (c); Butera* (c); Pijdura (c); Chichundra; Pangadi; Kateru	Found wherever fossils found; found in brackish sediments (Pangadi and Kateru)

Table 1 cont.

Taxon Number	Species	Lectotype	Localities	Notes
29	*Platyphysa* [*Physa*] *prinsepii inflata* (Hislop)	Plate V, fig. 23d (GS 10288) (Hislop, 1860)	Chikni; Takli (c); Telankhedi (c); Butera* (c); Pijdura (c); Chichundra; Pangadi; Kateru	Found wherever fossils found; found in brackish sediments (Pangadi and Kateru)
30	*Unio malcolmsoni* (Hislop)	Plate XLVII, figs. 12 (GS 10417) (Sowerby, 1840)	Mekalgandi Ghat*	Hislop renamed *U. tumida* (Sowerby) due to its usage for another species
31	*Unio deccanensis* (Sowerby)	Plate XLVII, figs. 4 (GS 10411-2) (Sowerby, 1840) (syntypes); Plate VI, figs. 14a-c (Hislop, 1860) (lectotype)	Munnoor*; Sip Ghat (c); north of Ellichpur (c); Karuni (c)	Hislop redescribed this species based on better preserved material
32	*Unio hunteri* (Hislop)	Plate VI, fig. 25 (GS 10291) (Hislop, 1860)	Karuni* (c)	Inward radiating sculpture
33	*Unio mamillatus* (Hislop)	Plate VII, fig. 26 (GS 10942) (Hislop, 1860)	Karuni* (c)	Single row of small tubercles centrally from umbo
34	*Unio imbricatus* (Hislop)	Plate VII, fig. 27a (GS 10293) (Hislop, 1860)	Mekalgandi Ghat* (c)	Single row of small tubercles centrally from umbo
35	*Unio malcolmsoni* (Hislop)	Plate VII, fig. 28 (GS 10355) (Hislop, 1860)	Karuni* (r)	Elongate

* Proposed type locality

(c) Common, (uc) Uncommon, (r) Rare

After 1860

Although much work has been conducted on the Deccan traps and its associated flora and some fauna, little study has been done on the continental molluscan fauna since Hislop (1860). Paul Fischer (1883) proposed the introduction of a new genus, *Platyphysa*, to apply to the large physid species of the Deccan trap sequence in India. He suggested the large size, enlargement of the final whorl near the suture, and the truncation of the columella, although similar to *Physopsis*, should be considered a separate group related to *Bulinus* (Fischer, 1887).

In the 1920s, N. Annandale and B. Prashad worked on the continental mollusks of India and the taxonomy of Hislop. Much of Annandale's work was on the modern mollusks of India and the surrounding regions, but he also examined the taxonomic placement of *Physa prinsepii* (Sowerby). Annandale (1920) argued for the generic change from *Physa* to *Bulinus* based on the predominance of *Bulinus* in the southern hemisphere. He also asserted that *Physa prinsepii elongata* was the only valid variation of *P. prinsepii* and that *P. prinsepii inflata* was simply a common morphology of *P. prinsepii* (Annandale, 1920). He proposed that *P. prinsepii elongata* be changed to *Bulinus elongatus*. Finally, he suggested the introduction of a distinct variation of *P. prinsepii normalis* (and *inflata*) on the basis of its occurrence with estuarine species, and he proposed the names *Bulinus prinsepii* for the freshwater forms and *Bulinus prinsepii euryhalinus* for the estuarine forms (Annandale, 1920). Annandale (1921) also revised the fossil viviparids of India. Although he relied on Sowerby's and Hislop's illustrations without actual specimens, he suggested that *Viviparus normalis* was a true viviparid while *V. rawesi* was not (Annandale, 1921). He left the taxonomic status of the rest of Sowerby's and Hislop's species of *Viviparus* unresolved.

A colleague of Annandale, B. Prashad worked mostly on the modern freshwater mollusks of India and surrounding regions, but he also studied India's fossil mollusks. Prashad (1928) completed an extensive work on the recent and fossil Viviparidae around the world, including discussion of the species of Sowerby and Hislop. Prashad reexamined the type species of *Viviparus deccanensis*, which was identified by Sowerby (1840) and confirmed in the genus *Viviparus* by Newton (1920). Prashad (1928) suggested that the group Hislop called *Viviparus* was heterogeneous and that the species *V. deccanensis* was actually a member of Hydrobiidae. He proposed that all members of Hislop's *Viviparus*, aside from *V. conoidea*, which he considered juvenile examples of *V. normalis*, were members of either Hydrobiidae or Thiaridae (Prashad, 1928). Prashad also asserted that Annandale's alliance between *Viviparus normalis* Hislop and *Viviparus dissimilis* Müller was correct, and that not only does *V. normalis* represent the first occurrence of Viviparidae in India but the ancestral stock of the *V. dissimilis* group (Annandale, 1918; Prashad, 1928). According to Prashad (1928) and Annandale (1921), *Physa prinsepii,* as well as the viviparids, most likely lived in marshy (paludal) environments instead of lacustrine or fluvial. The viviparids may also have inhabited flowing streams. Prashad also worked on the condition of bivalves of the intertrappean beds by reexamining a mislabeled specimen in the Geological Survey of India collections. The specimen was from the intertrappean beds of Goraha, Narbada and was labeled as *Pisidium medlicottianum* Hislop. The specimen was neither a *Pisidium* nor a member of a related genus. Prashad identified the specimen as belonging to the unionoid genus *Lamellidens* and named his new species *Lamellidens vredenburgi* (Prashad, 1921).

Several publications mention the continental mollusks, but most often secondarily as components of the overall assemblage. In these instances, the authors use Sowerby's and Hislop's original identifications and taxonomy with little to no further investigation. In Rana (1984), mollusk species were described for the purposes of illustrating the assemblage occurring at Takli but not for the purpose of molluscan study. The preservation of the mollusk species was described with their geographic and stratigraphic occurrence. This type of account of molluscan fauna is repeated in other studies (e.g., Sahni et al., 1984; Sahni, 1986; Sahni, 1987; Mohabey, 1996). Here the authors reported the occurrence of mollusks as constituents of the assemblages or localities they studied, but they did not describe or report further on the species.

CHAPTER III

GEOLOGY

The geology of India and the Deccan Plateau is diverse spanning Precambrian to present day and recording India's complex paleogeographic history. Understanding the geologic history of India is important in comprehending the living and depositional context of the molluscan assemblage. Determining the geologic context will help resolve extinction scenarios and volcanism response. Knowledge of the history of interpretation of India's geology is also important in understanding the evolution of theory changes.

Pioneering Geological Studies in the Deccan Plateau

Early studies in Indian geology were completed mostly by members of the Geological Survey of India in the mid-1800s when Britain was surveying for India's natural resources. Joseph Medlicott (1859) wrote "On the geological structure of the central portion of the Narbadda (Nerbudda) District" while conducting a geologic survey of central India (Figure 1). Medlicott's (1859) work mostly concerned the examination of the volcanic rocks of the region and identified three major periods of basalt intrusion in India instead of just the phase that created the main Deccan Plateau. He recognized a period of volcanism before the oldest Talchir (Talcheer) beds (Carboniferous), a period before the Lower Damuda beds (Permian) and Mahadeva beds (Upper Triassic), and the period of major Deccan volcanism previously called the "great Basaltic period" that constitutes the overlying trap exposed throughout India (Medlicott, 1859). The first two traps are not distinct lithologically or mineralogically from each other and are distinguishable from the more recent phase by its terrace morphology (Medlicott, 1859).

Medlicott (1859) also recognized multiple flows within the most recent trap that are mineralogically distinct but not consistent in exposure. He identified at least two common types of basalt within these flows, which were granular subcrystalline diorite and ferruginous basalt (Medlicott, 1859). Although he identified multiple eruption events and was able to recognize differences in the intensity of volcanic activity based on geography, Medlicott was unable to locate the eruption center.

Medlicott (1859) provided an alternative theory of the relationship between the traps and their associated intertrappean beds to that of Hislop and Hunter (1854). Hislop and Hunter proposed formation of the sedimentary beds (stage 2) occurred in a vast lake covering all of central and western India (stage 1) prior to the outpouring of lava. When the volcanism began the lava worked its way in between the freshwater beds creating the infra- and intertrappean intervals (stage 3) (Figure 3).

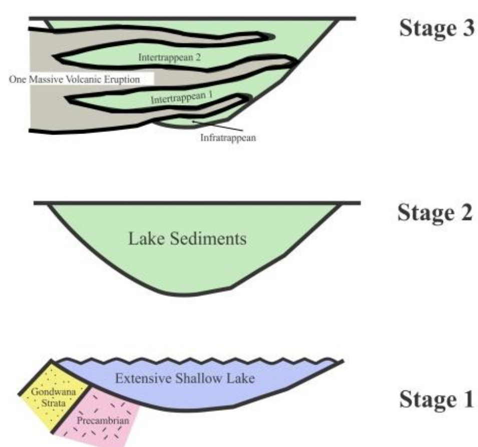

Figure 3. Hislop and Hunter's (1854) view on the eruption of the Deccan basalts and the deposition of infra- and intertrappean sediments.

Medlicott suggested that to support Hislop and Hunter's theory there should be chemical alteration of the lower and upper surfaces of the intertrappean interval. He observed only the upper surface of the sediments altered by the lava with the lower surface completely unaltered (Medlicott, 1859). This scenario is only possible if the underlying basalt was completely cooled by the time the freshwater sediments were deposited, and the overlying basalt flowed over the sediments chemically altering them before cooling.

William Blanford (1867) also published on the Deccan traps and their intertrappean intervals, especially in the Narmada (Narbadda; Nerbudda) and Taptee Valleys in central India and Kachchh (Cutch) in western India (Figure 1). Blanford studied in greater detail the morphology, petrology, and a potential origin of the basalt flows. He suggested a potential center of volcanic eruption during the most recent Deccan eruption north of the Narmada River in the Rajpeepla hills (Blanford, 1867). He cited a large amount of dykes and a volcanic mass that appeared to be the center of a volcano as evidence for the eruptive center in this area (Blanford, 1867). Blanford found several more potential volcanic nuclei, one (or maybe two) in the lower Narmada Valley and several in the Kachchh region; however, he stressed the difficulty in proving these to be centers.

Blanford (1867) suggested the original extent was far greater before erosion as evidenced by the occurrence of basalt outliers outside the Deccan Plateau shown on the Malcolmson (1840) map. Hislop (1860) noticed a similarity between the freshwater fossils of these outlying regions and those of the main Deccan Plateau province. Blanford (1867) demonstrated that the mineralology of the outliers was comparable to that of the main Deccan Plateau basalt and therefore verified Hislop's account of the fossils. Blanford amended the idea of the presence of volcanic (or basaltic) breccias previously reported by Malcolmson (1840) to that of volcanic ash.

He compared the rocks found within the Deccan Plateau with those of known volcanic eruptions and concluded that they must have been formed of ejecta (Blanford, 1867).

Blanford also supported Hislop's (1860) theory that the Deccan traps were not extruded into submarine conditions as was the general consensus at the time. He argued that the presence of vesicular basalt and freshwater and brackish fossils suggested that the lava must have extruded at least partially under subaerial and continental conditions (Blanford, 1867).

Blanford (1867) supported the theory that of a succession of multiple mineralogically distinct flows with intertrappean intervals deposited, likely in lakes, between the flows. He also suggested that the intertrappean beds represented individual lakes with a small geographic extent based on the discontinuous distribution of the deposits. Lava flowing over an irregular surface would fill in existing depressions from previous erosion into which subsequent shallow lakes can form once the lava cools. Blanford (1867) suggested this sequence would repeat itself forming the series of flows he observed. This theory represents the current view on the formation of the Deccan traps and intertrappean intervals (Figure 7).

Blanford (1867) noticed a similarity between the estuarine fossils from the intertraps of Rajahmundry and those of the Cretaceous marine Trichinopoly beds. Blanford concluded that at least some traps were likely Upper Cretaceous in age with the lower traps possibly as old as middle Cretaceous. This not only contradicted the previous estimation of Eocene age, considered correct by most at the time, but also argued for longer eruption duration than previously proposed.

Geological History of the Deccan Plateau

During the Precambrian, India was part of the supercontinent Gondwana, which was located around the equator. The oldest rocks are roughly 3.5 Ga and are mainly gneisses and schists (Figure 4). The remainder of the Precambrian is divided into the Bijawar Group and the Gwalior Group. These Archean rocks underwent significant erosion before later deposition. Lower Proterozoic sediments were deposited 2 Ga and are characterized by a series of sedimentary and metasedimentary rocks (Figure 4).

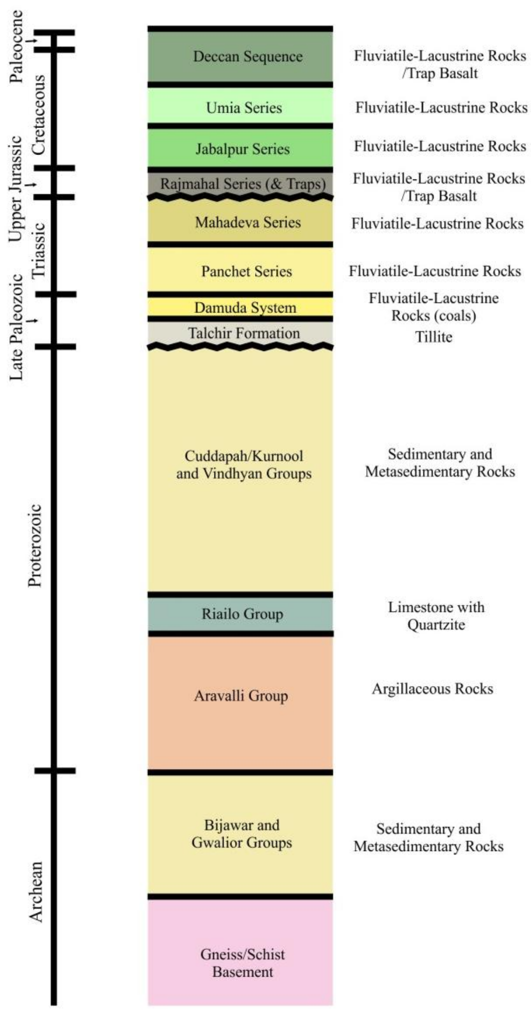

Figure 4. Generalized stratigraphic column of India.

A substantial period of erosion and/or nondeposition followed the deposition of the Vindhyan Supergroup that resulted in an unconformity that encompasses most of the Paleozoic. Upper Carboniferous sediments, however, were preserved with the formation of Pangaea. The Upper Carboniferous is characterized by a glaciation that is represented by a tillite at the base of the Talchir Formation. The Talchir Formation is overlain by a series of fluvial and lacustrine shale, sandstone, and freshwater limestone beds that constitute the Gondwana Group, which is prevalent until the Jurassic or mid Cretaceous (Figure 4). During the Late Jurassic the Rajmahal traps are formed, which are mineralogically similar to the Deccan traps, and constitute the Rajmahal Formation with interbedded fossiliferous shale beds. Fossils are common throughout the Gondwana Group and consist of fish, mollusks (unionoids), reptiles, amphibians, and plants. The Deccan trap sequence, including the infratrappean Lameta beds, overlies either these Gondwanan sediments or Precambrian basement rocks depending on locality (Figure 5).

Continental and marine Cretaceous rocks occur mainly along the western and southern margins of the Deccan Plateau while mostly continental rocks occur in the eastern part of the plateau. The continental rocks are composed of mainly of claystone, silty sandstone, and freshwater limestone beds. The Deccan trap sequence is mostly Maastrichtian based on microvertebrate assemblages (Courtillot et al., 1986; Buffetaut, 1987; Sahni and Bajpai, 1988; Jaeger et al., 1989). Palynofloral evidence from the Nand-Dongargaon Basin also suggests a Maastrichtian age for at least the infratrappean through the first three intertrappean beds of the Deccan trap sequence (Samant and Mohabey, 2005). The Deccan trap sequence continued into the earliest Paleocene with at least one intertrappean interval, which occurs about 500 km north of Nagpur near Papro, Lalitpur (Uttar Pradesh) (Sharma et al., 2008). The Deccan Trap sequence, including the infratrappean sediments, was deposited unconformably in the topographic lows of the underlying Gondwanan and Precambrian rocks (Figure 5, stage 1). Intertrappean intervals are formed as the basal trap covers the infratrappean beds and erosion creates a basin for a new lake (Figure 5, stages 2-4). This new lake becomes lithified and is covered by the next trap, and the sequence continues (Figure 5, stage 5). Often the intertrappean sediments are converted to chert still reflecting the original stratification of the lacustrine sediments. Each intertrappean unit is numbered based on its relation to its boundary flows. Intertrappean 1 lies between the first flow (flow 1) and flow 2, intertrappean 2 lies between flows 2 and 3, etc. (Figure 5).

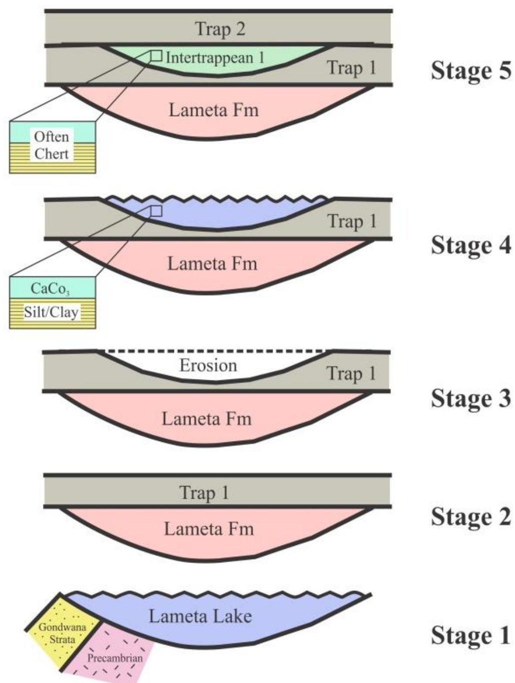

Figure 5. The Deccan Trap sequence and the deposition of infra- and intertrappean sediments (stage 1 is earliest in the sequence).

Infratrappean sediments are referred to as the Lameta Formation or Lameta beds based on exposures at Lameta Ghat on the Narmada River, west of Jabalpur. The Lameta Formation ranges from 0.5-70 m thick and covers an area of roughly 5000 km^2 (Salil et al., 1997; Samant and Mohabey, 2009). The Lameta Formation is exposed in discontinuous outcrops in five depositional basins in Maharashtra, Madhya Pradesh, and Gujarat (Mohabey, 1996; Samant and Mohabey, 2009). In the Chandrapur District (Maharashtra) the Lameta Formation sediments is silty claystone and channel sandstone, with interbedded calcareous mudstone and limestone (Mohabey, 1996). In general, the Lameta Formation was deposited in a channel-overbank-lacustrine setting in a semi-arid yet seasonal climate (Mohabey et al., 1993). These sediments are fossiliferous containing dinosaurs, fish, turtles, frogs, gastropods, bivalves, ostracodes, charophytes, conifers, algae, fungus, pteridophytes, and multiple species of gymnosperm and angiosperm micro- and macroflora (Mohabey et al., 1993; Mohabey, 1996; Mohabey and Udhoji, 1996; Mohabey and Samant, 2003; Ghosh et al., 2003; Sharma et al., 2004; Samant and Mohabey, 2005; Samant and Mohabey, 2009).

Intertrappean sediments are defined by their position between an under- and overlying basalt flow. However, both flows may not be present in all localities. Intertrappean sediments are exposed in multiple depositional basins in Maharashtra (Nand-Dongargaon Basin, the Yeotmal-Nanded region, and Mumbai), Madhya Pradesh (the Chhindwara-Mandla-Jabalpur region), Gujarat (Kachchh), and parts of Andra Pradesh (Rajahmundry) and Utter Pradesh (Lalitpur) (Figure 1). Intertrappean sediments are similar to infratrappean and are mostly lacustrine silty-sandy claystone, limestone, and marlstone beds. There is, however, evidence of channel influence from the significant sand component in the sediments and the presence of riverine mollusks. Intertrappean beds are generally thin, only a few centimeters to approximately a meter in thickness, and discontinuous. They are generally fossiliferous containing end-Cretaceous assemblages generally comparable to infratrappean beds. The biota of the intertrappean beds include multiple species of fish, turtles, dinosaurs, ostracodes, charophytes, mollusks, and mammals.

Paleobio- and Paleogeography of India

The western half of Gondwana (Africa and South America) began to separate from the eastern half (Antarctica, Australia, India, and Madagascar) during the Jurassic (~ 160 Ma) (Plummer and Belle, 1995). Separation continued as India, the Seychelles, and Madagascar separated from Antarctica (~ 130 Ma) and then India and the Seychelles separated from Madagascar (~90 Ma) (Gnos et al., 1997, Chand et al., 2001, Storey et al., 1995). The separation of India from Madagascar was caused by a mantle plume called the Marion hotspot, which currently lies south of Madagascar. India separates from the Seychelles at roughly 65 Ma, which coincides with the Deccan volcanism and the initial opening of the northwest Indian Ocean (Gnos et al., 1997, Chand et al., 2001, Storey et al., 1995) (Figure 6).

Biostratigraphic relationships observed in northwestern Pakistan indicate an initial contact between India and Eurasia between 58 and 55 Ma (Shafique, 2001). Marine biostratigraphy from Tibet indicates a contact between 51 and 53 Ma (Najman et al., 2010). Shallow marine rocks indicate a final suturing of India and Eurasia around 49 Ma (Beck et al., 1995). This suturing occurred as a two part event with suturing in western half of India occurring around 50 Ma and in the eastern half around 42 Ma. With the collision completed, India's momentum slowed, but there still could have been as much as 1500 to 4000 km of "freeboard" sediments lost after convergence.

Analyzing the paleobiogeographic relationships of the Indian assemblage is complex due to the existence of the Indian Plate tectonically as a subcontinent with an individual paleogeographic history. India was connected to Gondwana for most of the Proterozoic and Paleozoic and the beginning of the Mesozoic providing uninhibited migration throughout

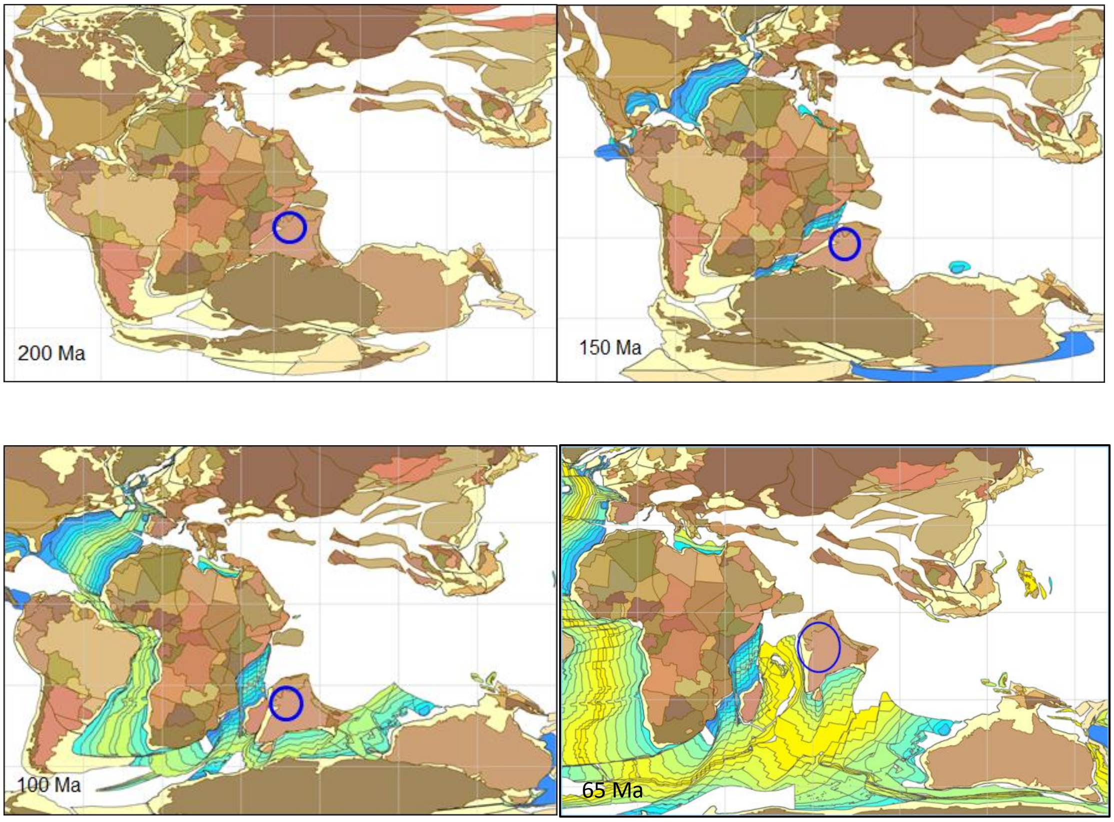

Figure 6. Paleogeography of India at 200 Ma, 150 Ma, 100 Ma, and 65 Ma time slices with the Deccan Plateau represented by the blue circle (PaleoGIS v. 3.0).

Antarctica, Australia, Africa, South America, Madagascar, and India. In the Jurassic (~160 Ma) Gondwana separated into an eastern half containing Antarctica, Australia, India, and Madagascar and a western half containing Africa and South America (Plummer and Belle, 1995). India and Madagascar separate from Antarctica around 130 Ma and India and the Seychelles break away from Madagascar around 90 Ma (Gnos et al., 1997, Chand et al., 2001, Storey et al., 1995). India then separates from the Seychelles around 65 Ma but has been isolated from a major landmass since around 130 Ma. India remains on its own, travelling northward until its initial collision with Asia between 58 and 55 Ma and a final suturing around 49 Ma (Shafique, 2001; Beck et al., 1995). In other words India was isolated from simple biogeographic migrations through land connection from the Early Cretaceous to the middle Eocene. Therefore, in order for new continental species to arrive in India after the separation there needed to be dynamic dispersal mechanisms. Since India was isolated for almost 100 million years, these continental dispersal mechanisms are likely through filter corridors where there is intermittent connection with other landmasses or sweepstakes corridors where migration is through chance (e.g., rafts, etc.). The Chagos-Laccadive Ridge is a potential corridor where the Deep Sea Drilling Project showed that Paleocene sediments with progressive sinking suggesting that during the Cretaceous this could have been above sea level (Sahni, 1986). Island arcs are another possible source for migration between Tibet and India. There is evidence of volcanism during the Cretaceous in Pakistan and the eastern Himalayas, which could have produced volcanic island arcs as a means of leap-frogging between India and Asia (Sahni, 1986).

The Indian biota shows a strong affinity to Africa and Madagascar. There are several lines of evidence suggesting a close proximity between India and Africa/Madagascar during the Cretaceous. There are several species of fish (e.g., *Lepisosteus*, *Lepidotes*, *Amia*, etc.), turtles (e.g., pelomedusids), and dinosaurs (common genera with a common species, *Laplatosaurus madagascarensis*) common to Niger, Madagascar, and the Deccan sequence of India (Jain and Sahni, 1983; Sahni, 1984, 1986). The paleomedusid turtles are found in infratrappean sediments of Pijdura, the Senonian of Niger, and the Early Cretaceous of the Saharan region (Sahni, 1984). These turtles also common in the Paleogene sediments throughout India and the Lesser Himalayas suggesting this group migrated from Africa sometime prior to the Deccan (Sahni, 1984). Also, there are some plant fossils and charophytes that are similar between Africa, Madagascar, and India (Sahni, 1986). The dinosaur fauna from Jabalpur (central India) is comparable to Madagascar and Africa (Sahni, 1984). Sereno, Wilson, and Conrad (2004) used similar abelisaurid dinosaurs from South America, India, and Madagascar to suggest there were intermittent land bridges between the major Gondwanan regions during the Early Cretaceous that persisted until the Late Cretaceous (100-90 Ma). This “pan-Gondwana” model allowed unproblematic migration between the Gondwanan landmasses for much of the Cretaceous (Sereno et al., 1996, 2004). Chatterjee (2002) suggests there was a previously unrecognized landmass between eastern Arabia and northwest India called “Greater Somalia.” He proposes that as India moved closer to Africa during the latest Cretaceous, this landmass would have provided a corridor for which biota could have migrated from Africa and possibly even Europe into India. This would explain why the earliest occurrence of many groups in India is the Upper Cretaceous. Regardless of the exact dating of the lingering connection between India and other parts of Gondwana, there are several lines of evidence to support the existence of corridors of migration through much of the Cretaceous. The mammals show a slightly different paleobiogeographic history. Ninety mammalian dental specimens were reported and exist in Geological Survey of India collections (Prasad and Sahni, 1988; Prasad et al., 1994; Rana and Wilson, 2003; Khosla et al., 2004) and 90% of these are considered to be eutherians of Laurasian affinity (Wilson et al., 2007). The mammal fossil assemblage of India suggests there was a connection with the northern landmasses perhaps through the “Greater Somalia” scenario or some other means (e.g., island arcs, etc.). Nevertheless, the high degree of endemism that should exist in the Indian assemblage from a lengthy isolation is not observed.

Molluscan paleobiogeography during the evolution of the Indian subcontinent is difficult owing to consistent similarities between species of the same genus regardless of biogeographic origin. Prashad (1928) noticed a strong similarity between *Viviparus normalis* of the Deccan and *V. leai* from North America, *V. sublentus* from Paris, and *V. lentus* from England, which all are of a comparable age. Also, the Upper Cretaceous Deccan sequence is the first occurrence of many of the species of gastropods in India (e.g., Viviparidae) (Prashad, 1928). Older material for comparison is scarce. *V. normalis* was considered by Annandale (1921) to be closely related to the modern *V. dissimilis*, with a southern Asian distribution, and should be considered to be the ancestral stock for the group. This similarity may suggest the Cretaceous Indian gastropods dispersed after the collision with Asia and became the ancestral forms for modern Asian gastropods. Newton (1920) compared *V. deccanensis* from the Deccan assemblage with several unidentified fossil specimens in Matabeleland, Central South Africa and concluded there were sufficient similarities between the species to consider a connection between the two land masses during the Cretaceous. Newton described these specimens from poorly preserved material but concluded that they were similar to the modern African species *V. unicolor*. Another fossil species, *V. passargei*, from the Kalahari area could potentially be Cretaceous based on Newton's inference that Cretaceous beds extended from the Zambesi River to the Cape Colony. This species is considered to be also related to *V. unicolor* but distinct as an intermediate form between the Matabeleland fossil and the modern forms. Viviparids have existed in Africa since the early to middle Cretaceous according to Fischer (1963) who identified from poorly preserved material what he called ?*Campeloma* from the Continental Intercalaire beds in Mali. So it is possible that the occurrence of viviparids in India originated from Africa as India passed closely in the early to middle Cretaceous.

Understanding the paleobiogeographic relationships of the Deccan Trap contintental molluscan assemblage is important to understanding its evolution and the evolution of the Indian Plate. The specific assemblage appears in the fossil record at the end of the Cretaceous in the Deccan Traps and is not reported in older strata. The evolution of such a diverse assemblage seems geologically abrupt and its origins are currently uncertain. There are potential African affinities, but more detailed work is needed. Determining the origins of the Deccan Trap contintental molluscan assemblage will also track the movements of the Indian Plate as it moved northward.

The Deccan Flood Basalts

The Deccan flood basalts occupy an area of at least 500,000 km^2 across peninsular India and a current volume of roughly 1.5 million km^3 (Jay and Widdowson, 2008; Pande, 2002) (Figure 1). Estimates ten million km^2 have been reported for the area covered prior to erosion, with an initial volume up to six or seven times that currently preserved (Courtillot et al., 1986; Courtillot and Renne, 2003; Cripps et al., 2005). Regardless of the total area and volume covered by basalt, the Deccan Plateau is a major geologic feature covering about one sixth of the surface area of present-day India. The timing and duration of volcanism has also been a topic of much discussion for many years. Some argue for a very short duration lasting at most one million years (Duncan and Pyle, 1988; Cande and Kent, 1995; Hoffman et al., 2000; Chenet et al., 2007).

On the basis of $^{40}Ar/^{39}Ar$ dates of several trap basalts from multiple regions across the Deccan Plateau, three main pulses of volcanism during the main Deccan extrusion have been recognized (Chenet et al., 2007). Pulse one, which is restricted to the northern Deccan Plateau, occurred around 67.5 Ma at the C30r/C30n reversal boundary. Pulse two began after roughly 2.5 million years of quiescence at around 65-66 Ma. This is the largest phase of volcanism and began in C29r before the end of the Cretaceous and ended roughly at the K/Pg boundary. The final pulse began in the Paleocene of C29r and ended in C29n with the reversal boundary dated at 64.7 Ma.

Others have argued for a much longer duration of Deccan volcanism from at least three million years to as much as eight million years long (Sheth et al., 2001; Pande, 2002; Courtillot and Renne, 2003). Pande (2002) demonstrated an age range of 69-62 Ma for the Deccan trap basalts based on their paleomagnetic record (Pande, 2002). He postulated that the largest pulse in volcanism was during C30r, but admits that the paleomagnetic record is incomplete in the Deccan sequence because the basalts flows were episodic. Radiometric dating also supports a longer duration for Deccan volcanism. Alkaline rocks from the northern Deccan Plateau date to 68.5 Ma (Basu et al., 1993). Trachytes and basalts from Mumbai date to roughly 60.5 Ma (Sheth et al., 2001a,b; Lightfoot et al., 1987). Although these dates illustrate a much longer duration for the Deccan sequence, they do agree with previous statements that initial volcanism occurred in the north and moved farther south as India moved toward Eurasia. Volcanism reached its peak around 65-66 Ma and ended around the K/Pg boundary (Chenet et al., 2007). Patterns in the marine microfossil record from the intertrappean sediments found near Rajahmundry also show that the largest period of Deccan volcanism ended at the K/Pg boundary (Keller et al., 2008).

The origin of Deccan flood basalts is also a subject of contention. The mantle plume model is a widely held explanation (e.g., Morgan, 1981; Richards et al., 1989; Campbell and Griffiths, 1990). Flood basalts originated during a large plume diaper (head) initiating along a hot spot track (Richards et al., 1989; Campbell and Griffiths, 1990). The Deccan flood basalts are considered, according to the mantle plume model, to be related to the initiation of the Reunion hot spot (e.g., Richards et al., 1989). During the height of Deccan flood volcanism there were periods of elevated lava production separated by times of inactivity (Richards et al., 1989; Courtillot et al., 1988). Deccan volcanism was connected with the Reunion hot spot by a series of submarine volcanic lineaments. The Laccadive, Chagos, and Mascarene lineaments get progressively younger to the south demonstrating the northward movement of India towards Eurasia (Richards et al., 1989).

The alternative hypothesis for the origin of Deccan Trap volcanism suggests that it is the result of continental rifting. The separation of India from the Seychelles caused mantle convection and decompression melting that resulted in volcanism (Sheth, 2005). The separation is also suggested to be associated with the initiation of the Reunion hotspot (Sheth, 2005). Radial and focused flow from rifting instead of vertical flow from a mantle plume would not only account for the sizable volume of basalt, but it also explains the near circular shape of the Deccan Plateau (Sheth, 2005).

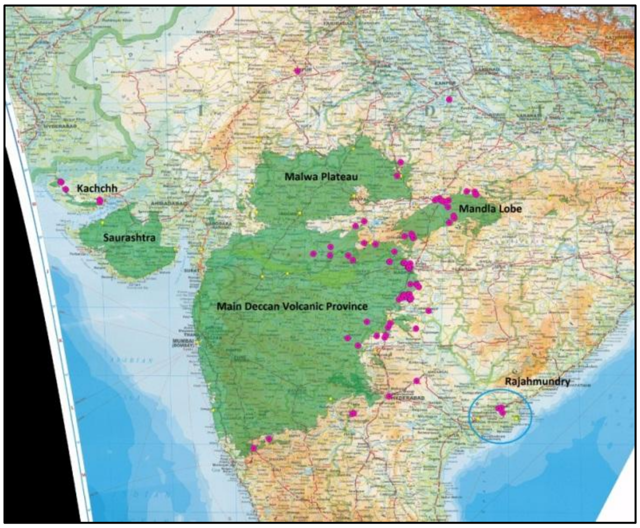

Figure 7. Major subregions of the Deccan flood basaltic province. Continental mollusk localities are shown in pink (Geology – GSI, 1998; Base Map – Gizi Map, 2005).

The Deccan basaltic province is split into four major subregions (Jay and Widdowson, 2008) (Figure 7). The main Deccan Volcanic Province (73-78°N, 16-22°E) includes the majority of the basaltic province, and is where much of Deccan research has been concentrated. Saurashtra and Kachchh together are smaller isolated lobes in the northwestern part of the province. The important Anjar locality, which contains iridium below the K/Pg boundary, is located in Kachchh. The Malwa Plateau is the northern lobe of the main Deccan Volcanic Province but is considered distinct. The Mandla lobe is an isolated portion of the province to the northeast of the main Deccan Volcanic Province. The Mandla lobe has been considered by some to represent a separate lava source, but geochemical analysis suggests a definite correlation to the main Deccan event

(Shrivastava and Ahmad, 2005). A small outlier of Deccan trap basalt also occurs in the Rajahmundry area southeast of the main Deccan Volcanic Province.

Deccan volcanics are mainly tholeiitic basalts and are classified into two main flow types (Cripps et al., 2005). Simple flows are generally nonamygdaloidal except for their vesicular and oxidized flow tops with joints perpendicular to their lower contacts. Compound flows are generally massive, amygdaloidal flows that have poorly developed joints. This type is composed of several individual flows that are a few centimeters to a few meters thick and are laterally discontinuous.

Extensive geochemical work was completed in the Western Ghats where researchers developed a detailed stratigraphic framework for the Deccan basalts. Ten chemically distinct formations in three subgroups were identified on the basis of their flow type, phenocryst mineralogy, grainsize, and chemical signature (Beane et al., 1986) (Table 2).

Table 2. Deccan trap basalt subgroups (shown in stratigraphic order).

Subgroup	Number of Formations	Thickness (m)	Flow Type
Wai	3	1100	Simple
Lonavala	2	525	Simple (lower); Compound (upper)
Kalsubai	5	2000	Compound

The three subgroups, Kalsubai, Lonavala, and Wai, were recognized in the Western Ghats and have been correlated to other regions of the Deccan. Jay and Widdowson (2008) correlated the Wai Subgroup formation boundaries to the Rajahmundry area based on $^{87}Sr/^{86}Sr$ ratios, Sr and Ba concentrations, and Ba/Y and Zr/Nb ratios. Correlation of the Rajahmundry basalts with the Western Ghats suggests that the stratigraphic nomenclature developed for the western Deccan basalts may be appropriate for usage in other regions of the province.

Geology of the Study Area

For this study, five localities were chosen based on their stratigraphic placement and quality of fossil material. One infratrappean (Pijdura), one intertrappean 1 (Takli), one intertrappean 2 (Kalmeshwar), and two intertrappean 3 (Butera and Sindhi) localities represent changes in geology and paleontology before and during the initial stages of Deccan trap volcanism (Figure 1). Two intertrappean 3 localities were used because although they are both stratigraphically intertrappean 3, Sindhi is chronologically younger than Butera due to the lack of an intertrappean bed between flows 3 and 4 at Sindhi. The sequence from infratrappean (Pijdura) to intertrappean 3 (Sindhi) is considered here to represent a continuous biotic and abiotic response to volcanism starting with the unaffected infratrappean locality.

Infratrappean–InL009 Pijdura

The Pijdura fossil locality (Maharashtra: Chandrapur District) is located approximately 100 km south of Nagpur just east of the village of Pijdura (Figure 1). The fossil bearing sediments are infratrappean underlying an exposed basalt (flow 1), and is locally referred to as the Lameta Formation. At Pijdura, the Lameta Formation (Maastrichtian) disconformably overlies the Kamthi Formation (Gondwana Group; Permian). Lameta Formation sediments were deposited in the paleotopographic lows of the Kamthi Formation.

The Lameta Formation is predominantly a lacustrine deposit containing mainly red and green overbank clay beds, with some intermittent sandstone lenses indicating fluvial influx. The majority of the site is red clay beds, which weather into agricultural fields. The hills above the fields display the red clay beds grading into green clay beds that are then overlain by the trap. The green clay beds often contain microvertebrates, which are not found in the red clay beds. The reddish color to the clays suggests that the lake sequence deposited in the Pijdura was well oxidized. Within the red clay beds are intermittent lenses of coarse-grained light gray sandstone that contain some fossil snails and clams. Most of the fossils are acquired from the fields as float in isolated patches, which are most likely the result of the weathering (either natural or through agricultural activity) of fossil rich layers in the relatively thin Lameta Formation. The exposure observed by Samant and Mohabey (2005) consists of roughly 4.5 m of alternating clay and sandstone beds with a few thin carbonate layers (Figure 8). The lower carbonates and upper sandstone are the only fossiliferous beds with the carbonates containing gastropods, bivalves, diatoms, charophytes, dinosaurs, ostracodes, phytoliths, pollen, and plants and the sandstone containing gastropods, dinosaurs, fish, and diatoms (Samant and Mohabey, 2005). The majority of molluscan fossils were preserved as silicified steinkerns.

Intertrappean 1– InL004 Takli

The Takli fossil locality is located within the city limits of Nagpur (Maharashtra: Nagpur District). Takli is considered intertrappean 1 (Maastrichtian) because it occurs between flows 1 and 2 in the Takli section known as the Takli Formation. The section is composed mainly of green clay sediments. In the area of Takli, the first flow directly overlies Gondwana Group beds thus there are no Lameta beds present (Figure 9). The underlying trap is amygdaloidal, and the overlying trap is nodular. The Takli locality has two distinct sites of collection, the Takli hill site (considered similar in location to the original Hislop locality) and the Girl’s Hostel site located downslope from the hill locality. Most of the sediments occurring at both sites are the green clays that are typical of the lacustrine Takli Formation, however there are some silts and sands that suggest some fluvial influence. The intertrappean sediments, especially the green clays, weather

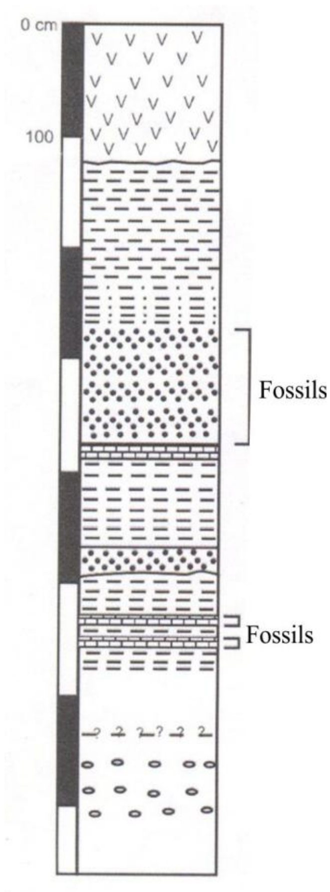

Figure 8. Stratigraphic section at Pijdura (20.36° N, 79.04° E) as interpreted by Samant and Mohabey (2005).

to a rust color and the greatest producing layers seem to be found in these weathered sediments. No measurements of the intertrap were taken on the hill due to the quality of the exposure, but the Girl's Hostel intertrap was approximately 1.5-2 m (Figure 9).

Fossils were collected at both sites; however the preservation and faunal assemblage varied slightly. The hill site assemblage consisted mainly of *Physa* casts, while the Girl's Hostel site assemblage was much more diverse with better preservation. The Girl's Hostel site also contained a diverse microsnail (<5 mm) assemblage. Fish have also been reported from Takli

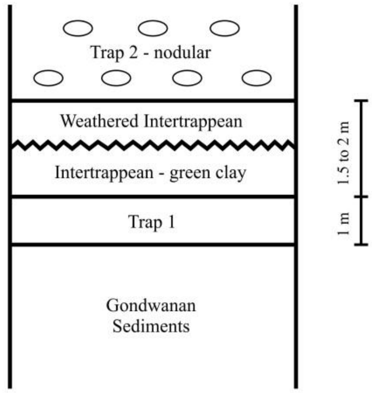

Figure 9. Stratigraphic section at Takli Girl's Hostel (21.17° N, 79.05° E) locality.

(Rana and Sahni, 1989). The majority of specimens collected at the Girl's Hostel site were silicified steinkerns but some specimens retained original shell material as evidenced by the presence of shell coloration (keel). Specimens are commonly crushed along bedding planes.

Intertrappean 2–InL096 Kalmeshwar

The Kalmeshwar locality is located close to the town of Kalmeshwar (Maharashtra: Nagpur District), which is just west of Nagpur. The locality is Maastrichtian in age. The outcrop is very extensive in overall vertical and horizontal magnitude, and it consists of both an underlying trap (flow 2), an intertrappean bed (intertrappean 2), and an overlying trap (flow 3) (Figure 10). The underlying trap is nodular and/or vesicular and constitutes the ground and base of the outcrop. The overlying trap is at least three meters of the upper portion of the outcrop and has columnar (vertical) jointing. The intertrappean sediments are divided up into three lithologies. A basal chert directly overlies the underlying trap and is only a few centimeters thick. This chert is overlain by a bed of alternating reddish brown claystone beds with carbonate nodules and white to light-yellow colored siltstone beds, which is then overlain by another thin chert before the overlying trap. A layer of carbonate occurs at the base of the silt-clay unit but is discontinuous.

The chert beds are discontinuous and vary in thickness. The clay-silt unit has a greater volume of clay at the base and a greater volume of silt toward the top, although both lithologies are present throughout. Kalmeshwar preserved the contact between the upper and lower traps, which is a unique opportunity to observe the actual paleoshoreline of the intertrappean lake.

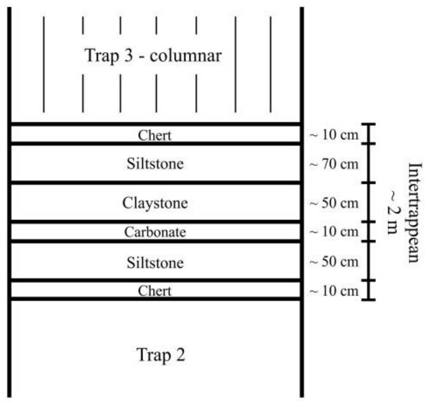

Figure 10. Stratigraphic section at Kalmeshwar (21.29° N, 78.92° E).

The fossil assemblage of Kalmeshwar includes gastropods, ostracodes, and floral remnants. Fossils are found in the basal chert, but they are completely silicified and often incomplete. Fossils, mainly small snails and plants, are found in the brown claystone but were often broken or crushed. The siltstone contains much higher fossil diversity and abundance. Most specimens are silicified steinkerns, but the external impression is well preserved and shows shell sculpture. There are also a substantial proportion of microsnails (< 5 mm).

Intertrappean 3–InL017 Butera

The Butera locality, in the Jabalpur-Mandla-Chhindwara sector, is located near the villages of Butera and Machhaghoda (Chhindwara District: Madhya Pradesh) roughly 160 km north of Nagpur (22.11 N, 79.14 E). The sedimentary beds are intertrappean 3 (Maastrichtian) and were deposited during magnetochron C29r (Samant and Mohabey, 2009). Bulk material brought to the laboratory for preparation was found as float as no actual outcrop is found at the fossil locality. Fossils are found in chert and siliciclastic rock and consist of gastropods, ostracodes, and some plants. There is some preservation of shell material, but most specimens are silicified steinkerns.

Intertrappean 3–InL106 Sindhi

The Sindhi locality lies in the Nand-Dongargaon Basin around 100 km west of Pijdura (Maharashtra: Yavatmal District). Fossil bearing sediments are considered intertrappean 3, but the sediments occur between flows four and five in the region. Due to absence of an intertrappean bed between flows three and four, Sindhi is considered stratigraphically intertrappean 3. Chronologically Sindhi is considered of a younger age than Butera. The Sindhi intertrappean interval was deposited during magnetochron C29r (Samant and Mohabey, 2009). Lithology is predominantly chert including the complete silicification of fossils. The section exposed at the Sindhi locality has intertrappean sediments in between two observable traps. The intertrappean interval is roughly three meters thick with a lower unfossiliferous carbonate bed (~1.5 m thick) and upper fossiliferous chert and porcellanitic claystone beds (~1.5 m thick) (Samant and Mohabey, 2005) (Figure 11).

The fossil assemblage reported from Sindhi includes pollen and megaflora, charophytes, ostracodes, bivalves, and gastropods (Samant and Mohabey, 2005; Samant and Mohabey, 2009). The locality was not visited during the 2006 field season and a small amount of bulk material was sent from D. M. Mohabey of the Geological Survey of India. Because of preservation of fossils in chert, preparation of the material was impossible without damaging the specimens.

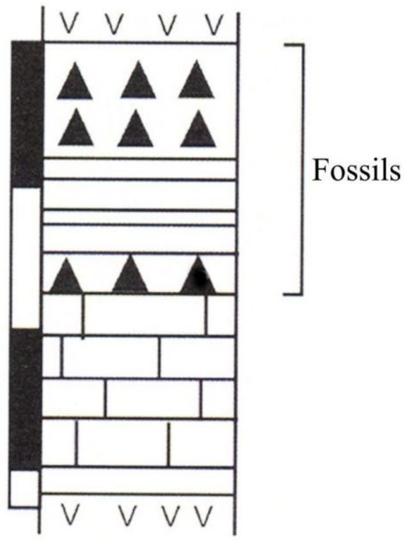

Figure 11. Stratigraphic section at Sindhi (~20.33° N, 78.54° E) as interpreted by Samant and Mohabey (2005).

CHAPTER IV

METHODS

Field Methods

Locating Original Localities

Stephen Hislop (1860) and his contemporaries (e.g., Malcolmson, 1840) described their fossil localities very generally citing adjacent villages or military landmarks as the only reference to their location. According to these descriptions a locality like Pijdura was found “60 mi S. of Nagpur” with no other reference to the fossil locality’s location (Hislop, 1860). Additionally, these studies were conducted in the mid-1800s when spelling or names of these landmarks were different (e.g., Phizdura = Pijdura). An attempt was made to more precisely locate all the molluscan localities on current topographic maps prior to field work. However, it was difficult to locate the actual fossil locality, so once the general area was located, local colleagues (e.g., D.M. Mohabey) helped trace Hislop’s and his contemporaries’ potential fossil sites. These sites are designated as potential because there is no definitive means of determining the original locations based on the information provided by Hislop. Therefore, any comparison to the species collected by Hislop should be considered close but not exact in terms of species typology and geology.

During field work precise locations were obtained using a Global Positioning System (GPS). During the field investigation twenty localities (eleven potential Hislop localities, five new localities in central India, and four new localities in western India) were precisely located

(Table 3). Due to previous extensive work, greater stratigraphic control is known for these localities in their relation to flow stratigraphy (i.e., Samant and Mohabey, 2005, 2009, etc.).

Fossil surveying was conducted at all localities where possible (i.e., Chickni was covered by construction and Sitabuldi is a military site and was inaccessible), but fossils were not always found even if they had been reported (i.e., no fossils were discovered at Telankhedi).

Five localities are used for the present study encompassing the infra- through intertrappean 3 stratigraphic levels; Infratrappean Pijdura (InL009), intertrappean 1 Takli (InL004), intertrappean 2 Kalmeshwar (InL096), intertrappean 3 Butera (InL017), and intertrappean 3 Sindhi (InL106). Sindhi was not visited during the 2006 field season but is found in the Nand-Dongargaon Basin like Pijdura. Samples were obtained from Dr. D.M. Mohabey.

Sample Collection

Fossil surveying and collection was conducted in central and western India in the 2006 field season (Table 3). Bulk matrix and specimens were extracted and removed to the laboratory for processing. Roughly 270 kg of material was shipped to the University of North Dakota from India, which included matrix and individual specimens. This amount of molluscan fossil material has more than doubled the amount of previously collected Deccan Plateau mollusk material and noticeably expanded the number of localities sampled.

Section Measurement

The stratigraphic section was measured where a sufficient exposure was available. The detail recorded for each section varied on the quality of the section. In several cases, section measurement was not possible due to time constraints or accessibility to the section. In all cases measurements were recorded in metric and were completed by Dr. Henning Schölz.

Table 3. Locality information from 2006 field trip.

Locality Number	Locality Name	Latitude °N	Longitude °E	State	Stratigraphic Level*	Notes
InL002	Karwad	20.33	78.88	Maharashtra	Int 2	G/B^
InL003	Telankhedi	21.15	79.03	Maharashtra	Int 1	No fossils
InL004	Takli†	21.17	79.05	Maharashtra	Int 1	G/O/V/C
InL007	Chikni	20.35	78.93	Maharashtra	Int 1	Locality destroyed
InL008	Gidad Hill	20.66	79.11	Maharashtra	Ints 2-3	No fossils
InL009	Pijdura†	20.36	79.04	Maharashtra	Inf	G/V
InL010	Kotbala	20.37	79.07	Maharashtra	Inf	G/B/V
InL011	Dongargaon	20.21	79.09	Maharashtra	Inf	V/C
InL017	Butera†	22.11	79.14	Madhya Pradesh	Int 3	G/O/P
InL019	Pahadsingha	21.32	78.48	Maharashtra	Int 2	G
InL026	Sitabaldi	21.15	79.08	Maharashtra	Int 1	No Access
InL096	Kalmeshwar†	21.29	78.92	Maharashtra	Int 2	G/O
InL097	Dhamni	20.25	79.13	Maharashtra	Inf	G/O
InL098	Daiwal	79.13	78.92	Maharashtra	Int 1	O/C
InL099-101	Mohagaon Kalan	22.02	79.18	Madhya Pradesh	Int 2	G/P
InL102	Lakshmipur	23.44	69.02	Gujarat	Int 3?	G/O
InL103	Dayapur	23.64	68.90	Gujarat	Inf	G/O/P
InL104	Kora	23.65	68.88	Gujarat	Inf	G/O/P
InL105	Ram Nagar	21.14	79.05	Maharashtra	Int 1	No fossils
InL123	Viri-Anjar	23.07	70.02	Gujarat	Int 3	G/B/V/P-K/Pg

†Denotes study locality (InL106 Sindhi is a study locality but was not visited in the field)

*Inf = Infratrappean, Int = Intertrappean.

^G = Gastropods, B = Bivalves, O = Ostracodes, V = Vertebrates, C = Charophtyes, P = Plants

Laboratory Methods

Sample Preparation

Individual specimens were collected from Pijdura as surface float and required little to no preparation. Takli and Kalmeshwar were composed mostly of softer matrix (i.e., siltstone and claystone) and preparation was accomplished with dental picks. Butera was composed of siltstone matrix surrounding chert and was prepared using a series of different sized air scribes. Once mechanical preparation was accomplished, residual matrix was washed using calgon soap, screened, and picked under magnification for specimens. This method was especially successful in Takli, which contained a vast abundance of microspecimens (<5 mm).

Individual specimens were separated by quality and identifiable and/or measureable specimens were assigned an "InS" number for ascension into the University of North Dakota fossil collection. A specimen of highest quality was considered to be mostly complete and/or uncrushed and labeled with a green dot on the specimen tag. A specimen of moderate quality was considered to be almost complete and/or uncrushed or crushed and was labeled with a purple dot on the specimen tag. A specimen of lowest quality was considered to be complete enough for identification but not necessarily measurement and was labeled with a red dot on the specimen tag. A total of 1461 specimens were numbered and sorted.

Photography

Specimens of highest quality were photographed for character measurement. Macrophotography was accomplished using a standard digital camera. Microphotography was used for specimens less than ten mm in length and was accomplished using the Spot Insight© series digital microscope camera. The Spot© computer program was utilized to capture and calibrate images. Due to problems in the range of depth of field in microspecimens, a secondary program, Helicon Focus©, was employed to create a focused composite image through combining a series of partially focused images. Specimens' apertural, apertural flush, and right lateral views were photographed (Figure 12). Apical views were also photographed for the most complete specimens and umbilical views were photographed for potential members of Valvatidae (Figure 12). Of the 1461 total specimens numbered, 679 specimens were photographed.

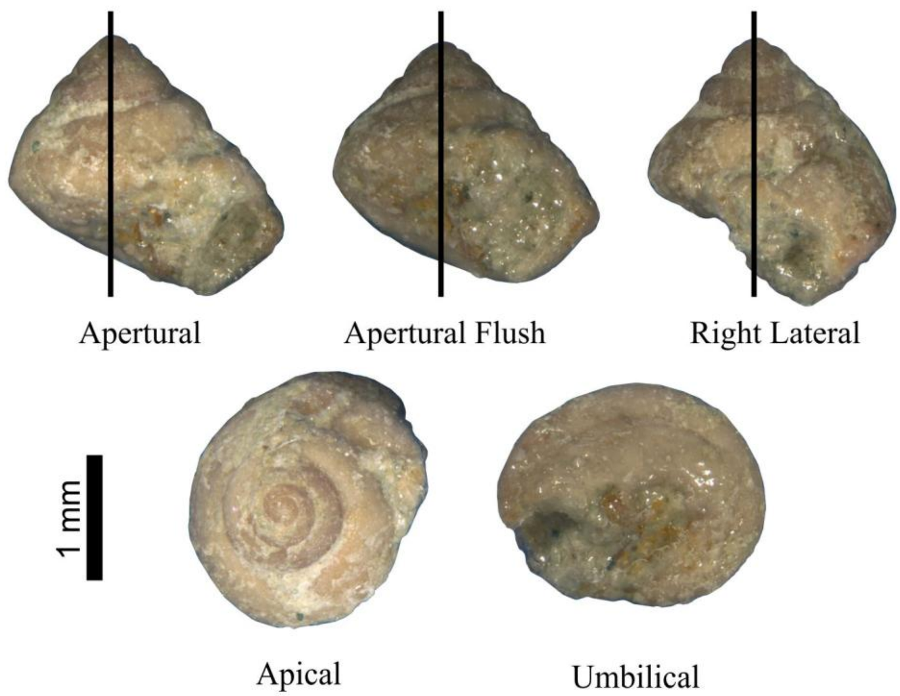

Figure 12. Standard photographed gastropod views.

Orienting and Scaling Images

Specimens were photographed with the axis of coiling parallel to the plane of view for apertural and right lateral views (Figure 12, apertural). For apertural flush the specimen was photographed with the aperture surface parallel to the plane of view. The apical and umbilical views were photographed with the axis of coiling perpendicular to the plane of view. Specimen photographs were oriented for measurement using Photoshop CS5©. They were oriented along the axis of coiling, or the closest approximate axis of coiling for less than complete specimens (Figure 12). Once properly oriented the images were scaled for measurement in CorelDraw X5©. Each photographed was individually scaled according to their calibration scale bars and the internal metric scale available in the CorelDraw X5© program.

Character Measurement

Basic Parameters

The basic dimensions of each specimen were measured using CorelDraw X5© in millimeters to the thousandth place. A ratio was calculated for each basic measurement against another for use in analysis. Ratios were used in this study due to the drastic difference in sizes of similar morphotypes between localities. Almost all of the specimens are steinkerns, so measurements are of the internal cast. Maximum height was measured from the apex to the base of the aperture (Figure 13). Maximum width represents the widest point on the specimens and was measured from the outside of the final whorl to the outside of the aperture (Figure 13). Aperture height was measured from the base of the aperture to the point where the aperture meets the final whorl but is sometimes approximated due to preservation (Figure 13). Aperture width is measured from the inside to outside edges of the aperture (Figure 13). The height of the spire was measured from the apex to the plane where the body whorl intersects the axis of coiling (Figure 13). The height of the body whorl as measured from the plane where the body whorl intersects the axis of coiling to the base of the aperture (Figure 13). Both of these measurements are also subject to preservation. Character trait ratios from basic measurements included in this analysis consist of maximum height to maximum width, aperture height to aperture width, spire height to maximum height, body whorl height to maximum height, aperture height to maximum height, and aperture width to maximum width (Figure 13).

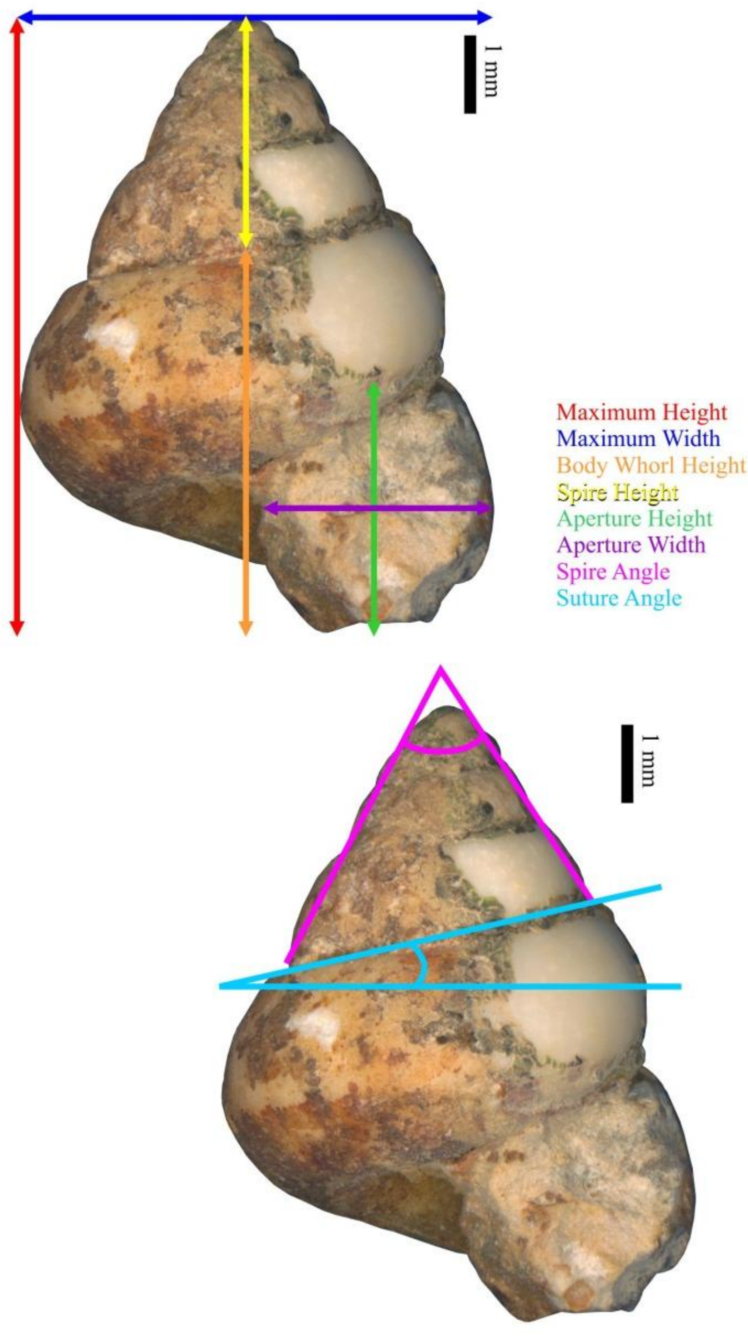

Figure 13. Basic gastropod shell parameters.

General Shell Shape

The shell shape is a qualitative character trait based on the general outline shape. This outline shape is separated into distinct categories. For example, the shape category “ovate” refers to a general oval shape to the shell outline (Figure 14). Categories that contain two categories hyphenated retain qualities of both shapes such that the shape can only be described as a mixture of both. Shape categories modified from Burch (1989).

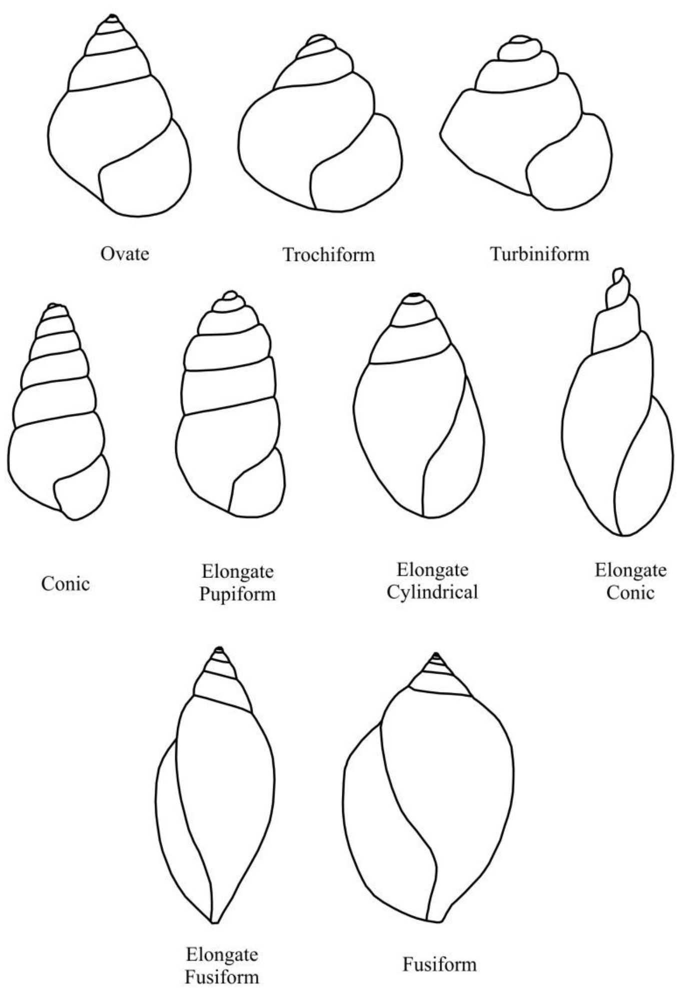

Figure 14. Named gastropod shell shapes.

Suture Angle

The suture angle represents the angle of growth of the individual whorls. This measurement is taken as the angle between the suture slope plane and the plane where the suture intersects the axis of coiling (Figure 13). The suture angle was acquired using the Photoshop CS5© angle function and is a continuous character.

Number of Whorls

The number of whorls for a given specimen represents the number of whorls from the initiation of growth (protoconch) to where the inside edge of the aperture intersects the body whorl (Figure 15). This was accomplished using Photoshop CS5© by orienting the edge of the aperture to the apex (approximated if poorly preserved) along a horizontal line. A secondary line is made through the apex to the initiation of growth, which represents the beginning of whorl measurement. The number of whorls is then the number of full whorls from the aperture edge towards the secondary line plus the remaining number of degrees to the secondary line (Figure 15). The remaining degrees are converted into a decimal, and the number of whorls is reported as the whole number of whorls plus the decimal degrees (e.g., 4.8 whorls).

Figure 15. Measurement of the number of whorls.

Coiling Direction

The coiling direction represents the direction of specimen growth during the course of its lifetime. Gastropods coil dextrally (to the right) or sinistrally (to the left) (Figure 16). This character trait is a fundamental difference between certain families of gastropods (i.e., physids coil sinistrally). If the aperture is located on the right side of the body then it coils dextrally and vice versa. The character trait is reported as dextral or sinistral.

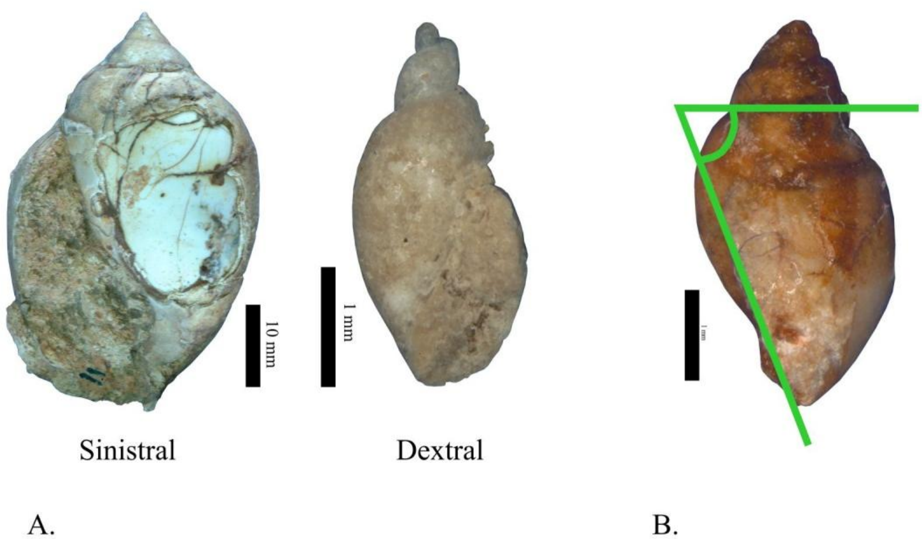

Figure 16. A. Gastropod coiling direction. B. Plane of aperture to axis of shell.

Spire Angle

The spire angle represents the angle at which the specimen grows outward from the initiation of growth. It is measured as the angle from the apex to the maximum width of the shell (Figure 13). The spire angle was acquired using the Photoshop CS5© angle function and is a continuous character.

Plane of Aperture to Axis of Shell

The plane of the aperture represents the slope of the aperture from the right lateral view. It is measured using the Photoshop CS5© angle function and is a continuous character. The angle of the aperture is measured where the plane of the aperture crosses the intersection of the axis of coiling and the horizontal plane at the body whorl suture (Figure 16).

Umbilicus

The shape of the umbilicus is important in distinguishing certain gastropod families. The umbilicus is reported as open or closed. It is deemed open when it has not been covered by the callus, which is a thickening of the shell covering the umbilicus (Figure 17a).

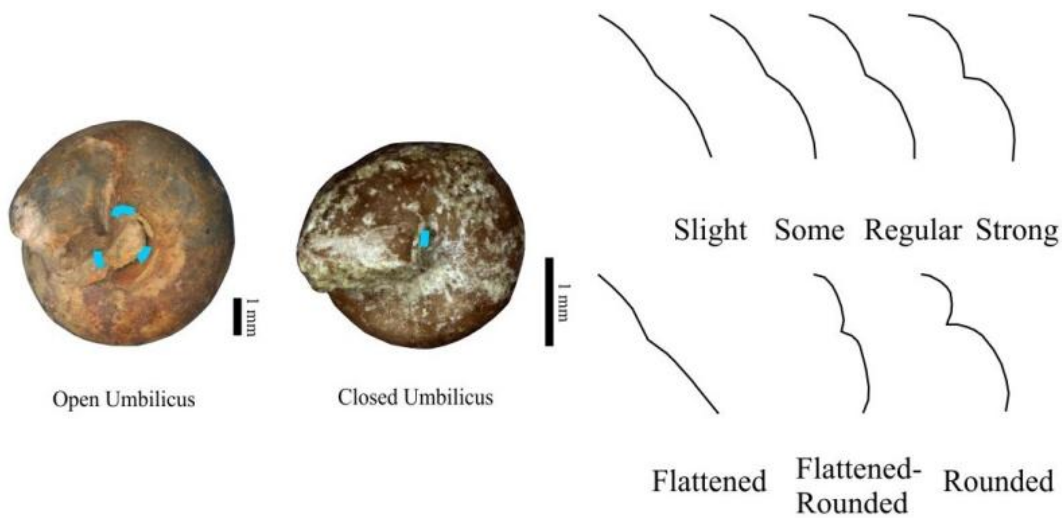

A. B.

Figure 17. A. Umbilicus description. B. Suture depression (upper), Whorl shape (lower).

Suture Depression

The depression of sutures describes the degree of indentation from the shell margin. Suture depression is related to strength of curvature of individual whorls. It is qualitative and classified slight, some, regular or strong depression (Figure 17b, upper).

Whorl Shape

The whorl shape describes the overall roundness of the whorls as applied to the all whorls. Whorls are described as being rounded, flattened-rounded, or flattened (Figure 17b, lower). Flattened-rounded is considered to be a whorl that has a rounded shape but is flat along the apex (Figure 17b, lower). If the spire whorls are collectively a different shape then the body whorl, then the trait is reported as two shape categories.

Presence of Keel

The keel is shell surface ornamentation that is not reflected on the steinkern. Most specimens from the study localities lack shell material and do not have the keel preserved. The character trait is reported as either present or absent (Figure 18a). However, this trait does not entirely describe the population because of the abundance of steinkerns.

Shell Sculpture

Shell sculpture in continental gastropods is strictly surface ornamentation and is not reflected on steinkerns. The sculpture present in most study specimens is found in the corresponding mold. To observe the sculpture in 3-dimensional form, a cast was made using Image Plus Impression Material by Parkell©. In rare occurrences (Kalmeshwar only) there was enough shell material remaining to preserve sculpture. The character trait is recorded as none, revolving, or axial sculpture (Figure 18b).

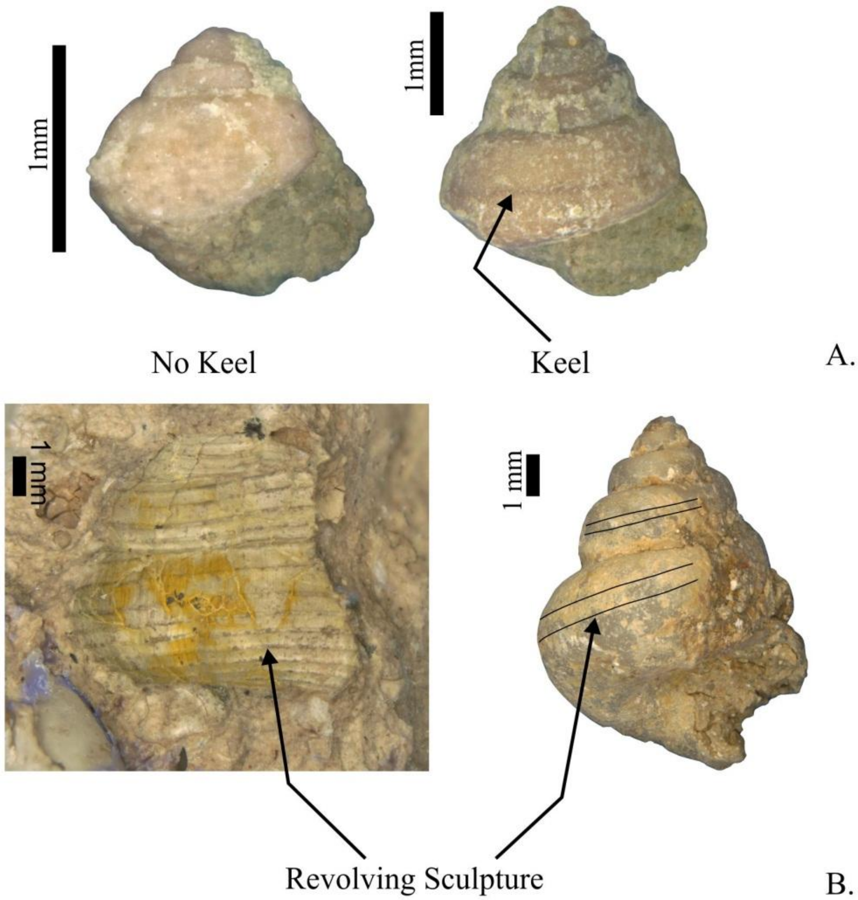

Figure 18. A. Keel description on viviparid specimens from Takli. B. Sculpture description on valvatid specimens from Kalmeshwar.

Statistical Analyses

Lectotype specimens of Sowerby (1840) and Hislop (1860), four paralectotype specimens with higher measurable quality, and nineteen modern specimens from comparable families (e.g., Viviparidae, Hydrobiidae, and Subulinidae) were included in analysis for comparison to the study specimens. Specimens with missing data were removed from analysis due to the difficulty of statistical software packages to interpret data gaps.

Cluster Analysis

Cluster analyses were used to identify morphotypes based on overall morphologic similarity. These morphotypes are interpreted as distinct species. The StatistiXL© v. 1.8 statistics package for Microsoft Excel 2007© using a mixed dataset, both quantitative (reported as numeric values) and qualitative traits (reported as categories), and the group average method calculated each dendrogram. The group average method is equivalent to the unweighted pair-group mean average method (UPGMA) where a dendrogram is built based on the calculated minimum distance between individuals.

A separate cluster analysis was conducted for each of the following datasets; all study specimens plus all Sowerby (1840) and Hislop (1860) types (443 specimens), all study specimens plus all modern representatives (437 specimens), and all study specimens plus all types and all modern representatives (462 specimens). All aforementioned character traits were included in these analyses except for the presence or absence of a keel. This character trait was considered uninformative due to the presence of a keel only in specimens with original shell material. To define morphotypes, all three analyses were evaluated in combination to identify consistent groupings. To further reinforce consistent groupings of specimens, individual cluster analyses were conducted using members of similar families only. These analyses included a physid, lymnaeid, valvatid, stylommatophoran, viviparid/hydrobiid, and viviparid/hydrobiid/valvatid/ stylommatophoran analysis. To evaluate the strength of individual clusters within a dendrogram, a correlation coefficient (R) was calculated by StatistiXL. A correlation coefficient value of 1.0 means 100% of the clusters can be explained by the relationships between the specimens or, in other words, the dendrogram is perfect. For the purposes of this study, a correlation coefficient of 0.7 or higher is considered to be a dendrogram with statistically significant clusters. A correlation coefficient of 0.6 or higher is considered to be a dendrogram with reasonably satisfactory clusters.

Cluster analysis will be used as a tool to establish taxonomic identity, including the revision of previous nomenclature and placement. These modifications will be described herein, but a more detailed analysis of evolutionary history, biogeography, and taxonomic relationships will be conducted and described in subsequent work thus the presented herein is a work in progress.

Analysis of Variance

Two-way analysis of variance (ANOVA) was used to examine the change in each morphotype through the Deccan trap sequence. This was to determine whether or not stratigraphic levels (or localities) are distinct based on the character traits of each morphotype. ANOVA was conducted using R: A Language and Environment for Statistical Computing v. 2.13.0 (2011)©. R calculated an F statistic and probability (p) to determine the statistical significance (Bates et al., 2011). The dataset was tested for normality and equal variance prior to analysis. Since there is no nonparametric equivalent for the 2-way ANOVA, if the assumptions were not met then a nonparametric Kruskall-Wallis test was utilized using only height or height to width ratio and the locality. A post-hoc Tukey's test, or pairwise t-test with bonferroni adjustment for the nonparametric test, was conducted to determine locality grouping if the analysis was significant with 95% confidence ($\alpha = 0.05$).

Each of the sixteen morphotypes was tested using both raw data and transformed ratios. The separation of raw data from ratio data was to observe the effect of specimen size in stratigraphic level distinction. Maximum height or the height to width ratio and the locality combined with outline shape, whorl shape, or suture depression were used.

χ^2 *Tests*

χ^2 tests were utilized to examine the difference between stratigraphic levels based on the number of species (diversity) and number of specimens (abundance). The number of species and number of specimens were obtained by counting the number of identified morphotypes for each locality. χ^2 tests were accomplished using Microsoft Excel 2007©. 95% confidence was used to determine whether the outcome was statistically significant.

Morphologic Trends

Linear plots were created to show changes in morphology for each morphotype through time. Overall change was shown using mean measured maximum height, mean measured maximum width, mean measured spire height, mean measured body whorl height, and height to width ratio plotted against time. Mean number of whorls, mean suture angle, and mean spire angle were also plotted against time. Linear plots were created using Microsoft Excel 2007©.

CHAPTER V

RESULTS

Cluster Analysis for Gastropod Morphotype Identification

Using cluster analysis to differentiate morphotypes provides a quantitative approach to identifying similar morphologies based on shell characters. Distinctive clusters were recognized on each dendrogram based on overall grouping patterns. These distinctive clusters, or sets of clusters, were interpreted to be individual morphotypes (Figure 19). The clusters were compared between different trees, as previously discussed, to reinforce their repeatability and therefore morphotypes' validity.

Sixteen morphotypes were recognized from different freshwater and terrestrial gastropod families (Figure 20). Four morphotypes from Hydrobiidae, or a related family, are designated "hydA," "hydB," "hydC," and "hydD," with the morphology "hydD" possibly a member of Thiaridae. These four morphotypes are distinguishable based primarily on outline shape. Two morphotypes ("vivA" and "vivB") belong to Viviparidae, or a related family, and are distinguishable by whorl shape. There are two morphotypes ("valA" and "valB") from Valvatidae, or a related family, and are distinguishable by differences in the height to width ratios and whorl shape. Two morphotypes ("phyA" and "phyB") are from Physidae, or a related family, which is contrary to the three identified by Hislop (1860) but consistent with Annandale (1920). "PhyA" is more slender and elongate and is equivalent to the *Physa prinsepii elongata* species of Hislop (1860), while "phyB" is wider and more robust and is equivalent to *Physa prinsepii* *normalis* and *P. p. inflata* of Hislop (1860). There are at least three morphotypes ("lymA," "lymB," and "lymC) of Lymnaeidae, or a related family, recognizable in the study sample. Three other morphotypes ("lymD," "lymE," and "lymF") are represented by the Hislop's type specimens of *Lymnaea attenuata, L. telankhediensis peracuminata*/*L. t. radiolus,* and *L. spina*, but were not found in the study sample. "LymA," "lymB," and "lymC are distinguishable by outline shape and height to width ratios. There are three morphotypes belonging to the terrestrial group Stylommatophora ("styA," "styB," "styC"). These are differentiated by outline shape.

"HydA" clusters with *Viviparus virapai* Hislop, 1860, but the close relationship with other clusters containing modern hydrobiids suggests this morphotype belongs in Hydrobiidae or a related family (Figure 19). "HydB" is a large cluster that includes modern representatives from Hydrobiidae (*Incertihydrobia teesdalei* Verdcourt, 1958) and Pleuroceridae (*Elimia livescens* Menke, 1830), as well as Hislop's (1860) types *Viviparus conoidea* and *V. takliensis*. Two distinctive morphologies are found within this cluster, which are denoted "hydB1" and "hydB2." "HydB1" includes *Incertihydrobia teesdalei* and *V. conoidea* and "hydB2" includes *Elimia livescens* and *V. takliensis*. "HydC" clusters with modern representatives from the freshwater families Hydrobiidae (*Littoridina australis* Marcus & Marcus, 1965) and Micromelanidae (*Micromelania grimani* Brusina, 1874) and the terrestrial family Pomatiopsidae (*Blanfordia simplex* Pilsbry, 1902) as well as *Viviparus sankeyi* Hislop, 1860. There are only a few specimens of "hydD," which may be a thiarid, and they form a distinct minor cluster found within the major cluster containing the "hydC" morphology. "HydD" is considered a distinct morphotype rather than a common morphology within "hydC" based on its unique shell and aperture shape.

"LymA" is found in two distinctive clusters yet appears to be the same morphotype (Figure 19). "LymA" groups with a modern lymnaeid, *Galba truncatula* Müller, 1774, and *Lymnaea oviformis* Hislop, 1860 suggesting it is a member of Lymnaeidae. "LymB" is

Figure 19. Dendrogram of analysis with all specimens (types and modern equivalents) (R=0.71).

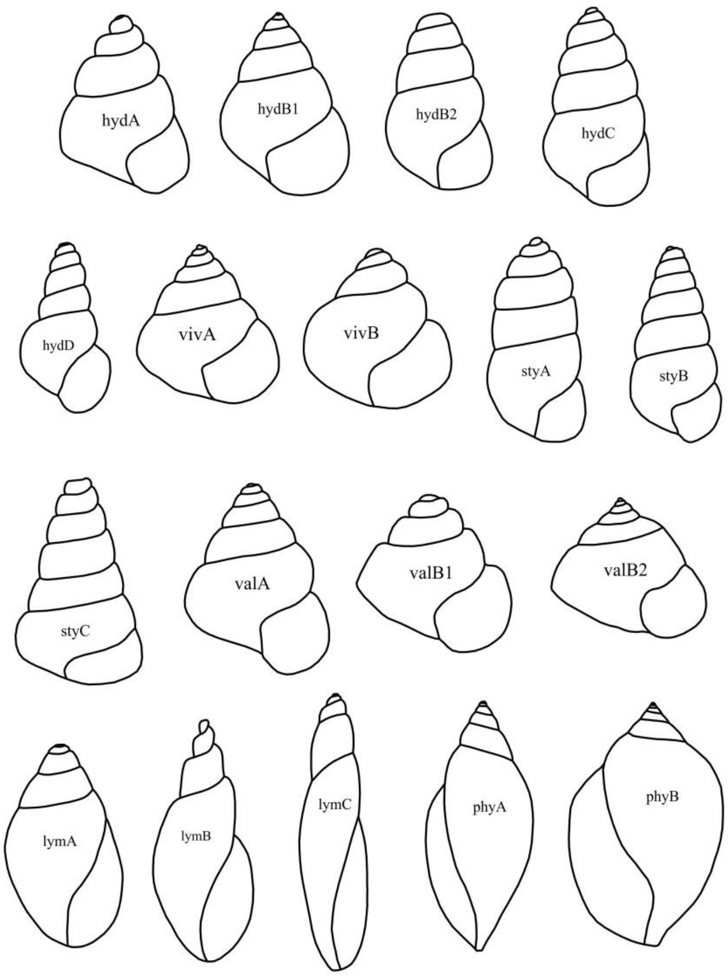

Figure 20. Distinct gastropod morphotype outlines.

not found with modern representatives or type specimens, but it is closely related to the "lymC" cluster suggesting a taxonomic relationship. "LymC" clusters with a modern lymnaeid, *Stagnicola elodes* Say, 1821, and all other Deccan trap type lymnaeids (*Lymnaea subulata* Sowerby, 1840, *L. telankhediensis peracuminata* Hislop, 1860, *L. t. radiolus* Hislop, 1860, *L. spina* Hislop, 1860, and *L. attenuate* Hislop, 1860). "LymC" is considered equivalent to *L. subulata*, and although *L. attenuata*, *L. spina*, and *L. t. peracuminata*/*L. t. radiolus* cluster with "lymC," they appear to be distinct morphologies.

“PhyA” clusters with the modern physid, *Aplexa niteus* Say, 1821, and *Physa prinsepii elongata* Hislop, 1860 (Figure 19). “PhyB” clusters with two modern representatives of Physidae, *Physella parkeri* Currier, 1881 and *P. gyrina* Say, 1821, and *Physa prinsepii normalis* Hislop, 1860 and *P. p. inflata* Hislop, 1860. Although Hislop (1860) considered *P. p. normalis* and *P. p. inflata* to be two separate, there is no evidence to support these subspecies in the dendrogram.

Morphotypes were placed within each potential family based on overall appearance and clustering patterns with modern representatives (Figure 19). Both morphotypes considered as members of Valvatidae clustered with the modern valvatid representatives, *Valvata virens* Tyron, 1863 and *V. utahensis* Call, 1884, *Valvata multicarinata* Hislop, 1860 and *V. unicarinifera* Hislop, 1860.

Clustering of “styA,” “styB,” and styC” is more complicated due to the relationship of both freshwater and terrestrial families to these forms in all analyses. The cluster includes representatives from the freshwater families Micromelanidae, Hydrobiidae, Pleuroceridae, and two families of the terrestrial Stylommatophora (Subulinidae and Ferussaciidae) (Figure 19). Although “styA,” “styB,” and styC” are found together, their individual morphologies are readily distinguishable and are considered distinct morphotypes. The presence of terrestrial families and the type of shell morphology suggests they are terrestrial rather than freshwater. The cluster incorporating “styB” contains *Viviparus acicularis* Hislop, 1860 and *V. subcylindracea* Hislop, 1860. The cluster containing “styC” contains *V. pyramis* Hislop, 1860 and *V. rawesi* Hislop, 1860. The clustering pattern suggests that *V. acicularis* and *V. subcylindracea* and *V. pyramis* and *V. rawesi*, respectively, are perhaps the same species.

Although both morphotypes of Viviparidae appear to be valid members of the family, only “vivB” clusters with the modern representative from India, *Bellamya bengalensis* Lamarck, 1801, and *Viviparus normalis* Hislop, 1860 (Figure 19). "VivA" forms two distinctive clusters yet the morphology appears consistent (Figure 19).

Analysis of Variance (ANOVA) for Locality Distinction

Locality distinction based on changes in morphotype characteristics reflects changes in species due potentially to the Deccan trap eruptions. Analysis of variance demonstrated these changes by determining if at least one locality was distinct on the basis of shape and size of the morphotype. Subsequent post hoc testing determined how localities were related. In general, localities could be consistently differentiated based on specimen size but not on overall morphology. Specimens in the infratrappean Pijdura locality are statistically larger than the remainder of the sequence; however species retained the same shape between all localities.

Morphotype "hydA"

"HydA" was found throughout the sequence at all study localities (Table 4). Differentiating localities using the height to width ratio and either outline shape showed that localities were not distinct (height/width: $F_{4,10}$= 0.7841, p= 0.5608; height/width:shape: $F_{4,1,10}$= 0.0804, p= 0.7826). Localities were not distinct based on the height to width ratio and whorl shape (height/width: $F_{4,10}$= 0.4254, p= 0.7872; height/width:whorl shape: $F_{4,2,10}$= 0.6340, p=0.5505). Localities also could not be differentiated based on the height to width ratio and suture depression (height/width: $F_{4,9}$= 0.6784, p= 0.6239, height/width:suture depression: $F_{4,2,9}$= 2.246, p= 0.1617).

Localities were statistically distinguishable based on maximum height and outline shape (height: $F_{4,10}$= 26.64, p= <0.0001*; height:shape: $F_{4,1,10}$= 9.777, p= 0.0108*). Two locality groups were formed, the Takli-Kalmeshwar-Sindhi group and Pijdura-Butera group. "hydA" in the Pijdura-Butera group has a greater mean maximum height than the Takli-Kalmeshwar-Sindhi

Table 4. Number of specimens of each gastropod morphotype found at each locality.

	Pijdura (Inf)	Takli (Int1)	Kalmeshwar (Int2)	Butera ($Int3_1$)	Sindhi ($Int3_2$)	Totals	% of Family	% of Assemblage
hydA	2	5	9	2	2	20	10%	3%
hydB	26	30	31	3	6	96	48%	14%
hydC	1	28	38	11	7	85	42%	13%
hydD	2	0	0	0	2	4	100%	<1%
lymA	0	2	11	15	0	28	24%	4%
lymB	5	34	21	4	1	65	56%	10%
lymC	15	2	0	6	1	24	20%	4%
phyA	14	9	4	5	0	32	34%	5%
phyB	20	16	15	12	0	63	66%	9%
styA	0	9	1	0	0	10	14%	1%
styB	0	19	21	11	4	55	78%	8%
styC	0	1	3	2	0	6	8%	<1%
valA	0	0	12	6	0	18	24%	3%
valB	0	10	29	19	0	58	76%	9%
vivA	0	13	7	11	0	31	30%	5%
vivB	25	14	23	7	2	71	70%	11%
Totals	110	192	225	114	25			
	17%	29%	34%	17%	4%			

group (Figure 21a). Localities can be distinguished based on the height when incorporating the whorl shape (height: $F_{4,10}$= 17.40, p= 0.0002*; height:whorl shape: $F_{4,2,10}$= 3.061, p= 0.0918). The resulting locality groups are the same. Similarly, localities are distinguishable based on the height when incorporating suture depression (height: $F_{4,9}$= 20.82, p= 0.0001*; height:suture depression: $F_{4,2,9}$= 1.341, p= 0.3092). The same resulting locality groups occurred in this analysis (Figure 21a).

Overall, localities are not distinguishable when the morphology is corrected for size variation, as when using the height to width ratio, but are distinct forming two subgroups, the

Takli-Kalmeshwar-Sindhi group and Pijdura-Butera group, when analyzing the actual specimen dimensions.

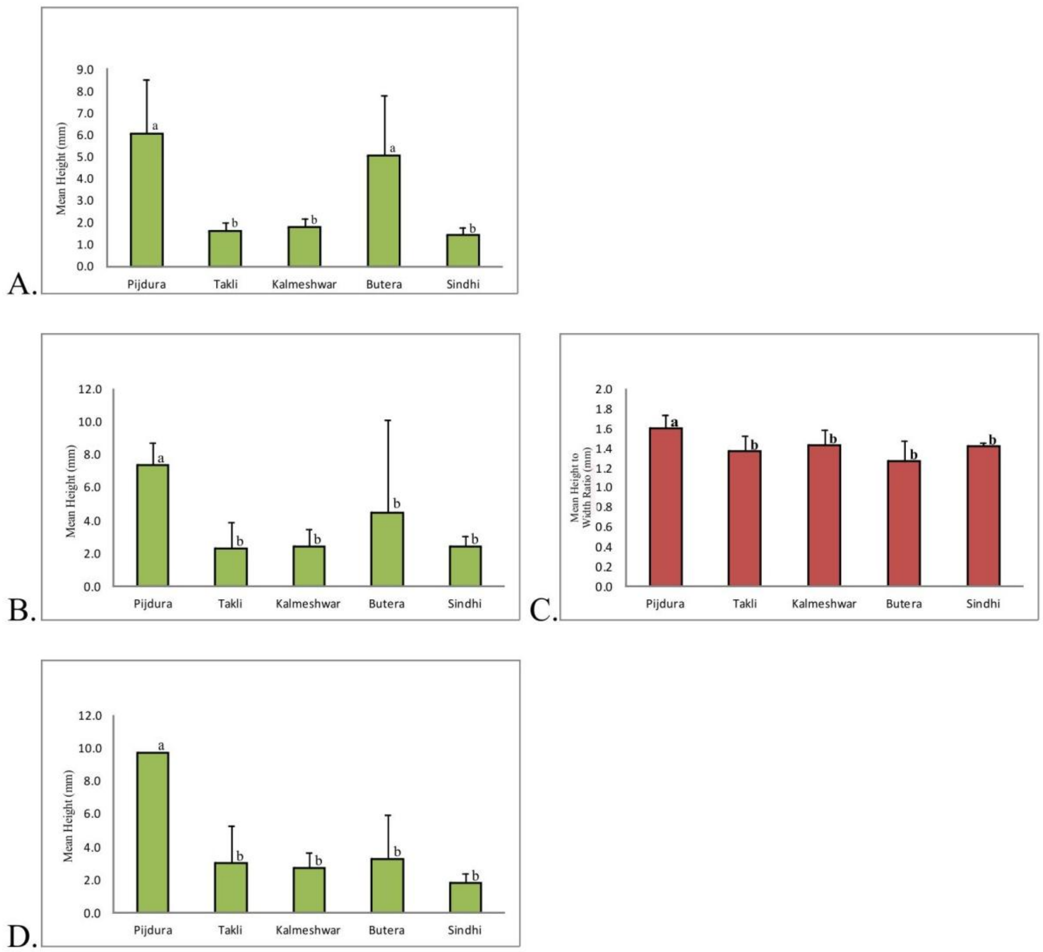

Figure 21. ANOVA results from post-hoc Tukey's test for "hydA," "hydB," and "hydC." For each gastropod morphotype, members of group "a" are distinct from group "b." A. Results from raw data analysis for "hydA." B. Results from raw data analysis for "hydB." C. Results from ratio data analysis for "hydB." D. Results from raw data analysis for "hydC." Error bars = one standard deviation above mean, $\alpha = 0.05$.

Morphotype "hydB"

"HydB" was common throughout the sequence at all study localities (Table 4). Differences between "hydB" distinguish localities based on the height to width ratio and outline shape (height/width: $F_{4,70}$= 10.99, *p*= <0.0001*; height/width:shape: $F_{4,5,70}$= 0.5632, *p*= 0.7278). Two locality groups are formed. The Takli-Kalmeshwar-Butera-Sindhi group has a lower height to width ratio than the Pijdura group (Figure 21c). "HydB" morphology differentiates localities based on the height to width ratio and whorl shape (height: $F_{4,74}$= 10.30, *p*= <0.0001*; height/width:whorl shape: $F_{4,4,74}$= 1.880, *p*= 0.1229). The resulting locality groups are the same.

Using the height to width ratio with the suture depression distinguished localities (height/width: $F_{4,71}$= 9.856, *p*= <0.0001* height/width:suture depression: $F_{4,5,71}$= 1.390, *p*= 0.2383). Locality groups are the same as previous analyses. Localities are distinguishable based on the actual maximum height when incorporating outline shape (height: $F_{4,70}$= 35.9757, *p*= <0.0001*; height:shape: $F_{4,5,70}$= 1.911, *p*= 0.1034). "hydB" is divided into two locality groups. The Takli-Kalmeshwar-Butera-Sindhi group has a lower mean height than the Pijdura group (Figure 21b). Localities are distinguishable based on actual height and whorl shape (height: $F_{4,74}$= 73.20, *p*= <0.0001*; height:whorl shape: $F_{4,4,74}$= 11.12, *p*= <0.0001*). Locality groups are the same as the previous analysis. The height and suture depression distinguish localities (height: $F_{4,71}$= 48.51, *p*= <0.0001*; height:suture depression: $F_{4,5,71}$= 3.254, *p*= 0.0104*). Resulting locality groups are the same as previous analyses.

Overall, "hydB" forms two locality groups based on ratio and raw data. The Pijdura group has a greater height or height to width ratio than the Takli-Kalmeshwar-Butera-Sindhi group.

Morphotype "hydC"

"HydC" was common throughout the sequence at all study sites (Table 4). Height to width ratio with outline shape does not distinguish localities (height/width: $F_{4,67}$= 1.063, *p*= 0.3819; height/width:shape: $F_{4,3,67}$= 0.6102, *p*= 0.6107). When incorporating height to width ratio and whorl shape, localities were not distinguishable (height/width: $F_{4,69}$= 1.013, *p*= 0.4071; height/width:whorl shape: $F_{4,3,69}$= 0.2959, *p*= 0.8283). Localities are also not distinguishable based on the height to width ratio with suture depression (height/width: $F_{4,66}$= 1.075, *p*= 0.3761; height/width:suture depression: $F_{4,3,66}$= 0.7682, *p*= 0.5159).

Incorporating the actual maximum height and outline shape produced a statistically significant result (height: $F_{4,67}$= 3.935, *p*= 0.0063*; height:shape: $F_{4,3,67}$= 4.389, *p*= 0.0070*). "hydC" specimens are divided into two locality groups. The Takli-Kalmeshwar-Butera-Sindhi group has a lower mean height than the Pijdura group (Figure 21d). Localities are also differentiable based on the height and whorl shape (height: $F_{4,69}$= 3.726, *p*= 0.0084*; height:whorl shape: $F_{4,3,69}$= 3.486, *p*= 0.0203*). The resulting locality groups are the same as the previous analysis. Localities were differentiable into two groups based on the height and suture depression (height: $F_{4,66}$= 3.659, *p*= 0.0094*; height:suture depression: $F_{4,3,66}$= 1.515, *p*= 0.2188) (Figure 21d).

Generally, localities are not distinguishable when "hydC" is corrected for size variation, but are distinct forming two groups, the Takli-Kalmeshwar-Butera-Sindhi group and Pijdura group, when analyzing the actual specimen dimensions. "HydC" in the Pijdura group have a greater mean height than those in the Takli-Kalmeshwar-Butera-Sindhi group.

Morphotype "hydD"

"HydD" is a rare morphology and was restricted to Pijdura and Sindhi (Table 4). The distribution of this morphology was not normal and a nonparametric Kruskall-Wallis test was used. Localities were not differentiable based on the height to width ratio (χ^2_1 = 2.4, p= 0.1213) or the actual measured height (χ^2_1 = 2.4, *p*= 0.1213).

Morphotype "lymA"

"LymA" is an uncommon morphology found at Takli, Kalmeshwar, and Butera (Table 4). Localities were not differentiable based on the height to width ratio when incorporating the outline shape (height/width: $F_{2,21}$= 0.1861, *p*= 0.8316). There is no interaction between the height to width ratio and outline shape indicating these factors have equal effect on locality separation. The height to width ratio with whorl shape could not be used to distinguish localities (height/width: $F_{2,20}$= 0.1798, *p*= 0.8368; height/width:whorl shape: $F_{2,1,20}$= 0.0720, *p*= 0.7912). Similarly, localities are not distinguishable based on the height to width ratio with the suture depression (height/width: $F_{2,19}$= 0.1733, *p*= 0.8422; height/width:suture depression: $F_{2,1,19}$= 4.128, *p*= 0.0564).

The assumptions were not met when using the actual measured height due to a lack of a normal distribution, so a nonparametric Kruskall-Wallis test was used. Localities could not be distinguished based on specimen height (χ^2_2 = 2.457, *p*= 0.2927).

Morphotype "lymB"

"LymB" was common throughout the sequence found at all study localities (Table 4). The height to width ratio of "lymB" nor its interaction with the outline shape could be used to distinguish localities (height/width: $F_{4,53}$= 1.061, *p*= 0.3851; height/width:shape: $F_{4,3,53}$= 0.6351,

p= 0.5957). Localities were also not differentiable based on the height to width ratio with the whorl shape (height/width: $F_{4,54}$= 1.001, p= 0.4154; height/width:whorl shape: $F_{4,2,54}$= 0.0972, p= 0.9075). The height to width ratio with the suture depression did not distinguish localities (height/width: $F_{4,53}$= 1.068, p= 0.3814; height/width:suture depression: $F_{4,1,53}$= 1.498, p= 0.2264).

The actual measured height with outline shape differentiated localities into three groups (height: $F_{4,53}$= 13.78, p= <0.0001*; height:shape: $F_{4,3,53}$= 0.9849, p= 0.4070). The Takli group has a lower mean height than the Takli-Kalmeshwar-Butera-Sindhi group, which has a lower mean height than the Pijdura group (Figure 22a). Localities are also distinguishable based on the height with whorl shape (height: $F_{4,54}$= 12.36, p= <0.0001*; height:whorl shape: $F_{4,2,54}$= 0.0352, p= 0.9654). The resulting groups are the same as the previous analysis. Localities are also differentiable using the height and suture depression (height: $F_{4,53}$= 13.54, p= <0.0001*; height:suture depression: $F_{4,1,53}$= 2.943, p= 0.1240). Similarly, specimens are divided into three locality groups (Figure 22a).

In general, localities are distinguishable based on the actual measured height but not the height to width ratio. The specimens of "lymB" form three locality groups. The Takli group has a lower mean height than the Takli-Kalmeshwar-Butera-Sindhi group, which have a lower height than the Pijdura group.

Morphotype "lymC"

"LymC" was found at all study localities (Table 4). The outline shape is constant throughout this morphology and therefore it cannot be used in the analysis. The height to width ratio distinguishes localities ($F_{3,18}$= 8.270, p= 0.0011*). The Pijdura-Sindhi group has a greater mean height to width ratio than the Takli-Butera group (Figure 22c). Localities are differentiable based on the height to width ratio when incorporating the whorl shape (height/width: $F_{3,16}$= 8.091,

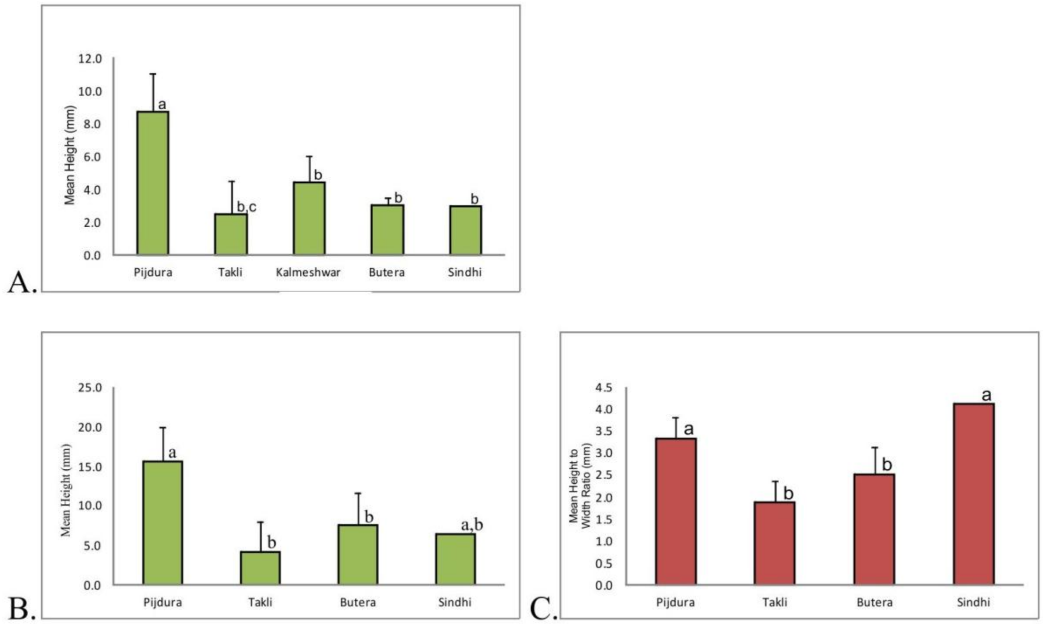

Figure 22. ANOVA results from post-hoc Tukey's test for "lymB" and "lymC." For each gastropod morphotype, members of group "a" are distinct from group "b" and group "c." A. Results from raw data analysis for "lymB." B. Results from raw data analysis for "lymC." C. Results from ratio data analysis for "lymC." Error bars = one standard deviation above mean, α = 0.05.

p= 0.0017*; height/width:whorl shape: $F_{3,1,16}$= 1.065, *p*= 0.3174). There are two resulting locality groups (Figure 22c). The height to width ratio distinguishes localities when incorporating the suture depression (height/width: $F_{3,16}$= 7.692, *p*= 0.0021*). There is no interaction between the height to width ratio and the suture depression indicating equal effects on the differentiation of localities. Localities are divided into two groups (Figure 22c).

Since the outline shape is constant throughout the morphotype, a 2-way analysis of variance using the outline shape and actual measured height was not possible. Localities are differentiable into two groups ($F_{3,18}$= 8.2719, *p*= 0.0011*). The Pijdura-Sindhi group has a greater mean height than the Takli-Butera-Sindhi group (Figure 22b). Localities are distinguishable based on height when incorporating the whorl shape and suture depression (Whorl Shape: $F_{3,16=}$ 9.250, *p*= 0.0009*; Suture Depression: $F_{3,16}$= 8.3260, *p*= 0.0015*). The interaction of height and whorl shape is not significant and there is no interaction between height and suture depression indicating an equal effect on locality distinction (height:whorl shape: $F_{3,1,16}$= 0.9566, *p*= 0.3426). There were two resulting locality groups (Figure 22b).

Overall, localities are differentiable based on "lymC" morphology and size. The Pijdura-Sindhi group has a greater mean height to width ratio than the Takli-Butera group. The Pijdura-Sindhi group had a greater mean height than the Takli-Butera-Sindhi group.

Morphotype "phyA"

"PhyA" was found in all study localities except Sindhi (Table 4). The height to width ratio when including the outline shape differentiated localities into two groups (height/width: $F_{3,24}$= 4.425, *p*= 0.0130*) (Figure 23b). There is no interaction between the outline shape and height to width ratio indicating an equal effect on the analysis. Localities are differentiable based on the height to width ratio when incorporating the whorl shape (height/width: $F_{3,24}$= 3.960, *p*= 0.0200*; height/width:whorl shape: $F_{3,1,24}$= 0.4698, *p*= 0.4997). Using the height to width ratio when including the suture depression differentiates localities into two groups (height/width: $F_{3,21}$= 4.019, *p*= 0.0209*; height/width:suture depression: $F_{3,3,21}$= 1.229, *p*= 0.3242). In all analyses, the Pijdura-Kalmeshwar-Butera group has a greater mean height to width ratio than the Takli-Kalmeshwar group (Figure 23b).

The distribution of the actual height of "phyA" was not normal, so a nonparametric Kruskall-Wallis test was used. Localities were differentiable into three groups (χ^2_3 = 22.71, p=

<0.0001*). The Pijdura group has a noticeably greater mean height than the Kalmeshwar-Butera group, which has a greater mean height than the Takli-Kalmeshwar group (Figure 23a).

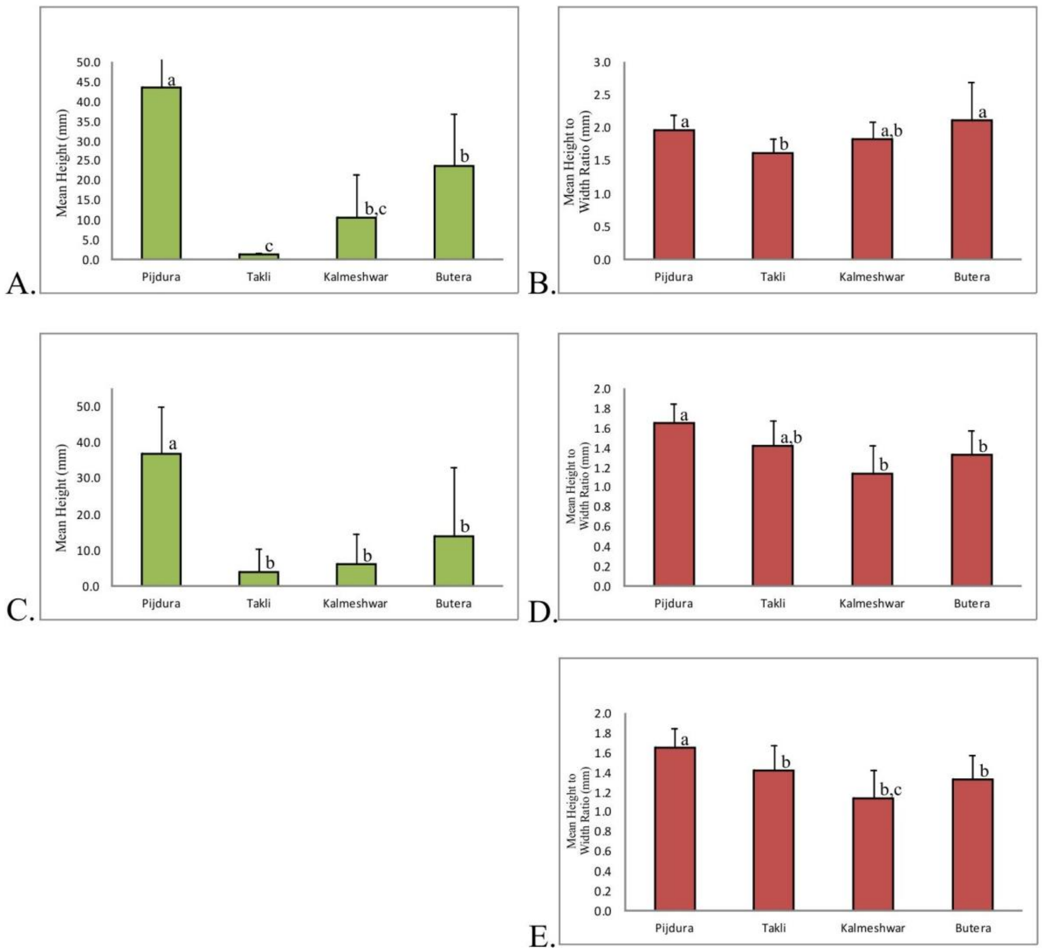

Figure 23. ANOVA results from post-hoc Tukey's test for "phyA" and "phyB." For each gastropod morphotype, members of group "a" are distinct from group "b" and group "c." A. Results from raw data analysis for "phyA." B. Results from ratio data analysis for "phyA." C. Results from raw data analysis for "phyB." D. Results from ratio data analysis for "phyB." E. Results from ratio data analysis incorporating whorl shape for "phyB." Error bars = one standard deviation above mean, α = 0.05.

Generally, using the size corrected values and the actual dimensions of "phyA" differentiate localities. The Pijdura-Kalmeshwar-Butera group has a greater mean height to width ratio than the Takli-Kalmeshwar group. In order by mean height are the Pijdura group, the Kalmeshwar-Butera group, and the Takli-Kalmeshwar group.

Morphotype "phyB"

"PhyB" was common in all study localities except Sindhi (Table 4). Localities are distinguishable based on the height to width ratio and outline shape (height/width: $F_{3,48}$= 10.35, *p*= <0.0001*; height/width:shape: $F_{3,1,48}$= 0.0378, *p*= 0.8466). The Pijdura-Takli group has a greater mean height to width ratio than the Takli-Kalmeshwar-Butera group (Figure 23d). The height to width ratio with whorl shape differentiates localities into three groups (height/width: $F_{3,44}$= 10.79, *p*= <0.0001*; height/width:whorl shape: $F_{3,4,44}$= 1.431, *p*= 0.2398). The Pijdura group has a greater mean height to width ratio than the Takli-Kalmeshwar-Butera group, which has a greater mean height to width ratio than the Kalmeshwar group (Figure 23e). Localities are separated into two groups based on the height to width ratio when including the suture depression(height/width: $F_{3,40}$= 10.18, *p*= <0.0001*; height/width:suture depression: $F_{3,6,40}$= 0.9408, *p*= 0.4769). The resulting locality groups are the same as when including outline shape.

The assumptions were not met when including the actual measured height because of the lack of a normal distribution, so a nonparametric Kruskall-Wallis test was used. Localities were differentiable into two groups (χ^2_3 = 28.24, p= <0.0001*). The Pijdura group has a noticeably greater mean height than the Takli-Kalmeshwar-Butera group (Figure 23c). Specimens from Butera have a broad distribution of shell heights ranging from one mm to almost 50 mm, which gives the locality a lower mean height although some specimens are comparable to those in the Pijdura group.

Overall, both the size corrected values and the actual dimensions of specimens of the "phyB" morphotype differentiate localities. The groups resulting from the height to width ratio and the outline shape or suture depression are the Pijdura-Takli group and the Takli-Kalmeshwar-Butera group, while those from the whorl shape are the Pijdura group, the Takli-Kalmeshwar-Butera group, and the Kalmeshwar group. Groups containing Pijdura have greater mean height to width ratios. The analysis with the actual height resulted in two locality groups. The Pijdura group has a greater mean height than the Takli-Kalmeshwar-Butera group.

Morphotype "styA"

"StyA" was rare and occurred only at Takli and Kalmeshwar (Table 4). Localities were not differentiable based on the height to width ratio when incorporating the outline shape, whorl shape, or suture depression (Outline Shape: $F_{1,7}$= 1.438, *p*= 0.2695; Whorl Shape: $F_{1,7}$= 1.248, *p*= 0.3608; Suture Depression: $F_{1,6}$= 1.143, *p*= 0.3262). There are no interactions between variables indicating that they have an equal effect on distinguishing localities.

Localities were not differentiable based on height with outline shape, whorl shape, or suture depression did not differentiate localities (Outline Shape: $F_{1,7}$= 0.1441, *p*= 0.7155; Whorl Shape: $F_{1,7}$= 0.0724, *p*= 0.7956; Suture Depression: $F_{1,6}$= 0.0651, *p*= 0.8071). There are no interactions between variables indicating an equal effect on distinguishing localities. In general, "styA" remains the same throughout all localities where present and cannot be used to differentiate localities.

Morphotype "styB"

"StyB" was relatively common at all study localities except Pijdura (Table 4). Height to width ratio when including outline shape, whorl shape, or suture depression did not distinguish localities (Outline Shape: $F_{3,37}$= 0.3196, *p*= 0.8111; Whorl Shape: $F_{3,35}$= 0.3209, *p*= 0.8102;

Suture Depression: $F_{3,32}$= 0.3428, *p*= 0.7945). There is no interaction between height and outline shape, indicating the variables have an equal effect, and the interaction between height and the whorl shape and suture depression did not differentiate localities (Height:Whorl shape: $F_{3,2,35}$= 1.440, *p*= 0.2507; Height:Suture depression: $F_{3,3,32}$= 2.181, *p*= 0.1095).

Localities are also not differentiable based on actual height when including outline shape, whorl shape, or suture depression (Outline Shape: $F_{3,37}$= 2.746, *p*= 0.0567; Whorl Shape: $F_{3,35}$= 2.655, *p*= 0.0636; Suture Depression: $F_{3,32}$= 2.480, *p*= 0.0789). There is no interaction between height and outline shape, indicating the variables have an equal effect, and the interaction between height and whorl shape and suture depression did not differentiate localities (Height:whorl shape: $F_{3,2,35}$= 0.2923, *p*= 0.7484; Height:suture depression: $F_{3,3,32}$= 0.0308, *p*= 0.9926). Overall, “styB” remains the same throughout all localities and cannot be used to differentiate the localities.

Morphotype “styC”

“StyC” was rare and found only at Takli, Kalmeshwar, and Butera (Table 4). The distribution of the height to width ratio was not normal, so a nonparametric Kruskall-Wallis test was used. “StyC” cannot differentiate localities based on the height to width ratio (χ^2_2 = 0.0952, *p*= 0.9535).

The assumptions were also not met when incorporating the measured height due to normality, so a nonparametric Kruskall-Wallis test was used. Localities are not differentiable based on height (χ^2_2 = 0.8095, *p*= 0.6671). In general, using the morphologic characters of “styC” cannot distinguish localities.

Morphotype "valA"

"ValA" was rare and found only in Kalmeshwar and Butera (Table 4). The height to width ratio when incorporating outline shape, whorl shape, or suture depression did not differentiate localities (Outline Shape: $F_{1,12}$= 1.133, p= 0.8080; Whorl Shape: $F_{1,13}$= 1.227, p= 0.2881; Suture Depression: $F_{1,12}$= 1.199, p= 0.2950). The interaction between height to width ratio and outline shape, whorl shape, or suture depression also did not differentiate localities (Height:Outline shape: $F_{1,1,12}$= 0.3228, p= 0.5804; Height:Whorl shape: $F_{1,1,13}$= 0.0885, p= 0.7708; Height:Suture depression: $F_{1,1,12}$= 0.4713, p= 0.5054).

Localities were not differentiable based on the measured height when including the outline shape, whorl shape, or suture depression (Outline Shape: $F_{1,12}$= 1.505, p= 0.2435; Whorl Shape: $F_{1,13}$= 1.319, p= 0.2715; Suture Depression: $F_{1,12}$= 1.529, p= 0.2399). The interaction between height and outline shape, whorl shape, or suture depression also did not differentiate localities (Height:Outline shape: $F_{1,1,12}$= 0.5119, p= 0.4880; Height:Whorl shape: $F_{1,1,13}$= 1.929, p= 0.1883; Height:Suture depression: $F_{1,1,12}$= 0.4633, p= 0.5090). Overall, "valA" is consistent through the sequence where it is present and cannot be used to distinguish localities.

Morphotype "valB"

"ValB" was found at Takli, Kalmeshwar, and Butera (Table 4). The height to width ratio only differentiates localities with the interaction with outline shape (height/width: $F_{2,45}$= 0.7124, p= 0.4959; height/width:shape: $F_{2,1,45}$= 4.225, p= 0.0457*). The height to width ratio with whorl shape and suture depression do not differentiate localities (height/width: $F_{2,43}$= 0.6046, p= 0.5509; height/width:whorl shape: $F_{2,2,43}$= 0.1273, p= 0.8808; height/width: $F_{2,42}$= 0.6072, p= 0.5496; height/width:suture depression: $F_{2,2,42}$= 0.6984, p= 0.5031).

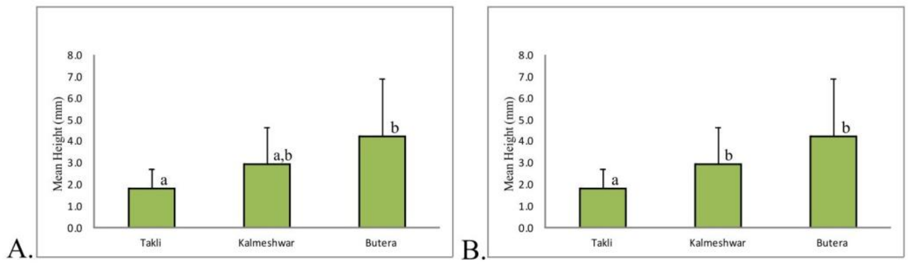

Figure 24. ANOVA results from post-hoc Tukey's test for "valB." For each gastropod morphotype, members of group "a" are distinct from group "b." A. Results from raw data analysis. B. Results from raw data analysis incorporating the suture depression. Error bars = one standard deviation above mean, $\alpha = 0.05$.

Localities are distinguishable based on the measured height with outline shape (height: $F_{2,45}= 4.486$, *p*= 0.0167*; height:shape: $F_{2,1,45}= 5.621$, *p*= 0.0221*). The Takli-Kalmeshwar group has a lower mean height than the Kalmeshwar-Butera group (Figure 24a). The height with whorl shape differentiates localities into the same groups as with outline shape (height: $F_{2,43}= 5.248$, *p*= 0.0091*; height:whorl shape: $F_{2,2,43}= 0.8041$, *p*= 0.4541). The height with suture depression also differentiates localities (height: $F_{2,42}= 8.734$, *p*= 0.0007*; height:suture depression: $F_{2,2,42}= 10.59$, *p*= 0.0002*). Here, the Takli group has a lower mean height than the Kalmeshwar-Butera group (Figure 24b).

Morphotype "vivA"

"VivA" was found at Takli, Kalmeshwar, and Butera (Table 4). Localities are differentiable based on the height to width ratio with outline shape (height/width: $F_{2,24}= 10.60$, *p*= 0.0005*; height/width:shape: $F_{2,2,24}= 0.2434$, *p*= 0.7858). Localities are differentiable based on the height to width ratio and whorl shape and suture depression (Whorl Shape: height/width: $F_{2,24}= 6.961$, *p*= 0.0041*; interaction: $F_{2,2,24}= 0.8721$, *p*= 0.4309; Suture Depression: $F_{2,22}= 7.141$,

p= 0.0041*; interaction: $F_{2,2,22}$= 1.258, p= 0.3038). In all analyses, the Takli-Kalmeshwar group has a greater mean height to width ratio than the Takli-Butera group (Figure 25b).

Localities are distinguishable based on the interaction of height and outline shape (height: $F_{2,24}$= 2.713, p= 0.0867; height:shape: $F_{2,2,24}$= 4.267, p= 0.0260*). The Takli-Kalmeshwar group has a lower mean height than the Kalmeshwar-Butera group (Figure 25a). Height with whorl shape and suture depression do not differentiate localities (Whorl Shape: $F_{2,24}$= 2.066, p=0.1487; interaction: $F_{2,2,24}$= 0.0467, p= 0.9544; Suture Depression: $F_{2,22}$= 3.064, p= 0.0670; interaction: $F_{2,2,22}$= 0.3884, p= 0.6827).

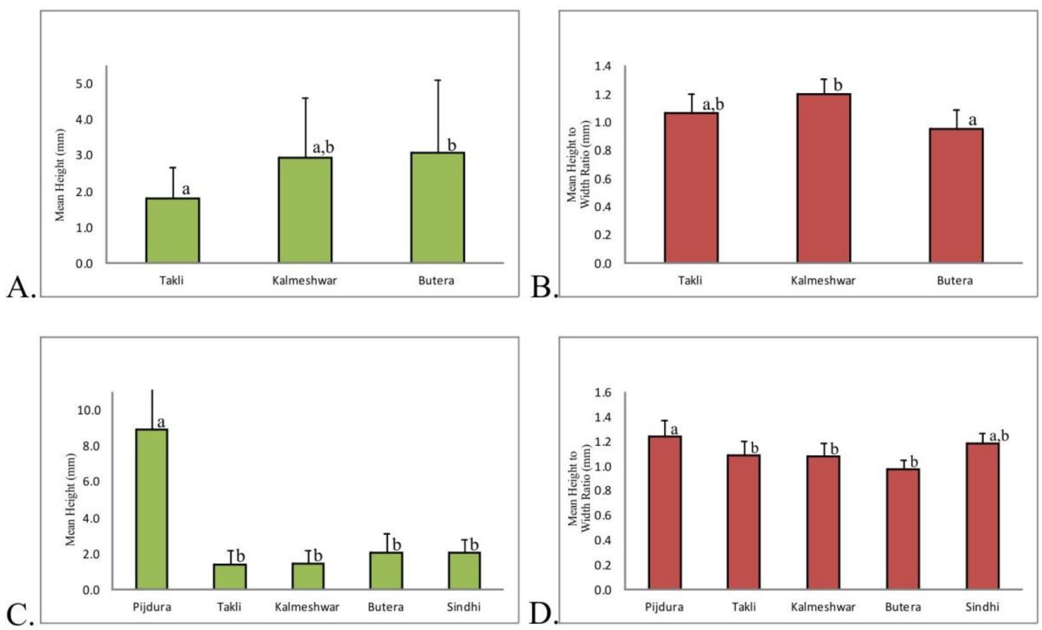

Figure 25. ANOVA results from post-hoc Tukey's test for "vivA" and "vivB." For each gastropod morphotype, members of group "a" are distinct from group "b." A. Results from raw data analysis for "vivA." B. Results from ratio data analysis for "vivA." C. Results from raw data analysis for "vivB." D. Results from ratio data analysis for "vivB." Error bars = one standard deviation above mean, α = 0.05.

In general, localities are differentiable when using the height to width ratio and measured height. The Takli-Kalmeshwar group has a greater mean height to width ratio than the Takli-Butera group. The Takli-Kalmeshwar group has a lower mean height than the Kalmeshwar-Butera group.

Morphotype "vivB"

"VivB" was common throughout the sequence at all study sites (Table 4). Localities are distinguishable based on the height to width ratio with outline shape, whorl shape, and suture depression (Outline Shape: $F_{4,62}$= 10.22, *p*= <0.0001*; Whorl Shape: $F_{4,62}$= 9.910, *p*= <0.0001*; Suture Depression: $F_{4,57}$= 10.80, *p*= <0.0001*). There are no interactions between the height to width ratio and the outline shape and whorl shape indicating the equal effects of the variables on the analyses; however, there is an interaction between the ratio and suture depression but it is not significant ($F_{4,2,57}$= 0.5304, *p*= 0.7138). The resulting groups for all analyses are the Pijdura-Sindhi, which has a greater mean height to width ratio than the Takli-Kalmeshwar-Butera-Sindhi group (Figure 25d).

The distribution of the actual height is not normal, so a nonparametric Kruskall-Wallis test was used. Localities are differentiated into two groups based on height (χ^2_4 = 47.90, *p*= <0.0001*). The Pijdura group has a noticeably greater mean height than the Takli-Kalmeshwar-Butera-Sindhi group (Figure 25c).

Overall, localities are distinguishable when using ratios and the actual specimen dimensions. The Pijdura-Sindhi group has a greater height to width ration than the Takli-Kalmeshwar-Butera-Sindhi. The Pijdura group has a greater mean height than the Takli-Kalmeshwar-Butera-Sindhi group. Specimens from Sindhi are slightly narrower giving them a greater height to width ratio comparable to specimens from Pijdura, but Sindhi specimens are still significantly smaller than Pijdura specimens so that they are not comparable when using the actual height measurements.

χ^2 Analysis for Locality Distinction

Changes in the diversity, or number of species, and abundance, or number of specimens, through the locality sequence illustrate potential effects of the Deccan trap eruptions on the molluscan population. χ^2 analyses measured differences between localities based on the number of species, total number of specimens measured for the study, and total number of specimens cataloged for each locality.

Localities are not distinguishable based on species diversity ($\chi^2_4 = 5.445$) (Table 5). The results were significant based on the total number of study specimens photographed and measured ($\chi^2_4 = 183.9$) (Table 5). Sindhi has noticeably fewer specimens; however, this is likely due to the small amount of material processed and the difficulty in preparing fossils from chert. Pijdura and Butera have fewer specimens than average while Takli and Kalmeshwar have more. Sindhi was removed to avoid skewing the results based on the amount of material processed and the test was conducted again. Localities were still distinct when removing Sindhi ($\chi^2_3 = 61.56$). Localities were distinct based on the total number of species identified to morphotype but not necessarily measured ($\chi^2_4 = 486.3$) (Table 5). Again, Sindhi has noticeably fewer specimens, which is likely due to the amount of material. Sindhi was removed and the analysis was conducted a second time. Localities were still distinguishable without Sindhi ($\chi^2_3 = 148.5$). Pijdura and Kalmeshwar have fewer specimens than average while Takli and Butera have more.

Table 5. Number of species and specimens for each locality.

	Species	Specimens Measured	Specimens Identified
Pijdura	9	110	201
Takli	14	192	508
Kalmeshwar	14	225	306
Butera	14	114	415
Sindhi	8	25	30
Totals		666	1460

CHAPTER VI

DISCUSSION

Systematics

Cluster analysis is highly effective in identifying grouping patterns in paleontologic specimens that may coincide with taxonomic categories. Grouping patterns not only show distinct morphotypes but how these morphotypes are related to each other, which may identify higher taxonomic categories. Once potential taxonomic clusters are identified, knowledge of the group's taxonomy, geologic history, and biogeography is applied to flesh out more accurate systematics. In cluster analysis, the correlation coefficient (R) determines the goodness of fit of the resulting dendrogram or the degree of similarity of the data points. The correlation coefficient is given as a number between zero and one where one equals perfect correlation. Values between 0.9 and one are considered very strongly correlated, values between 0.7 and 0.9 are strongly correlated, values between 0.5 and 0.7 are moderately correlated, and values less than 0.5 have poor to no correlation (Calkins, 2005). The calculated correlation coefficients for analyses incorporating all specimens range from 0.70 to 0.71, so the resulting clusters interpreted as morphotypes are considered strong.

According to the cluster analysis for taxonomic placement, "hydA" is distinct but is related to "hydB," "hydC," and "hydD" (Figure 26). It is distinguishable by an angular body whorl and a more triangular outline shape. "HydA" is also related to *Viviparus virapai* Hislop, 1860. Although it is not found with modern representatives, the closely related clusters contain *Incertihydrobia teesdalei* Verdcourt, 1958 and *Littoridina australis* Marcus & Marcus, 1965 (Hydrobiidae), *Elimia livescens* Menke, 1830 (Pleuroceridae), *Micromelania grimani* Brusina, 1874 (Micromelaniinae), and *Blanfordia simplex* Pilsbry, 1902 (Pomatiopsidae).

Pleurocerids have a similar morphology to "hydA," and although originally the family included members from Asia, they are now considered restricted to North America. Micromelaniinae is a freshwater family very similar in shell morphology to the hydrobiids and are now included in Hydrobiidae (Bouchet and Rocroi, 2005). Micromelanids are found in many areas of the world including eastern India. Pomatiopsids are very similar in morphology to hydrobiids and were previously included as a Hydrobiidae subfamily (Davis, 1967). The pomatiopsids have a worldwide distribution with one modern species in northern India. Pomatiopsids evolved in Gondwana and migrated north through India, while hydrobiids evolved in Laurasia and migrated south (Davis, 1979). Most hydrobiids occur in Europe, North America, and Turkey (Davis, 1979). There are possible pomatiopsid fossils, which resemble the modern subfamily Triculinae, from the Cretaceous of India and South Africa (Davis, 1979). Although Davis did not discuss the Indian fossils in detail, he referenced Hislop (1860) and Malcolmson (1836) so he was likely referring to the Deccan trap fauna. Hydrobiids, pomatiopsids, and micromelanids are typically small and higher spired (2-8 whorls) with an ovate aperture. Hydrobiids are completely aquatic while pomatiopsids are aquatic, semi aquatic, or terrestrial.

Since pleurocerids are restricted to North America, Deccan Trap gastropod morphologies do not likely belong to this taxon. Micromelaniinae is currently included in the Hydrobiidae and are not considered a separate family. Shell morphology is very similar between hydrobiids and pomatiopsids and distinction is often based on habit, so it is difficult to identify with certainty which family applies to "hydA," "hydB," and "hydC." Since pomatiopsids evolved in Gondwana before migrating north (Davis, 1979), it is likely that the Cretaceous Deccan trap species are in Pomatiopsidae rather than the Laurasian Hydrobiidae. "HydA" is closely related to *Viviparus* *virapai*, so they are considered the equivalent. The revised genus *Tricula* is applied to this species based on general morphologic similarity combined with the modern occurrence of the genus in India (Davis and Rao, 1997) and the fossil record of potential Triculinae from the Cretaceous (Davis, 1979).

Superfamily Rissooidea (Rissoacea) Adams and Adams, 1854

Family Pomatiopsidae Stimpson, 1865

Subfamily Triculinae Annandale, 1924

Genus *Tricula* Benson, 1843

Description: "Shell elongated ovate cone-shaped, not umbilicate; apex somewhat blunt; whorls moderately bulging, the last somewhat stretched downward; aperture oval, angular above, produced below: apertural margin blunt, continuous, in most cases somewhat broadened; operculum thin, with nearly marginal nucleus and rapidly increasing growth. Central plate of the radula trapezoidal, posteriorly with 2 (or 3) teeth, cutting edge with fairly large. triangular median cusp and 1 or 2 lateral cusps; intermediate plate with fairly short lateral process, cutting edge with large main cusp and few inner and outer lateral cusps; cutting edges of the lateral plates distinctly denticulate. *T. montana* Benson. Few species in India and South China (Thiele, 1992)."

Tricula virapai (Hislop), new genus assignment

Paludina virapai Hislop, 1860

Description: "Shell turreted; apex acute, commonly truncate; eight, perhaps nearly 10, planar whorls; suture moderately impressed; aperture ovate, peristome interrupted; labial margin reflexed. Length 1.1?, width 0.5 inch [27.9? mm, 12.7 mm] (Hislop, 1860; translated in Hartman et al., 2008)."

Distribution: Uncommon across Deccan Plateau infra- and intertrappean beds at Pijdura, Takli, Kalmeshwar, Butera, and Sindhi.

Holotype: GS 10271a; Plate V, fig. 12a (Hislop, 1860); Type locality: Takli.

Repository: Natural History Museum, London, England.

"HydB" clusters with *Incertihydrobia teesdalei* Verdcourt, 1958 (Hydrobiidae) and *Elimia livescens* Menke, 1830 (Pleuroceridae) and *Viviparus conoidea* Hislop, 1860 and *V. takliensis* Hislop, 1860. "HydB" is also closely related to "hydA," "hydC," and "hydD" (Figure 26). The taxonomic relationships discussed for "hydA" apply to "hydB" due to a close relationship between these morphologies.

"HydB" can also be separated into two distinctive morphologies that are distinguishable by whorl shape and shell width. "HydB1" has rounder whorls and a slightly wider body whorl than "hydB2" with flatter whorls and a narrower body whorl. These two morphs correspond to *Viviparus conoidea* Hislop, 1860 and *V. takliensis* Hislop, 1860, respectively. "HydB1" is more common than "hydB2." On the basis of clustering patterns and shell morphology, "hydB1" and "hydB2" are considered subspecies. Due to predominance of "hydB1," the two morphologies will be considered subspecies of the revised *Tricula conoidea* Hislop, 1860. The two subspecies proposed here are *Tricula conoidea conoidea* and *Tricula conoidea hislopi* to honor the extensive work done by Hislop.

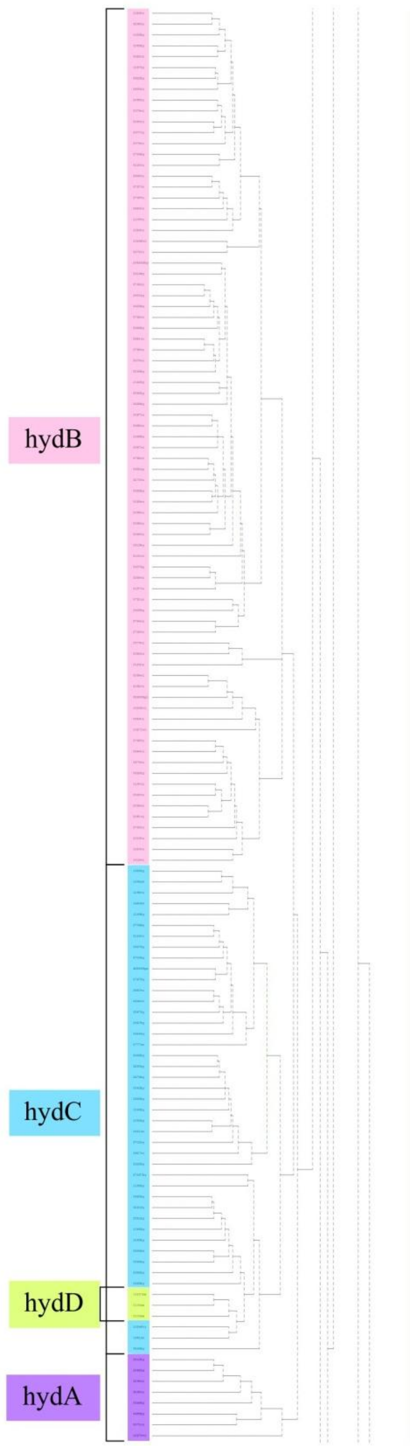

Figure 26. Portion of complete dendrogram with all specimens (including types and modern) containing the "hyd" morphologies (R = 0.71).

Genus *Tricula* Benson, 1843

Tricula conoidea conoidea (Hislop), original morphotype

Paludina conoidea Hislop, 1860

Diagnosis: Morphology differs from *T. conoidea hislopi* in having rounded whorls and a wider body whorl. More common subspecies of *T. conoidea*.

Description: Shell is small, ovate. Whorls rounded with strongly depressed sutures. Aperture small, ovate. Shell has 5-7 whorls. A single revolving keel has been documented on specimens with original shell material preserved. Shell smooth. Spire angle is roughly 50-60 degrees. Sutures are at around 14 degrees. Aperture is about 65 degrees to the axis of coiling.

Holotype: InS0187 (appendix 2, figure B; 9.9 mm x 6.0 mm); Type locality: Pijdura (InL009).

Distribution: Common across Deccan Plateau infra- and intertrappean beds at Pijdura, Takli, Kalmeshwar, Butera, Sindhi.

Repository: University of North Dakota, Grand Forks, North Dakota.

Tricula conoidea hislopi n. subsp.

Diagnosis: Morphology differs from *T. conoidea conoidea* in having flattened whorls and a narrower body whorl.

Description: Shell is small, ovate. Whorls flattened with regularly depressed sutures. Aperture small, ovate. Shell has 3-5 whorls. Shell smooth. Spire angle is roughly 50-60 degrees. Sutures are at around 15-16 degrees. Aperture is about 60 degrees to the axis of coiling.

Distribution: Relatively common across Deccan Plateau infra- and intertrappean beds at Pijdura, Takli, Kalmeshwar, and Butera.

Holotype: InS0730, (Appendix 2, Figure C; 4.0 mm x 2.8 mm); Type locality: Takli (InL004b-3).
Repository: University of North Dakota, Grand Forks, North Dakota.
Remarks: Named in honor of Stephen Hislop.

"HydC" clusters with *Littoridina australis* Marcus & Marcus, 1965 (Hydrobiidae), *Micromelania grimani* Brusina, 1874 (Micromelaniinae), and *Blanfordia simplex* Pilsbry, 1902 (Pomatiopsidae) and *Viviparus sankeyi* Hislop, 1860. Although related to "hydA," "hydB," and "hydD," it is distinguishable by a more elongate outline shape (Figure 26). "HydD" is found within the "hydC" cluster, but "hydD" shell morphology is considered distinctive. The two morphologies are grouped together likely due to the rarity of "hydD" specimens and the overall elongate shell shape of both morphotypes. Taxonomic relationships discussed for "hydA" correspond to "hydC." "HydC" is considered equivalent to *Viviparus sankeyi* and revised to Pomatiopsidae.

Genus *Tricula* Benson, 1843

Tricula sankeyi (Hislop), new genus assignment

Paludina sankeyi Hislop, 1860

> Description: "Shell subfusiform, single-banded; nine very or slightly convex whorls; suture impressed; aperture ovate, angular above. Length 0.4, width 0.17 inch [10.2 mm, 4.32 mm] (Hislop, 1860; translated in Hartman et al., 2008)."

Distribution: Common across Deccan Plateau infra- and intertrappean beds at Pijdura, Takli, Kalmeshwar, Butera, Sindhi, and Telankhedi.

Holotype: GS 10246; Plate V, fig. 7 (Hislop, 1860); Type locality: Telankhedi.

Repository: Natural History Museum, London, England.

"HydD" is found within the "hydC" cluster but is considered distinct on the basis of a wider body whorl and more circular aperture shape (Figure 26). The group contains *Thiara hunteri* Hislop, 1860. *Thiara quadrilineata* Sowerby, 1840 was not included due to the poor preservation of the type specimen providing limited opportunity for character measurement. These species were originally placed in the genus "*Melania*" Lamarck, 1799 in the family "Melaniidae," which is now considered a junior synonym of *Thiara* Röding, 1798. The familial placement of the two Deccan Trap species is revised to Thiaridae. Thiarids are found worldwide in temperate to tropical environments, but are most common in subtropical to tropical areas.

"HydD" is considered a member of Thiaridae because of a turreted outline shape and almost circular aperture shape. Although the specimens included in the analysis do not have sculpture, the type specimen of *Thiara quadrilineata* Sowerby, 1840 has the revolving sculpture that is common within thiarids. *Thiara hunteri* Hislop, 1860 and *T. quadrilineata* Sowerby, 1840 are considered one species because the only apparent difference between these species is shell sculpture. The type specimen of *Thiara quadrilineata* Sowerby, 1840 is an impression while the *T. hunteri* Hislop, 1860 type specimen is a steinkern. Sculpture is not preserved on a steinkern so it is likely that these are actually one sculptured species. Since the species has sculpture, it is considered equivalent to *Thiara quadrilineata* Hislop, 1860.

Superfamily Cerithioidea Fleming, 1822

Family Thiaridae Gill, 1871

Genus *Thiara* Röding, 1798

Description: “Mantle edge papillate; males generally absent (parthenogenetic reproduction common, often the rule); females brood their young in an adventitious ("subhaemocoelic"; not uterine) brood pouch in the postero-dorsal head-foot region (Burch, 1989).”

Thiara quadrilineata (Sowerby), new genus assignment

Melania quadrilineata Sowerby, 1840

Description: “Subulate, whorls about eight, with four striae upon each; aperture nearly round (Hislop, 1860; translated in Hartman et al., 2008).”

Distribution: Rare across Deccan Plateau infra- and intertrappean beds at Pijdura, Sindhi, Chikni, Karwad, Pahadsingha, and Karuni.

Holotype: GS 10421; Plate 47, fig. 18 (Sowerby, 1840); Type locality: Chikni.

Repository: Natural History Museum, London, England.

“LymA” clusters with the modern *Galba truncatula* Müller, 1774 (Lymnaeidae) and *Lymnaea oviformis* Hislop, 1860. It does not cluster with the remainder of the Deccan lymnaeids and forms two separate clusters (Figure 27). Despite the clustering configuration, there is no noticeable difference between “lymA” in the two clusters. The morphology is distinguishable by a wider body whorl and typical lymnaeid large aperture. Lymnaeids are found worldwide but are in greatest diversity in temperate regions of North America (Burch, 1989). Genetically the family has three evolutionary clades separated geographically into the American, Eurasian, and Indo-Pacific groups (including Indian forms) (Correa et al., 2010). The shells are typically narrow with large apertures that are often wide. “LymA” is considered a member of Lymnaeidae based on its relationship in the dendrogram, the existence of lymnaeids in modern India, and shell morphology (specifically the large, wide aperture).

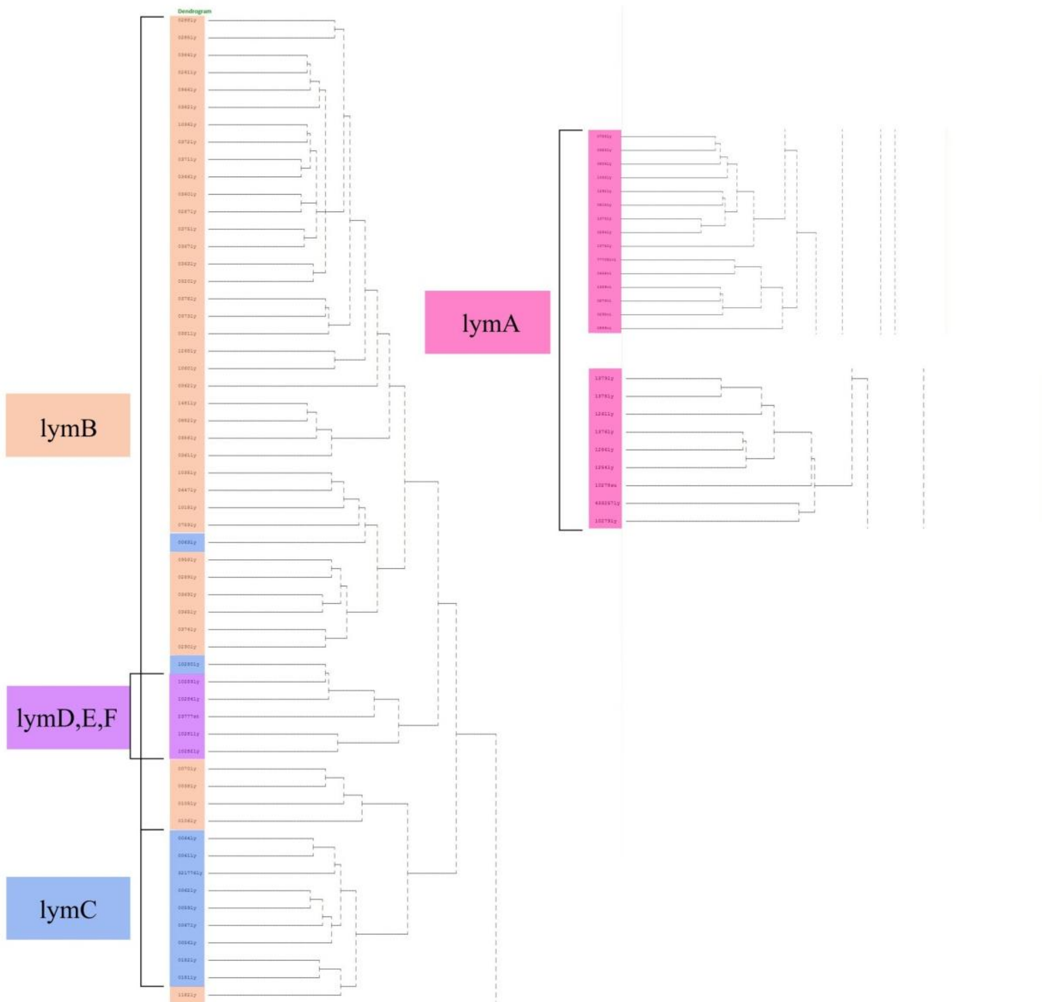

Figure 27. Portion of the complete dendrogram with all specimens (including types and modern) containing the “lym” morphologies (R = 0.71).

“LymA” is considered equivalent to *Lymnaea oviformis* Hislop, 1860 and will retain Hislop’s (1860) diagnosis.

Superfamily Lymnaeoidea Rafinesque, 1815

Family Lymnaeidae Rafinesque, 1815

Genus *Lymnaea* Lamarck, 1799

> Description: “Shell not covered by the mantle; spire nearly always elevated; columella twisted; aperture variably wide. The receptaculum seminis, which arises close to the female genital opening, has a duct which is sometimes short, sometimes fairly long; the prostate is variable in length (Thiele, 1992).”

Lymnaea oviformis Hislop, 1860

“LymB” does not cluster with modern representatives or Deccan trap species, but it is closely related to “lymC” and the modern *Ferussacia vescoi* Bourguignat, 1864 (Stylommatophora: Ferussaciidae) and *Stagnicola elodes* Say, 1821 (Lymnaeidae) and *Lymnaea subulata*, *L. attenuata* Hislop, 1860, *L. telankhediensis peracuminata* Hislop, 1860, *L. telankhediensis radiolus* Hislop, 1860, and *L. spina* Hislop, 1860 (Figure 27). Although the terrestrial species *Ferussacia vescoi* Bourguignat, 1864 clusters with “lymC,” neither “lymB” nor “lymC” are considered terrestrial. “LymB” has a typical lymnaeid shape with the narrow shell and a large aperture and is placed within this family. The proposed name for this new species is *Lymnaea pokhariensis* from the Hindi word for pond.

Lymnaea pokhariensis n. sp.

Diagnosis: Intermediate morphology between *L. oviformis* and *L. subulata*. Body whorl is narrower than *L. oviformis* and wider than *L. subulata*. Whorls are more strongly depressed than other species of *Lymnaea* of the Deccan Traps.

Description: Shell small to medium, elongate conic. Whorls subrounded with strongly depressed sutures. Aperture large, narrow, loop-shaped. Shell has 3-4 whorls. Shell smooth. Spire angle narrow at 30-40 degrees. Sutures are at roughly 20-21 degrees. Aperture is about 67 degrees to the axis of coiling.

Distribution: Common across Deccan Plateau infra- and intertrappean beds at Pijdura, Takli, Kalmeshwar, Butera, and Sindhi.

Holotype: InS0261 (Appendix, Figure K; 2.6 mm x 1.1 mm); Type locality: Takli (InL004b-3).

Repository: University of North Dakota, Grand Forks, North Dakota.
Remarks: Species name derived from the Hindi word for pond. Closely related to *L. subulata* Sowerby, 1840.

"LymC" is related to the modern species *Ferussacia vescoi* Bourguignat, 1864 (Stylommatophora: Ferussaciidae) and *Stagnicola elodes* Say, 1821 (Lymnaeidae) and *Lymnaea subulata* Sowerby, 1840, *L. attenuata* Hislop, 1860, *L. telankhediensis peracuminata* Hislop, 1860, *L. telankhediensis radiolus* Hislop, 1860, and *L. spina* Hislop, 1860. "LymC" is closely related to "lymB" so the familial relationships discussed previously apply to "lymC" (Figure 27). "LymB" and "lymC" are distinguishable by the width of the body whorl. "LymB" has a wider and rounder body whorl than "lymC," which is more needlelike in shape. Both morphologies have narrower body whorls than "lymA." "LymC" is considered equivalent to *Lymnaea subulata* Sowerby, 1840 based on an elongate outline shape and whorl morphology.

Lymnaea subulata Sowerby, 1840

There are at least three other recognizable morphotypes within the "lymC" cluster, which are not found in the study sample. "LymD" is considered equivalent to *Lymnaea attenuata* Hislop, 1860, "lymE" is considered equivalent to both subspecies of *L. telankhediensis* Hislop, 1860, and "lymF" is considered equivalent to *L. spina* Hislop, 1860 (Figure 27). All are regarded as discrete species and at least *L. attenuata* Hislop, 1860 and *L. telankhediensis* Hislop, 1860 appear belong to Lymnaeidae. Both of these species and the two subspecies of *L. telankhediensis* Hislop, 1860 will retain their Hislop (1860) names. *L. spina* Hislop, 1860 is still elongate like lymnaeids, but does not have the characteristic large body whorl and large aperture. It is possible that *L. spina* Hislop, 1860 may belong to Stylommatophora but more work is needed before any conclusions are drawn.

Lymnaea attenuata Hislop, 1860

Lymnaea telankhediensis radiolus Hislop, 1860

Lymnaea telankhediensis peracuminata Hislop, 1860

Lymnaea? spina Hislop, 1860 *sedis mutabilis*

"PhyA" clusters with the modern *Aplexa niteus* Say, 1821 (Physidae) and *Physa prinsepii elongata* Hislop, 1860 (Figure 28). It is also closely related to the "phyB." Shell morphology is distinguished by a slender, more elongate outline shape. Fischer (1883) argued that the genus be revised to *Platyphysa* based on a relationship to *Bulinus* and the physids but with a discrete evolutionary history. Annandale (1920) suggested that the physid-types from the Deccan traps were actually members of *Bulinus* and not a new genus. The predominance of *Bulinus* in the southern hemisphere in tropical environments suggested the placement of the Deccan trap species

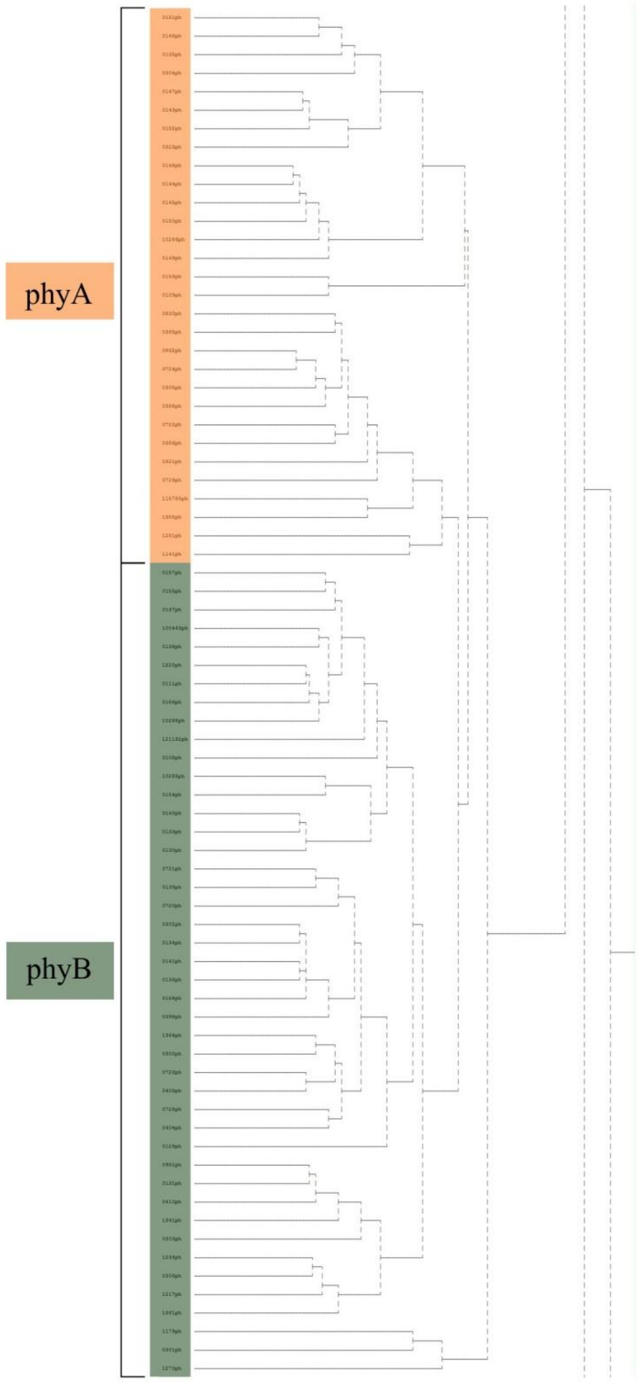

Figure 28. Portion of the complete dendrogram with all specimens (including types and modern) containing the “phy” morphologies (R = 0.71).

into that genus (Annandale, 1920). Annandale (1920) also argued that *Physa prinsepii inflata* Hislop, 1860 was simply a common variation of *Physa prinsepii normalis* Hislop, 1860. The current study supports the distinction of only two physid species. “PhyA” is considered to be equivalent to *Physa prinsepii elongata* Hislop, 1860. The revised *Platyphysa* proposed by Fischer (1883) is applied due to the unique morphology of the Deccan trap species suggesting an isolated evolution.

Superfamily Planorboidea Rafinesque, 1815

Family Planorbidae Rafinesque, 1815

Genus *Platyphysa* Fischer, 1883

> Description: “Shell like *Physa*, but columella truncate below. Last whorl enlarged at the shoulder; columella truncate below (Tyron, 1884).”

Platyphysa prinsepii elongata Hislop, 1860

> Description: “Shell subturreted-elongate; spire extended; apex rather acute; 7–8 convex whorls separated by a distinct suture, the last whorl nearly equal to half of the length; aperture ovate-oblong, angular above; columella incrassate. Length 2.67, width 1.2 inch [67.82 mm, 30.48 mm] (Hislop, 1860; translated in Hartman et al., 2008).”

Distribution: Very common across Deccan Plateau infra- and intertrappean beds at Pijdura, Takli, Kalmeshwar, Butera, Chikni, Telankhedi, Chichundra, Pangadi and Kateru.

Holotype: GS 10286; Plate V, fig. 23b (Hislop, 1860); Type locality: Butera.

Repository: Natural History Museum, London, England.

"PhyB" clusters with the modern species *Physella gyrina* Say, 1821 and *Physella parkeri* Currier, 1881 (Physidae) and *Physa prinsepii normalis* Hislop, 1860 and P*hysa prinsepii inflata* Hislop, 1860 (Figure 28). It is also closely related to "phyA." The aforementioned taxonomic relationships and assumptions of "phyA" apply to "phyB." The cluster analysis, and Annandale (1920), does not support *Physa prinsepii normalis* Hislop, 1860 and *Physa prinsepii inflata* Hislop, 1860 as two separate subspecies. One subspecies under the revised name *Platyphysa prinsepii normalis* Hislop, 1860 is proposed here.

Platyphysa prinsepii normalis Hislop, 1860

> Description: "Shell huge, ovate, elegantly striated; spire moderately long; 7–8 convex whorls separated by an impressed suture, the last whorl fully two times greater in length than the spire; aperture ovate-oblong, angular above; columella incrassate. Length 2.75, width 1.56 inch [69.85 mm, 39.62 mm] (Hislop, 1860; translated in Hartman et al., 2008)."

Distribution: Very common across Deccan Plateau infra- and intertrappean beds at Pijdura, Takli, Kalmeshwar, Butera, Chikni, Telankhedi, Chichundra, Pangadi and Kateru.

Holotype: GS 10285; Plate V, fig. 23a (Hislop, 1860); Type locality: Chikni.

Repository: Natural History Museum, London, England.

The cluster considered to be the terrestrial stylommatophorans is complicated. All specimens were in one major cluster with no distinct minor clusters; however, there are two to three noticeable morphotypes present (Figure 29). These morphotypes cluster with the modern species *Micromelania caspia* Eichwald, 1829 (Micromelaniinae), *Diala dubia* Sowerby, 1892 (Dialidae), and *Subulina normalis* Morelet, 1885 (Subulinidae) and *Viviparus acicularis*

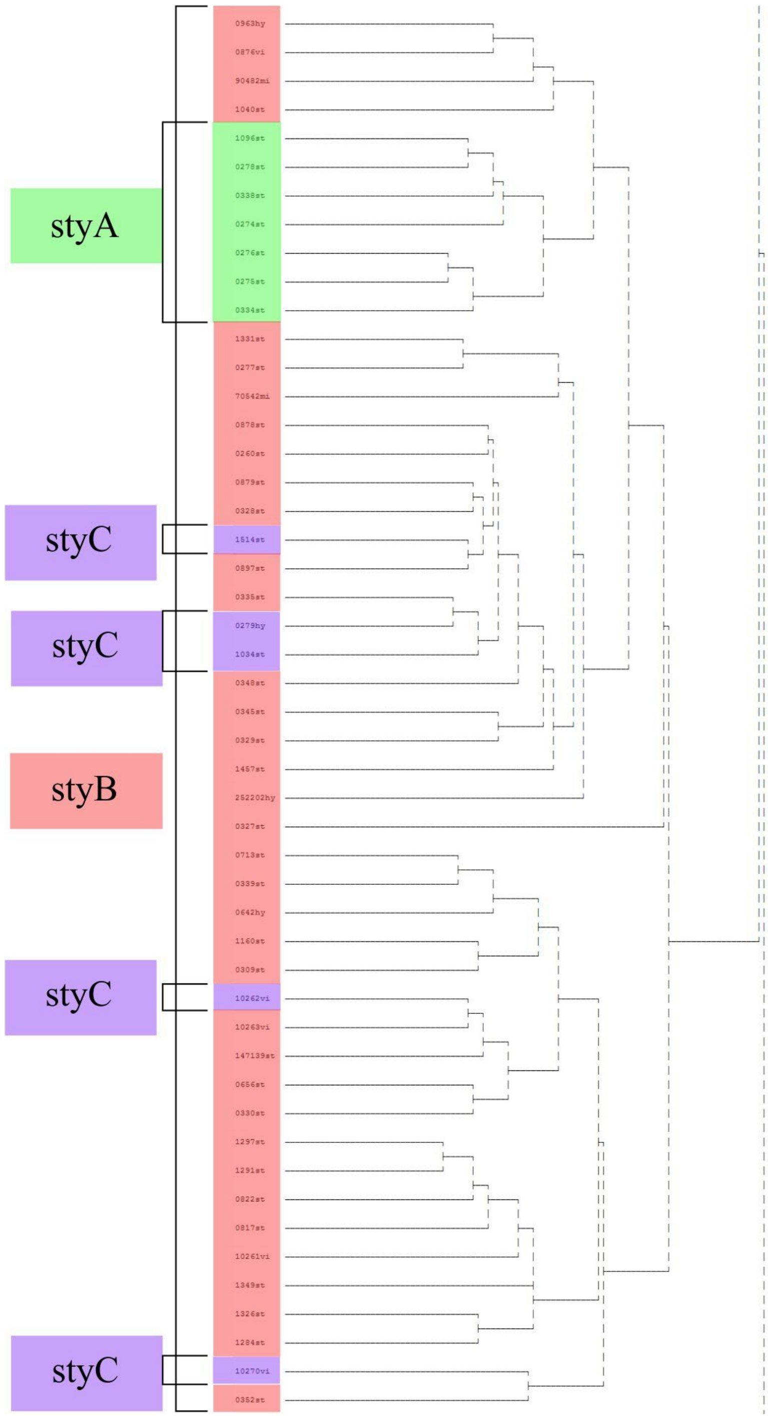

Figure 29. Portion of the complete dendrogram with all specimens (including types and modern) containing the “sty” morphologies (R = 0.71).

Hislop, 1860, *V. subcylindracea* Hislop, 1860, *V. pyramis* Hislop, 1860, and *V. rawesi* Hislop, 1860.

"StyA" forms a small cluster and is distinctive with an elongate pupiform outline shape. This morphology superficially resembles the modern *Diala dubia* Sowerby, 1892. It was mislabeled as a hydrobiid but is actually a member of the marine family Dialidae, so it is highly unlikely that "styA" is in Dialidae. Hydrobiids (micromelanids) are often high-spired like "styA," "styB," and "styC," but they have a different aperture shape. Hydrobiids have an ovate aperture shape while the terrestrials, more specifically the subulinids, have a more trapezoidal shaped aperture. Stylommatophorans are also commonly narrower with a greater number of whorls than the hydrobiids. Subulinids are terrestrial species that live in tropical environments and typically have a narrowly conical and tapering outline shape (Kerney and Cameron, 1979). The subulinds originated on Gondwana and dispersed after the breakup of the supercontinent in the Mesozoic (Wade et al., 2001). Modern subulinds are found worldwide but are common throughout India, Africa, and Asia. Subulinid species that are very similar in shell morphology to the Deccan trap species are the most common gastropod component of the Pliocene Laetoli locality in eastern Africa (Harrison, 2011) (Figure 30).

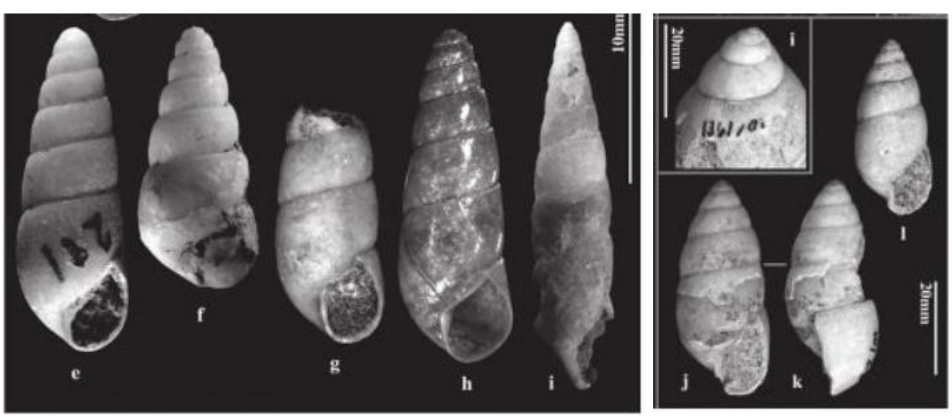

Figure 30. Species of subulinidae from the African Laetoli locality (Harrison, 2011).

On the basis of aperture shape, high-spired shell, and abundance of subulinids in gastropod assemblages of Gondwana suggest that "styA," "styB," and "styC" are members of Subulinidae. The first recorded members of this family are from the early Paleocene (Wenz and Zilch, 1959-1960), but the probable divergence of the clade containing subulinids coinciding with the breakup of Gondwana (Wade et al., 2001) allows for the possibility of the existence of subulinids in the Cretaceous.

The morphology of "styA" is comparable to the modern subulinid genus *Zootecus* Westerlund, 1887 (Figure 31). There are modern species of *Zootecus* in India as well as Africa and Asia, but the earliest recorded species of *Zootecus* is from the Miocene of Abu Dhabi (Mordan, 1999). Although the fossil record of *Zootecus* only extends to the Miocene, there is a possibility of its existence in the Cretaceous due to the divergence of the family with the separation of Gondwana. Therefore, the species will be placed in *Zootecus* due to the strong morphologic comparison. The species name proposed is *burji* based on the Hindi word for turret.

Figure 31. The modern species *Zootecus insularis* Ehrenberg, 1831.

Superfamily Achatinoidea Swainson, 1840

Family Subulinidae Fischer & Crosse, 1877

Genus *Zootecus* Westerlund, 1887

Description: "Shell very narrowly umbilicate, in most cases translucent, cylindrical with cone-shaped apex, with fine wrinkled striae, somewhat shiny; aperture small, oval; columellar margin callously thickened; apertural margin blunt. Lateral plates of the radula as in *Xerocerastus*; marginal plates tricuspid. Live-bearing (Thiele, 1992)."

Zootecus burji n. sp.

Diagnosis: Distinguished from other Deccan Trap stylommatophorans by its pupiform shape and flattened whorls on the lower spire whorls and body whorl.

Description: Shell small, pupiform. Apical whorls rounded with remainder of the whorls flattened to subrounded. Sutures with some to regular depression. Aperture small and trapezoidal shaped. Shell has 5-6 whorls. Shell smooth. Spire angle narrow at 30-40 degrees. Sutures at 10 degrees. Aperture is about 69 degrees to the axis of coiling.

Distribution: Rare across Deccan Plateau infra- and intertrappean beds at Takli and Kalmeshwar.

Holotype: InS0275 (Appendix 2, Figure P; 2.9 mm x 1.4 mm); Type locality: Takli (InL004b-3).

Repository: University of North Dakota, Grand Forks, North Dakota.

Remarks: Species name is derived from the Hindi for turret.

"StyB" and "styC" are found within the same major cluster as "styA," so the familial relationships discussed previously apply (Figure 29). "StyB" and "styC" are similar in overall morphology, but "styB" has a narrower conic outline shape while "styC" has a wider conic shape. These may be two subspecies instead of two separate species; however, for this study they are considered discrete species based on the degree of difference in spire angle. "StyB" is similar to

Viviparus acicularis Hislop, 1860 and *V. subcylindracea* Hislop, 1860. Although Hislop (1860) diagnosed these as two separate species, there is no evidence from the cluster analysis to support the separation. The only difference appears to be that *V. subcylindracea* Hislop, 1860 is larger than *V. acicularis* Hislop, 1860. A modern representative of the genus *Subulina*, which is the type genus of the family, is present in India, and based on this and before more detailed taxonomic analysis, "styB" will be considered in *Subulina*. The species name s*ubcylindracea* was chosen because the more robust form is more common throughout the sequence.

Superfamily Achatinoidea Swainson, 1840

Family Subulinidae Fischer & Crosse, 1877

Genus *Subulina* Beck, 1837

Description: "Shell nonumbilicate, more or less high turreted, thin-walled; apex rounded; aperture small, oblique; columella twisted, truncated below. Central plate of the radula narrow; lateral plates nearly symmetrical, with inner and outer cusp; marginal plates tricuspid. Eggs with calcareous shell (Thiele, 1992)."

Subulina subcylindracea (Hislop), new genus assignment

Paludina subcylindracea Hislop, 1860

Description: "Shell elongate-turreted, single-banded; apex subacute; 8–10 rather convex whorls; aperture small, ovate, narrow, angular above; labial margin subreflexed. Length 0.45, width 0.17 inch [11.43 mm, 4.32 mm] (Hislop, 1860; translated in Hartman et al., 2008)."

Distribution: Common across Deccan Plateau infra- and intertrappean beds at Takli, Kalmeshwar, Butera, Sindhi, and Telankhedi.

Holotype: GS 10263; Plate V, fig. 6 (Hislop, 1860); Type locality: Telankhedi.

Repository: Natural History Museum, London, England.

"StyC" is comparable to *Viviparus pyramis* Hislop, 1860 and *V. rawesi* Hislop, 1860. Hislop (1860) diagnosed these as two separate species, but this is not supported by the analysis. The only noticeable difference is *V. rawesi* is larger than *V. pyramis*. Due to its similarity to the "styB" morphology, "styC" will be considered in the genus *Subulina*. This is a rare morphology but the slighter *V. pyramis* Hislop, 1860 appears to be more common. Therefore, the suggested species revision is *Subulina pyramis*.

Genus *Subulina* Beck, 1837

Subulina pyramis (Hislop), new genus assignment

Paludina pyramis Hislop, 1860

> Description: "Shell chinked, pyramidal; apex acute; nine subconvex whorls with uniform growth in size; aperture ovate, angular above. Length 0.25, width 0.1 inch [6.35 mm, 2.5 mm] (Hislop, 1860; translated in Hartman et al., 2008)."

Distribution: Rare across Deccan Plateau infra- and intertrappean beds at Takli, Kalmeshwar, Butera, and Telankhedi.

Holotype: GS 10262; Plate V, fig. 5 (Hislop, 1860); Type locality: Telankhedi.

Repository: Natural History Museum, London, England.

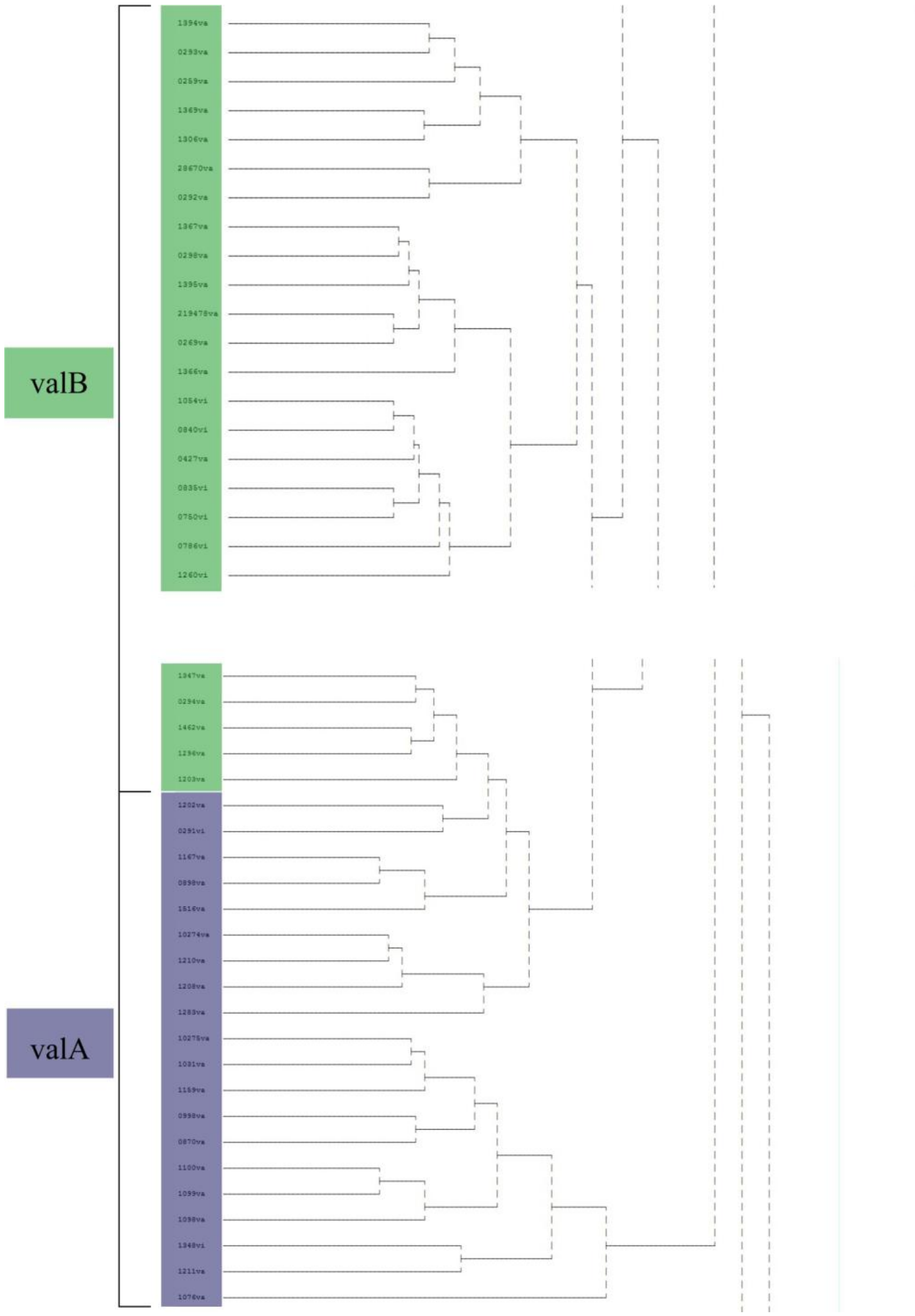

Figure 32. Portion of the complete dendrogram with all specimens (including types and modern) containing the “val” morphologies (R = 0.71).

“ValA” clusters with *Valvata multicarinata* Hislop, 1860 (Figure 32). It is closely related to “valB,” the modern valvatids, *Valvata virens* Tyron, 1863 and *Valvata utahensis* Call, 1884, and *Valvata unicarinifera* Hislop, 1860. “ValA” is considered in Valvatidae based on its open, wide umbilicus combined with a turbiniform to trochiform outline shape. It has revolving sculpture, which is common in Valvatidae. The distinguishing feature between “valA” and “valB” is a higher-spired more trochiform shell in “valA” compared with the shorter more turbiniform shell shape of “valB.”

Although valvatids are generally found in temperate to cooler climates in the northern hemisphere, there is at least one modern species in India (*Valvata piscinalis* Müller, 1774). The predominance of valvatids in the northern hemisphere suggests they evolved in Laurasia before moving south, which complicates the existence of Cretaceous valvatids in India. The family is found in northern Africa, and although there is no record of valvatids from the Cretaceous, Africa could have been a corridor for dispersion. The dispersion of valvatids from Europe or western Asia to northern Africa and then to India is explainable if India’s plate movements brought it near Africa as it headed toward Asia. Therefore, even though there is no fossil evidence to support the dispersal of valvatids from Africa to India in the Cretaceous prior to the Deccan trap eruptions, these assertions are possible.

“ValA” is considered equivalent to *Valvata multicarinata* until further taxonomic analysis identifies a more appropriate genus.

Superfamily Valvatoidea Gray, 1840

Family Valvatidae Gray, 1840

Genus *Valvata* Müller, 1773

Description: “Shell in most cases small, without indentations of the apertural margin. Living in fresh water. Animal oviparous; lateral plates of the radula with denticulate cutting edges (Thiele, 1992).”

Valvata multicarinata Hislop, 1860 sedis mutabilis

“ValB” clusters with modern species, *Valvata virens* Tyron, 1863 and *Valvata utahensis* Call, 1884 (Valvatidae), and *Valvata unicarinifera* Hislop, 1860 (Figure 32). It is related to “valA,” so the taxonomic relationships previously discussed apply to “valB.” Although “valB” are present in two distinct clusters, the morphotype appears to be the same. In one cluster the specimens have rounder whorls while in the other they have flatter whorls. Due to the uniqueness of each cluster, it is likely that these are subspecies. “ValB” is considered to be equivalent to *Valvata unicarinifera* Hislop, 1860 based on the association in the dendrogram. The two proposed subspecies are *V. unicarinifera unicarinifera* (“valB1”) and *V. unicarinifera chiknaformis* (“valB2”). The rounded whorl morphology is *V. u. unicarinifera* and the flattened whorl morphology is *V. u. chiknaformis* from the Hindi word for flat. Although Hislop’s (1860) type specimen does not have revolving sculpture, several study specimens of this morphology preserve it within the impression suggesting that *V. unicarinifera* is sculptured.

Valvata unicarinifera Hislop, 1860

Description: “Shell turbinate-conoid; apex subacute; 5–6 subventricose whorls that are unicarinate below the suture; umbilicus large; aperture subrounded. Length 0.4, width 0.27–0.38 inch [10.2 mm, 6.86–9.65 mm] (Hislop, 1860; translated in Hartman et al., 2008).”

Valvata unicarinifera unicarinifera Hislop, 1860, original morphotype

Diagnosis: Differs from *V. unicarinifera chiknaformis* in having rounded whorls and strongly depressed sutures. Differs from *V. multicarinata* by a lower height to width ratio.

Description: Shell small to medium, turbiniform. Whorls rounded. Sutures at 7 degrees and strongly depressed. Aperture circular. Shell has 4-5 whorls. Spire angle wide at 80-85 degrees. Aperture is about 70-80 degrees to the axis of coiling. Wide, open umbilicus. Revolving sculpture present in specimen impressions.

Distribution: Relatively uncommon across Deccan Plateau infra- and intertrappean beds at Takli, Kalmeshwar, and Butera.

Holotype: InS1159 (Appendix 2, Figure O; 1.5 mm x 1.7 mm); Type locality: Kalmeshwar (InL0096b).

Repository: University of North Dakota, Grand Forks, North Dakota.

Valvata unicarinifera Hislop, 1860

Valvata unicarinifera chiknaformis n subsp.

Diagnosis: Differs from *V. unicarinifera unicarinifera* in having flattened whorls and mildly depressed sutures. Differs from *V. multicarinata* by a lower height to width ratio.

Description: Shell small to medium, turbiniform. Whorls flattened. Sutures at 8 degrees with some depression. Aperture circular. Shell has 4-7 whorls. Spire angle wide at 80-85 degrees. Aperture is about 70 degrees to the axis of coiling. Wide, open umbilicus. Sculpture not recorded but is proposed based on the presence in the species.

Distribution: Uncommon across Deccan Plateau infra- and intertrappean beds at Takli, Kalmeshwar, and Butera.

Holotype: InS1199 (Appendix 2, Figure N; 6.8 mm x 7.6 mm); Type locality: Butera (InL017).

Repository: University of North Dakota, Grand Forks, North Dakota.

Remarks: Species name derived from the Hindi for flat.

The Deccan trap species *Valvata decollata* Hislop, 1860 does not cluster with the rest of the valvatids, but the shell morphology is analogous to *V. multicarinata* Hislop, 1860 with a more high-spired, trochiform shape. The type specimen is poorly preserved so it is likely that the subtle differences between these two species are due to preservation. Therefore, it is proposed that *Valvata decollata* is not a valid species but simply a poorly preserved specimen of *V. multicarinata*. The taxonomic status of the Deccan species *Valvata minima* Hislop, 1860, which was not included in the analysis, is not discussed further due to the poor preservation of the only specimen.

Although "vivA" and "vivB" form distinct clusters, their morphologies are very similar and it is difficult to diagnose these as two species or two subspecies (Figure 33). "VivA" has flatter whorls and a slightly more angled body whorl with a more triangular outline shape than "vivB." They will be considered two separate species based on their separation into two definite clusters. Although "vivA" does not group with any modern representatives or Deccan trap species, it is closely related to "vivB," the modern *Bellamya bengalensis* Lamarck, 1822 (Viviparidae) and *Viviparus normalis* Hislop, 1860.

Viviparids are currently found worldwide except for South America (fossil only) in temperate to tropical environments with several genera in India. They are typically trochiform in

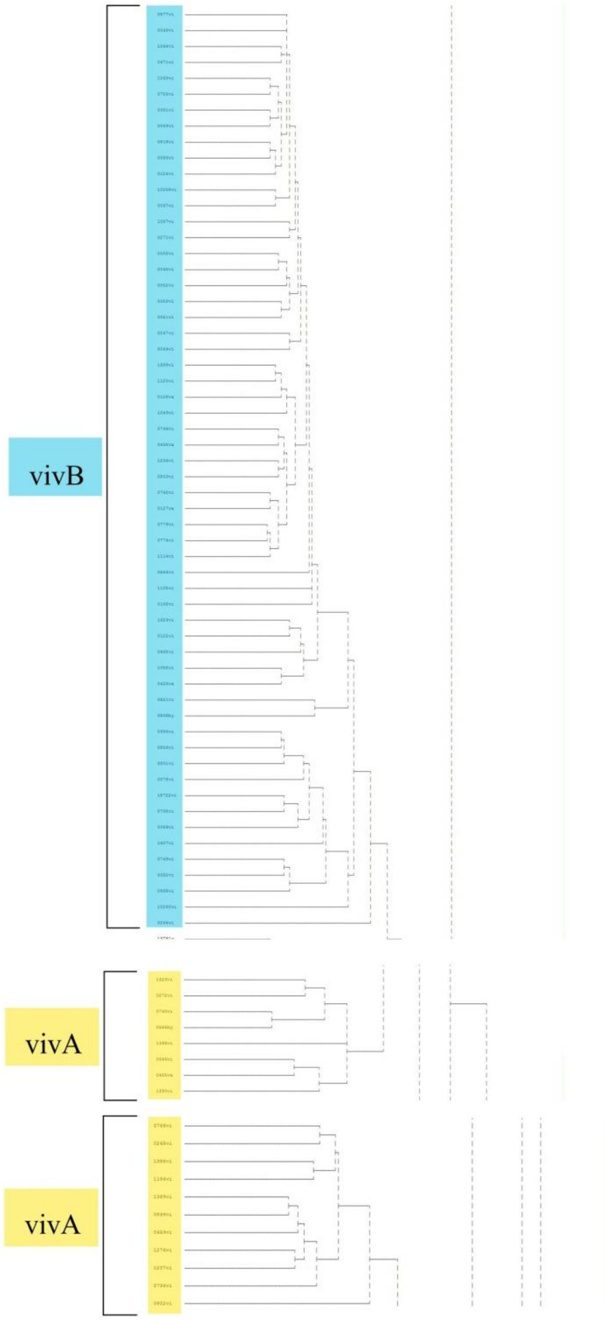

Figure 33. Portion of the complete dendrogram with all specimens (including types and modern) containing the “viv” morphologies (R = 0.71).

shape with an ovate aperture. Annandale (1921) regarded *V. normalis* as the only of Hislop's (1860) "*Paludina*" forms to be a true viviparid. Based on the morphology of "vivA" and Annandale's (1921) argument, "vivA" is considered to be a member of Viviparidae. The genus *Viviparus* is typically of holarctic distribution so it is not likely that the Deccan viviparids are in this genus. It is more likely that the Deccan viviparids belong to the genus *Bellamya*, which is common in modern India as well as other tropical regions (e.g., Africa and Southeast Asia). The occurrence of *Bellamya* in these areas suggests a possible Gondwanan origin, which coincides with the existence of the genus in India during the Cretaceous. Therefore, based on biogeographic relationships, Deccan viviparids are revised to the genus *Bellamya*. The proposed new species name is *Bellamya lattooformis* from the Hindi word for top-shaped.

Superfamily Viviparoidea Gray, 1847

Family Viviparidae Gray, 1847

Subfamily Bellamyinae Rohrbach, 1937

Genus *Bellamya* Jousseaume, 1886

> Description: "Shell of moderate size, often with a more or less distinct edge, in most cases narrowly umbilicate. Dorsum of the animal with a strong crest which ends behind the right tentacle which is considerably elongated in the male (Thiele, 1992)."

Bellamya lattooformis n. sp.

> Diagnosis: Differs from B. normalis in having flattened whorls and regularly depressed sutures.

Description: Shell is small to medium, trochiform. Whorls flattened with sutures regularly depressed. Typically 5-6 whorls. Shell smooth. Spire angle wide at roughly 70 degrees. Suture angled at 10-11 degrees. Aperture broadly ovate, at 70 degrees to the axis of coiling. A single revolving keel has been documented on specimens with original shell material.

Distribution: Relatively uncommon across Deccan Plateau infra- and intertrappean beds at Takli, Kalmeshwar, and Butera.

Holotype: InS1207 (Appendix 2, Figure F; 6.2 mm x 5.6 mm); Type locality: Butera (InL017).

Repository: University of North Dakota, Grand Forks, North Dakota.
Remarks: Species name derived from Hindi for top-shaped.

"VivB" clusters with the modern *Bellamya bengalensis* Lamarck, 1822 (Viviparidae) and *Viviparus normalis* Hislop, 1860 (Figure 33). This morphotype is related to "vivA," so familial relationships discussed previously apply to "vivB." "VivB" is considered equivalent to *V. normalis* Hislop, 1860, and will therefore retain the species name with the revised genus *Bellamya*.

Genus *Bellamya* Jousseaume, 1886

Bellamya normalis (Hislop), new genus assignment

Paludina normalis Hislop, 1860

> Description: "Shell chinked, ovate-conical; apex subacute but rather often truncate; 5–6 ventricose whorls separated by a deep suture; aperture round, peristome continuous. Length 0.8, width 0.5 inch [20.3 mm, 12.7 mm] (Hislop, 1860; translated in Hartman et al., 2008)."

Distribution: Very common across Deccan Plateau infra- and intertrappean beds at Pijdura, Takli, Kalmeshwar, Butera, Sindhi, Karwad, Ambiakanti, Tandra, and Kateru.

Holotype: GS 10259; Plate V, fig. 2b (Hislop, 1860); Type locality: Pijdura.

Repository: Natural History Museum, London, England.

Viviparus wapsharei Hislop, 1860 has two different morphologies. There is a shorter form similar in morphology to *V. normalis* Hislop, 1860 and a taller form similar to *V. conoidea* Hislop, 1860. Although morphology is similar, it appears that Hislop (1860) distinguished *V. wapsharei* based on its smaller size (< 1 cm). The cluster analysis does not support *V. wapsharei* as a distinct species but a close relationship to *V. normalis* and "vivB." Using shell morphology as an indicator of taxonomic relationships rather than size, the shorter form of *V. wapsharei* should be included in "vivB" equivalent to *V. normalis* while the taller form should be included in "hydB" equivalent to *V. conoidea*. The extensive size variation observed in the study localities suggests that difference in specimen size does not denote discrete species, but instead is likely an indicator of ecology or some external environmental pressure.

Viviparus soluta Hislop, 1860 was not included in the analysis due to the inability to measure most character traits. Hislop (1860) placed this species within Viviparidae, and initial observation of the type specimen suggests that it is similar in overall shell morphology to *V. normalis*. *V. soluta* is narrower and taller but has similar strongly rounded whorls and overall outline shape. The type specimen of *V. soluta* Hislop, 1860 is the only example of this species, and the preservation is poor so that the aperture is obscured. More work is needed on taxonomic relationships of this species.

The type specimen of *Succinea nagpurensis* Hislop, 1860 was included in the analysis, but no other examples of this species have been identified. The cluster analysis placed *S.*

nagpurensis with the “lymA” morphology, but this is likely due to the similar body whorl and aperture shape. Since the type specimen is the only occurrence of the species, it is difficult to ascertain the validity of the species or its taxonomic relationships. More work is needed on the relationships of this species.

Morphologic Changes Through Time

Tricula virapai (“hydA”) is an uncommon morphology although it occurs in all study localities. Its greatest abundance is in Kalmeshwar. Specimens are largest in Pijdura (Table 6) and decrease significantly in size in Takli and Kalmeshwar (Figure 34). Specimens are larger in Butera before decreasing in Sindhi to a comparable size as in Takli and Kalmeshwar. Statistically Pijdura, although with larger specimens, is similar to Butera while Takli, Kalmeshwar, and Sindhi are similar. The general morphology of specimens, as depicted by dimension ratios, is relatively consistent through the sequence suggesting that although the specimen size changes their overall morphology remains the same. The spire and suture angles and the number of whorls display no obvious pattern. Specimens of *Tricula virapai* are largest prior to the Deccan eruptive events, which suggest an influence of the Deccan volcanism on the size of individual specimens causing a drastic decrease in size after the initial phase. The morphology does not appear affected by the volcanism.

Tricula conoidea (“hydB”) is very common occurring in all study localities. Its greatest abundance is in Kalmeshwar although Takli also contains a significant amount. The specimens are largest in Pijdura (Table 6) and decrease in size dramatically in Takli (Figure 35). There is a slight increase in Kalmeshwar and more in Butera before decreasing again in Sindhi. Specimens in Pijdura are statistically larger than the remainder of the study sample. The general morphology of *Tricula conoidea* (dimension ratios) changes through time with Pijdura having a greater height

Table 6. Distribution of specimen shell minimum, maximum, and mean heights for each morphotype at each locality.

	Pijdura			Takli			Kalmeshwar			Butera			Sindhi		
	Specimen Height (mm)														
	Min	Max	Mean	Min	Max	Mean	Min	Max	Mean	Min	Max	Mean	Min	Max	Mean
hydA	4.3	7.8	6.0	1.3	2.3	1.6	1.1	2.2	1.8	3.1	7	5.1	1.2	1.7	1.4
hydB	5.3	9.9	7.4	0.8	6.2	2.3	1.1	5.2	2.4	1.2	11	4.5	1.8	3.5	2.4
hydC	9.7		9.7	1.3	9.7	3.0	1.2	5.4	2.7	1.4	10.9	3.3	0.8	2.7	1.8
hydD	10.7	11.1	10.9										4.9	6.6	5.7
lymA				1.2	4.6	2.9	2	4.1	3.2	0.9	4.4	2.3			
lymB	6.4	12.4	8.7	1.1	11.6	2.5	1.7	8	4.4	2.7	3.7	3.1	3		3.0
lymC	9.7	23.2	15.6	1.3	6.9	4.1				3	14.7	7.6	6.5		6.5
phyA	21.4	57.3	43.6	1.1	1.7	1.3	1.2	22.6	10.7	11.4	35.9	23.8			
phyB	5.4	52.2	37.0	1	26.2	4.0	1	29.9	6.2	0.8	48.7	13.9			
styA				2.1	4.8	2.8	3.1		3.0						
styB				1.9	8.5	3.0	1.4	4.2	3.0	2.5	6.3	4.3	2.2	6.7	4.3
styC				2.9		2.9	2.6	5.3	3.8	3.2	5.3	4.3			
valA							0.7	9.4	6.0	4.9	12.4	7.6			
valB				0.9	3.8	1.8	1.2	8.4	3.0	0.8	7.9	4.3			
vivA				0.7	3.5	1.8	1.1	6.4	2.9	1.2	7.8	3.1			
vivB	3	13.4	9.0	0.8	3.4	1.4	0.6	3	1.4	0.6	3.8	2.1	1.5	2.6	2.1

Figure 34. Changes in *Tricula virapai*. Scale bar is 1 mm.

to width ratio resulting in narrower specimens. There is no trend in the spire or suture angles through the sequence. The number of whorls is greatest in Pijdura (5.1) decreasing in Takli (4.1), increasing slightly in Kalmeshwar (4.4), and then decreasing in Butera (4.1) and Sindhi (3.9). The decrease in size and number of whorls and the slight change in morphology following the initiation of volcanism suggest a potential effect on the fauna.

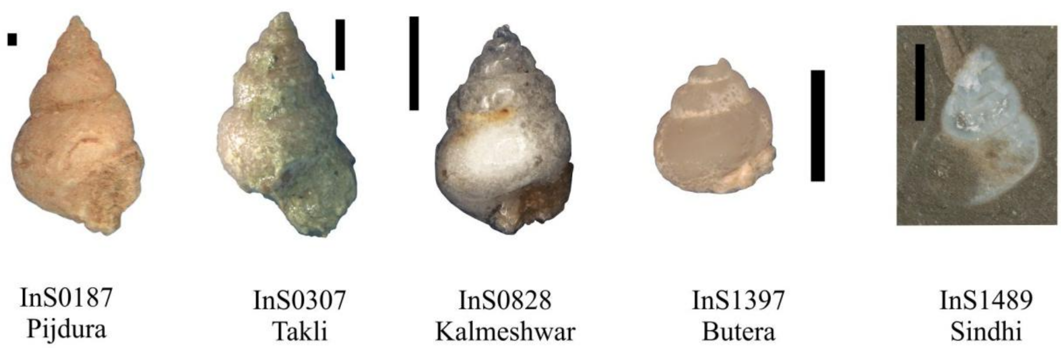

Figure 35. Changes in *Tricula conoidea*. Scale bar is 1 mm.

Tricula sankeyi (“hydC”) is very common occurring in all localities. Its greatest abundance is in Kalmeshwar. Although there is only one specimen from Pijdura (Table 6), it is noticeably larger than those in the remainder of the localities (Figure 36). The size decreases dramatically in Takli and Kalmeshwar before increasing slightly in Butera and decreasing again in Sindhi. The general morphology remains consistent through the sequence. Statistically specimens of *Tricula sankeyi* in Pijdura are larger than specimens in all other study localities. There is no noticeable trend in the spire angles or suture angles of *Tricula sankeyi* specimens. The number of whorls is greatest in Pijdura averaging about 6.2 whorls. The number of whorls decreases in Takli (4.5) before increasing in Kalmeshwar (4.5), Butera (5.5), and Sindhi (5.0). Specimens of *Tricula sankeyi* are largest with the greatest number of whorls prior to volcanism suggesting a possible relationship.

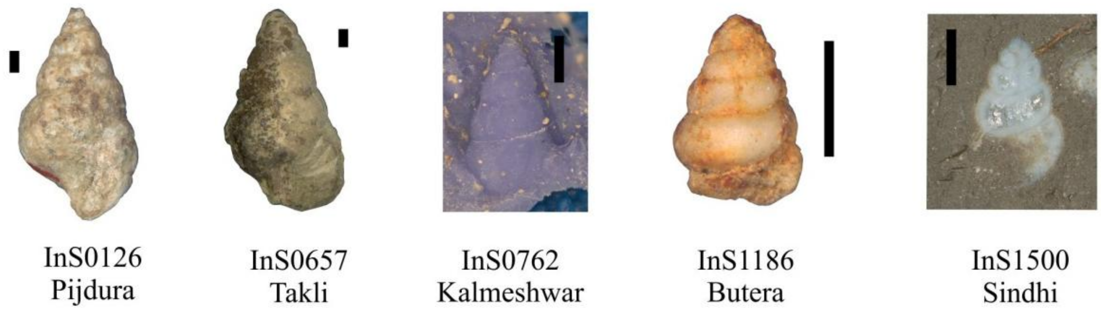

Figure 36. Changes in *Tricula sankeyi*. Scale bar is 1 mm.

Thiara quadrilineata (“hydD”) is a rare morphology occurring only in Pijdura and Sindhi with a total of four specimens. Due to the scarcity of specimens it is difficult to ascertain any patterns in this species. Specimens are roughly twice as large in Pijdura as in Sindhi but are not statistically distinct (Table 6) (Figure 37). Their general morphology is consistent between the two localities. The number of whorls, suture angle, and spire angle are greater in Pijdura than in Sindhi. Since there are so few specimens to establish a trend, there can be no conclusion as to the effects of Deccan volcanism. However, based on the sample obtained, the volcanism does appear to affect the size of *Thiara quadrilineata* specimens but not the overall morphology.

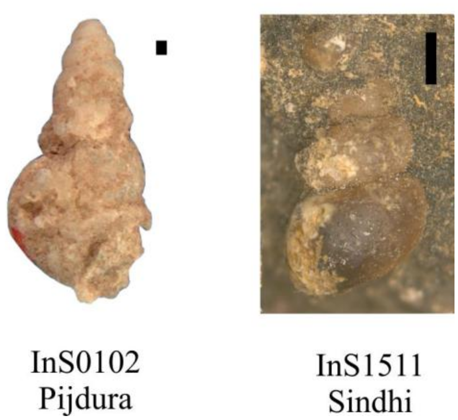

Figure 37. Changes in *Thiara quadrilineata*. Scale bar is 1 mm.

Lymnaea oviformis (“lymA”) is uncommon occurring only in Takli, Kalmeshwar, and Butera. Its greatest abundance is in Butera. There is a complete absence of specimens in Pijdura prior to the onset of volcanic activity, so it is difficult to determine changes throughout the entirety of the sequence. Specimens are larger in Kalmeshwar than in Takli or Butera but with no statistical pattern (Table 6) (Figure 38). Similarly the general morphology remains statistically consistent over time. There is no overall pattern to the spire and suture angles or the number of whorls, but specimens in Kalmeshwar do have more whorls than Takli or Butera. Although conclusions as to the direct effect of volcanism cannot be gleaned from specimens of *Lymnaea oviformis,* the larger specimens in Kalmeshwar may indicate a preferential ecology for this type of snail and more research is needed to analyze relationships.

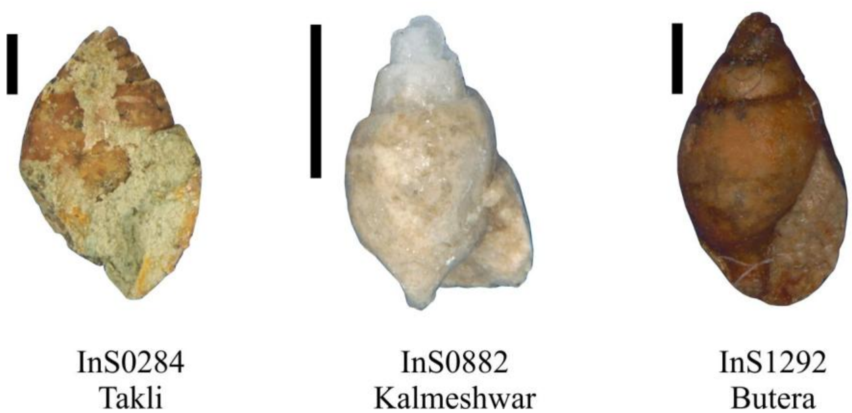

Figure 38. Changes in *Lymnaea oviformis*. Scale bar is 1 mm.

Lymnaea pokhariensis (“lymB”) is a common lymnaeid morphology occurring in all localities although only one specimen was obtained from Sindhi. Its greatest abundance is in Takli. Specimens from Pijdura are noticeably and statistically larger before drastically reducing in size into Takli (Table 6) (Figure 39). Specimens increase slightly in Kalmeshwar before decreasing in Butera and remaining small in Sindhi. Specimens in Takli are statistically distinct from the remainder of the sample. The overall morphology remains relatively constant through time supported by the lack of statistical significance. There is no observable pattern in the number of whorls of *Lymnaea pokhariensis,* although Pijdura has the greatest number of whorls (4.5 whorls). There is also no pattern within the spire or suture angles through time. The noticeably larger specimens of *Lymnaea pokhariensis* from Pijdura and smaller specimens in Takli may suggest some reaction to the onset of volcanism in the area.

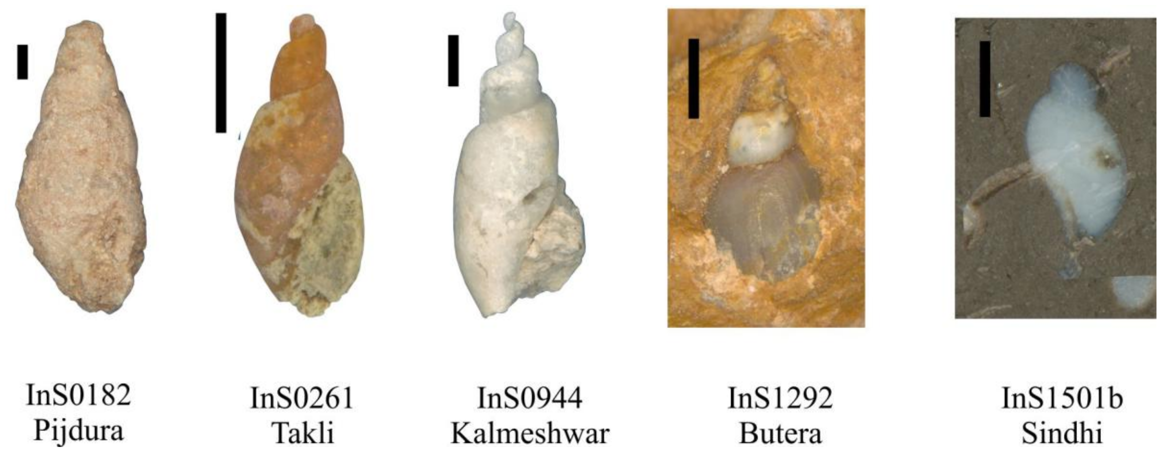

Figure 39. Changes in *Lymnaea pokhariensis*. Scale bar is 1 mm.

Lymnaea subulata ("lymC") is relatively uncommon occurring in all localities except Kalmeshwar with only one specimen from Sindhi and two from Takli. The majority of specimens are found in Pijdura suggesting a possible pattern of reduction in population due to the onset of volcanism. Specimens are much larger in Pijdura creating a statistically distinct group with the specimen from Sindhi. Specimens reduce dramatically in size into Takli and increase in Butera and Sindhi (Table 6) (Figure 40). Although the specimen from Sindhi is found in both groups, the analysis of only one specimen should not be used as a definitive judgment of the nature of the morphology at the end of the sequence. The overall morphology is statistically different in Takli and Butera from Pijdura and Sindhi. Pijdura and Sindhi have much narrower specimens giving the group its greater height to width ratio than Takli and Butera. There is no observable trend in the number of whorls through the sequence, however, the number of whorls is greatest in Pijdura (4.6 whorls). There is also no noticeable trend in the spire and suture angles. The larger specimens in Pijdura compared to the rest of the sample suggests a possible relationship between the size and shape of the morphology and volcanic activity. More specimens are needed before any conclusive statements are made regarding the *Lymnaea subulata* morphology.

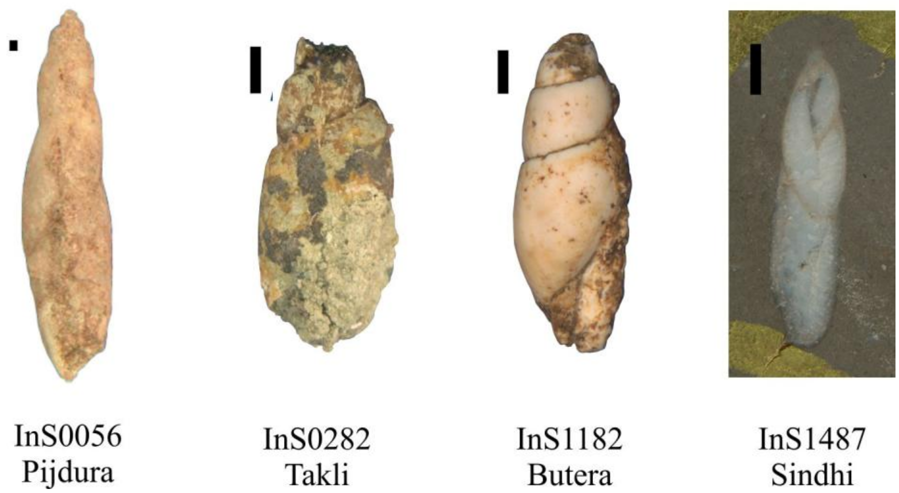

Figure 40. Changes in *Lymnaea subulata*. Scale bar is 1 mm.

Platyphysa prinsepii elongata (“phyA”) is common occurring in all localities but Sindhi, where planorbids are absent. Its greatest abundance is in Pijdura. Specimens from Pijdura are consistently larger than the rest of the specimens while those from Takli are consistently small with its largest specimen around two millimeters long (Table 6) (Figure 41). There is a slight increase in size in Kalmeshwar and again in Butera. Although there are a few specimens of comparable size to Pijdura in Kalmeshwar and Butera, the average size is small suggesting the dominant form is comparable to Takli. Specimens in Pijdura are statistically different from those in Takli and Kalmeshwar and those in Kalmeshwar and Butera. The overall morphology forms two statistically distinct groups. Specimens in Pijdura, Kalmeshwar, and Butera are thinner than in Takli and Kalmeshwar. There is no discernible trend in the number of whorls or the spire or suture angles. The larger specimens in Pijdura with a dramatic decrease in size into Takli may indicate a response to the onset of volcanism, but more work is needed to explain the intermixing of micro- and macro specimens of *Platyphysa prinsepii elongata*.

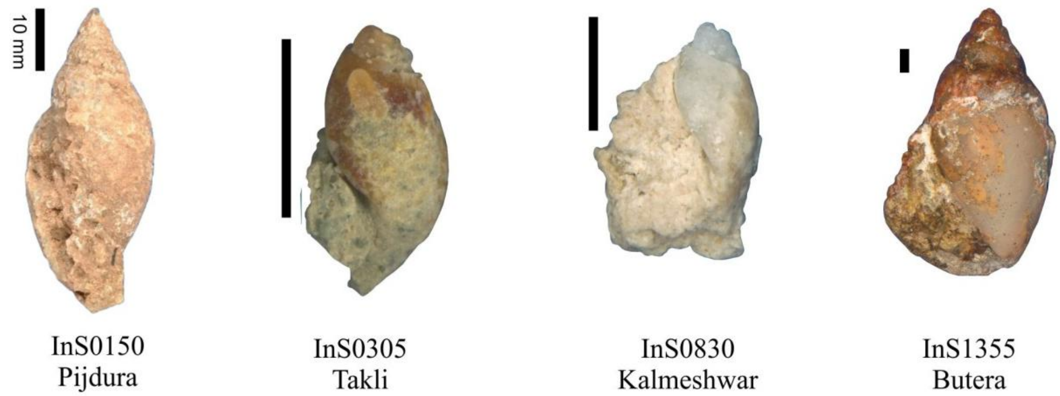

Figure 41. Changes in *Platyphysa prinsepii elongata*. Scale bar is 1 mm unless otherwise noted.

Platyphysa prinsepii normalis (“phyB”) is common occurring in all localities but Sindhi. The greatest abundance is in Pijdura but the number of specimens in the remaining localities is comparable. Specimens are much larger in Pijdura forming a statistically distinct group (Table 6) (Figure 42). The average specimen size in Takli, Kalmeshwar, and Butera is small, but there are also a few larger specimens of comparable size to Pijdura. The overall morphology changes through time. Pijdura has narrower specimens than Takli, Kalmeshwar, and Butera and specimens in Kalmeshwar are slightly broader than Takli and Butera. There is no apparent trend in the number of whorls or the spire and suture angles, but specimens from Pijdura do have the greatest number of whorls (~4.1) suggesting a possible relationship between number of whorls and the Deccan volcanism. The larger specimens of *Platyphysa prinsepii normalis* in Pijdura may suggest effects of volcanism, but the intermixing of micro- and macrosnails is interesting and needs further scrutiny.

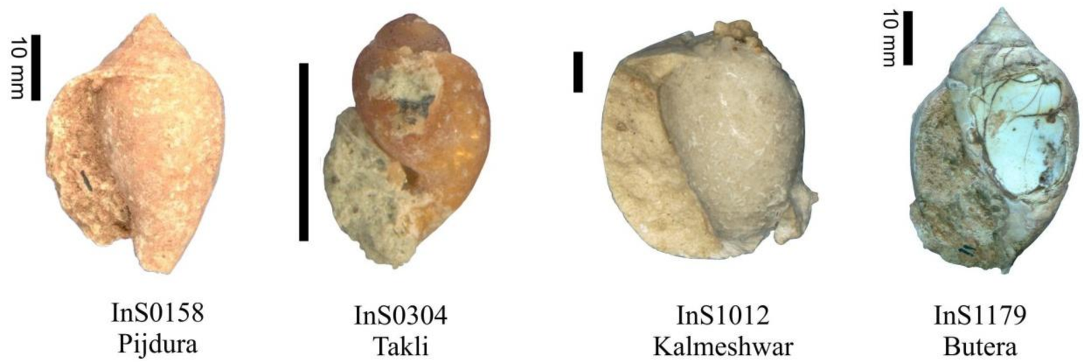

Figure 42. Changes in *Platyphysa prinsepii normalis*. Scale bar is 1 mm unless otherwise noted.

Zootecus burji ("styA") is a rare morphology occurring only at Takli and Kalmeshwar. Most specimens are found in Takli. There is a slight increase in size from Takli into Kalmeshwar but this is not statistically significant (Table 6) (Figure 43). The overall morphology does not change from Takli into Kalmeshwar. There is no pattern in the number of whorls or the spire and suture angles. Since specimens are only present in two localities it is difficult to discern a trend through time although the slight increase in size from Takli into Kalmeshwar is comparable to other morphologies.

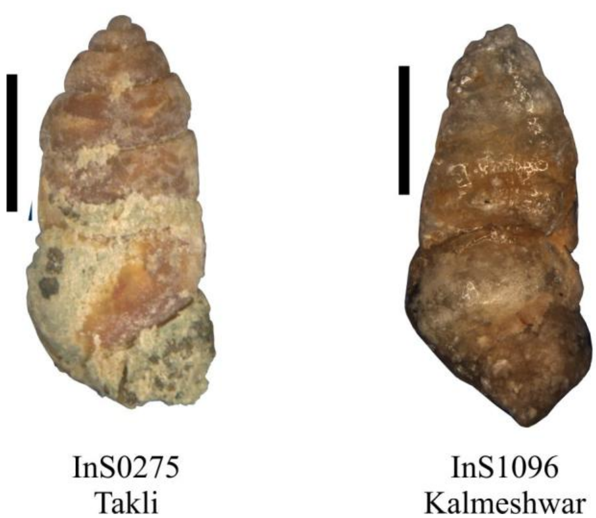

Figure 43. Changes in *Zootecus burji*. Scale bar is 1 mm.

Subulina subcylindracea (“styB”) is common occurring in all localities but Pijdura, where terrestrial morphologies are absent. The greatest abundance is in Kalmeshwar, but the population size between this locality, Takli, and Butera are not markedly different. Specimens from Butera and Sindhi are slightly larger than those from Takli and Kalmeshwar but this is not statistically significant (Table 6) (Figure 44). Similarly, the overall morphology stays consistent throughout the sequence. There is no trend in the number of whorls or the spire and suture angles. The *Subulina subcylindracea* morphology remains statistically constant through time suggesting no noticeable response to volcanism, but the increase in size after Takli is comparable to other morphologies.

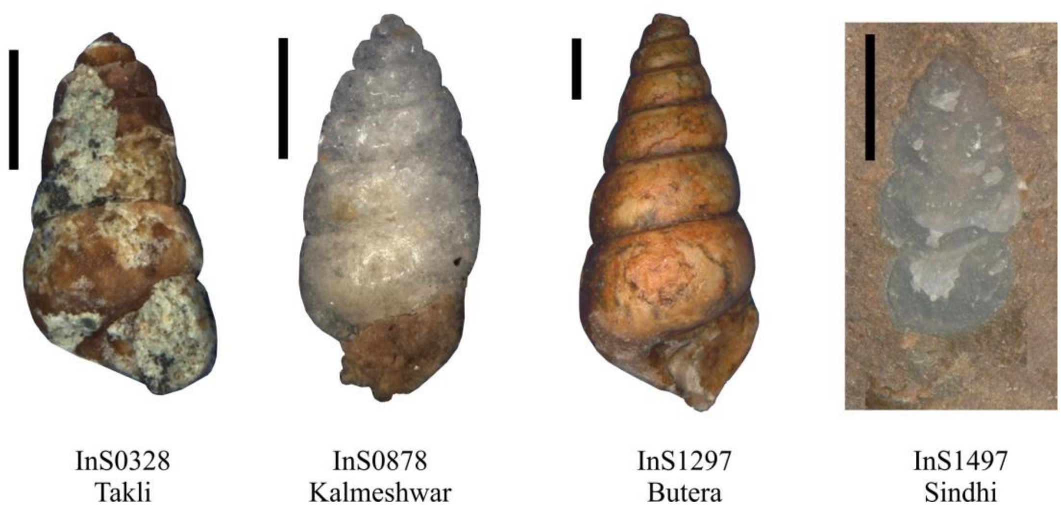

Figure 44. Changes in *Subulina subcylindracea.* Scale bar is 1 mm.

Subulina pyramis (“styC”) is rare occurring in Takli, Kalmeshwar, and Butera. The abundance is greatest in Kalmeshwar with only three specimens. There is an increase in size consistently but slightly through time but this is not statistically significant (Table 6) (Figure 45). The overall morphology stays relatively the same. The number of whorls is consistent in Takli and Kalmeshwar before increasing in Butera. The spire angle is highest in Takli and then decreases steadily through Butera. There is no apparent pattern to the suture angles. *Subulina pyramis* stays consistent through time suggesting little to no effects of volcanism.

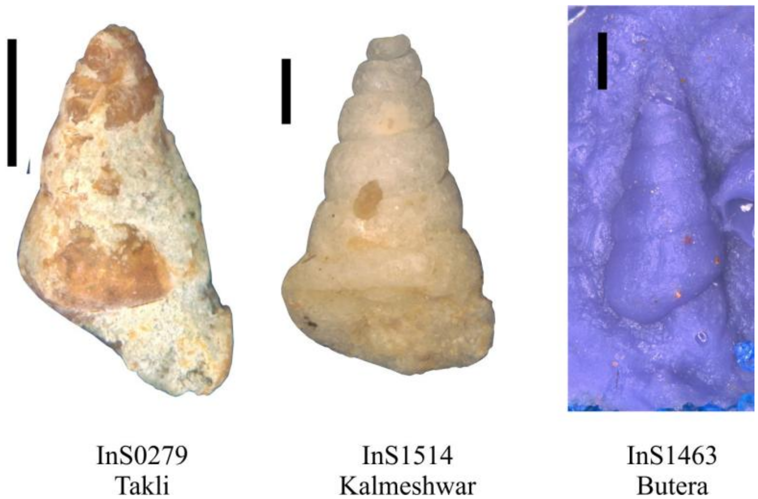

Figure 45. Changes in *Subulina pyramis.* Scale bar is 1 mm.

Valvata multicarinata ("valA") is uncommon occurring only at Kalmeshwar and Butera. Its greatest abundance is in Kalmeshwar. There is a slight increase in specimen size from Kalmeshwar into Butera but this is not statistically significant (Table 6) (Figure 46). The overall morphology remains constant through the sequence. The number of whorls and suture angles increase while the spire angles decrease over time. Since *Valvata multicarinata* is only present in two localities, it is difficult to identify a response to volcanism. However, the increase in size from Kalmeshwar into Butera is comparable to other morphologies.

Valvata unicarinifera ("valB") is relatively common existing in Takli, Kalmeshwar, and Butera. Its greatest abundance is in Kalmeshwar. Kalmeshwar apparently supported desirable conditions for valvatids to thrive as this locality has a conspicuously larger population. Specimens are smallest in Takli and increase in size steadily through time (Table 6) (Figure 47). Specimens from Takli form a statistically distinct group. The overall morphology remains constant through

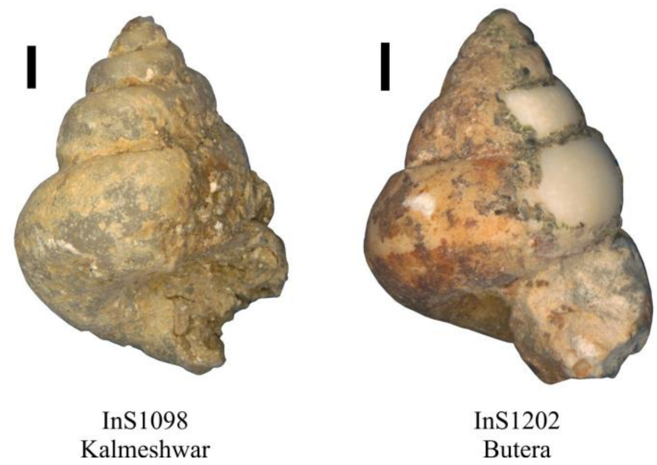

Figure 46. Changes in *Valvata multicarinata.* Scale bar is 1 mm.

time. The number of whorls increases through time while the suture angle decreases. There is no visible trend in the spire angle. Although there are no identified valvatids in Pijdura hindering examination of their response to Deccan volcanism, the steady increase in size from Takli to Butera is comparable to other morphologies.

Figure 47. Changes in *Valvata unicarinifera.* Scale bar is 1 mm.

Bellamya lattooformis ("vivA") is uncommon occurring in Takli, Kalmeshwar, and Butera. Its greatest abundance is in Takli. Specimens are smallest in Takli and increase in size in Kalmeshwar and Butera, but this trend is only statistically significant when there is an interaction of the size and outline shape meaning the size changes only when effected by changes in the outline shape (Table 6) (Figure 48). Under these conditions specimens in Takli and Kalmeshwar form one group while Kalmeshwar and Butera form another. The overall morphology changes through time with Kalmeshwar retaining a narrower morphology than Takli and Butera. The number of whorls is lowest in Takli and then increases and remains stable through Kalmeshwar and Butera. There is a steady increase in the suture angle while no apparent trend in the spire angle is recognizable. Although there is little statistical evidence to support a change in size of *Bellamya lattooformis* through time, the increase from Takli through Butera is comparable to other morphologies. The change in overall morphology suggests volcanism may have had an effect on the shape of *Bellamya lattooformis*.

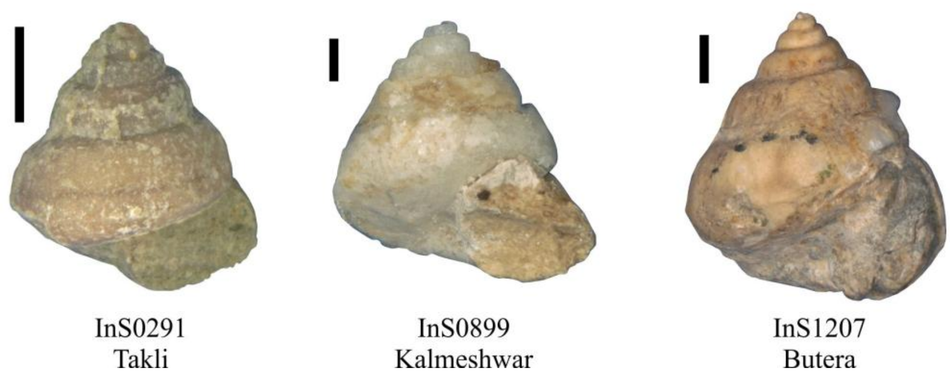

Figure 48. Changes in *Bellamya lattooformis.* Scale bar is 1 mm.

Bellamya normalis (“vivB”) is very common existing in all localities. Its greatest abundance is in Pijdura. Specimens are markedly larger in Pijdura forming a distinct group while all other specimens are statistically similar (Table 6) (Figure 49). There is a decrease in size into Takli before increasing very slightly in Kalmeshwar and stabilizing for the remainder of the sequence. The overall morphology changes through time. Pijdura and Sindhi have a narrower shape than Takli and Kalmeshwar, which in turn are narrower than Butera. There is no pattern in the number of whorls or the spire and suture angles, although Pijdura has the greatest number of whorls (~4.2). The larger specimens in Pijdura suggest volcanism may have affected specimen size, but the lack of a trend in the change in morphology suggests volcanism was not likely the cause.

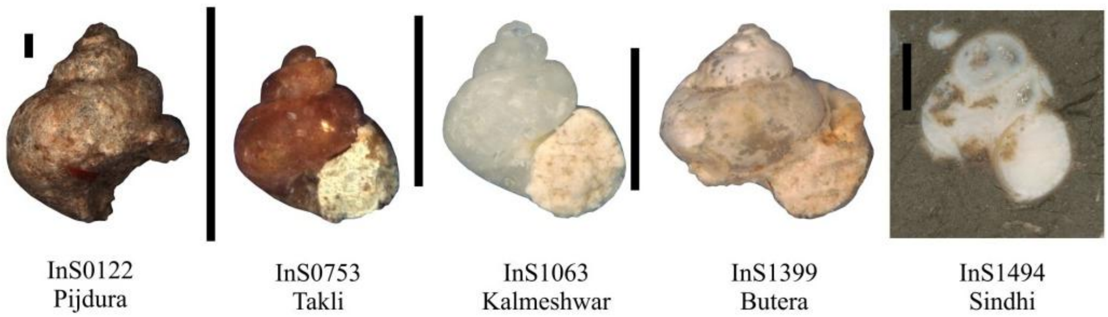

Figure 49. Changes in *Bellamya normalis.* Scale bar is 1 mm.

CHAPTER VII

CONCLUSIONS

Between Sowerby and Hislop, 35 species of continental mollusks (gastropods [28 species] and bivalves [7 species]) were identified in the Deccan Trap sedimentary sequence. Sowerby and Hislop placed the 28 gastropod species into six families that are Viviparidae (12 species), Thiaridae (2 species), Valvatidae (4 species), Succinidae (1 species), Lymnaeidae (6 species), and Physidae (3 species) (Table 7). The analyses indicate that at least seven of these original species are no longer considered valid taxa (i.e., *Viviparus wapsharei*, *V. deccanensis*, *V. takliensis*, *V. acicularis*, *V. rawesi*, *Thiara hunteri*, and *Valvata decollata*), three need revision (*V. soluta*, *Valvata minima*, and *Succinea nagpurensis*) that was not included in this analysis, and three families, including one terrestrial, and one genus were revised to a more accurate taxonomic status. Furthermore, three new species and four new subspecies were identified and described. From this current study, there are now 23 species (plus three that still need revision) in seven families (Succinidae in revision). The revised family Pomatiopsidae includes four species, the family Thiaridae includes one species, the family Lymnaeidae includes six species with a questionable seventh, the revised family Planorbidae includes two species, the revised terrestrial family Subulinidae includes three species, the family Valvatidae includes three species, and the family Viviparidae includes two species (Table 7).

Table 7. List of historic and revised nomenclature, including revised family and new genus and species names.

Morphotype	Revised Family	Historic Nomenclature	Revised Nomenclature	New Species
hydA	Pomatiopsidae	*Paludina virapai*	*Tricula virapai*	
hydB		*Paludina conoidea*	*Tricula conoidea*	*Tricula conoidea conoidea*
hydB		*Paludina takliensis*		*Tricula conoidea hislopi*
hydC		*Paludina sankeyi*	*Tricula sankeyi*	
hydD	Thiaridae	*Melania quadrilineata*	*Thiara quadrilineata*	
		Melania hunteri	*Not valid species	
lymA	Lymnaeidae	*Limnea oviformis*	*Lymnaea oviformis*	
lymC		*Limnea subulata*	*Lymnaea subulata*	
lymD		*Limnea attenuata*	*Lymnaea attenuata*	
lymE		*Limnea telankhediensis radiolus*	*Lymnaea telankhediensis radiolus*	
lymE		*Limnea telankhediensis peracuminata*	*Lymnaea telankhediensis peracuminata*	
lymF		*Limnea spina*	*Lymnaea*? *spina*	
lymB				*Lymnaea pokhariensis*
phyB	Planorbidae	*Physa (Platyphysa) prinsepii normalis*	*Platyphysa prinsepii normalis*	
phyB		*Physa (Platyphysa) prinsepii inflata*	*Platyphysa prinsepii normalis*	
phyA		*Physa (Platyphysa) prinsepii elongata*	*Platyphysa prinsepii elongata*	
styB	Subulinidae	*Paludina subcylindracea*	*Subulina subcylindracea*	
styC		*Paludina pyramis*	*Subulina pyramis*	
styA				*Zootecus burji*
		Paludina acicularis	*Not valid species	
		Paludina rawesi	*Not valid species	
	Succinidae	*Succinea nagpurensis*	*Needs revision	
valA	Valvatidae	*Valvata multicarinata*	*Valvata multicarinata*	

Table 7 cont.

Morphotype	Revised Family	Historic Nomenclature	Revised Nomenclature	New Species
valB		*Valvata unicarinifera*	*Valvata unicarinifera*	*Valvata unicarinifera unicarinifera*
valB				*Valvata unicarinifera chiknaformis*
		Valvata decollata	*Valvata multicarinata*	
		Valvata minima	*Needs revision	
vivB	Viviparidae	*Paludina normalis*	*Bellamya normalis*	
vivA				*Bellamya lattooformis*
		Paludina wapsharei	*Not valid species	
		Paludina deccanensis	*Not valid species	
		Paludina soluta	*Needs revision	

There is no change or trend in the number of species in the faunule at each locality through time as supported by the χ^2 analyses. Takli, Kalmeshwar, and Butera all have fourteen of the sixteen species present while Pijdura and Sindhi, despite the reduced amount of processed material, have nine and eight species, respectively. Therefore there is no evidence to support volcanism or any other environmental or other condition had an effect on molluscan diversity through the Deccan sequence. The species abundance, however, does change between the localities. Kalmeshwar and Takli have the greatest number of specimens, which is likely a result of the quality of preservation. Despite the statistical significant difference in abundance, there is no distinct trend over time. This is likely due to the varying amounts of material able to be collected and processed for specimens and/or the conditions for inhabitability and fossilization in the localities.

Collectively, species size changes through time, with the exception of the “hydD,” “lymA,” and the three terrestrial morphologies. Species begin noticeably larger in the infratrappean Pijdura before the onset of volcanism. In some cases, specimens of the same species average about two to three times greater in size at Pijdura (e.g., “phyB” at Pijdura is 40 mm long, while 15 mm in Butera). In intertrappean 1 sediments, the species size is decreased dramatically to microsnail level. The species that exist at Takli appear to be equivalent in morphology to those in Pijdura only reduced in size (e.g., the average height of “vivB” in Pijdura is 9 mm, while Takli is only 1.4 mm). This decline in species size after the onset of volcanism is consistent throughout most species and could be described as dwarfing of the molluscan population. There is a slight consistent increase in size in most species throughout the remainder of the stratigraphic sequence, but species never obtain equivalent sizes as Pijdura.

The morphology of certain species changes through the sequence (i.e., “hydB,” “lymC,” and both planorbid and viviparid species), but this is likely not the result of volcanism due to the lack of an obvious pattern to these changes. Generally, through the sequence the size of species changes but not their morphology; however it is not certain that this is the result of volcanism. More research is needed before an accurate correlation between volcanism and molluscan morphology can be made.

Also to be considered when addressing the effects of volcanism on the molluscan population is the intermixing of some species of micro- and macrosnails (e.g., “phyB” occurs as both types in Takli, Kalmeshwar, and Butera). Despite intermixing, the microfauna is noticeably predominant in the intertrappean strata. Intermixing may indicate the beginning of a “return to normal conditions” situation in each intertrappean interval before the onset of another lava flow. In this case one would expect to find a few “normal” sized specimens occurring with the dwarfed forms, especially in the upper interval of the intertrappean strata as time progressed. Volcanism as a cause for dwarfism also explains why there are no identified microsnails in the infratrappean Pijdura. The lack of local volcanism in Pijdura would not produce dwarfs to be intermixed.

Overall the results suggest the molluscan population is considered to be “normal” in Pijdura prior to volcanism in the area. After the initial phase of volcanism there is a dramatic reduction in species size in the first intertrappean interval (Takli). After this period species increased slightly with each subsequent intertrappean interval but never fully recovered to “normal” conditions observed at Pijdura. Molluscan diversity remains statistically constant through time suggesting little effect of volcanism. Species abundance changes, but this is most likely not from volcanism due to the lack of an obvious pattern through time.

The molluscan assemblage has not been studied in detail since the mid-1800s and was in need of restudy. This study of the taxonomy, changes through the sequence, and origins of the continental molluscan assemblage has identified several interesting aspects of the Deccan Plateau infra- and intertrappean strata. Cluster analysis assisted in the revision of the current taxonomic status as well as the recognition of new taxa in the molluscan assemblage. Seven continental gastropod families are represented including the terrestrial Subulinidae that was not recognized by Sowerby (1840) and Hislop (1860). This more accurate revised taxonomy is necessary in order to identify patterns in evolution, extinction, and spatial and temporal relationships in the molluscan assemblage. The occurrence of this assemblage just prior to the K/Pg boundary provides a unique window into the analysis of extinction patterns related to the massive Deccan volcanism. Analysis of variance and χ^2 tests demonstrated these changes through the Deccan Trap sequence. There was a dramatic decrease in species size after the initial onset of volcanism, although no pattern in species diversity or abundance is observable. More research is needed before there is a better understanding of the actual relationships between changes in the molluscan population and volcanism. This study provides preliminary insights into how the molluscan assemblage is reacting to volcanism that can be further expanded. There is something happening to these species, which may eventually provide answers to how Deccan Trap volcanism affected the biota.

APPENDICES

Appendix 1. Sowerby (1840) and Hislop (1860) type specimens. Plates 1–6.

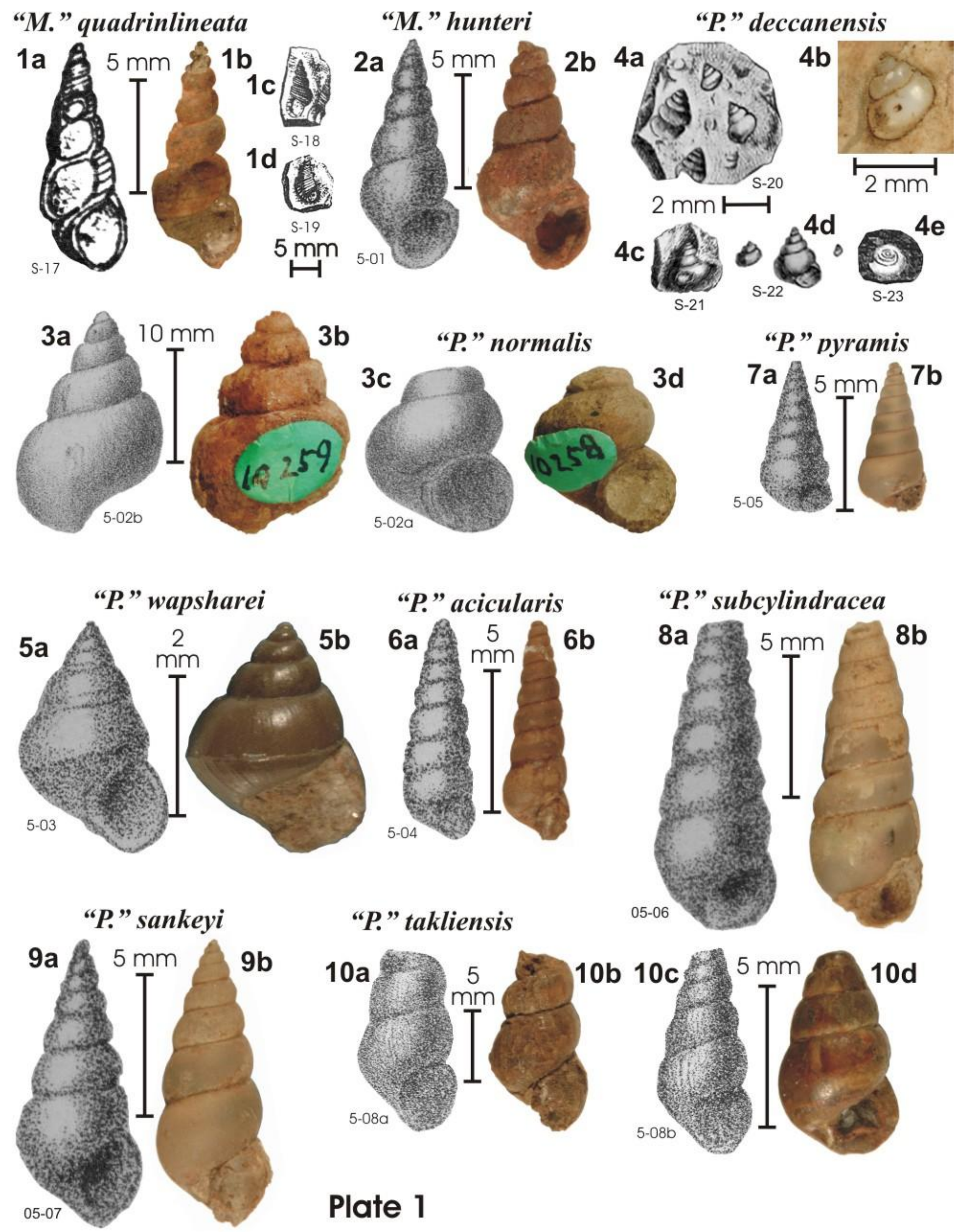

Plate 1

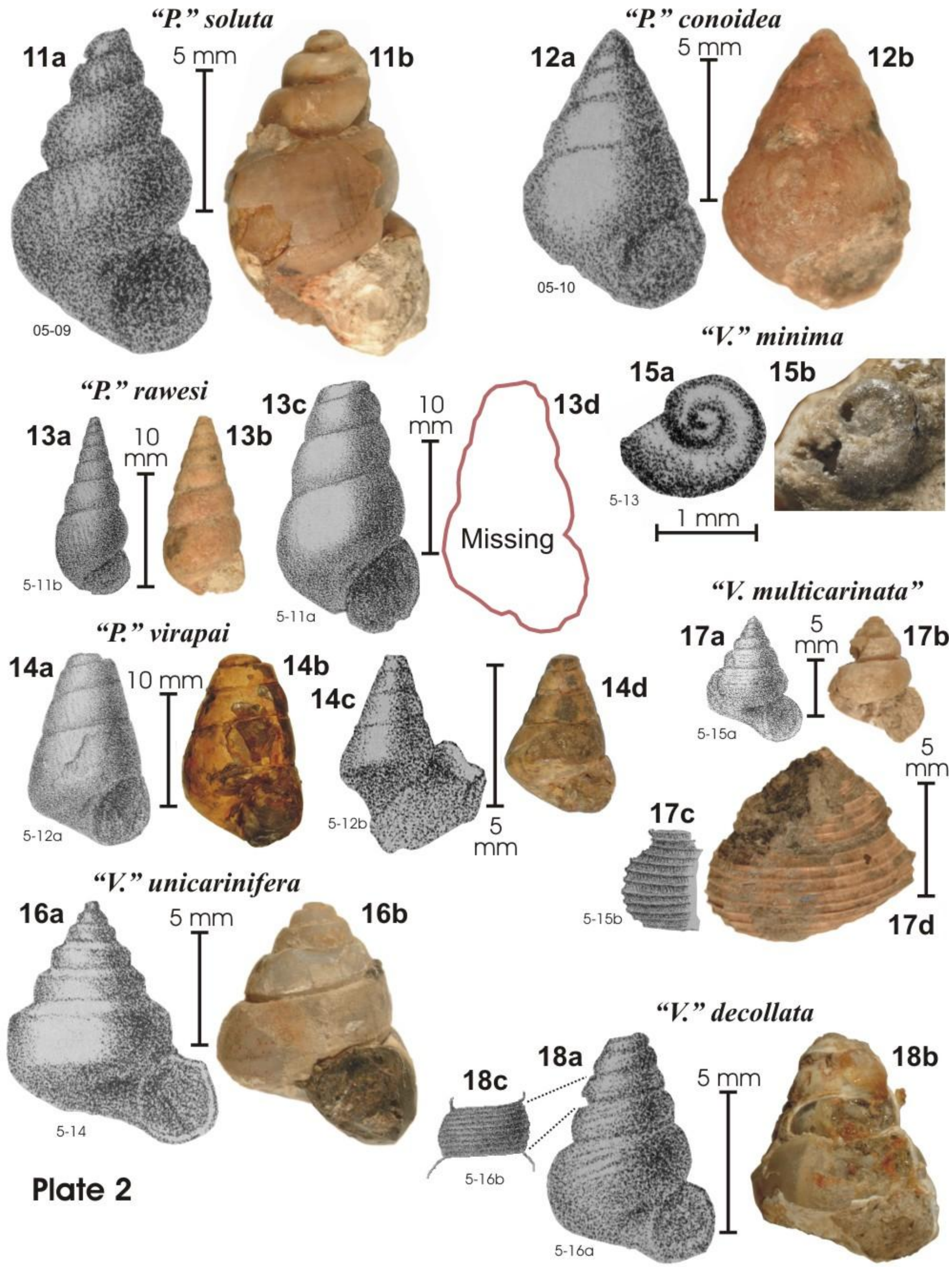
"P." soluta
11a
5 mm
11b
05-09
"P." conoidea
12a
5 mm
12b
05-10
"V." minima
15a
15b
5-13
1 mm
"P." rawesi
13a
10 mm
13b
5-11b
13c
10 mm
13d
Missing
5-11a
"V. multicarinata"
17a
5 mm
17b
5-15a
"P." virapai
14a
10 mm
14b
5-12a
14c
5-12b
5 mm
14d
5 mm
17c
5-15b
17d
"V." unicarinifera
16a
5 mm
16b
5-14
"V." decollata
18a
5 mm
18b
18c
5-16b
5-16a

Plate 2

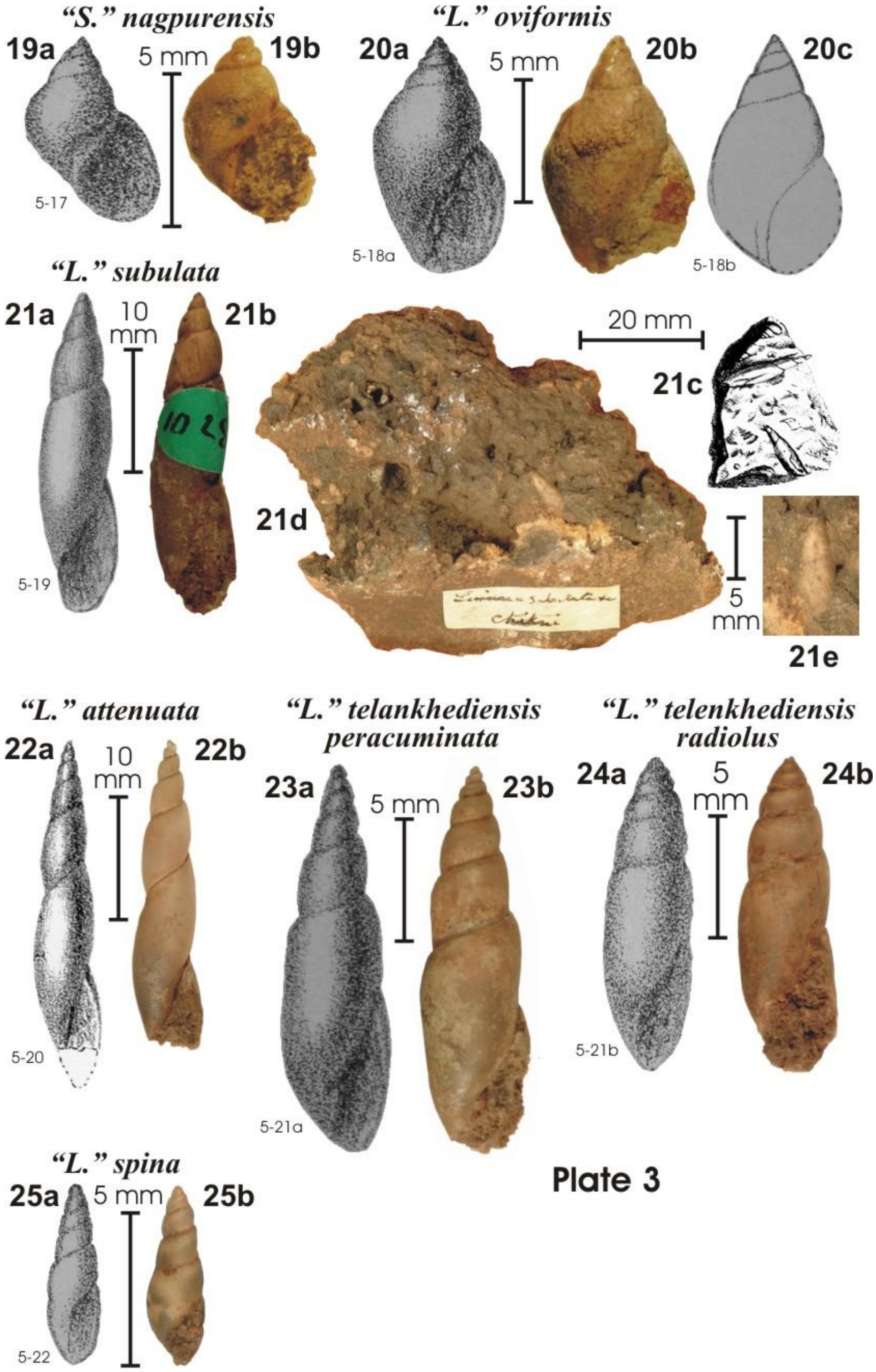
"S." nagpurensis
19a
5 mm
19b
5-17
"L." oviformis
20a
5 mm
20b
20c
5-18a
5-18b
"L." subulata
21a
10 mm
21b
5-19
20 mm
21c
21d
5 mm
21e
"L." attenuata
22a
10 mm
22b
5-20
"L." telankhediensis peracuminata
23a
5 mm
23b
5-21a
"L." telenkhediensis radiolus
24a
5 mm
24b
5-21b
"L." spina
25a
5 mm
25b
5-22

Plate 3

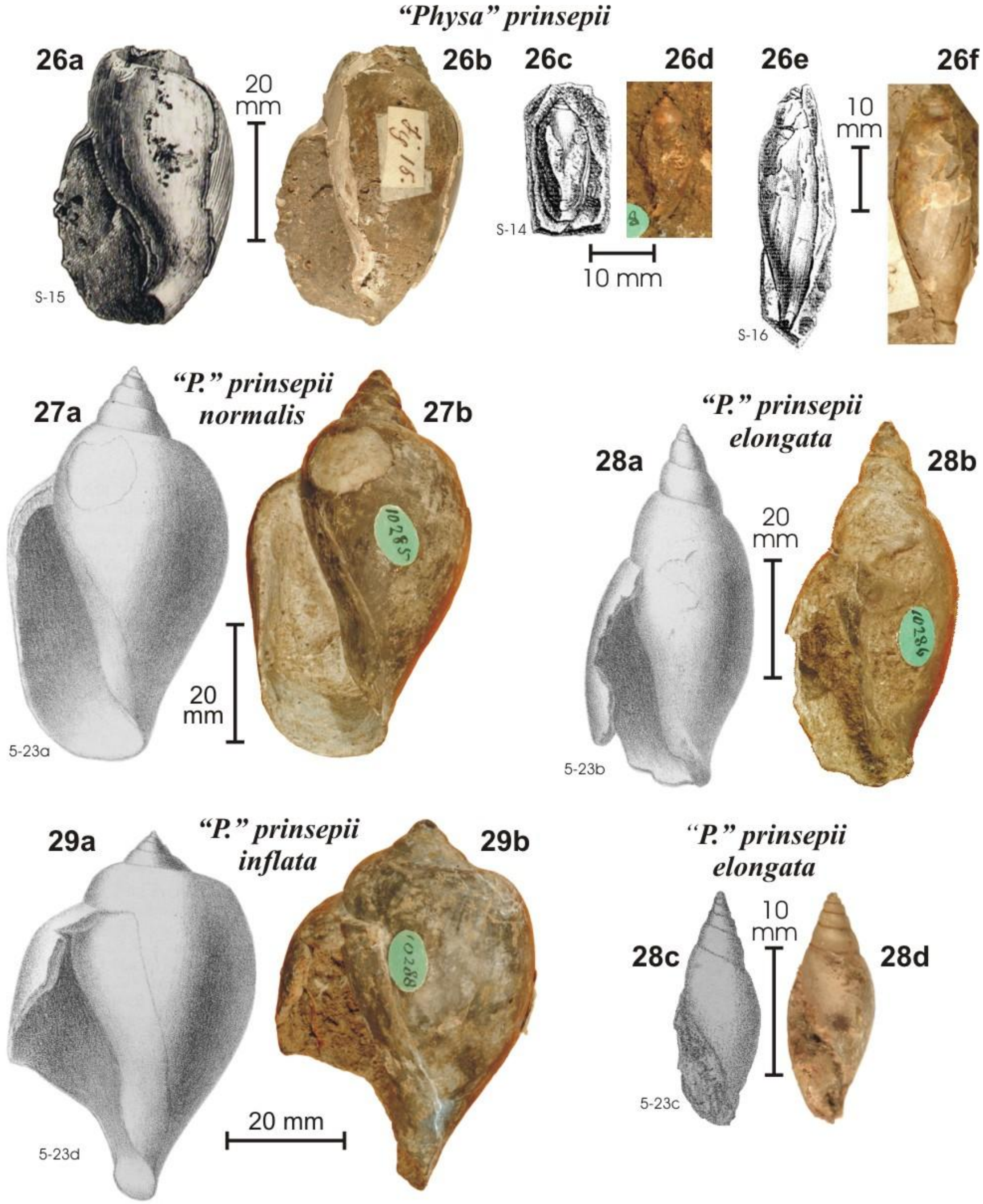
"Physa" prinsepii
26a
20 mm
26b
Fg 16.
S-15
26c
26d
S-14
10 mm
26e
26f
10 mm
S-16
"P." prinsepii normalis
27a
27b
10285
20 mm
5-23a
"P." prinsepii elongata
28a
28b
20 mm
10286
5-23b
"P." prinsepii inflata
29a
29b
10288
20 mm
5-23d
"P." prinsepii elongata
10 mm
28c
28d
5-23c

Plate 4

"Unio" malcolmsoni (Unio tumida of Sowerby*)*

"Unio" deccanensis

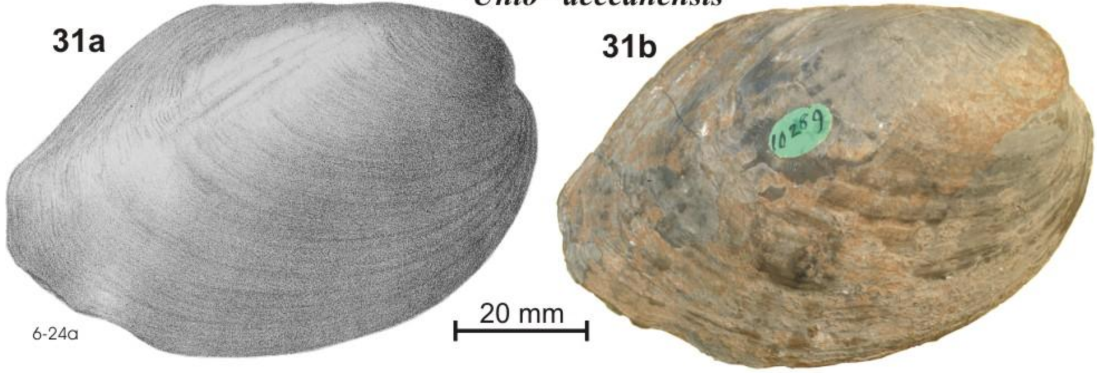

"Unio" hunteri

"Unio" mamillatus

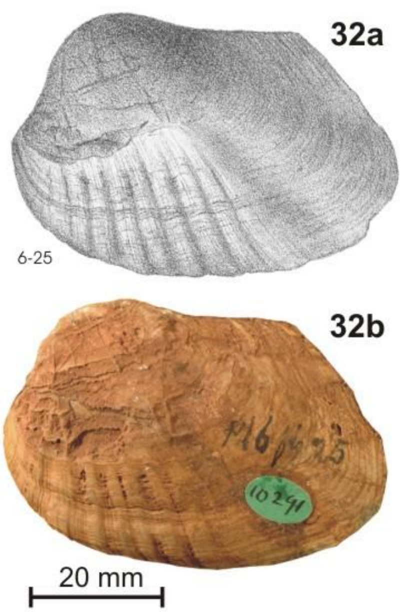

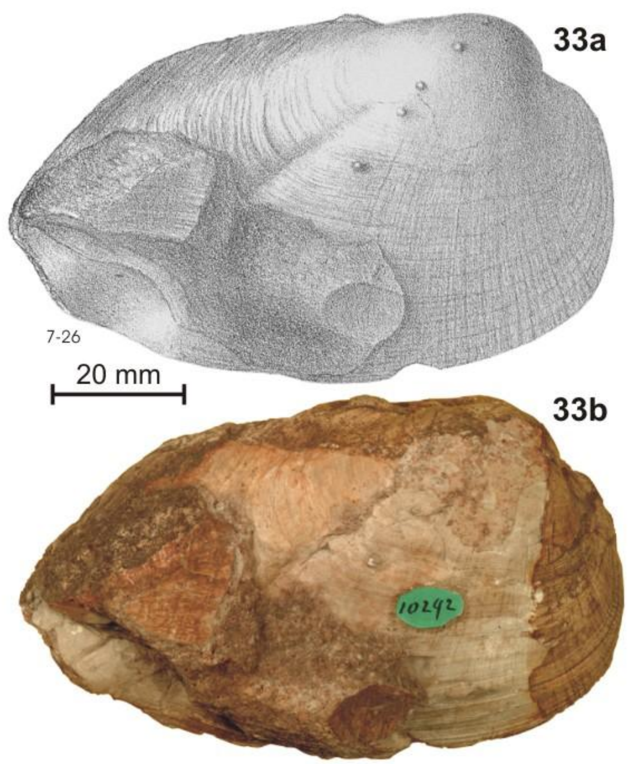

Plate 5

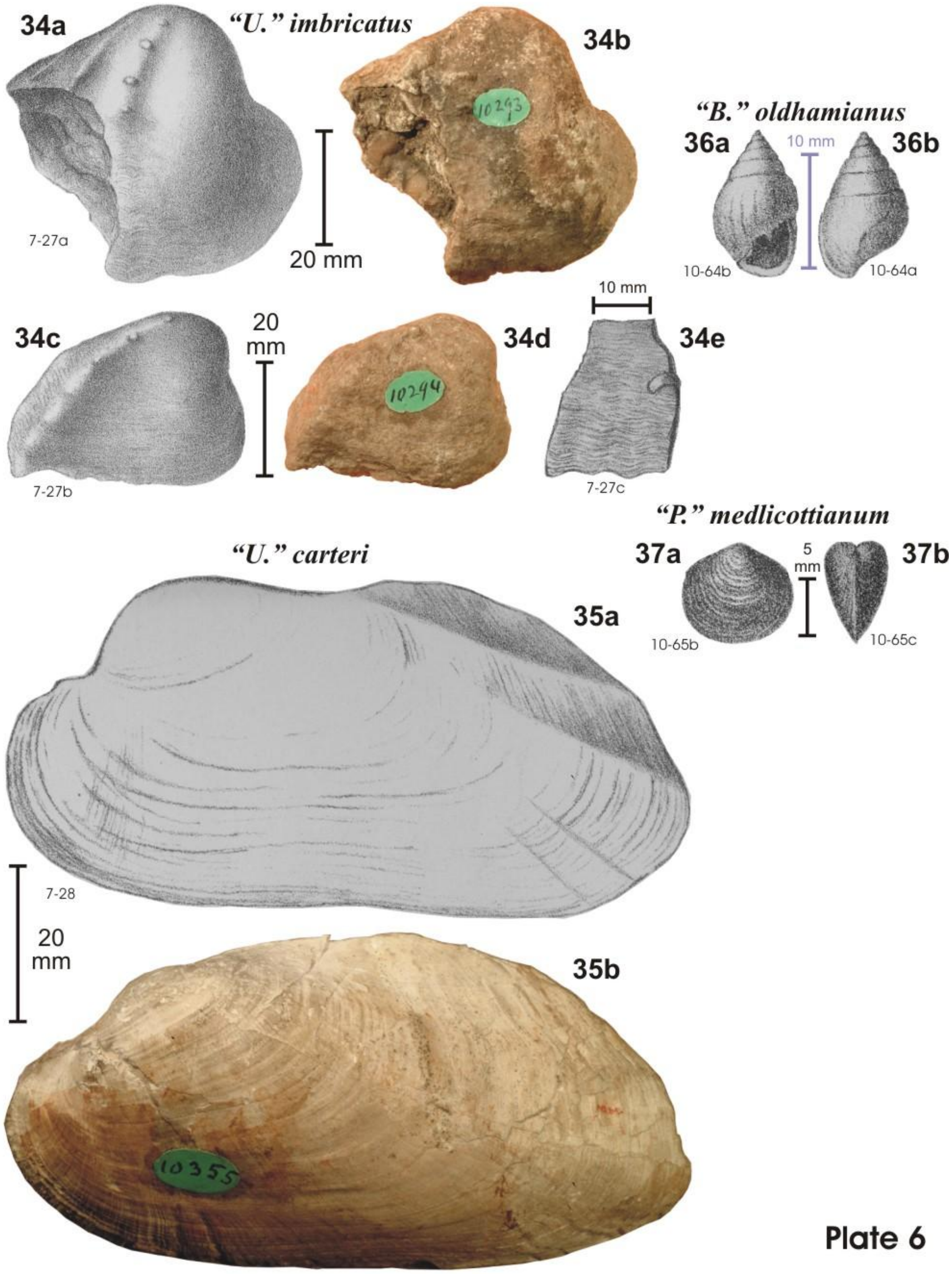

34a
"U." imbricatus
34b
10293
20 mm
7-27a
"B." oldhamianus
36a
10 mm
36b
10-64b
10-64a
10 mm
34c
20
mm
34d
10294
34e
7-27b
7-27c
"P." medlicottianum
37a
5
mm
37b
10-65b
10-65c
"U." carteri
35a
7-28
20
mm
35b
10355

Plate 6

Appendix 2. Revised taxonomy of the Deccan Trap gastropods.

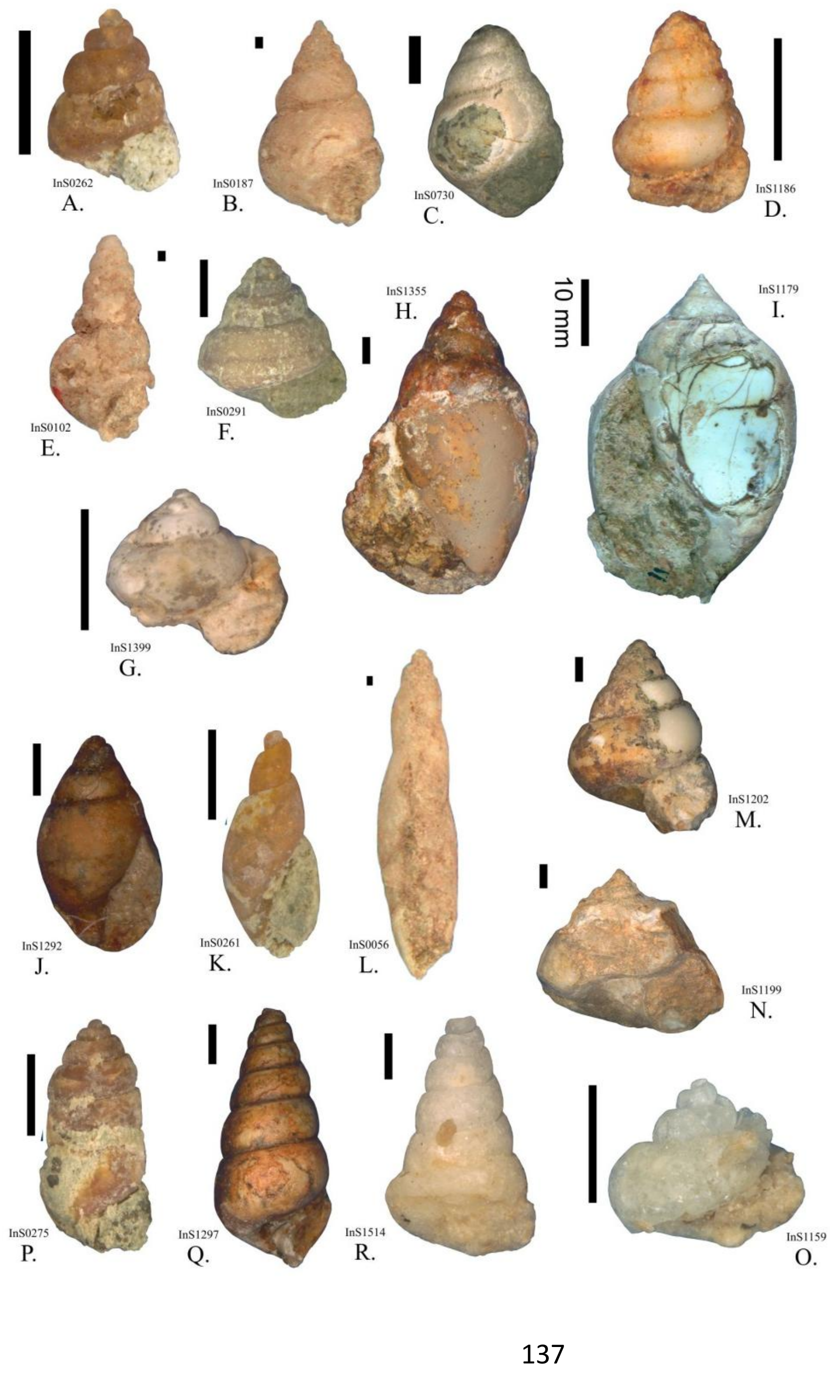

Explanation of plate.

A. *Tricula virapai*
B. *Tricula conoidea conoidea*
C. *Tricula conoidea hislopi* n. subsp.
D. *Tricula sankeyi*
E. *Thiara quadrilineata*
F. *Bellamya lattooformis* n. sp.
G. *Bellamya normalis*
H. *Platyphysa prinsepii elongata*
I. *Platyphysa prinsepii normalis*
J. *Lymnaea oviformis*
K. *Lymnaea pokhariensis* n. sp.
L. *Lymnaea subulata*
M. *Valvata multicarinata*
N. *Valvata unicarinifera unicarinifera*
O. *Valvata unicarinifera chiknaformis* n. subsp.
P. *Zootecus burji* n. sp.
Q. *Subulina subcylindracea*
R. *Subulina pyramis*

Appendix 3. Morphologic trends of each morphoptype.

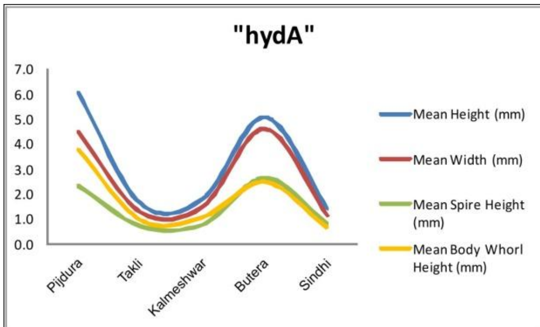

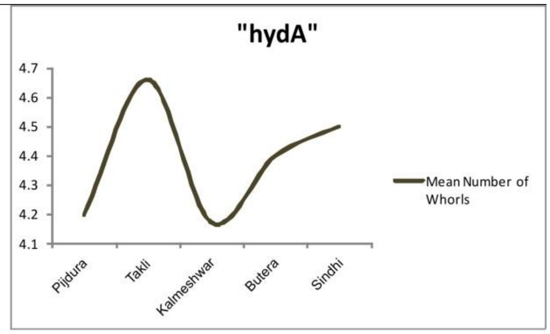

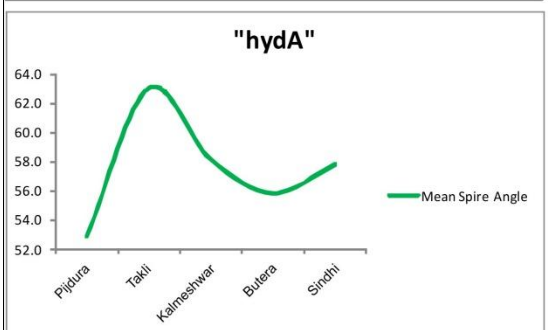

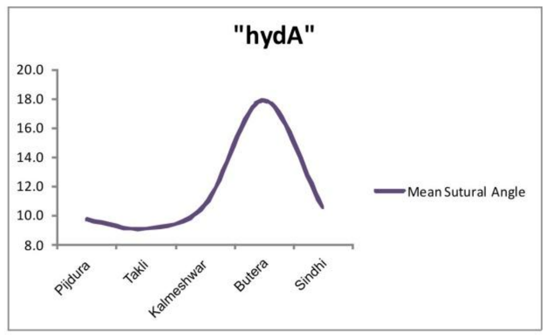

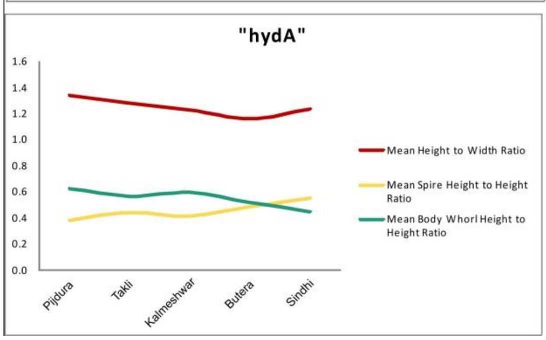

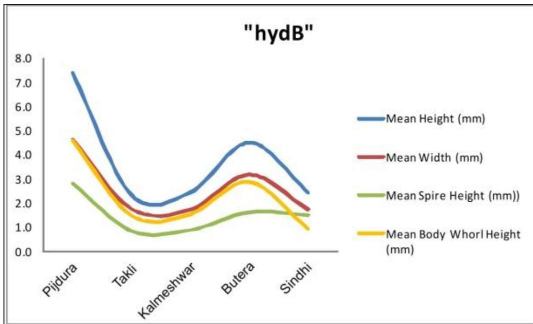
"hydB"
8.0
7.0
6.0
5.0
4.0
3.0
2.0
1.0
0.0
Pijdura
Takli
Kalmeshwar
Butera
Sindhi
Mean Height (mm)
Mean Width (mm)
Mean Spire Height (mm))
Mean Body Whorl Height (mm)

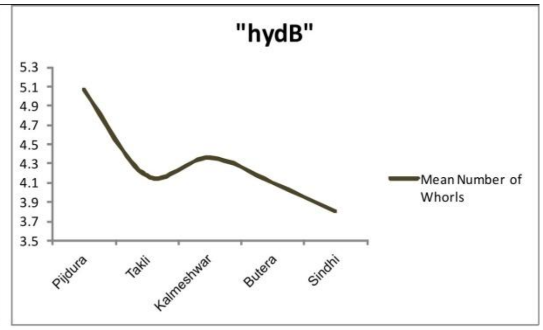
"hydB"
5.3
5.1
4.9
4.7
4.5
4.3
4.1
3.9
3.7
3.5
Pijdura
Takli
Kalmeshwar
Butera
Sindhi
Mean Number of Whorls

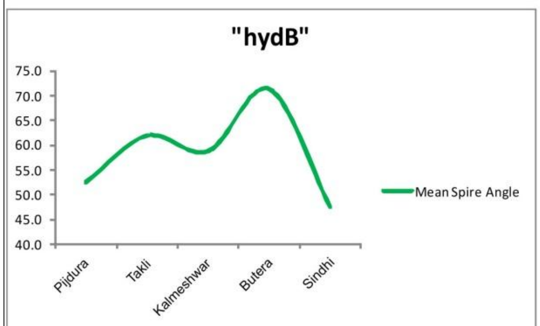
"hydB"
75.0
70.0
65.0
60.0
55.0
50.0
45.0
40.0
Pijdura
Takli
Kalmeshwar
Butera
Sindhi
Mean Spire Angle

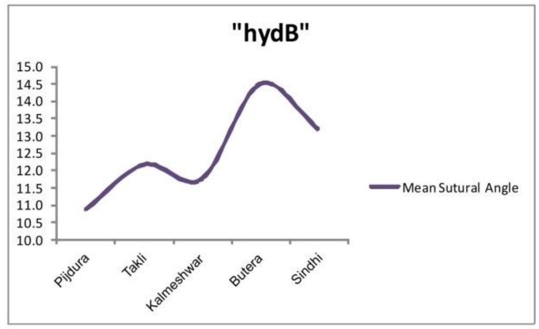
"hydB"
15.0
14.5
14.0
13.5
13.0
12.5
12.0
11.5
11.0
10.5
10.0
Pijdura
Takli
Kalmeshwar
Butera
Sindhi
Mean Sutural Angle

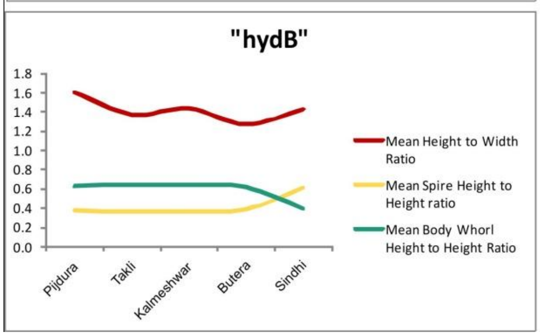
"hydB"
1.8
1.6
1.4
1.2
1.0
0.8
0.6
0.4
0.2
0.0
Pijdura
Takli
Kalmeshwar
Butera
Sindhi
Mean Height to Width Ratio
Mean Spire Height to Height ratio
Mean Body Whorl Height to Height Ratio

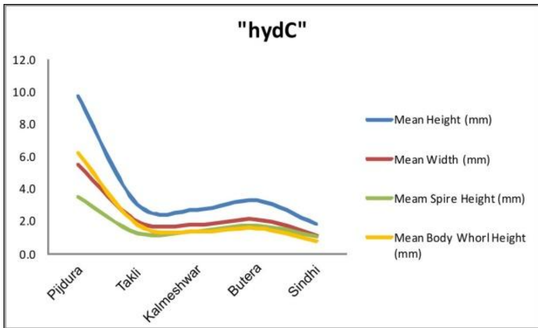
"hydC"
12.0
10.0
8.0
6.0
4.0
2.0
0.0
Pijdura
Takli
Kalmeshwar
Butera
Sindhi
Mean Height (mm)
Mean Width (mm)
Meam Spire Height (mm)
Mean Body Whorl Height (mm)

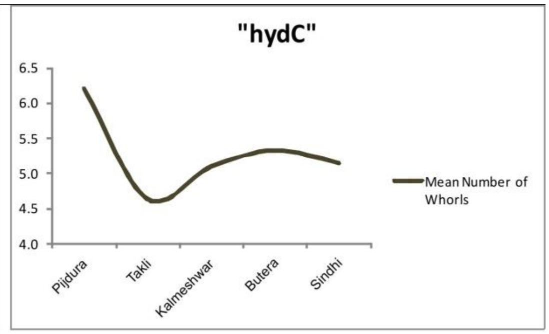
"hydC"
6.5
6.0
5.5
5.0
4.5
4.0
Pijdura
Takli
Kalmeshwar
Butera
Sindhi
Mean Number of Whorls

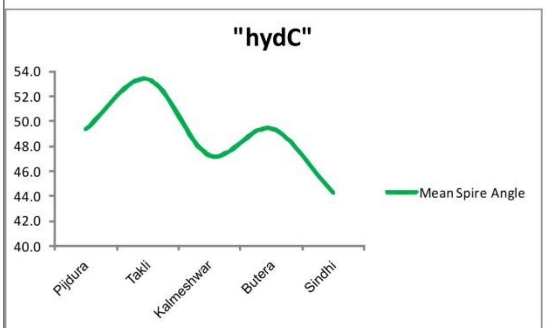
"hydC"
54.0
52.0
50.0
48.0
46.0
44.0
42.0
40.0
Pijdura
Takli
Kalmeshwar
Butera
Sindhi
Mean Spire Angle

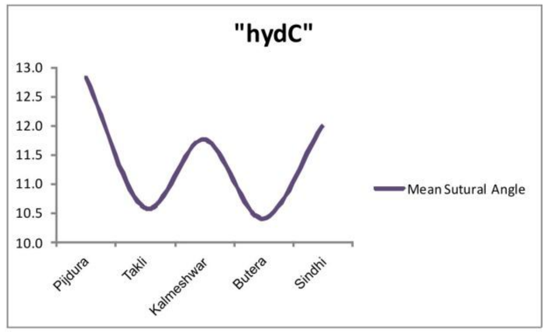
"hydC"
13.0
12.5
12.0
11.5
11.0
10.5
10.0
Pijdura
Takli
Kalmeshwar
Butera
Sindhi
Mean Sutural Angle

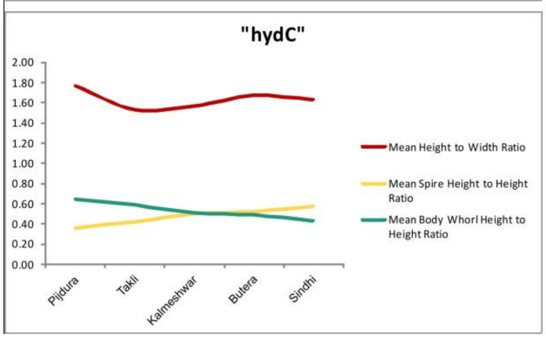
"hydC"
2.00
1.80
1.60
1.40
1.20
1.00
0.80
0.60
0.40
0.20
0.00
Pijdura
Takli
Kalmeshwar
Butera
Sindhi
Mean Height to Width Ratio
Mean Spire Height to Height Ratio
Mean Body Whorl Height to Height Ratio

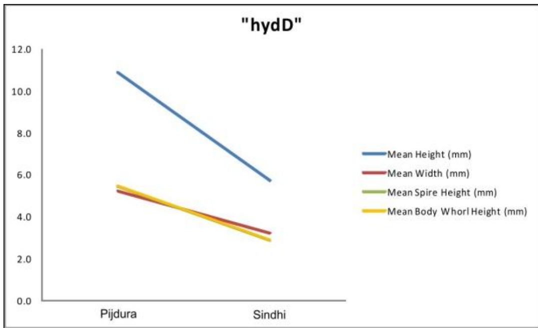
"hydD"
12.0
10.0
8.0
6.0
4.0
2.0
0.0
Pijdura
Sindhi
Mean Height (mm)
Mean Width (mm)
Mean Spire Height (mm)
Mean Body Whorl Height (mm)

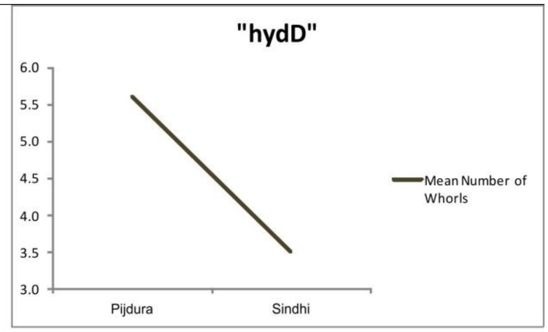
"hydD"
6.0
5.5
5.0
4.5
4.0
3.5
3.0
Pijdura
Sindhi
Mean Number of Whorls

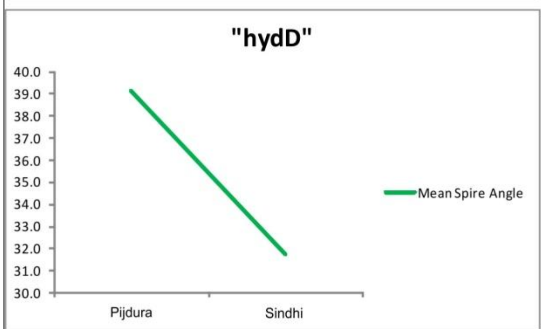
"hydD"
40.0
39.0
38.0
37.0
36.0
35.0
34.0
33.0
32.0
31.0
30.0
Pijdura
Sindhi
Mean Spire Angle

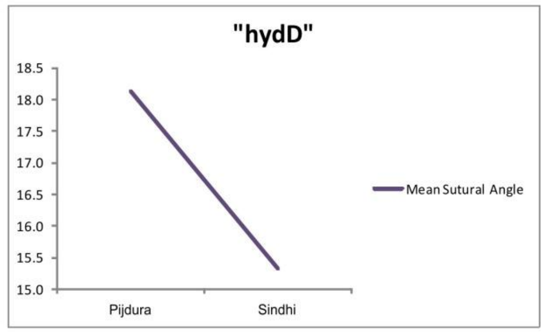
"hydD"
18.5
18.0
17.5
17.0
16.5
16.0
15.5
15.0
Pijdura
Sindhi
Mean Sutural Angle

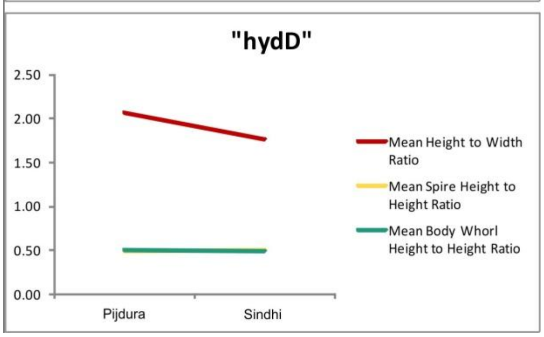
"hydD"
2.50
2.00
1.50
1.00
0.50
0.00
Pijdura
Sindhi
Mean Height to Width Ratio
Mean Spire Height to Height Ratio
Mean Body Whorl Height to Height Ratio

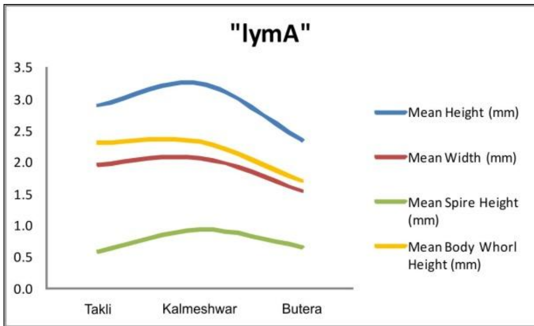
"lymA"
3.5
3.0
2.5
2.0
1.5
1.0
0.5
0.0
Takli
Kalmeshwar
Butera
Mean Height (mm)
Mean Width (mm)
Mean Spire Height (mm)
Mean Body Whorl Height (mm)

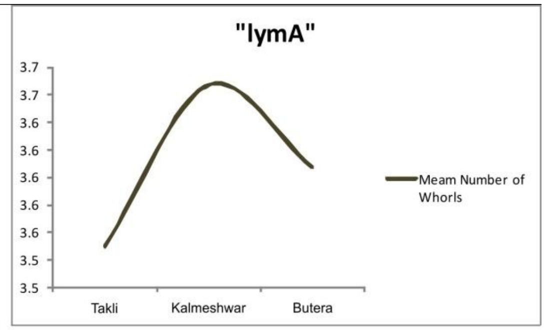
"lymA"
3.7
3.7
3.6
3.6
3.6
3.6
3.6
3.5
3.5
Takli
Kalmeshwar
Butera
Meam Number of Whorls

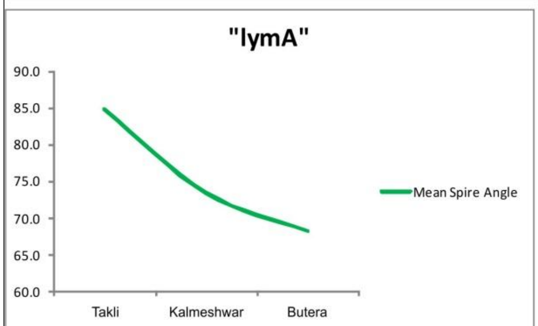
"lymA"
90.0
85.0
80.0
75.0
70.0
65.0
60.0
Takli
Kalmeshwar
Butera
Mean Spire Angle

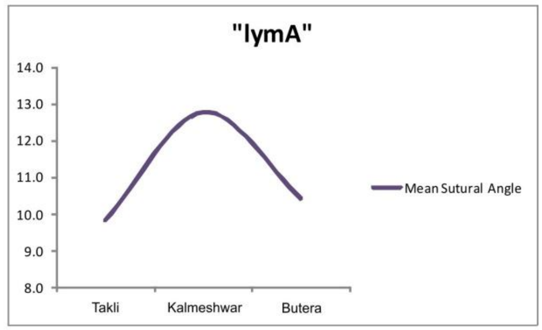
"lymA"
14.0
13.0
12.0
11.0
10.0
9.0
8.0
Takli
Kalmeshwar
Butera
Mean Sutural Angle

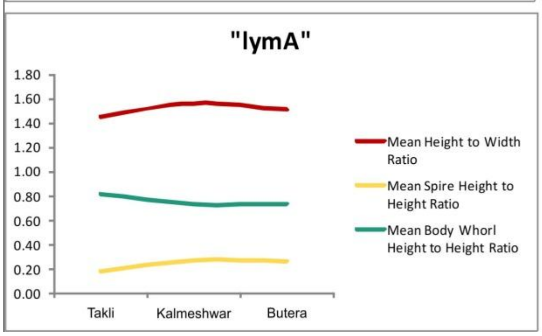
"lymA"
1.80
1.60
1.40
1.20
1.00
0.80
0.60
0.40
0.20
0.00
Takli
Kalmeshwar
Butera
Mean Height to Width Ratio
Mean Spire Height to Height Ratio
Mean Body Whorl Height to Height Ratio

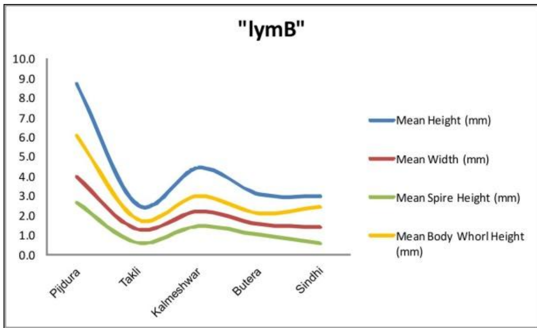
"lymB"
10.0
9.0
8.0
7.0
6.0
5.0
4.0
3.0
2.0
1.0
0.0
Mean Height (mm)
Mean Width (mm)
Mean Spire Height (mm)
Mean Body Whorl Height (mm)
Pijdura
Takli
Kalmeshwar
Butera
Sindhi

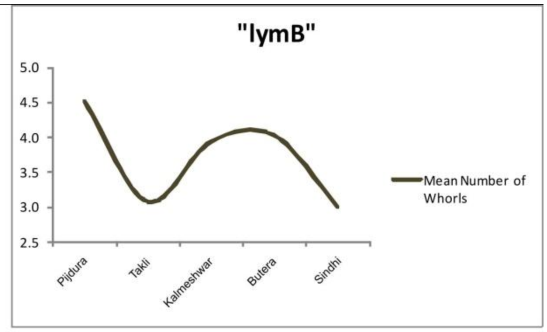
"lymB"
5.0
4.5
4.0
3.5
3.0
2.5
Mean Number of Whorls
Pijdura
Takli
Kalmeshwar
Butera
Sindhi

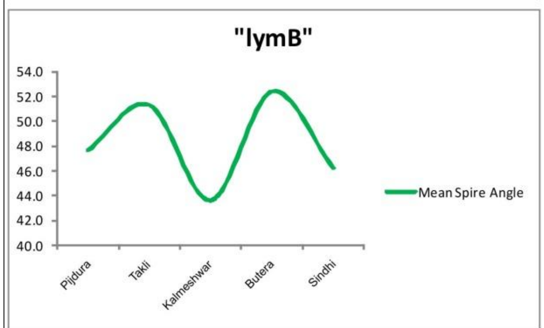
"lymB"
54.0
52.0
50.0
48.0
46.0
44.0
42.0
40.0
Mean Spire Angle
Pijdura
Takli
Kalmeshwar
Butera
Sindhi

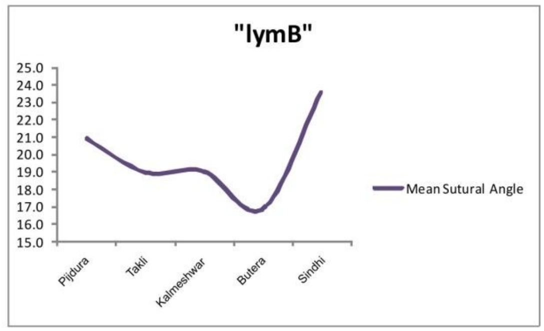
"lymB"
25.0
24.0
23.0
22.0
21.0
20.0
19.0
18.0
17.0
16.0
15.0
Mean Sutural Angle
Pijdura
Takli
Kalmeshwar
Butera
Sindhi

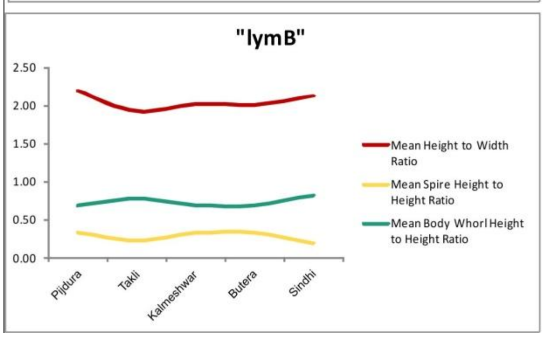
"lymB"
2.50
2.00
1.50
1.00
0.50
0.00
Mean Height to Width Ratio
Mean Spire Height to Height Ratio
Mean Body Whorl Height to Height Ratio
Pijdura
Takli
Kalmeshwar
Butera
Sindhi

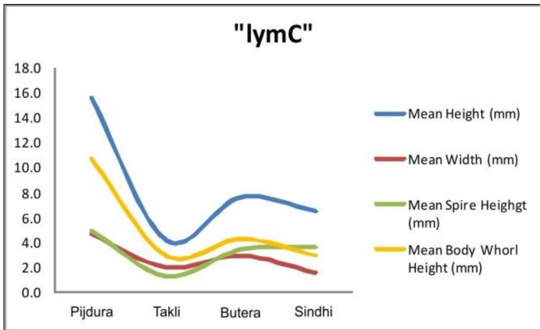
"lymC"
Mean Height (mm)
Mean Width (mm)
Mean Spire Heighgt (mm)
Mean Body Whorl Height (mm)
Pijdura
Takli
Butera
Sindhi

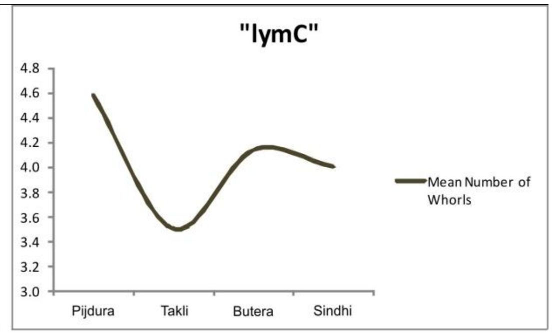
"lymC"
Mean Number of Whorls
Pijdura
Takli
Butera
Sindhi

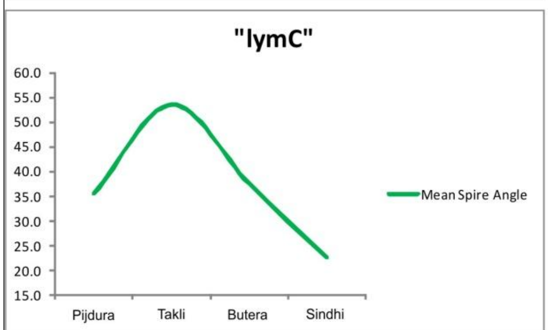
"lymC"
Mean Spire Angle
Pijdura
Takli
Butera
Sindhi

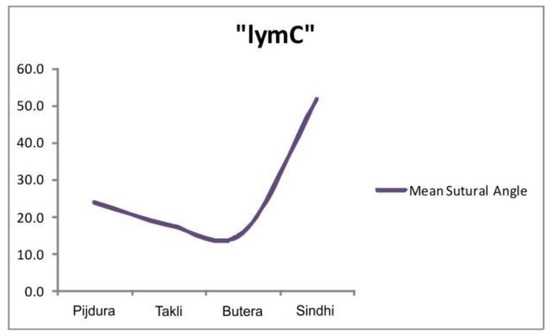
"lymC"
Mean Sutural Angle
Pijdura
Takli
Butera
Sindhi

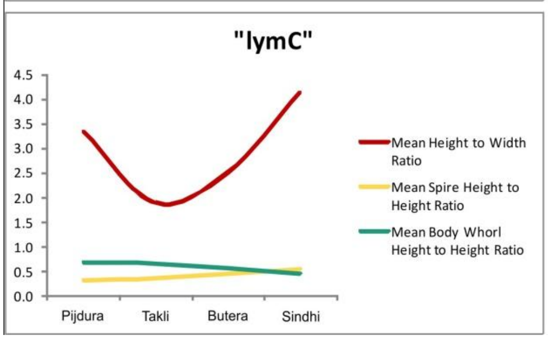
"lymC"
Mean Height to Width Ratio
Mean Spire Height to Height Ratio
Mean Body Whorl Height to Height Ratio
Pijdura
Takli
Butera
Sindhi

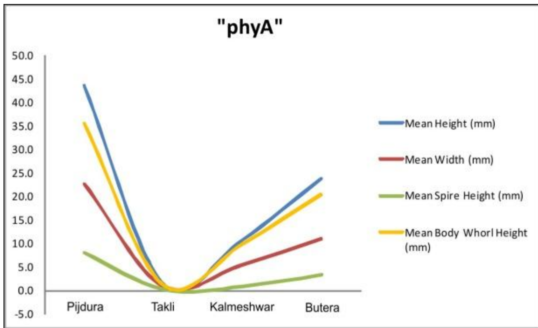
"phyA"
50.0
45.0
40.0
35.0
30.0
25.0
20.0
15.0
10.0
5.0
0.0
-5.0
Pijdura
Takli
Kalmeshwar
Butera
Mean Height (mm)
Mean Width (mm)
Mean Spire Height (mm)
Mean Body Whorl Height (mm)

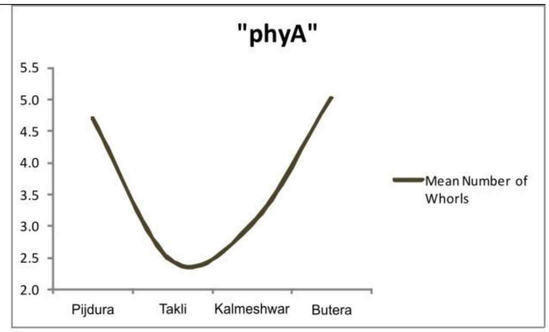
"phyA"
5.5
5.0
4.5
4.0
3.5
3.0
2.5
2.0
Pijdura
Takli
Kalmeshwar
Butera
Mean Number of Whorls

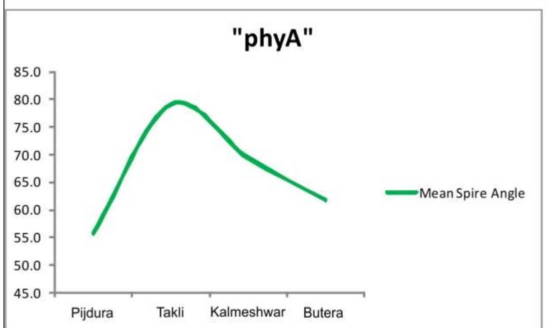
"phyA"
85.0
80.0
75.0
70.0
65.0
60.0
55.0
50.0
45.0
Pijdura
Takli
Kalmeshwar
Butera
Mean Spire Angle

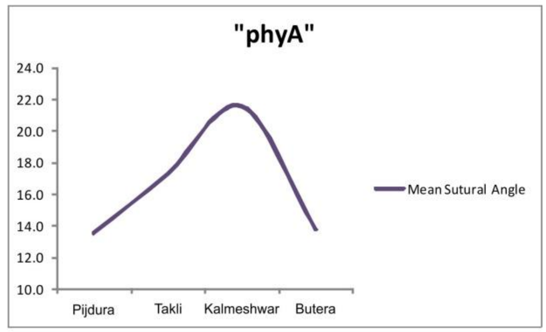
"phyA"
24.0
22.0
20.0
18.0
16.0
14.0
12.0
10.0
Pijdura
Takli
Kalmeshwar
Butera
Mean Sutural Angle

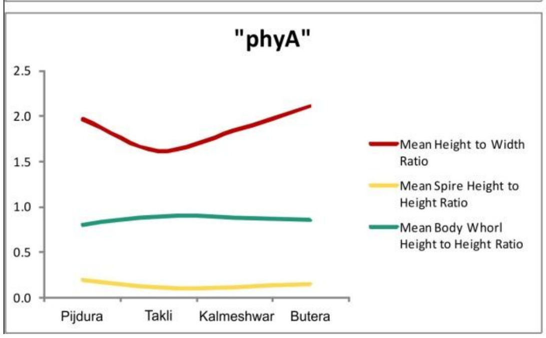
"phyA"
2.5
2.0
1.5
1.0
0.5
0.0
Pijdura
Takli
Kalmeshwar
Butera
Mean Height to Width Ratio
Mean Spire Height to Height Ratio
Mean Body Whorl Height to Height Ratio

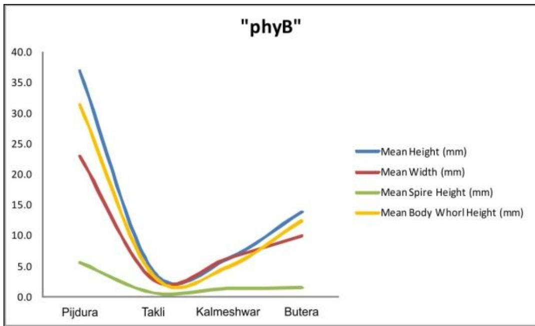
"phyB"
40.0
35.0
30.0
25.0
20.0
15.0
10.0
5.0
0.0
Pijdura
Takli
Kalmeshwar
Butera
Mean Height (mm)
Mean Width (mm)
Mean Spire Height (mm)
Mean Body Whorl Height (mm)

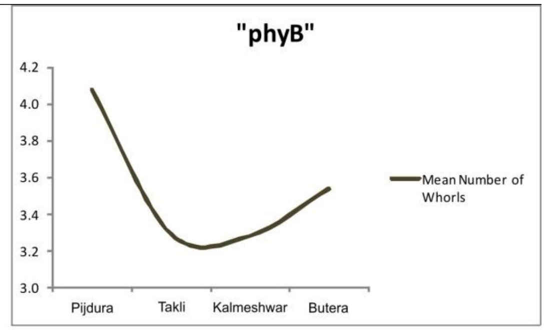
"phyB"
4.2
4.0
3.8
3.6
3.4
3.2
3.0
Pijdura
Takli
Kalmeshwar
Butera
Mean Number of Whorls

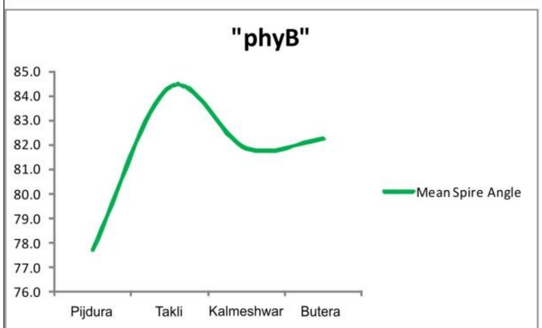
"phyB"
85.0
84.0
83.0
82.0
81.0
80.0
79.0
78.0
77.0
76.0
Pijdura
Takli
Kalmeshwar
Butera
Mean Spire Angle

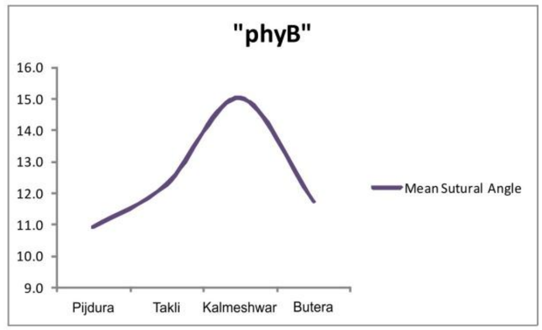
"phyB"
16.0
15.0
14.0
13.0
12.0
11.0
10.0
9.0
Pijdura
Takli
Kalmeshwar
Butera
Mean Sutural Angle

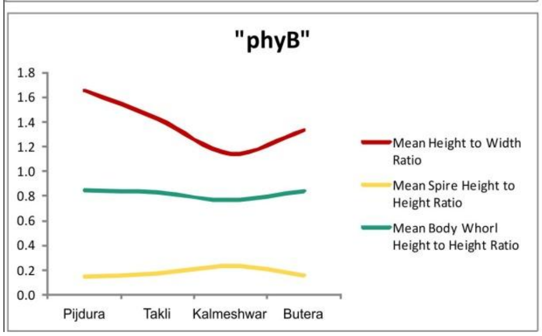
"phyB"
1.8
1.6
1.4
1.2
1.0
0.8
0.6
0.4
0.2
0.0
Pijdura
Takli
Kalmeshwar
Butera
Mean Height to Width Ratio
Mean Spire Height to Height Ratio
Mean Body Whorl Height to Height Ratio

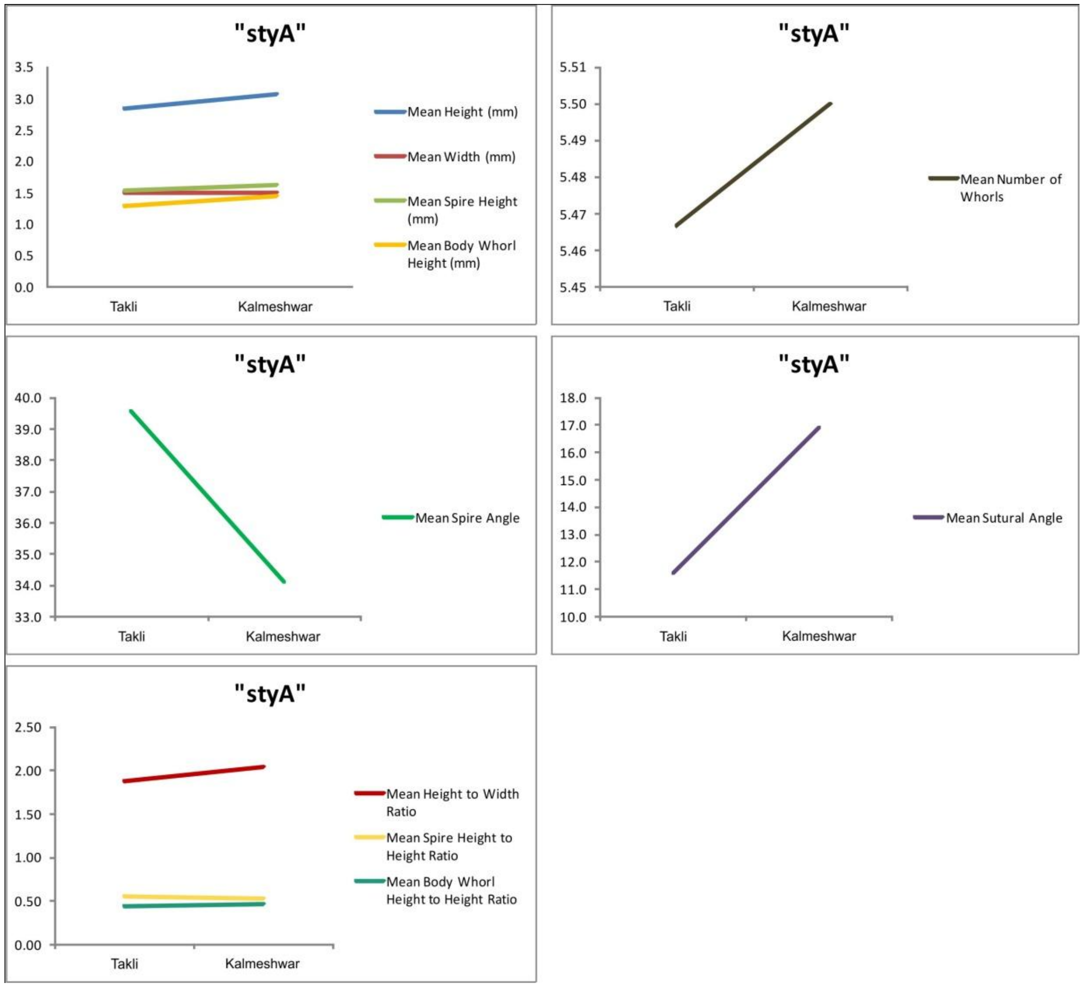

"styA"
Mean Height (mm)
Mean Width (mm)
Mean Spire Height (mm)
Mean Body Whorl Height (mm)
Takli
Kalmeshwar
"styA"
Mean Number of Whorls
Takli
Kalmeshwar
"styA"
Mean Spire Angle
Takli
Kalmeshwar
"styA"
Mean Sutural Angle
Takli
Kalmeshwar
"styA"
Mean Height to Width Ratio
Mean Spire Height to Height Ratio
Mean Body Whorl Height to Height Ratio
Takli
Kalmeshwar

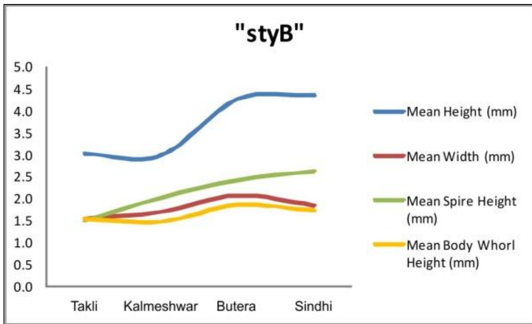
"styB"
5.0
4.5
4.0
3.5
3.0
2.5
2.0
1.5
1.0
0.5
0.0
Takli
Kalmeshwar
Butera
Sindhi
Mean Height (mm)
Mean Width (mm)
Mean Spire Height (mm)
Mean Body Whorl Height (mm)

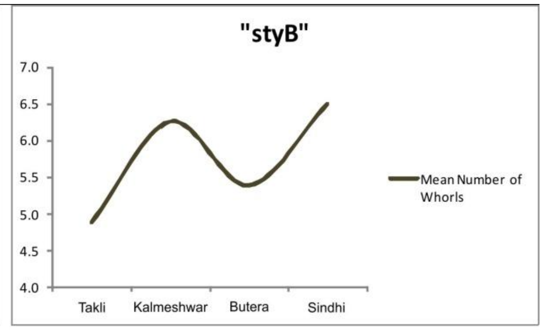
"styB"
7.0
6.5
6.0
5.5
5.0
4.5
4.0
Takli
Kalmeshwar
Butera
Sindhi
Mean Number of Whorls

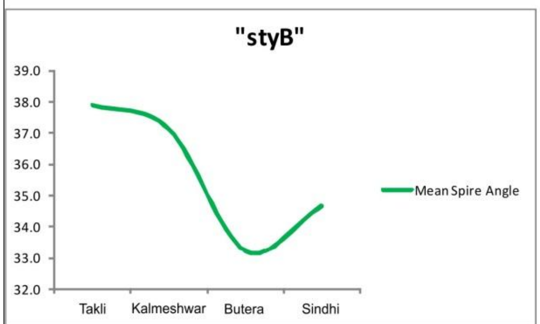
"styB"
39.0
38.0
37.0
36.0
35.0
34.0
33.0
32.0
Takli
Kalmeshwar
Butera
Sindhi
Mean Spire Angle

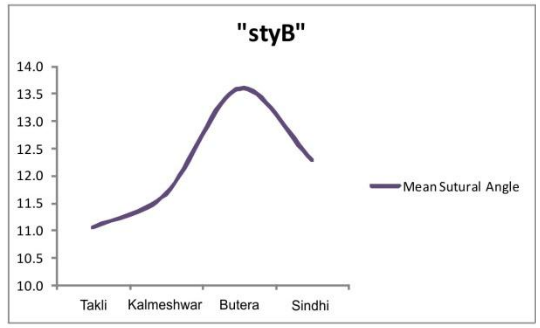
"styB"
14.0
13.5
13.0
12.5
12.0
11.5
11.0
10.5
10.0
Takli
Kalmeshwar
Butera
Sindhi
Mean Sutural Angle

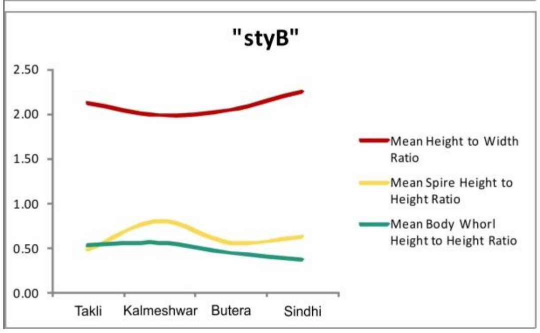
"styB"
2.50
2.00
1.50
1.00
0.50
0.00
Takli
Kalmeshwar
Butera
Sindhi
Mean Height to Width Ratio
Mean Spire Height to Height Ratio
Mean Body Whorl Height to Height Ratio

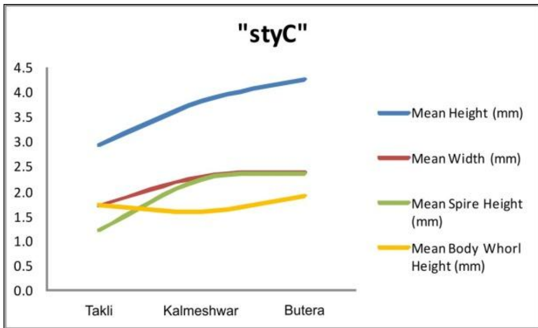
"styC"
4.5
4.0
3.5
3.0
2.5
2.0
1.5
1.0
0.5
0.0
Takli
Kalmeshwar
Butera
Mean Height (mm)
Mean Width (mm)
Mean Spire Height (mm)
Mean Body Whorl Height (mm)

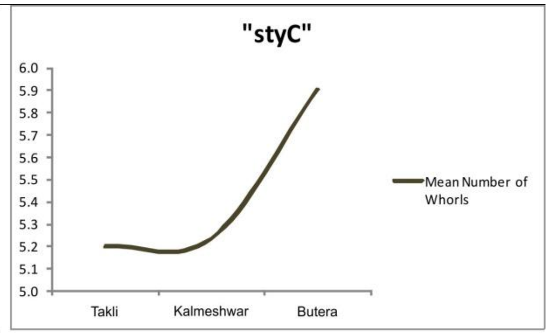
"styC"
6.0
5.9
5.8
5.7
5.6
5.5
5.4
5.3
5.2
5.1
5.0
Takli
Kalmeshwar
Butera
Mean Number of Whorls

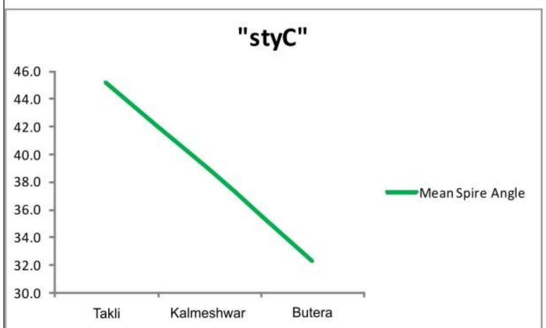
"styC"
46.0
44.0
42.0
40.0
38.0
36.0
34.0
32.0
30.0
Takli
Kalmeshwar
Butera
Mean Spire Angle

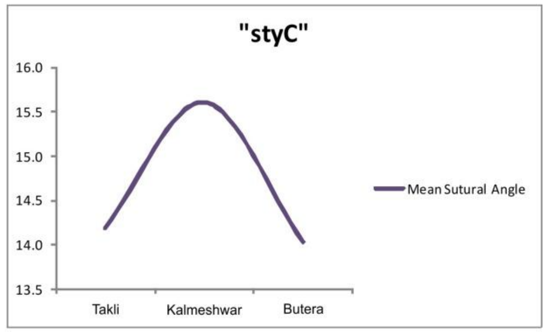
"styC"
16.0
15.5
15.0
14.5
14.0
13.5
Takli
Kalmeshwar
Butera
Mean Sutural Angle

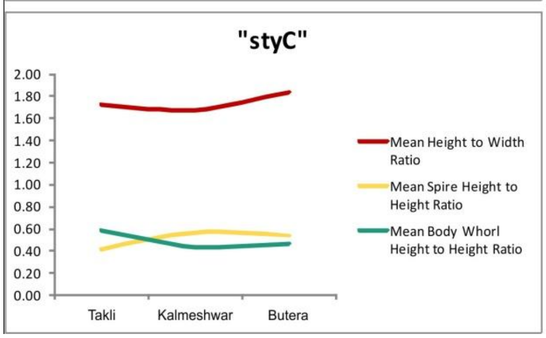
"styC"
2.00
1.80
1.60
1.40
1.20
1.00
0.80
0.60
0.40
0.20
0.00
Takli
Kalmeshwar
Butera
Mean Height to Width Ratio
Mean Spire Height to Height Ratio
Mean Body Whorl Height to Height Ratio

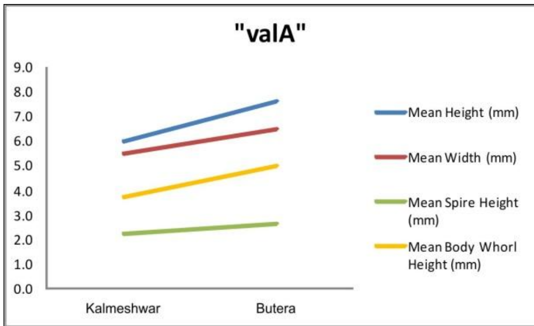
"valA"
9.0
8.0
7.0
6.0
5.0
4.0
3.0
2.0
1.0
0.0
Kalmeshwar
Butera
Mean Height (mm)
Mean Width (mm)
Mean Spire Height (mm)
Mean Body Whorl Height (mm)

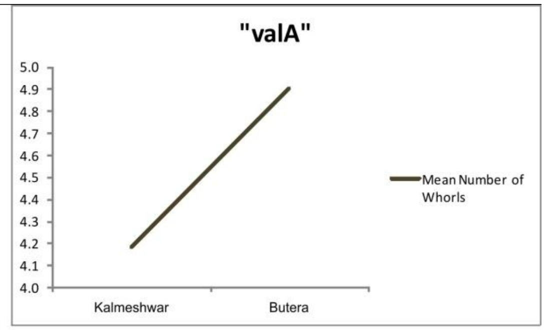
"valA"
5.0
4.9
4.8
4.7
4.6
4.5
4.4
4.3
4.2
4.1
4.0
Kalmeshwar
Butera
Mean Number of Whorls

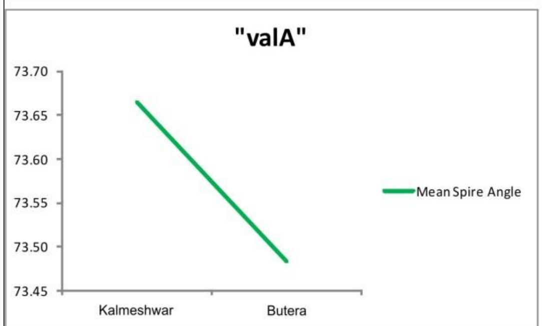
"valA"
73.70
73.65
73.60
73.55
73.50
73.45
Kalmeshwar
Butera
Mean Spire Angle

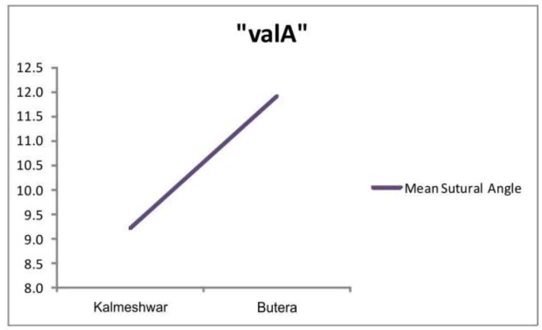
"valA"
12.5
12.0
11.5
11.0
10.5
10.0
9.5
9.0
8.5
8.0
Kalmeshwar
Butera
Mean Sutural Angle

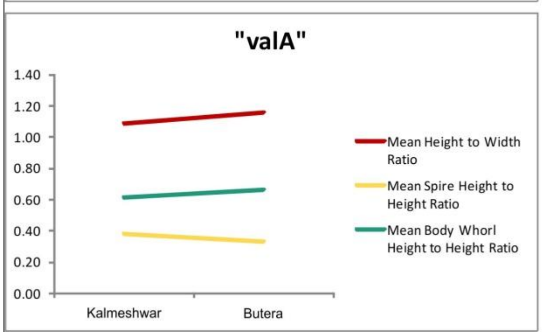
"valA"
1.40
1.20
1.00
0.80
0.60
0.40
0.20
0.00
Kalmeshwar
Butera
Mean Height to Width Ratio
Mean Spire Height to Height Ratio
Mean Body Whorl Height to Height Ratio

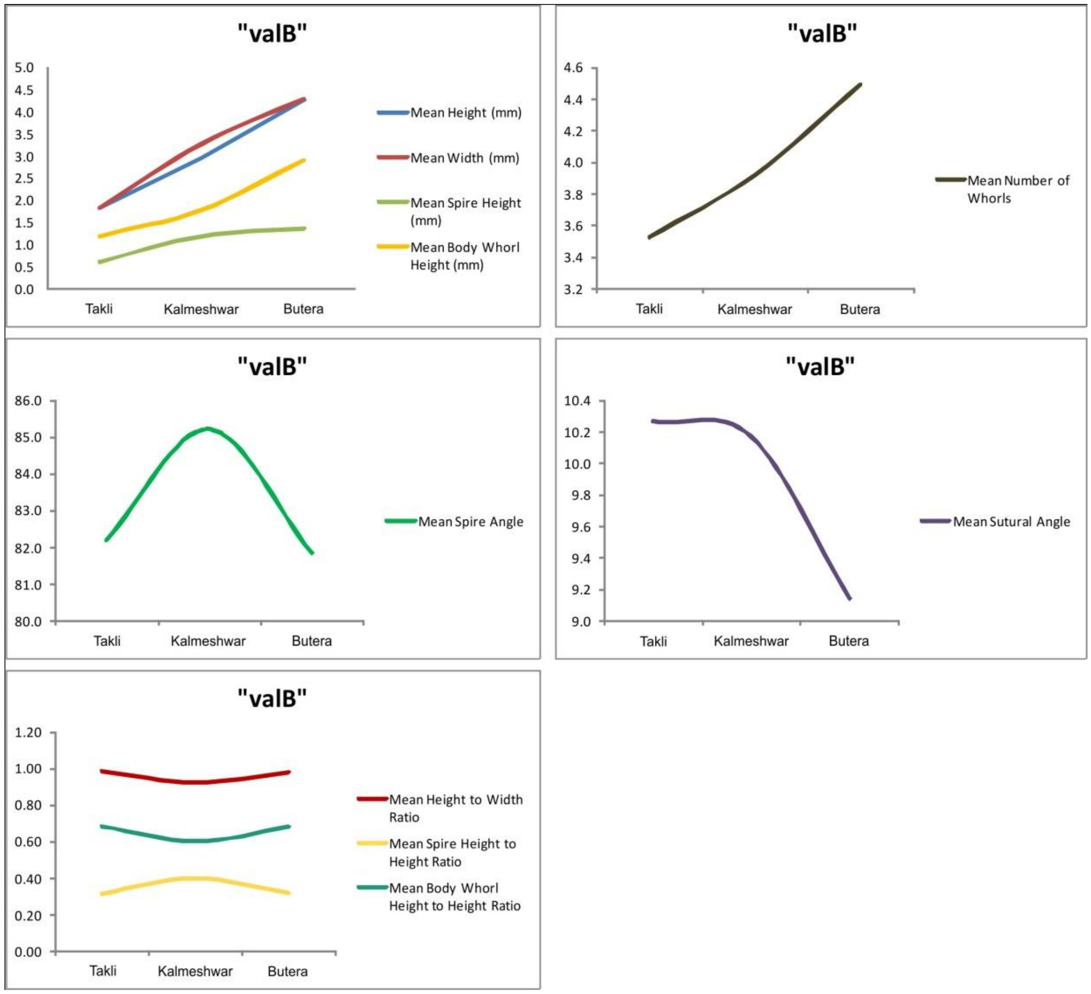
"valB"
Mean Height (mm)
Mean Width (mm)
Mean Spire Height (mm)
Mean Body Whorl Height (mm)
Takli
Kalmeshwar
Butera
"valB"
Mean Number of Whorls
Takli
Kalmeshwar
Butera
"valB"
Mean Spire Angle
Takli
Kalmeshwar
Butera
"valB"
Mean Sutural Angle
Takli
Kalmeshwar
Butera
"valB"
Mean Height to Width Ratio
Mean Spire Height to Height Ratio
Mean Body Whorl Height to Height Ratio
Takli
Kalmeshwar
Butera

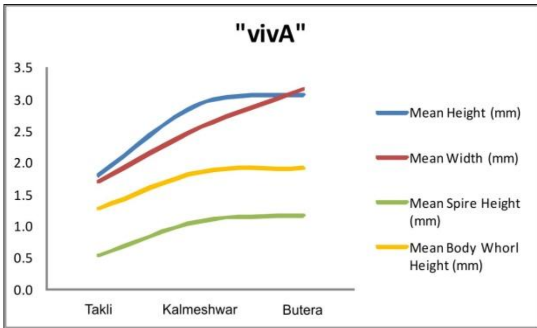
"vivA"
3.5
3.0
2.5
2.0
1.5
1.0
0.5
0.0
Takli
Kalmeshwar
Butera
Mean Height (mm)
Mean Width (mm)
Mean Spire Height (mm)
Mean Body Whorl Height (mm)

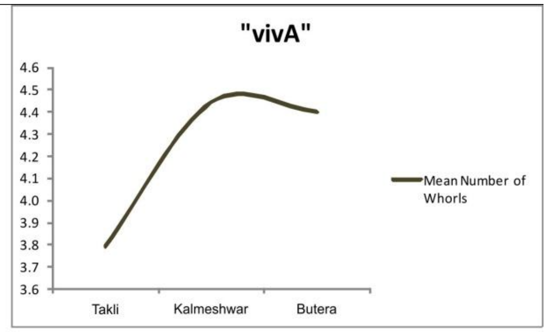
"vivA"
4.6
4.5
4.4
4.3
4.2
4.1
4.0
3.9
3.8
3.7
3.6
Takli
Kalmeshwar
Butera
Mean Number of Whorls

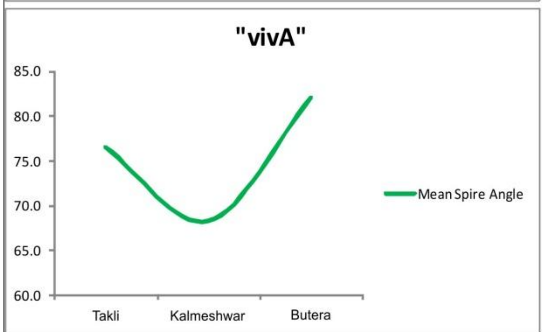
"vivA"
85.0
80.0
75.0
70.0
65.0
60.0
Takli
Kalmeshwar
Butera
Mean Spire Angle

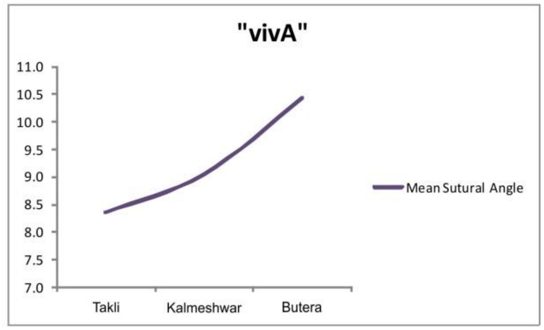
"vivA"
11.0
10.5
10.0
9.5
9.0
8.5
8.0
7.5
7.0
Takli
Kalmeshwar
Butera
Mean Sutural Angle

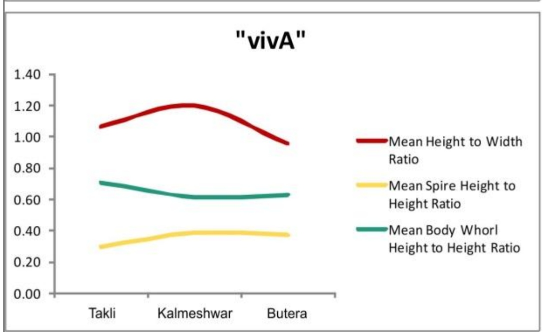
"vivA"
1.40
1.20
1.00
0.80
0.60
0.40
0.20
0.00
Takli
Kalmeshwar
Butera
Mean Height to Width Ratio
Mean Spire Height to Height Ratio
Mean Body Whorl Height to Height Ratio

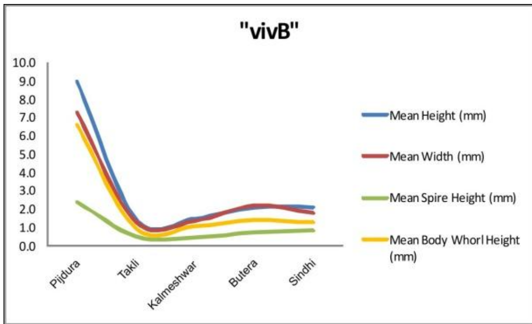
"vivB"
Mean Height (mm)
Mean Width (mm)
Mean Spire Height (mm)
Mean Body Whorl Height (mm)
Pijdura
Takli
Kalmeshwar
Butera
Sindhi

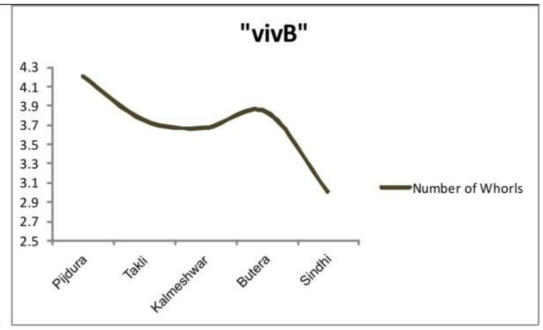
"vivB"
Number of Whorls
Pijdura
Takli
Kalmeshwar
Butera
Sindhi

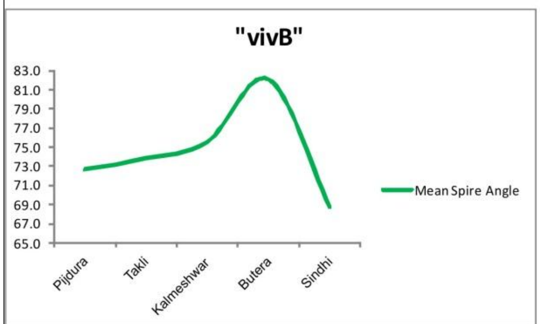
"vivB"
Mean Spire Angle
Pijdura
Takli
Kalmeshwar
Butera
Sindhi

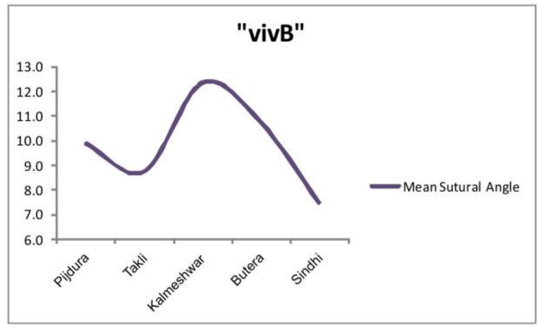
"vivB"
Mean Sutural Angle
Pijdura
Takli
Kalmeshwar
Butera
Sindhi

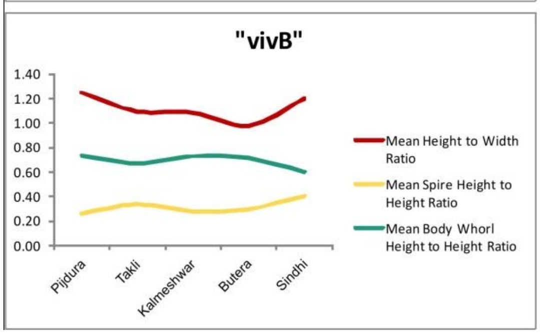
"vivB"
Mean Height to Width Ratio
Mean Spire Height to Height Ratio
Mean Body Whorl Height to Height Ratio
Pijdura
Takli
Kalmeshwar
Butera
Sindhi

Appendix 4. Statistical analyses results.

ANOVA with Ratio Data																		
	Outline Shape			Outline Shape:Height/Width			Whorl Shape			Whorl Shape:Height/Width			Suture Depression			Suture Depression:Height/Width		
	df	F	*p*	df	F	*p*	df	F	*p*	df	F	*p*	df	F	*p*	df	F	*p*
hydA	4,10	0.7841	0.5608	4,1,10	0.0804	0.7826	4,10	0.4254	0.7872	4,2,10	0.6340	0.5505	4,9	2.354	0.1505	4,2,9	2.246	0.1617
hydB	4,70	10.99	<0.0001*	4,5,70	0.5632	0.7278	4,74	10.30	<0.0001*	4,4,74	1.880	0.1229	4,71	9.856	<0.0001*	4,5,71	1.390	0.2383
hydC	4,67	1.063	0.3819	4,3,67	0.6102	0.6107	4,69	1.013	0.4071	4,3,69	0.2959	0.8283	4,66	1.075	0.3761	4,3,66	0.7682	0.5159
hydD	1	X^2=2.400	0.1213															
lymA	2,21	0.1861	0.8316				2,20	0.1798	0.8368	2,1,20	0.0720	0.7912	2,19	0.1733	0.8422	2,1,19	4.128	0.0564
lymB	4,53	1.061	0.3851	4,3,53	0.6351	0.5957	4,54	1.001	0.4154	4,2,54	0.0972	0.9075	4,53	1.068	0.3814	4,1,53	1.498	0.2264
lymC	3,18	8.270	0.0011*				3,16	8.091	0.0017*	3,1,16	1.065	0.3174	3,15	7.692	0.0021*			
phyA	3,24	4.425	0.0130*				3,24	3.960	0.0200*	3,1,24	0.4698	0.4997	3,21	4.019	0.0209*	3,3,21	1.229	0.3242
phyB	3,48	10.35	<0.0001*	3,1,48	0.0378	0.8466	3,44	10.79	<0.0001*	3,4,44	1.431	0.2398	3,40	10.18	<0.0001*	3,6,40	0.9408	0.4769
styA	1,7	1.438	0.2695				1,7	1.248	0.3608				1,6	1.143	0.3262			
styB	3,37	0.3196	0.8111				3,35	0.3209	0.8102	3,2,35	1.440	0.2507	3,32	0.3428	0.7945	3,3,32	2.181	0.1095
styC	2	X^2=0.0952	0.9535															
valA	1,12	1.133	0.8080	1,1,12	0.3228	0.5804	1,13	1.227	0.2881	1,1,13	0.0885	0.7708	1,12	1.199	0.2950	1,1,12	0.4713	0.5054
valB	2,45	0.7124	0.4959	2,1,45	4.225	0.0457	2,43	0.6046	0.5509	2,2,43	0.1273	0.8808	2,42	0.6072	0.5496	2,2,42	0.6984	0.5031
vivA	2,24	10.60	0.0005*	2,2,24	0.2434	0.7858	2,24	6.961	0.0041*	2,2,24	0.8721	0.4309	2,22	7.141	0.0041*	2,2,22	1.258	0.3038
vivB	4,62	0.3038	<0.0001*				4,62	9.910	<0.0001*				4,57	10.80	0.0014*	4,2,57	0.5304	0.7138

ANOVA with Raw Data																		
	Outline Shape			Outline Shape:Height			Whorl Shape			Whorl Shape:Height			Suture Depression			Suture Depression:Height		
	df	F	*p*	df	F	*p*	df	F	*p*	df	F	*p*	df	F	*p*	df	F	*p*
hydA	4,10	26.65	<0.0001*	4,1,10	9.777	0.0108*	4,10	17.40	0.0002*	4,2,10	3.061	0.0918	4,9	20.82	0.0001*	4,2,9	1.341	0.3092
hydB	4,70	35.98	<0.0001*	4,5,70	1.911	0.1034	4,74	73.20	<0.0001*	4,4,74	11.12	<0.0001*	4,71	48.51	<0.0001*	4,5,71	3.254	0.0104*
hydC	4,67	3.935	0.0063*	4,3,67	4.389	0.0070*	4,69	3.726	0.0084*	4,3,69	3.486	0.0202*	4,66	3.659	0.0094*	4,3,66	1.515	0.2188
hydD	1	X^2=2.400	0.1213															
lymA	2	X^2=2.457	0.2927															
lymB	4,53	13.78	<0.0001*	4,3,53	0.9849	0.4070	4,54	12.36	<0.0001*	4,2,54	0.0352	0.9654	4,53	13.54	<0.0001*	4,1,53	2.943	0.1240
lymC	3,18	8.272	0.0011*				3,16	9.250	0.0009*	3,1,16	0.9566	0.3426	3,15	8.326	0.0015*			
phyA	3	X^2=22.72	<0.0001*															
phyB	3	X^2=28.24	<0.0001*															
styA	1,7	0.1441	0.7155				1,7	0.0724	0.7956					0.0651	0.8071			
styB	3,37	2.746	0.0567				3,35	2.655	0.0636	3,2,35	0.2923	0.7484	3,32	2.480	0.0789	3,3,32	0.0308	0.9926
styC	2	X^2=0.8095	0.6671															
valA	1,12	1.505	0.2435	1,1,12	0.5119	0.4880	1,13	1.319	0.2715	1,1,13	1.929	0.1883	1,12	1.529	0.2399	1,1,12	0.4633	0.5090
valB	2,45	4.486	0.0167*	2,1,45	5.621	0.0221*	2,43	5.248	0.0091*	2,2,43	0.8041	0.4541	2,42	8.734	0.0007*	2,2,42	10.59	0.0002*
vivA	2,24	2.713	0.0867	2,2,24	4.267	0.0260*	2,24	2.066	0.1487	2,2,24	0.0467	0.9544	2,22	3.064	0.0670	2,2,22	0.3884	0.6827
vivB	4	X^2=47.90	<0.0001*															

Cluster Analysis with Both Modern and Type Specimens				
	R	df	*p*	
All Specimens	0.706	106489	0.0000	
VivHydStyVal	0.699	49139	0.0000	
VivHydSty	0.674	35243	0.0000	
VivHyd	0.683	23869	0.0000	
Sty	0.680	1223	0.0000	
Val	0.679	944	0.0000	
Lym	0.720	2699	0.0000	
Phy	0.709	2699	0.0000	

Cluster Analysis with Modern Specimens				
	R	df	*p*	
All Specimens	0.704	95264	0.0000	
VivHydStyVal	0.658	44251	0.0000	
VivHydSty	0.671	32383	0.0000	
VivHyd	0.676	21526	0.0000	
Sty	0.759	1126	0.0000	
Val	0.631	818	0.0000	
Lym	0.728	2276	0.0000	
Phy	0.674	2483	0.0000	

Cluster Analysis with Type Specimens				
	R	df	p	
All Specimens	0.708	97901	0.0000	
VivHydStyVal	0.677	44848	0.0000	
VivHydSty	0.668	32129	0.0000	
VivHyd	0.685	22153	0.0000	
Sty	0.651	988	0.0000	
Val	0.673	859	0.0000	
Lym	0.724	2483	0.0000	
Phy	0.719	2483	0.0000	

X^2 Analysis for Changes in Diversity and Abundance					
	X^2	df			
Diversity	5.445	4			
Abundance - mesaured specimens	183.9*	4			
Abundance - mesaured specimens - Sindhi Removed	61.56*	3			
Abundance - identified specimens	486.3*	4			
Abundance - identified specimens - Sindhi Removed	148.5*	3			

X^2 Analysis for Changes in Individual Morphotype Abundance					
	X^2	df			
hydA	9.500*	4			
hydB	38.48*	4			
hydC	56.12*	4			
hydD	6.000	4			
lymA	34.50*	4			
lymB	61.08*	4			
lymC	31.42*	4			
phyA	17.69*	4			
phyB	18.35*	4			
styA	31.00*	4			
styB	30.36*	4			
styC	5.667	4			
valA	32.00*	4			
valB	54.24*	4			
vivA	23.68*	4			
vivB	27.80*	4			

* denotes significance with 95% confidence (α = 0.05)

Appendix 5. Specimens numbered and measured.

InS#	Locality	Morph	Height	Width	SpireH	BWhH	ApertH	ApertW	SutAng	SpAng	ApAng	#Wh	Keel	Umb	SutDep	WhShp	ShShp	Sculpt	Coil Dir
0001	InL009	viv																	Dextral
0002	InL009	viv																	Dextral
0003	InL009	viv																	Dextral
0004	InL009	viv																	Dextral
0005	InL009	viv																	Dextral
0006	InL009	viv																	Dextral
0007	InL009	viv																	Dextral
0008	InL009	viv																	Dextral
0009	InL009	lym																	Dextral
0010	InL009	lym																	Dextral
0011	InL009	lym																	Dextral
0012	InL009	lym																	Dextral
0013	InL009	phy																	Sinistral

0030	0029	0028	0027	0026	0025	0024	0023	0022	0021	0020	0019	0018	0017	0016	0015	0014
InL009	InL009	InL009	InL009	InL009	InL009	InL009	InL009	InL009	InL009	InL009	InL009	InL009	InL009	InL009	InL009	InL009
viv	viv	viv	viv	bivalve	viv	viv	viv	viv	viv	viv	viv	viv	viv	viv	viv	viv
Dextral	Dextral	Dextral	Dextral		Sinistral	Dextral	Dextral	Dextral	Dextral	Dextral	Dextral	Dextral	Dextral	Dextral	Dextral	Dextral

0031	InL009	viv																Dextral
0032	InL009	viv																Dextral
0033	InL009	viv																Dextral
0034	InL009	viv																Dextral
0035	InL009	viv																Dextral
0036	InL009	val																Dextral
0037	InL009	vivB	6.791	5.380	1.556	5.235	3.978	2.994	11.810	73.4	63.642		Yes?	Closed	Strong	Rounded	Trochiform	No	Dextral
0038	InL009	lymB	6.443	3.149	1.852	4.591	3.186	1.676	17.802	49.8	66.318	4.4	No	Closed	Regular	Rounded	Elongate Cylindrical	No	Dextral
0039	InL009	viv																Dextral
0040	InL009	viv																Dextral
0041	InL009	phy																Sinistral
0042	InL009	phy																Sinistral
0043	InL009	phy																Sinistral
0044	InL009	vivB	12.146	8.371	3.015	9.131	6.474	5.326	10.856	61.5	76.891	4.4	No	Closed	Strong	Rounded	Trochiform	No	Dextral
0045	InL009	vivB	13.212	10.515	3.248	9.964	7.647	6.895	6.152	73.3	66.453	4.7	No	Closed	Strong	Rounded	Trochiform	No	Dextral
0046	InL009	viv																Dextral
0047	InL009	vivB	10.636	7.858	3.254	7.382	6.218	5.314	14.349	59.5	63.435		No	Closed	Strong	Rounded	Trochiform	No	Dextral

0064	0063	0062	0061	0060	0059	0058	0057	0056	0055	0054	0053	0052	0051	0050	0049	0048
InL009	InL009	InL009	InL009	InL009	InL009	InL009	InL009	InL009	InL009	InL009	InL009	InL009	InL009	InL009	InL009	InL009
lymC	lymC	lymC	lymC	lymC	lymC	lymC	lymC	lymC	vivB	vivB	vivB	vivB	vivB	vivB	vivB	vivB
11.131	18.013	16.185	12.211	20.826	15.241	17.738	20.586	23.220	10.986	14.251	10.989	9.217	11.284	11.866	11.245	12.277
3.716	5.537	5.116	4.183	5.056	5.030	4.960	5.547	5.763	8.739	10.092	8.371	7.926	9.472	10.323	8.750	10.689
2.686	3.234	3.711	3.586	11.341	4.262	4.887	6.275	6.314	2.176	3.886	2.606	2.227	2.859	2.117	2.816	3.387
8.445	14.779	12.474	8.625	9.485	10.979	12.851	14.311	16.906	8.810	10.365	8.383	6.990	8.425	9.749	8.429	8.890
4.747	9.724	8.686	5.483		7.705			12.003	6.313	7.214	5.916	4.749	6.102	6.131	6.294	7.629
2.666	3.223	3.680	2.907		3.703			4.194	5.775	5.607	6.115	4.561	7.180	6.272	4.755	5.600
9.689	17.103	22.765	13.079	33.232	29.100	24.711	29.560	27.834	5.947	12.529	7.169	5.231	11.583	4.532	13.841	18.652
37.9	43.4	34.9	39.1	32.9	38.5	34.9	43	26.2	78.4	61.7	72.5	76.2	72.7		64.7	70.7
67.380	56.470	75.399	73.474	63.682	75.087	77.925	72.784	71.671	74.636	56.821	66.801	59.421	66.121	60.789	67.203	63.087
5.5	5.2	4.4	4.6	4.8	4.2	4.4	4.7	5.4		5.3	3.4	4.0	4.2			4.1
No	No	No	No	No	No	No	No	No	No	No	No	No	No	No	No	No
Closed	Closed	Closed	Closed	Closed	Closed	Closed	Closed	Closed	Closed	Closed	Closed	Closed	Closed	Closed	Closed	Closed
Regular	Regular	Regular	Regular	Regular	Regular	Regular	Some	Regular	Strong	Regular	Strong	Strong	Strong	Strong	Strong	Strong
Rounded	Flattened-Rounded	Rounded	Rounded	Rounded	Rounded	Rounded	Rounded	Rounded	Rounded	Rounded	Rounded	Rounded	Rounded	Rounded	Rounded	Rounded
Elongate Conic	Elongate Conic	Elongate Conic	Elongate Conic	Elongate Conic	Elongate Conic	Elongate Conic	Elongate Conic	Elongate Conic	Trochiform	Ovate-Trochiform	Trochiform	Trochiform	Trochiform	Trochiform	Trochiform	Trochiform
No	No	No	No	No	No	No	No	No	No	No	No	No	No	No	No	No
Dextral	Dextral	Dextral	Dextral	Dextral	Dextral	Dextral	Dextral	Dextral	Dextral	Dextral	Dextral	Dextral	Dextral	Dextral	Dextral	Dextral

0081	0080	0079	0078	0077	0076	0075	0074	0073	0072	0071	0070	0069	0068	0067	0066	0065
InL009	InL009	InL009	InL009	InL009	InL009	InL009	InL009	InL009	InL009	InL009	InL009	InL009	InL009	InL009	InL009	InL009
vivB	hydB	hydA	vivB	hydB	hydB	hydB	hydB	vivB	hydB	hydB	lymB	lym	lym	lymC	lymC	lym
8.236	5.931	4.306	5.105	5.638	6.056	5.533	5.327	4.929	6.361	6.085	12.353			10.430	15.158	
6.740	4.168	3.389	3.554	3.724	3.610	4.041	3.263	3.721	3.263	4.274	4.771			3.146	4.029	
1.760	2.192	1.607	1.882	1.902	1.954	1.823	1.937	1.500	2.516	1.962	2.692			2.992	4.355	
6.476	3.739	2.699	3.223	3.736	4.102	3.710	3.390	3.429	3.845	4.123	9.661			7.438	10.803	
4.450	2.486	2.029	2.228	2.594	2.693	2.560	2.339		3.481	3.332	6.095			4.510		
3.839	2.376	2.114	1.910	2.094	2.247	2.240	1.712		1.827	2.415	2.822			2.034		
11.976	13.276	9.246	4.497	6.968	5.856	10.582	5.856	8.219	11.247	9.219	17.354			27.499	24.528	
66.3	53.7	55	64.2	52.6	51.9	61.9	52	73.9	41.3	56.7	44.1			33	35	
70.324	68.070	63.650	66.413	75.088	59.222	60.803	66.420		66.057	69.978	69.696			67.548	67.094	
	5.9	4.4	4.1		4.5	4.4		4.4	5.4	4.8	5.6	4.0		3.8		
No	No	No	No	No	No	No	No	No	No	No	No	No		No	No	No
Closed	Closed	Closed	Closed	Closed	Closed	Closed	Closed	Closed	Closed	Closed	Closed	Closed		Closed	Closed	Closed
Strong	Regular	Regular	Regular	Regular	Regular	Strong	Regular	Regular	Some-Regular	Strong	Regular	Some		Regular	Regular	Regular
Rounded	Flattened-Rounded	Rounded	Rounded	Rounded	Rounded	Rounded	Rounded	Rounded	Rounded	Rounded	Rounded	Rounded		Rounded	Rounded	Rounded
Trochiform	Ovate	Ovate-Trochiform	Trochiform	Ovate	Ovate	Ovate	Ovate	Trochiform	Ovate	Ovate-Trochiform	Elongate Cylindrical	Elongate Conic		Elongate Conic	Elongate Conic	Elongate Conic
No	No	No	No	No	No	No	No	No	No	No	No	No		No	No	No
Dextral	Dextral	Dextral	Dextral	Dextral	Dextral	Dextral	Dextral	Dextral	Dextral	Dextral	Dextral	Dextral	Dextral	Dextral	Dextral	Dextral

0097	0096	0095	0094	0093	0092	0091	0090	0089	0088	0087	0086	0085	0084	0083b	0083	0082
InL009	InL009	InL009	InL009	InL009	InL009	InL009	InL009	InL009	InL009	InL009	InL009	InL009	InL009	InL009	InL009	InL009
hydB	hydB	hydB	hydB	hydB	hydB	hydB	hydB	vivB	hydB	hydB	hydB	hydA	hydB	vivB	vivB	vivB
9.944	7.481	7.936	8.788	7.978	6.748	8.750	7.296	6.295	9.135	7.476	7.043	7.792	6.716	2.967	5.736	5.943
5.910	4.085	5.117	5.546	4.786	4.130	5.204	4.669	4.660	5.138	4.996	4.485	5.530	4.162	2.022	4.500	5.375
3.766	2.709	2.778	3.241	3.511	2.470	3.685	2.341	2.626	3.589	2.752	2.940	2.997	2.992	1.023	1.568	1.261
6.178	4.772	5.158	5.547	4.467	4.278	5.065	4.955	3.669	5.546	4.724	4.103	4.795	3.724	1.944	4.168	4.682
4.467	3.639	3.535	4.387	3.338	3.253	3.640	3.703	3.240	3.507	3.800	3.060	3.633	2.564		3.107	3.785
3.791	2.606	3.282	3.313	2.775	2.657	3.061	2.802	3.031	3.307	3.064	3.119	3.413	2.240		2.588	3.367
13.422	5.964	5.117	6.082	17.430	9.744	16.790	11.211	14.153	9.689	13.069	5.711	10.176	15.301	11.944	7.927	7.206
46.9	46	50.4	53.9	51.6	54.5	44.8	58.4	61	47.6	54.7	51.8	50.6	52.9	74.4	68	89.1
71.761	73.869	65.772	68.102	64.323	64.694	70.201	73.327	61.390	64.699	70.724	61.928	65.659	53.020		65.472	66.371
5.1			5.7		5.7	5.1	5.5		5.3	5.3			6.8	5.3	3.9	
No	No	No	No	No	No	No	No	No	No	No	No	No	No	No	No	No
Closed	Closed	Closed	Closed	Closed	Closed	Closed	Closed	Closed	Closed	Closed	Closed	Closed	Closed	Closed	Closed	Closed
Strong	Regular	Strong	Some-Regular	Regular	Some-Regular	Regular	Regular	Regular	Strong	Strong	Strong	Regular	Strong	Regular	Strong	Regular
Rounded	Rounded	Rounded	Flattened-Rounded	Flattened-Rounded	Flattened-Rounded	Flattened-Rounded	Rounded	Rounded	Rounded	Rounded	Rounded	Rounded	Rounded	Rounded	Rounded	Rounded
Ovate	Ovate	Ovate	Ovate	Ovate	Ovate	Ovate	Ovate	Trochiform	Ovate	Ovate	Ovate	Ovate	Ovate	Trochiform	Trochiform	Trochiform
No	No	No	No	No	No	No	No	No	No	No	No	No	No	No	No	No
Dextral	Dextral	Dextral	Dextral	Dextral	Dextral	Dextral	Dextral	Dextral	Dextral	Dextral	Dextral	Dextral	Dextral	Dextral	Dextral	Dextral

0114	0113	0112	0111	0110	0109	0108	0107	0106	0105	0104	0103	0102	0101	0100	0099	0098
InL009	InL009	InL009	InL009	InL009	InL009	InL009	InL009	InL009	InL009	InL009	InL009	InL009	InL009	InL009	InL009	InL009
phy	phy	phy	phyB	phy	phyA	phyB	lymC	lymB	lymB	hyd	hydD	hydD	hydB	hydB	hydB	hydB
			12.547		21.398	22.519	12.972	6.866	9.306		10.675	11.102	9.209	7.435	7.167	7.514
			8.407		10.040	9.881	4.236	3.399	4.576		5.214	5.293	5.188	4.893	4.479	4.706
			1.757		6.154	3.102	8.085	3.671	2.387		5.627	5.210	4.377	4.105	3.014	3.132
			10.790		15.244	19.417	4.887	3.195	6.919		5.048	5.892	4.832	3.330	4.153	4.382
			10.235		13.570	15.964		3.800	4.941		4.941	4.030	4.034	2.656	3.294	3.128
			4.505		4.523	5.661		1.786	2.586		2.586	3.123	2.884	3.547	2.629	2.814
			13.392		14.396	20.194	23.273	20.556	28.482		19.692	16.557	12.875	2.203	11.041	12.131
			86.9		52.1	57.6	27.1	56.3	48.5		47.2	31	48.5		56.7	51.4
			74.332		74.228	84.544	67.714	78.056	53.973		63.072	63.015	56.070		62.430	60.772
			4.6			4.6	3.3	4.7	3.7		5.7	5.5	2.9		4.7	3.4
			No		No	No	No	No	No		No	No	No	No	No	No
			Closed		Closed	Closed	Closed	Closed	Closed		Closed	Closed	Closed	Closed	Closed	Closed
			Some		Some	Some	Regular	Regular	Regular		Strong	Strong	Strong	Strong	Strong	Strong
			Flattened-Rounded		Flattened-Rounded	Flattened-Rounded	Rounded	Rounded	Rounded		Rounded	Rounded	Rounded	Flattened-Rounded	Rounded	Rounded
			Fusiform		Elongate Fusiform	Fusiform	Elongate Conic	Elongate Cylindrical	Elongate Cylindrical		Ovate-Conic	Ovate-Conic	Ovate	Ovate	Ovate	Ovate
			No		No	No	No	No	No		No	No	No	No	No	No
Sinistral	Sinistral	Sinistral	Sinistral	Sinistral	Sinistral	Sinistral	Dextral	Dextral	Dextral	Dextral	Dextral	Dextral	Dextral	Dextral	Dextral	Dextral

0131	0130	0129	0128	0127	0126	0125	0124	0123	0122	0121	0120	0119	0118	0117	0116	0115
InL009	InL009	InL009	InL009	InL009	InL009	InL009	InL009	InL009	InL009	InL009	InL009	InL009	InL009	InL009	InL009	InL009
phyB	phyB	phyB	vivB	vivB	hydC	hydB	vivB	hydB	vivB	viv	viv	vivB	phy	phy	phy	phy
47.837	48.484	5.424	4.837	6.879	9.717	8.599	5.837	6.615	8.444			13.384				
31.655	32.192	3.150	4.862	7.276	5.498	5.821	4.845	4.746	7.672			11.289				
10.927	5.668	0.591	1.339	1.621	3.475	3.340	1.554	1.323	2.413			5.887				
36.910	42.816	4.833	3.498	5.259	6.242	5.259	4.283	5.292	6.032			7.497				
37.184	37.245	4.341	3.183	3.989	4.683	3.850	3.287	3.872	5.771							
15.859	14.528	0.951	2.786	3.619	2.659	3.228	2.547	2.497	4.167							
10.731	17.645	10.229	9.527	8.049	12.817	11.936	8.812	16.417	12.197			14.140				
79.2	80.9	103.9	82.3	81.9	49.3	56.6	74.8	60.8	74.9			68.3				
73.511	80.764	71.350	64.263	61.949	72.181	65.726	66.615	63.138	53.768			63.975				
			4.6	3.2	6.2	6.6	4.6		4.7			5.1				
No	No	No	No	No	No	No	No	No	No			No				
Closed	Closed	Closed	Closed	Closed	Closed	Closed?	Closed	Closed	Closed			Closed				
Strong	Some	Regular	Strong	Strong	Regular	Regular	Strong	Regular	Strong			Strong				
Flattened-Rounded	Flattened	Flattened-Rounded	Rounded	Rounded	Rounded	Rounded	Rounded	Rounded	Rounded			Rounded				
Fusiform	Fusiform	Fusiform	Trochiform	Trochiform	Ovate-Conic	Ovate	Trochiform	Ovate-Trochiform	Trochiform			Trochiform				
No	No	No	No	No	No	No	No	No	No			No				
Sinistral	Sinistral	Sinistral	Dextral	Dextral	Dextral	Dextral	Dextral	Dextral	Dextral	Dextral	Dextral	Dextral	Sinistral	Sinistral	Sinistral	Sinistral

0132	InL009	phyB	45.001	28.456	5.358	39.643	32.026	16.258			76.149		No	Closed			Fusiform	No	Sinistral
0133	InL009	phyB	45.344	25.955	5.667	39.677	31.950	12.150	17.041	69.3	80.263		No	Closed	Some	Flattened	Fusiform	No	Sinistral
0134	InL009	phyB	52.195	28.293	5.535	46.660	39.818	13.762	10.592	73.9	79.739		No	Closed	Regular	Flattened-Rounded	Fusiform	No	Sinistral
0135	InL009	phyA	50.739	29.862	4.891	45.848	40.420	16.500	18.997	75.8	82.208		No	Closed	Regular	Rounded	Fusiform	No	Sinistral
0136	InL009	phyB	42.595	24.368	5.334	37.261	28.716	11.006	8.707	65	73.106		No	Closed	Regular	Flattened-Rounded	Fusiform	No	Sinistral
0137	InL009	phyB	30.503	17.359	4.145	26.358	19.210	7.454	9.039	67.4	76.206		No	Closed	Some	Flattened-Rounded	Elongate Fusiform-Fusiform	No	Sinistral
0138	InL009	phyB	50.044	33.523	6.278	43.766	38.235	18.962	2.663	81.2	72.678		No	Closed	Some	Flattened-Rounded	Fusiform	No	Sinistral
0139	InL009	phyB	39.518	25.847	9.594	29.924	31.440	13.451	14.494	76.6	79.266		No	Closed	Regular	Flattened-Rounded	Fusiform	No	Sinistral
0140	InL009	phyB	35.085	21.050	3.796	31.289	28.016	10.396	10.923	66.9	77.586		No	Closed	Some	Flattened	Fusiform	No	Sinistral
0141	InL009	phyB	28.109	15.754	3.839	24.270	20.014	7.838	11.449	75.6	72.474	4.4	No	Closed	Regular	Flattened-Rounded	Fusiform	No	Sinistral
0142	InL009	phy																	Sinistral
0143	InL009	phyA	57.330	27.024	8.697	48.633	40.112	12.512	10.620	60.9	73.348		No	Closed	Regular	Rounded	Elongate Fusiform	No	Sinistral
0144	InL009	phyA	50.179	26.245	9.533	40.646	33.049	12.227	12.047	50.2	72.235		No	Closed	Strong	Rounded	Elongate Fusiform	No	Sinistral
0145	InL009	phyA	42.040	19.924	9.290	32.750	26.057	9.583	17.728	43.2	74.258	4.6	No	Closed	Strong	Rounded	Elongate Fusiform	No	Sinistral
0146	InL009	phyA	51.752	32.801	8.758	42.994	35.459	17.486	15.240	69.1	67.775		No	Closed	Regular	Rounded	Elongate Fusiform-Fusiform	No	Sinistral
0147	InL009	phyA	55.092	28.865	8.305	46.787	37.274	14.062	18.672	57.5	73.761		No	Closed	Regular	Rounded	Elongate Fusiform	No	Sinistral
0148	InL009	phyA	56.026	26.527	10.274	45.752	36.680	12.523	15.038	47.9	75.964		No	Closed	Strong	Rounded	Elongate Fusiform	No	Sinistral

0149	InL009	phyA	51.688	31.193	12.498	39.190	30.974	13.338	11.046	54	68.199		No	Closed	Strong	Rounded	Elongate Fusiform	No	Sinistral
0150	InL009	phyA	50.067	21.252	9.585	40.482	33.774	12.282	15.823	45.9	68.334		No	Closed	Strong	Rounded	Elongate Fusiform	No	Sinistral
0151	InL009	phyA	33.009	16.686	5.476	27.533	21.096	8.425	8.957	61.5	69.075		No	Closed	Regular	Rounded	Elongate Fusiform-Fusiform	No	Sinistral
0152	InL009	phyA	31.753	17.310	4.940	26.813	21.678	9.124	7.943	65.6	74.560	4.1	No	Closed	Regular	Rounded	Elongate Fusiform	No	Sinistral
0153	InL009	phyA	33.527	14.532	9.780	23.747	15.328	5.278	12.689	38.3	71.333	6.7	No	Closed	Some	Flattened-Rounded	Elongate Fusiform	No	Sinistral
0154	InL009	phyA	25.711	13.690	5.027	20.684	18.416	6.427	10.268	58.1	76.822	4.5	No	Closed	Some-Regular	Rounded	Elongate Fusiform-Fusiform	No	Sinistral
0155	InL009	phyB	48.238	32.070	5.448	42.790	37.578	13.395	4.877	87.6	74.641		No	Closed	Some-Regular	Flattened-Rounded	Fusiform	No	Sinistral
0156	InL009	phyB	42.762	30.136	7.374	35.388	31.875	14.365	11.230	74.8	74.876		No	Closed	Some	Flattened-Rounded	Fusiform	No	Sinistral
0157	InL009	phyB	28.994	17.837	6.126	22.868	22.540	7.742	4.170	87.2	79.509	4.8	No	Closed	Some-Regular	Flattened-Rounded	Fusiform	No	Sinistral
0158	InL009	phyB	42.248	27.219	5.580	36.668	34.535	13.413	10.433	80.7	75.277		No	Closed	Regular	Flattened-Rounded	Fusiform	No	Sinistral
0159	InL009	phy																	Dextral
0160	InL009	bivalve																	
0161	InL009	phy																	Sinistral
0162	InL009	phyB	46.814	29.022		46.814	40.680	16.073			67.652		No	Closed			Fusiform	No	Sinistral
0163	InL009	phyB	42.664	28.046	9.260	33.404	32.850	14.164	8.222	83.5			No	Closed	Regular	Flattened-Rounded	Fusiform	No	Sinistral
0164	InL009	lym																	Dextral
0165	InL009	viv																	Dextral

0166	InL009	viv																	Dextral
0167	InL009	viv																	Dextral
0168	InL009	vivB	10.299	8.949	1.912	8.387	5.607	4.716	5.500	88.2	72.793		No	Closed	Strong	Rounded	Trochiform	No	Dextral
0169	InL009	viv																	Dextral
0170	InL009	viv																	Dextral
0171	InL009	viv																	Dextral
0172	InL009	viv																	Dextral
0173	InL009	viv																	Dextral
0174	InL009	viv																	Dextral
0175	InL009	viv																	Dextral
0176	InL009	viv																	Dextral
0177	InL009	lym																	Dextral
0178	InL009	lym																	Dextral
0179	InL009	lym																	Dextral
0180	InL009	lym																	Dextral
0181	InL009	lymC	9.657	3.853	2.299	7.359	5.119	2.020	27.687	35.2	72.504	4.2	No	Closed	Regular	Rounded	Elongate Conic	No	Dextral
0182	InL009	lymB	8.649	3.803	2.679	5.970	4.382	1.693	20.353	39.3	71.896	4.2	No	Closed	Regular	Rounded	Elongate Conic	No	Dextral

0199	0198	0197	0196	0195	0194	0193	0192	0191	0190	0189	0188	0187	0186	0185	0184	0183
InL009	InL009	InL009	InL009	InL009	InL009	InL009	InL009	InL009	InL009	InL009	InL009	InL009	InL009	InL009	InL009	InL009
phy	phy	phy	phy	phy	phy	phy	viv	viv	viv	viv	viv	hydB	viv	viv	viv	viv
												9.864				
												6.038				
												4.019				
												5.826				
												4.344				
												3.531				
												14.184				
												50.6				
												65.556				
												6.6				
												No				
												Closed				
												Strong				
												Rounded				
												Ovate				
												No				
Sinistral	Sinistral	Sinistral	Sinistral	Sinistral	Sinistral	Sinistral	Dextral	Dextral	Dextral	Dextral	Dextral	Dextral	Dextral	Dextral	Dextral	Dextral

0216	0215	0214	0213	0212	0211	0210	0209	0208	0207	0206	0205	0204	0203	0202	0201	0200
															InL009	InL009
															bivalve	phy
																Sinistral

0217																			
0218																			
0219																			
0220																			
0221																			
0222																			
0223																			
0224																			
0225																			
0226																			
0227																			
0228																			
0229																			
0230																			
0231																			
0232																			
0233																			

0250	0249	0248	0247	0246	0245	0244	0243	0242	0241	0240	0239	0238	0237	0236	0235	0234
InL073a	InL073a	InL073a														
viv	viv	viv														
Dextral	Dextral	Dextral														

0267	0266	0265	0264	0263	0262	0261	0260	0259	0258	0257	0256	0255	0254	0253	0252	0251
InL004b-3	InL004b-3	InL004b-3	InL004b-3	InL004b-3	InL004b-3	InL004b-3	InL004b-3	InL004b-3	InL073a	InL073a	InL073a	InL073a	InL073a	InL073a	InL073a	InL073a
vivB	hydB	hydB	vivB	hydB	hydA	lymB	styB	valB	viv	viv	viv	viv	viv	viv	viv	viv
1,538	2.468	5.51	0.79	1.015	1.496	2.548	4.104	3.828								
1.402	1.695	4.729	0.693	0.629	1.084	1.087	2.101	3.664								
0.162	0.947	2.15	0.61	0.337	0.643	0.657	1.939	1.688								
1.376	1.521	3.36	0.18	0.678	0.853	1.891	2.165	2.14								
0.992	1.208	2.712	0.437	0.511	0.572	1.387	1.465	1.698								
0.784	0.894	3.068	0.304	0.338	0.547	0.605	0.953	1.917								
3.814	18.534	11.310	10.087	9.643	9.142	20.915	11.659	12.781								
	50.6	53.2	84.9	60.7	59.2	30.8	26.8	63.9								
67.068	60.764	64.627	62.516	57.779	65.400	66.638	80.287	76.981								
		3.2		3.6	4.7	3.6	5.6	3.4								
No	No	No	No	No	No	No	No	No								
Closed	Closed	Closed	Closed	Closed	Closed	Closed	Closed	Open								
Strong	Regular	Strong	Strong	Strong	Strong	Strong	Regular	Strong								
Flattened-Rounded	Rounded	Flattened-Rounded	Rounded	Rounded	Flattened-Rounded	Flattened-Rounded	Flattened-Rounded	Flattened-Rounded								
Trochiform	Ovate	Ovate-Trochiform	Trochiform	Ovate	Ovate-Trochiform	Elongate Conic	Conic	Turbinifor m-Trochiform								
No	No	No	No	No	No	No	No	No								
Dextral	Dextral	Dextral	Dextral	Dextral	Dextral	Dextral	Dextral	Dextral			Dextral	Dextral	Dextral	Dextral	Dextral	Dextral

0284	0283	0282	0281	0280	0279	0278	0277	0276	0275	0274	0273	0272	0271	0270	0269	0268
InL004b-3	InL004b-3	InL004b-3	InL004b-3	InL004b-3	InL004b-3	InL004b-3	InL004b-3	InL004b-3	InL004b-3	InL004b-3	InL004b-3	InL004b-3	InL004b-3	InL004b-3	InL004b-3	InL004b-3
lymA	lymB	lymC	hydC	hydC	styC	styA	styB	styA	styA	styA	vivA	vivA	vivB	hydB	valB	vivA
4.592	4.969	6.887	1.74	1.691	2.93	2.61	2.528	2.928	2.86	4.834	1.298	1.031	0.847	1.319	1.3	2.639
3.056	3.01	3.084	1.24	1.121	1.7	1.401	1.145	1.474	1.377	2.602	1.328	0.835	0.746	0.889	1.224	2.249
0.973	0.909	1.91	0.751	0.702	1.204	1.664	1.37	1.547	1.45	2.018	0.323	0.314	0.239	0.519	0.301	0.437
3.619	4.06	4.977	0.988	0.989	1.726	0.945	1.158	1.381	1.41	2.817	0.976	0.717	0.608	0.8	0.999	2.203
2.925			0.64	0.587	0.886	0.695	0.779	0.795	0.896	1.574	1.03	0.532	0.419	0.6	0.734	1.591
1.621			0.653	0.513	0.837	0.684	0.437	0.733	0.652	1.032	0.666	0.488	0.301	0.424	0.589	1.237
9.462	25.224	14.105	11.560	7.921	14.178	16.202	13.632	11.855	9.634	9.660	4.378	9.503	12.075	13.325	7.543	7.485
80.7	36.4	53.6	41.6	56.1	45.2	38.1	35.3	31.8	33.4	30.4	88.1	70.9	67.4	58.2	76.5	74.9
77.905		72.366	65.433	69.821	75.417	68.394	65.606	70.270	68.532	64.320	69.349	71.200	76.079	63.435	66.292	69.677
4.6			4.3	4.8	5.2	5.3	5.7	6.1	5.4	4.8	4.1	4.1			3.1	
No	No	No	No	No	No	No	No	No	No	No	No	No	No	No	No	No
Closed	Closed	Closed	Closed	Closed	Closed	Closed	Closed	Closed	Closed	Closed	Closed	Closed	Closed	Closed	Open	Closed
Regular	Regular	Strong	Strong	Regular	Regular	Some-Regular	Strong	Some-Regular	Some-Regular	Some-Regular	Regular	Strong	Strong	Strong	Strong	Regular
Flattened-Rounded	Flattened-Rounded	Flattened-Rounded	Rounded	Flattened-Rounded	Flattened-Rounded	Flattened-Rounded	Flattened-Rounded	Flattened-Rounded	Flattened-Rounded	Flattened-Rounded	Flattened-Rounded	Flattened-Rounded	Rounded	Rounded	Rounded	Flattened-Rounded
Elongate Cylindrical	Elongate Conic	Elongate Conic	Ovate-Conic	Ovate-Conic	Conic	Conic	Conic	Elongate Pupiform	Elongate Pupiform	Conic	Turbiniform-Trochiform	Trochiform	Trochiform	Ovate	Turbiniform-Trochiform	Trochiform
No	No	No	No	No	No	No	No	No	No	No	No	No	No	No	No	No
Dextral	Dextral	Dextral	Dextral	Dextral	Dextral	Dextral	Dextral	Dextral	Dextral	Dextral	Dextral	Dextral	Dextral	Dextral	Dextral	Dextral

0301	0300	0299	0298	0297	0296	0295	0294	0293	0292	0291	0290	0289	0288	0287	0286	0285
InL004b	InL004b-3	InL004b-3	InL004b-3	InL004b-3	InL004b-3	InL004b-3	InL004b-3	InL004b-3	InL004b-3	InL004b-3	InL004b-3	InL004b-3	InL004b-3	InL004b-3	InL004b-3	InL004b-3
phyB	phyB	valB	valB	valB	hydA	vivA	valB	valB	valB	vivA	lymB	lymB	lymB	lymB	lymB	lymB
8.139	4.299		1.149	1.22	1.411	1.363	1.776	2.182	2.475	2.828	1.774	1.997	2.199	3.12		4.158
7.59	3.193		1.214	1.445	1.241	1.657	1.73	2.175	2.492	2.607	0.934	0.905	1.071	1.737		2.196
2.53	0.319		0.309	0.314	0.651	0.331	0.549	0.651	0.97	1.196	0.294	0.347	0.728	0.861		1.029
5.609	3.981		0.839	0.906	0.76	1.032	1.227	1.531	1.505	1.632	1.48	1.649	1.472	2.26		3.128
7.849	3.223		0.699	0.825	0.515	0.765	0.936	1.215	1.191	1.201	1.145	1.112	1.108	1.852		2.621
4.191	1.744		0.635	0.711	0.43	0.862	0.754	1.021	1.495	1.33	0.48	0.422	0.583	0.951		1.546
13.266	13.658	4.018	8.476	7.393	8.130	2.291	14.704	8.284	11.578	6.667	12.051	19.776	23.102	19.581	31.586	23.580
73.5	74.7		81.5		64.1	92.3	107.4	84.3	72.1	65.4	69.8	61.2	39.7	43.7	32.4	50.6
78.261	81.967	71.704	67.068	68.714	70.852	62.255	73.051	79.792	67.598	69.015	66.038	75.793	76.192	71.175	76.487	81.067
5.3	2.4		3.7		4.2		4.8	3.5	3.7	5.5		2.7	4.0			4.2
No	No	No	No	No	No	No	No	No	No	Yes	No	No	No	No	No	No
Closed	Closed		Open	Closed	Closed	Closed	Open	Open	Open	Closed	Closed	Closed	Closed	Closed	Closed	Closed
Some	Regular	Strong	Strong	Regular	Strong	Regular	Regular	Strong	Some-Regular	Regular	Regular	Regular	Strong	Strong	Strong	Strong
Flattened	Flattened-Rounded	Flattened-Rounded	Rounded	Flattened-Rounded	Flattened-Rounded	Flattened-Rounded	Flattened-Rounded	Flattened-Rounded	Flattened-Rounded	Flattened-Rounded	Flattened-Rounded	Flattened-Rounded	Flattened-Rounded	Flattened-Rounded	Flattened-Rounded	Flattened-Rounded
Fusiform	Fusiform	Turbinifor m-Trochiform	Turbinifor m-Trochiform	Turbinifor m-Trochiform	Ovate-Trochiform	Turbinifor m-Trochiform	Turbinifor m-Trochiform	Turbinifor m-Trochiform	Turbinifor m-Trochiform	Turbinifor m-Trochiform	Elongate Conic	Elongate Conic	Elongate Conic	Elongate Conic	Elongate Conic	Elongate Conic
No	No	No	No	No	No	No	No	No	No	No	No	No	No	No	No	No
Sinistral	Sinistral	Dextral	Dextral	Dextral	Dextral	Dextral	Dextral	Dextral	Dextral	Dextral	Dextral	Dextral	Dextral	Dextral	Dextral	Dextral

0302	InL004b	phyB	3.014	1.621	0.376	2.638	2.262	0.85	2.663	73.4	75.828	4.0	No	Closed	Regular	Flattened-Rounded	Fusiform	No	Sinistral
0303	InL004b-3	phyB	1.627	1.032	0.199	1.428	0.949	0.308	11.646	97.4	74.358		No	Closed	Strong	Flattened-Rounded	Fusiform	No	Sinistral
0304	InL004b-3	phyB	1.424	0.961	0.215	1.209	0.922	0.538	9.819	89.5	83.008	3.0	No	Closed	Regular	Rounded	Fusiform	No	Sinistral
0305	InL004b-3	phyA	1.522	0.804	0.235	1.287	0.866	0.446	18.435	77.7	82.355	2.6	No	Closed	Regular	Flattened-Rounded	Elongate Fusiform	No	Sinistral
0306	InL004b-3	phyB	1.22	0.901	0.287	0.932	1.006	0.458	15.327	83	77.338	3.0	No	Closed	Strong	Rounded	Fusiform	No	Sinistral
0307	InL004b-3	hydB	4.345	2.824	1.914	2.431	1.811	1.565	17.398	54.2	62.613	6.8	No	Closed	Strong	Rounded	Ovate	No	Dextral
0308	InL004b-3	hydB	3.816	2.303	1.112	2.704	1.997	0.909	9.654	63.6	65.807		No	Closed	Strong	Rounded	Ovate	No	Dextral
0309	InL004b-3	styB	2.299	1.029	1.052	1.247	0.932	0.369	4.785	32.3	69.574	5.1	Yes	Closed	Regular	Rounded	Conic	No	Dextral
0310	InL004b-3	hydB	2.092	1.61	0.602	1.491	1.004	0.804	13.791	61.1	69.894		No	Closed	Regular	Rounded	Ovate	No	Dextral
0311	InL004b-3	hydB							12.947	55	62.723		No	Closed	Strong	Flattened-Rounded	Ovate	No	Dextral
0312	InL004b-3	hydA	1.54	1.104	0.707	0.833	0.624	0.473	9.813	57.5	72.699	4.9	No	Closed	Strong	Flattened-Rounded	Ovate-Trochiform	No	Dextral
0313	InL004b-3	hydB	1.592	1.025	0.583	1.009	0.589	0.562	5.052	63.7	79.695	4.9	No	Closed	Strong	Rounded	Ovate	No	Dextral
0314	InL004b-3	hydB	1.865	1.273	0.773	1.091	0.791	0.633	17.103	61.6	76.849		No	Closed	Strong	Rounded	Ovate	No	Dextral
0315	InL004b-3	otolith?																	
0316	InL004b	hyd																	Dextral
0317	InL004b-3	viv																	Dextral
0318	InL004b-3	hydB							1.123	56.9	69.102		No	Closed	Strong	Rounded	Ovate	No	Dextral

0335	0334	0333	0332	0331	0330	0329	0328	0327	0326	0325	0324	0323	0322	0321	0320	0319
InL004b-3	InL004b-3	InL004b-3	InL004b-3	InL004b-3	InL004b-3	InL004b-3	InL004b-3	InL004b-3	InL004b-3	InL004b-3	InL004b-3	InL004b-3	InL004b-3	InL004b-3	InL004b-3	InL004b-3
styB	styA	hydC	styB	styB	styA	styB	styB	styB	hydC			phyA	vivB	phyA	lymB	styB
2.286	2.299	2.504	1.645	2.818	2.638	3.13	3.002	3.134	3.175			1.718	0.748	1.224	2.298	2.682
1.373	1.306	1.723	1.005	1.628	1.463	0.922	1.625	0.98	1.313			1.083	0.688	0.815	1.046	1.584
1.071	1.191	0.939	0.566	1.075	1.524	1.805	1.418	0.988	1.25			0.227	0.232	0.054	0.402	1.237
1.215	1.108	1.564	1.079	1.743	1.114	1.325	1.583	2.146	1.925			1.49	0.517	1.17	1.896	1.445
0.901	0.815	1.12	0.721	1.207	1.045	1.247	1.034	1.276	1.488			0.966	0.38	0.959	1.45	
0.69	0.608	0.842	0.523	0.84	0.762	0.486	0.691	0.38	0.526			0.598	0.349	0.474	0.493	
12.178	15.099	9.638	11.664	8.889	11.462	11.602	12.265	10.835	8.415			10.939	5.356	16.699	18.189	15.792
42.2	43.5	60.9			40.8	43.4	37	40.4	50			78.9	70.5	109.5	44.2	30.8
74.578	73.421	75.005	69.444	75.023	68.927	66.501	65.031	62.488	68.962			67.640		75.174	63.435	
4.4	4.6	5.5			6.7	5.3	7.2	3.8	3.9			3.3			3.8	4.7
No	No	No	No	No	Yes	No	No	No	No			No	No	No	No	No
Closed	Closed	Closed	Closed	Closed	Closed	Closed	Closed	Closed	Closed			Closed	Closed	Closed	Closed	Closed
Regular	Some-Regular	Regular	Regular	Regular	Regular	Regular	Regular	Some-Regular	Regular			Regular	Strong	Regular	Strong	Strong
Flattened-Rounded	Flattened-Rounded	Flattened-Rounded	Flattened-Rounded	Flattened-Rounded	Rounded	Flattened-Rounded	Flattened-Rounded	Flattened-Rounded	Flattened-Rounded			Rounded	Rounded	Flattened-Rounded	Flattened-Rounded	Rounded
Conic	Elongate Pupiform	Ovate-Conic	Conic	Conic	Conic	Conic	Conic	Conic	Ovate-Conic			Elongate Fusiform	Trochiform	Elongate Fusiform	Elongate Conic	Conic
No	No	No	No	No	No	No	No	No	No			No	No	No	No	No
Dextral	Dextral	Dextral	Dextral	Dextral	Dextral	Dextral	Dextral	Dextral	Dextral			Sinistral	Dextral	Sinistral	Dextral	Dextral

0352	0351	0350	0349	0348	0347	0346	0345	0344	0343	0342	0341	0340	0339	0338	0337	0336
InL004b-3	InL004b-3	InL004b-3	InL004b-3	InL004b-3	InL004b-3	InL004b-3	InL004b-3	InL004b-3	InL004b-3	InL004b-3	InL004b-3	InL004b-3	InL004b-3	InL004b-3	InL004b-3	InL004b-3
styB	hydC	hydC	hydC	styB	hydC	styB	styB	hydC	hydC	styB	hydC	sty	styB	styA	styA	hydA
2.633	1.612	1.657		1.929	1.485		1.982	2.068	1.836		2.166		1.883	2.106	2.403	2.329
1.531	1.028	1.196		1.287	1.029		0.703	1.298	1.22		1.449		1.144	1.268	1.245	1.816
1.452	0.797	0.816		1.091	0.453		0.956	0.977	0.933		0.698		0.612	1.122	1.641	0.81
1.181	0.816	0.841		0.838	1.032		1.025	1.09	0.903		1.468		1.271	0.984	0.762	1.518
0.917	0.567			0.625	0.719		0.623	0.769	0.659		1.149		0.898	0.75		1.071
0.846	0.567			0.678	0.537		0.251	0.631	0.456		0.8		0.591	0.675		0.862
6.009	12.804	12.926	12.695	8.302	8.702	8.622	9.012	5.774	10.995	7.690	8.705		11.240	9.338	11.310	9.958
50.9	44.8	51.8		53.6	58.9		52.7	45.1	56.9	52.4	61.8		27.5	52	52.1	64.6
61.294	72.047	70.665		57.588	63.726		68.385	51.760	75.964				66.114	70.989		66.267
5.5	4.3			5.7			5.3	4.7	5.1					5.1	5.2	4.6
Yes	No	No	No	No	No	No	No	No	No	Yes	No		No	No	No	No
Closed	Closed	Closed	Closed	Closed	Closed	Closed	Closed	Closed	Closed	Closed	Closed		Closed	Closed	Closed	Closed
Some-Regular	Strong	Regular	Strong	Regular	Regular	Regular	Regular	Strong	Regular	Some-Regular	Regular		Regular	Some-Regular	Regular	Regular
Rounded	Rounded	Flattened-Rounded	Rounded	Flattened-Rounded	Rounded	Rounded	Flattened-Rounded	Rounded	Flattened-Rounded	Rounded	Flattened-Rounded		Rounded	Flattened-Rounded	Flattened-Rounded	Flattened-Rounded
Conic	Ovate-Conic	Ovate-Conic	Ovate-Conic	Conic	Ovate-Conic	Conic	Conic	Ovate-Conic	Ovate-Conic	Conic	Ovate		Conic	Conic	Conic	Ovate-Trochiform
No	No	No	No	No	No	No	No	No	No	No	No		No	No	No	No
Dextral	Dextral	Dextral	Dextral	Dextral	Dextral	Dextral	Dextral	Dextral	Dextral	Dextral	Dextral	Dextral	Dextral	Dextral	Dextral	Dextral

0369	0368	0367	0366	0365	0364	0363	0362	0361	0360	0359	0358	0357	0356	0355	0354	0353
InL004b-3	InL004b-3	InL004b-3	InL004b-3	InL004b-3	InL004b-3	InL004b-3	InL004b-3	InL004b-3	InL004b-3	InL004b-3	InL004b-3	InL004b-3	InL004b-3	InL004b-3	InL004b-3	InL004b-3
lymB	lym	lymB	lymB	lymB	lymB	lymB	lymB	lymB	lymB	lym	lymB	hydC	hydC	hydC	hydC	sty
1.632		1.825	1.838	1.856	1.994	2.018	2.186	2.19	2.431		3.082	1.59	1.433	1.507	1.685	
0.865		0.846	0.97	0.894	0.972	0.873	1.204	1.201	1.442		2.123	1.04	1.019	0.945	1.085	
0.165		0.4	0.342	0.236	0.532	0.466	0.572	0.509	0.619		0.734	0.556	0.554	0.779	0.732	
1.466		1.425	1.497	1.619	1.462	1.551	1.624	1.68	1.812		2.348	1.034	0.878	0.728	0.953	
1.141		1.11	1.062	1.271	1.1	1.315	1.1	1.579	1.579		1.749	0.676	0.695			
0.43		0.46	0.492	0.547	0.505	0.451	0.674	0.604	0.769		1.1	0.387	0.577			
22.584		20.311	20.854	18.550	19.558	17.044	19.497	16.348	19.814		13.519	6.009	7.964	14.221	8.354	
70.4		46	44.6	65.4	41.5	48.6	55.2	56.3	48.9		50.4	59.7	43.6	39.3	59.7	
73.909		77.943	67.989	66.861	67.714	66.038	70.507	69.677	74.687		69.734	66.061	58.229	58.173	67.343	
		2.7			3.7	2.9		3.4	2.8		2.9				5.2	
No		No	No	No	No	No	No	No	No		No	No	No	No	No	
Closed		Closed	Closed	Closed	Closed	Closed	Closed	Closed	Closed		Closed	Closed	Closed	Closed	Closed	
Regular		Strong	Strong	Regular	Strong	Strong	Strong	Strong	Strong		Strong	Regular	Strong	Strong	Regular	
Flattened-Rounded		Flattened-Rounded	Flattened-Rounded	Flattened-Rounded	Flattened-Rounded	Flattened-Rounded	Rounded	Flattened-Rounded	Flattened-Rounded		Flattened-Rounded	Rounded	Rounded	Rounded	Flattened-Rounded	
Elongate Conic		Elongate Conic	Elongate Conic	Elongate Conic	Elongate Conic	Elongate Conic	Elongate Conic	Elongate Cylindrical	Elongate Conic		Elongate Cylindrical	Ovate-Conic	Ovate-Conic	Ovate-Conic	Ovate-Conic	
No		No	No	No	No	No	No	No	No		No	No	No	No	No	
Dextral	Dextral	Dextral	Dextral	Dextral	Dextral	Dextral	Dextral	Dextral	Dextral	Dextral	Dextral	Dextral	Dextral	Dextral	Dextral	Dextral

0386	0385	0384	0383	0382	0381	0380	0379	0378	0377	0376	0375	0374	0373	0372	0371	0370
InL004b-3	InL004b-3	InL004b-3	InL004b-3	InL004b-3	InL004b-3	InL004b-3	InL004b-3	InL004b-3	InL004b-3	InL004b-3	InL004b-3	InL004b-3	InL004b-3	InL004b-3	InL004b-3	InL004b-3
phyA	phyA	lym	lymA	lymB	lymB	lymC	lym	lymB	lymB	lymB	lymB	lymB	lymB	lymB	lymB	lymB
1.112	1.244		1.193	1.323	1.145	1.349		1.387	1.263	1.662	1.546	1.596	1.499	1.703	1.626	1.626
0.75	0.602		0.856	0.757	0.794	0.871		0.827	0.862	0.92	0.719	1.009	0.982	0.915	0.769	0.846
0.118	0.097		0.188	0.306	0.227	0.546		0.186	0.331	0.23	0.283	0.36	0.267	0.358	0.331	0.334
0.994	1.147		1.005	1.017	0.918	0.802		1.201	0.932	1.433	1.263	1.236	1.232	1.345	1.296	1.293
0.927	0.939		0.772	0.821	0.701			0.99	0.787	1.177	0.989	0.979	0.956	0.996	0.951	1.016
0.458	0.387		0.405	0.38	0.387			0.437	0.493	0.47	0.397	0.526	0.519	0.453	0.376	0.48
27.860	11.182		10.194	24.624	14.850	21.337	22.816	15.996	11.310	17.791	21.297	11.848	15.772	16.759	22.436	17.210
90	58.4		88.9	31.5	65.4	53.5		74	55.5	77.9	49.3	44.7	49.2	59.1	50.4	37.6
84.872	79.011		76.239	70.163	70.084			67.834			70.451	63.189	62.879	69.734	70.769	
2.7	2.3		2.5	2.8				2.9			2.5	2.7	2.7		3.4	2.7
No	No		No	No	No	No	No	No	No	No	No	No	No	No	No	No
Closed	Closed		Closed	Closed	Closed	Closed	Closed	Closed	Closed	Closed	Closed	Closed	Closed	Closed	Closed	Closed
Regular	Regular		Regular	Strong	Strong	Strong	Strong	Strong	Strong	Regular	Strong	Regular	Strong	Strong	Strong	Strong
Flattened-Rounded	Flattened-Rounded		Flattened-Rounded	Flattened-Rounded	Flattened-Rounded	Flattened-Rounded	Flattened-Rounded	Flattened-Rounded	Flattened-Rounded	Flattened-Rounded	Flattened-Rounded	Flattened-Rounded	Flattened-Rounded	Flattened-Rounded	Flattened-Rounded	Flattened-Rounded
Elongate Fusiform	Elongate Fusiform		Elongate Cylindrical	Elongate Conic	Elongate Conic	Elongate Conic	Elongate Conic	Elongate Conic	Elongate Conic	Elongate Conic	Elongate Conic	Elongate Conic	Elongate Conic	Elongate Conic	Elongate Conic	Elongate Conic
No	No		No	No	No	No	No	No	No	No	No	No	No	No	No	No
Sinistral	Sinistral	Dextral	Dextral	Dextral	Dextral	Dextral	Dextral	Dextral	Dextral	Dextral	Dextral	Dextral	Dextral	Dextral	Dextral	Dextral

0403	0402	0401	0400	0399	0398	0397	0396	0395	0394	0393	0392	0391	0390	0389	0388	0387
InL004b-3	InL004b-3	InL004b-3	InL004b-3	InL004b-3	InL004b-3	InL004b-3	InL004b-3	InL004b-3	InL004b-3	InL004b-3	InL004b-3	InL004b-3	InL004b-3	InL004b-3	InL004b-3	InL004b-3
phyB	phy	phy	phy	phy	phyB	lym	lym	lym	lym	lym	lym	lym	lym	phyB	phyA	lymB
1.439					2.53									1.101	1.072	
1.098					1.508									0.781	0.714	
0.241					0.41									0.026	0.089	
1.197					2.12									1.075	0.982	
0.974					1.82									0.845	0.75	
0.649					0.579									0.383	0.416	
6.911					6.710									21.092	15.767	17.435
90					88.4										87	
76.180					75.793									77.989	70.233	
3.1					3.5										2.4	
No					No									No	No	No
Closed					Closed									Closed	Closed	Closed
Regular					Regular									Regular	Regular	
Flattened-Rounded					Flattened-Rounded									Flattened-Rounded	Flattened-Rounded	
Fusiform					Fusiform									Fusiform	Elongate Fusiform	Elongate Conic
No					No									No	No	No
Sinistral	Sinistral	Sinistral	Sinistral	Sinistral	Sinistral	Dextral	Dextral	Dextral	Dextral	Dextral	Dextral	Dextral	Dextral	Sinistral	Sinistral	Dextral

0404	InL004b-3	phyB	1.411	1.164	0.169	1.242	1.041	0.676	18.258	99.9	74.427	2.3	No	Closed	Regular	Flattened-Rounded	Fusiform	No	Sinistral
0405	InL004b-3	phy																	Sinistral
0406	InL004b-3	phy																	Sinistral
0407	InL004b-3	phy																	Sinistral
0408	InL004b-3	phy																	Sinistral
0409	InL004b-3	phy																	Sinistral
0410	InL004b-3	phyB	1.024	0.84	0.185	0.838	0.718	0.382	12.926	80.4	80.159	2.5	No	Closed	Strong	Flattened-Rounded	Fusiform	No	Sinistral
0411	InL004b-3	phy																	Sinistral
0412	InL004b-3	phy																	Sinistral
0413	InL004b-3	phy																	Sinistral
0414	InL004b-3	phy																	Sinistral
0415	InL004b-3	phy																	Sinistral
0416	InL004b-3	phy																	Sinistral
0417	InL004b-3	phy																	Sinistral
0418	InL004b-3	phy																	Sinistral
0419	InL004b-3	phy																	Sinistral
0420	InL004b-3	phy																	Sinistral

0437	0436	0435	0434	0433	0432	0431	0430	0429	0428	0427	0426	0425	0424	0423	0422	0421
InL004b-3	InL004b-3	InL004b-3	InL004b-3	InL004b-3	InL004b-3	InL004b-3	InL004b-3	InL004b-3	InL004b-3	InL004b-3	InL004b-3	InL004b-3	InL004b-3	InL004b-3	InL004b-3	InL004b-3
val	val	vivB	val	val	val	val	val	val	val	valB	val	vivB	phy	phy	phy	phy
		1.048								1.476		3.352				
		1.087								1.645		2.696				
		0.327								0.533		1.373				
		0.722								0.943		1.98				
		0.496								0.824		1.676				
		0.579								0.857		1.561				
		6.116								10.465		6.435				
		77.3								82.4		63.6				
		67.184								70.084		65.624				
		3.3										5.1				
		No								No		No				
		Closed								Closed		Closed				
		Strong								Strong		Strong				
		Rounded								Rounded		Rounded				
		Trochiform								Turbinifor m- Trochiform		Trochiform				
		No								No		No				
Dextral	Dextral	Dextral	Dextral	Dextral	Dextral	Dextral	Dextral	Dextral	Dextral	Dextral	Dextral	Dextral	Sinistral	Sinistral	Sinistral	Sinistral

0454	0453	0452	0451	0450	0449	0448	0447	0446	0445	0444	0443	0442	0441	0440	0439	0438
InL004b-3	InL004b-3	InL004b-3	InL004b-3	InL004b-3	InL004b-3	InL004b-3	InL004b-3	InL004b-3	InL004b-3	InL004b-3	InL004b-3	InL004b-3	InL004b-3	InL004b-3	InL004b-3	InL004b-3
val	val	val	val	val	val	val	val	val	val	val	val	val	val	val	val	val
Dextral	Dextral	Dextral	Dextral	Dextral	Dextral	Dextral	Dextral	Dextral	Dextral	Dextral	Dextral	Dextral	Dextral	Dextral	Dextral	Dextral

0455	InL004b-3	vivA	0.709	0.753	0.193	0.516	0.427	0.422	7.463	89.3	63.778		No	Closed	Strong	Flattened-Rounded	Turbinifor m-Trochiform	No	Dextral
0456	InL004b-3	val																	Dextral
0457	InL004b-3	val																	Dextral
0458	InL004b-3	viv																	Dextral
0459	InL004b-3	vivA	3.481	2.931	0.972	2.51	1.994	1.462	10.850	72.7	62.560	5.2	Yes	Closed	Regular	Flattened-Rounded	Trochiform	No	Dextral
0460	InL004b-3	viv																	Dextral
0461	InL004b-3	viv																	Dextral
0462	InL004b-3	viv																	Dextral
0463	InL004b-3	viv																	Dextral
0464	InL004b-3	vivA	1.739	1.885	0.615	1.125	1.022	0.893	11.427	84.3	70.931	4.8	No	Closed	Regular	Rounded	Turbinifor m-Trochiform	No	Dextral
0465	InL004b-3	vivB	2.03	1.575	0.616	1.414	1.04	0.769	1.695	71.2	61.477	5.3	No	Closed	Strong	Rounded	Trochiform	No	Dextral
0466	InL004b-3	viv																	Dextral
0467	InL004b-3	viv																	Dextral
0468	InL004b-3	viv																	Dextral
0469	InL004b-3	viv																	Dextral
0470	InL004b-3	viv																	Dextral
0471	InL004b-3	vivB	1.477	1.386	0.441	1.036	0.912	0.825	11.508	69	67.003	4.3	Yes	Closed	Strong	Rounded	Trochiform	No	Dextral

0472	InL004b-3	viv																	Dextral
0473	InL004b-3	viv																	Dextral
0474	InL004b-3	viv																	Dextral
0475	InL004b-3	viv																	Dextral
0476	InL004b-3	viv																	Dextral
0477	InL004b-3	viv																	Dextral
0478	InL004b-3	viv																	Dextral
0479	InL004b-3	viv																	Dextral
0480	InL004b-3	viv																	Dextral
0481	InL004b-3	viv																	Dextral
0482	InL004b-3	viv																	Dextral
0483	InL004b-3	viv																	Dextral
0484	InL004b-3	viv																	Dextral
0485	InL004b-3	viv																	Dextral
0486	InL004b-3	viv																	Dextral
0487	InL004b-3	viv																	Dextral
0488	InL004b-3	viv																	Dextral

0489	InL004b-3	viv																	Dextral
0490	InL004b-3	viv																	Dextral
0491	InL004b-3	viv																	Dextral
0492	InL004b-3	viv																	Dextral
0493	InL004b-3	viv																	Dextral
0494	InL004b-3	viv																	Dextral
0495	InL004b-3	viv																	Dextral
0496	InL004b-3	viv																	Dextral
0497	InL004b-3	viv																	Dextral
0498	InL004b-3	viv																	Dextral
0499	InL004b-3	viv																	Dextral
0500	InL004b-3	viv																	Dextral
0501	InL004b-3	viv																	Dextral
0502	InL004b-3	viv																	Dextral
0503	InL004b-3	viv																	Dextral
0504	InL004b-3	viv																	Dextral
0505	InL004b-3	viv																	Dextral

0506	InL004b-3	viv																Dextral
0507	InL004b-3	viv																Dextral
0508	InL004b-3	viv																Dextral
0509	InL004b-3	viv																Dextral
0510	InL004b-3	viv																Dextral
0511	InL004b-3	viv																Dextral
0512	InL004b-3	viv																Dextral
0513	InL004b-3	viv																Dextral
0514	InL004b-3	viv																Dextral
0515	InL004b-3	viv																Dextral
0516	InL004b-3	viv																Dextral
0517	InL004b-3	viv																Dextral
0518	InL004b-3	viv																Dextral
0519	InL004b-3	viv																Dextral
0520	InL004b-3	viv																Dextral
0521	InL004b-3	viv																Dextral
0522	InL004b-3	viv																Dextral

0523	InL004b-3	viv																		Dextral
0524	InL004b-3	viv																		Dextral
0525	InL004b-3	viv																		Dextral
0526	InL004b-3	viv																		Dextral
0527	InL004b-3	viv																		Dextral
0528	InL004b-3	viv																		Dextral
0529	InL004b-3	viv																		Dextral
0530	InL004b-3	viv																		Dextral
0531	InL004b-3	viv																		Dextral
0532	InL004b-3	viv																		Dextral
0533	InL004b-3	viv																		Dextral
0534	InL004b-3	viv																		Dextral
0535	InL004b-3	viv																		Dextral
0536	InL004b-3	viv																		Dextral
0537	InL004b-3	viv																		Dextral
0538	InL004b-3	viv																		Dextral
0539	InL004b-3	viv																		Dextral

0540	InL004b-3	viv															Dextral
0541	InL004b-3	viv															Dextral
0542	InL004b-3	viv															Dextral
0543	InL004b-3	viv															Dextral
0544	InL004b-3	viv															Dextral
0545	InL004b-3	hyd															Dextral
0546	InL004b-3	hydC	2.663	1.852	1.228	1.475	1.356	1.116	14.715	49.2	61.280	4.9	No	Closed	Strong	Flattened-Rounded	Ovate-Conic	No	Dextral
0547	InL004b-3	hyd															Dextral
0548	InL004b-3	hyd															Dextral
0549	InL004b-3	hyd															Dextral
0550	InL004b-3	hyd															Dextral
0551	InL004b-3	hyd															Dextral
0552	InL004b-3	hyd															Dextral
0553	InL004b-3	hyd															Dextral
0554	InL004b-3	hyd															Dextral
0555	InL004b-3	hyd															Dextral
0556	InL004b-3	hyd															Dextral

0557	InL004b-3	hyd																Dextral
0558	InL004b-3	hyd																Dextral
0559	InL004b-3	hyd																Dextral
0560	InL004b-3	hyd																Dextral
0561	InL004b-3	hyd																Dextral
0562	InL004b-3	hyd																Dextral
0563	InL004b-3	hyd																Dextral
0564	InL004b-3	hyd																Dextral
0565	InL004b-3	hyd																Dextral
0566	InL004b-3	hyd																Dextral
0567	InL004b-3	hyd																Dextral
0568	InL004b-3	hyd																Dextral
0569	InL004b-3	hyd																Dextral
0570	InL004b-3	hyd																Dextral
0571	InL004b-3	hyd																Dextral
0572	InL004b-3	hyd																Dextral
0573	InL004b-3	hyd																Dextral

0574	InL004b-3	hydC	1.507	1.085	0.709	0.798	0.548	0.453	7.936	60.9	57.470	4.7	No	Closed	Regular	Flattened-Rounded	Ovate-Conic	No	Dextral
0575	InL004b-3	hyd																	Dextral
0576	InL004b-3	hyd																	Dextral
0577	InL004b-3	hyd																	Dextral
0578	InL004b-3	hyd																	Dextral
0579	InL004b-3	hyd																	Dextral
0580	InL004b-3	hyd																	Dextral
0581	InL004b-3	hyd																	Dextral
0582	InL004b-3	hyd																	Dextral
0583	InL004b-3	hyd																	Dextral
0584	InL004b-3	hyd																	Dextral
0585	InL004b-3	vivA	1.501	1.248	0.513	0.988	0.792	0.618	12.473	67.1	63.682		No	Closed	Strong	Flattened-Rounded	Ovate	No	Dextral
0586	InL004b-3	hyd																	Dextral
0587	InL004b-3	hyd																	Dextral
0588	InL004b-3	hyd																	Dextral
0589	InL004b-3	hydC	1.286	0.943	0.496	0.79	0.569	0.533	12.265	70.1	48.136	4.6	No	Closed	Strong	Rounded	Ovate-Conic	No	Dextral
0590	InL004b-3	hyd																	Dextral

0591	InL004b-3	hyd																	Dextral
0592	InL004b-3	hydB	1.276	1.024	0.39	0.886	0.597	0.591	11.409	75.7	71.241		No	Closed	Strong	Rounded	Ovate	No	Dextral
0593	InL004b-3	hyd																	Dextral
0594	InL004b-3	hyd																	Dextral
0595	InL004b-3	hyd																	Dextral
0596	InL004b-3	hyd																	Dextral
0597	InL004b-3	hyd																	Dextral
0598	InL004b-3	hydB	1.039	0.957	0.422	0.617	0.44	0.422	10.437	61.4	66.801		No	Closed	Strong	Rounded	Ovate	No	Dextral
0599	InL004b-3	hyd																	Dextral
0600	InL004b-3	hyd																	Dextral
0601	InL004b-3	hydB	1.144	0.833	0.416	0.777	0.59	0.423	10.008	58.8	69.334	4.0	No	Closed	Strong	Rounded	Ovate	No	Dextral
0602	InL004b-3	hyd																	Dextral
0603	InL004b-3	hyd																	Dextral
0604	InL004b-3	hyd																	Dextral
0605	InL004b-3	hydB	1.183	0.871	0.367	0.816	0.613	0.4	9.633	68.8	69.044		No	Closed	Strong	Rounded	Ovate	No	Dextral
0606	InL004b-3	hyd																	Dextral
0607	InL004b-3	hyd																	Dextral

0608	InL004b-3	hyd																	Dextral
0609	InL004b-3	hyd																	Dextral
0610	InL004b-3	hyd																	Dextral
0611	InL004b-3	hyd																	Dextral
0612	InL004b-3	hyd																	Dextral
0613	InL004b-3	hyd																	Dextral
0614	InL004b-3	hyd																	Dextral
0615	InL004b-3	hyd																	Dextral
0616	InL004b-3	hyd																	Dextral
0617	InL004b-3	hyd																	Dextral
0618	InL004b-3	hyd																	Dextral
0619	InL004b-3	hyd																	Dextral
0620	InL004b-3	hyd																	Dextral
0621	InL004b-3	hyd																	Dextral
0622	InL004b-3	hyd																	Dextral
0623	InL004b-3	hyd																	Dextral
0624	InL004b-3	hyd																	Dextral

0641	0640	0639	0638	0637	0636	0635	0634	0633	0632	0631	0630	0629	0628	0627	0626	0625
InL004b-3	InL004b-3	InL004b-3	InL004b-3	InL004b-3	InL004b-3	InL004b-3	InL004b-3	InL004b-3	InL004b-3	InL004b-3	InL004b-3	InL004b-3	InL004b-3	InL004b-3	InL004b-3	InL004b-3
hyd	hyd	hyd	hyd	hyd	hyd	hyd	hyd	hyd	hyd	hyd	hyd	hyd	hyd	hyd	hyd	hyd
Dextral	Dextral	Dextral	Dextral	Dextral	Dextral	Dextral	Dextral	Dextral	Dextral	Dextral	Dextral	Dextral	Dextral	Dextral	Dextral	Dextral

0642	InL004b-3	styB	8.467	5.391	4.911	3.556	4.364	2.815	7.431	35.2	62.003		No	Closed	Regular	Rounded	Conic	No	Dextral
0643	InL004b-3	hydB	6.174	5.193	2.635	3.539	3.462	2.558	12.113	52.9	70.498		No	Closed	Some-Regular	Flattened-Rounded	Ovate	No	Dextral
0644	InL004b-3	hydB	5.33	4.046	1.768	3.562	2.347	2.148	13.194	61	70.017		No	Closed	Regular	Flattened-Rounded	Ovate	No	Dextral
0645	InL004b-3	hydC	4.035	2.602	1.248	2.786	2.072	1.257	13.935	52.9	69.075	4.2	No	Closed	Regular	Rounded	Ovate-Conic	No	Dextral
0646	InL004b-3	vivA	2.684	2.569	0.876	1.808	1.515	1.431	12.385	68.4	63.869	3.1	No	Closed	Strong	Flattened-Rounded	Turbinifor m-Trochiform	No	Dextral
0647	InL004b-3	lymB	6.143	2.877	1.844	4.3	2.977	1.502	24.291	45.6	77.851	5.0	No	Closed	Regular	Flattened-Rounded	Elongate Conic	No	Dextral
0648	InL004b-3	phy																	Sinistral
0649	InL004b-3	viv																	Dextral
0650	InL004b-3	hydC	4.669	2.988	1.545	3.124	2.21	1.351	14.306	50.1	62.447	3.6	No	Closed	Regular	Rounded	Ovate-Conic	No	Dextral
0651	InL004b-3	viv																	Dextral
0652	InL004b-3	viv																	Dextral
0653	InL004b-3	viv																	Dextral
0654	InL004b-3	hydC	3.584	2.241	1.457	2.127	1.811	1.158	14.149	35.5	71.270	3.3	No	Closed	Regular	Rounded	Ovate-Conic	No	Dextral
0655	InL004b-3	sty																	Dextral
0656	InL004b-3	styA	2.832	1.443	1.701	1.131	1.025	0.717	9.776	34.1	53.409	6.0	No	Closed	Regular-Strong	Rounded	Conic	No	Dextral
0657	InL004b-3	hydC	9.713	5.711	3.914	5.799	4.377	2.811	12.004	55.6	67.999	4.7	No	Closed	Regular	Rounded	Ovate-Conic	No	Dextral
0658	InL004b-3	lym																	Dextral

0659	InL004b-3	lym																	Dextral
0660	InL004b-3	lym																	Dextral
0661	InL004b-3	lym																	Dextral
0662	InL004b-3	lym																	Dextral
0663	InL004b-3	lym																	Dextral
0664	InL004b-3	lym																	Dextral
0665	InL004b-3	lym																	Dextral
0666	InL004b-3	lym																	Dextral
0667	InL004b-3	lym																	Dextral
0668	InL004b-3	val																	Dextral
0669	InL004b-3	val																	Dextral
0670	InL004b-3	vivB							4.002	94.8	66.329		No	Closed	Strong	Rounded	Turbinifor m-Trochiform	No	Dextral
0671	InL004b-3	val																	Dextral
0672	InL004b-3	val																	Dextral
0673	InL004b-3	vivA	0.771	0.807	0.257	0.514	0.338	0.38	11.310	68	59.349		No	Closed	Strong	Rounded	Trochiform	No	Dextral
0674	InL004b-3	val																	Dextral
0675	InL004b-3	val																	Dextral

0692	0691	0690	0689	0688	0687	0686	0685	0684	0683	0682	0681	0680	0679	0678	0677	0676
InL004b-3	InL004b-3	InL004b-3	InL004b-3	InL004b-3	InL004b-3	InL004b-3	InL004b-3	InL004b-3	InL004b-3	InL004b-3	InL004b-3	InL004b-3	InL004b-3	InL004b-3	InL004b-3	InL004b-3
hyd	hydB	hyd	hyd	hydC	hyd	hydB	hyd	hyd	hyd	hyd	hyd	hyd	hyd	hyd	val	val
	1.603			1.844		2.175										
	1.039			1.257		1.56										
	0.659			0.856		0.73										
	0.945			0.988		1.444										
	0.631			0.79		1.145										
	0.519			0.593		0.784										
	11.493			9.838		14.818										
	47.4			59.9		69.5										
	66.105			68.199		66.975										
	4.4															
	No			No		No										
	Closed			Closed		Closed										
	Strong			Regular		Strong										
	Rounded			Flattened-Rounded		Rounded										
	Ovate			Ovate-Conic		Ovate										
	No			No		No										
Dextral	Dextral	Dextral	Dextral	Dextral	Dextral	Dextral	Dextral	Dextral	Dextral	Dextral	Dextral	Dextral	Dextral	Dextral	Dextral	Dextral

0693	InL004b-3	hyd															Dextral
0694	InL004b-3	hyd															Dextral
0695	InL004b-3	hyd															Dextral
0696	InL004b-3	hydA	1.327	1.1	0.647	0.68	0.539	0.564	8.383	69.6	68.443	4.9	No	Closed	Strong	Rounded	Ovate-Trochiform	No	Dextral
0697	InL004b-3	hyd																Dextral
0698	InL004b-3	hydB	1.273	0.807	0.49	0.784	0.579	0.475	11.254	58	70.887		No	Closed	Strong	Rounded	Ovate	No	Dextral
0699	InL004b-3	hyd																Dextral
0700	InL004b-3	hyd																Dextral
0701	InL004b-3	hyd																Dextral
0702	InL004b	hydC	7.951	5.345	3.546	4.405	3.764	2.646	10.954	60	67.471	7.5	No	Closed	Regular	Flattened-Rounded	Ovate-Conic	No	Dextral
0703	InL004b	hydC	6.436	4.333	2.388	4.048	2.639	2.163	9.728	57.5	65.253	6.6	No	Closed	Regular	Rounded	Ovate-Conic	No	Dextral
0704	InL004b	hydC	7.025	4.419	2.884	4.141	3.449	2.269	12.160	54.9	69.692	6.3	No	Closed	Regular	Rounded	Ovate-Conic	No	Dextral
0705	InL004b	hyd																Dextral
0706	InL004b	hydB	4.746	3.451	1.651	3.095	2.576	2.006	15.974	62.8	63.895	6.9	No	Closed	Regular	Rounded	Ovate	No	Dextral
0707	InL004b-3	sty																Dextral
0708	InL004b-3	sty																Dextral
0709	InL004b-3	sty																Dextral

0726	0725	0724	0723	0722	0721	0720	0719	0718	0717	0716	0715	0714	0713	0712	0711	0710
InL004b-3	InL004b-3	InL004b-3	InL004b-3	InL004b-3	InL004b-3	InL004b-3	InL004b-3	InL004b-3	InL004b-3	InL004b-3	InL004b-3	InL004b-3	InL004b-3	InL004b-3	InL004b-3	InL004b-3
phyA	phyB	phyA	phyB	phyA	phyB	phyB	phy	phy	phy	sty	sty	sty	styB	sty	sty	sty
1.224	1.116	1.264	1.568	1.531	2.696	3.116							2.137			
0.784	0.868	0.837	1.197	1.081	1.842	2.537							1.244			
0.083	0.18	0.129	0.353	0.241	0.556	0.701							0.889			
1.141	0.936	1.135	1.215	1.29	2.14	2.414							1.249			
0.914	1.012	0.928	1.008	1.232	1.807	2.324							1.075			
0.44	0.471	0.478	0.634	0.484	0.984	1.56							0.556			
14.153	14.715	15.642	10.929	24.821	16.422	21.393							14.801			
68.3	87.3	66.7	86	74.4	70.3	88.8							27.7			
73.009	80.538	76.452	78.232	80.685	70.509	76.715							64.983			
		2.7	2.7		4.3	4.9										
No	No	No	No	No	No	No							Yes			
Closed	Closed	Closed	Closed	Closed	Closed	Closed							Closed			
Strong	Regular	Regular	Regular	Regular	Regular	Regular							Regular			
Flattened-Rounded	Flattened-Rounded	Flattened-Rounded	Flattened-Rounded	Flattened-Rounded	Flattened-Rounded	Flattened-Rounded							Rounded			
Elongate Fusiform	Fusiform	Elongate Fusiform	Fusiform	Elongate Fusiform	Elongate Fusiform-Fusiform	Fusiform							Conic			
No	No	No	No	No	No	No							No			
Sinistral	Sinistral	Sinistral	Sinistral	Sinistral	Sinistral	Sinistral	Sinistral	Sinistral	Sinistral	Dextral	Dextral	Dextral	Dextral	Dextral	Dextral	Dextral

0743	0742	0741	0740	0739	0738	0737	0736	0735	0734	0733	0732	0731	0730	0729	0728	0727
InL004b-3	InL004b-3	InL004b-3	InL004b-3	InL004b-3	InL004b-3	InL004b-3	InL004b-3	InL004b-3	InL004b-3	InL004b-3	InL004b-3	InL004b-3	InL004b-3	InL004b-3	InL004b-3	InL004b-3
hydB	hydB	viv	vivA	viv	viv	hydB	hydB	vivB	vivA	hydB	viv	viv	hydB	viv	viv	phy
0.955	0.976		1.106			1.257	1.778	2.249	2.219	2.927			4.024			
0.686	0.734		0.88			0.99	1.378	1.912	2.204	2.646			2.822			
0.337	0.358		0.321			0.43	0.721	0.585	0.582	0.909			1.306			
0.618	0.618		0.785			0.857	1.056	1.664	1.637	2.023			2.718			
0.485	0.551		0.576			0.684	0.885	1.319	1.261	1.625			2.384			
0.349	0.389		0.452			0.496	0.628	1.137	1.054	1.409			1.669			
11.004	10.679		8.746			11.356	8.531	9.221	3.675	12.814			15.656			
62.8	65		71.5			69.9	65.4	71.8	81.4	63			57.4			
68.199	63.435		68.394			69.775	70.346	59.115	64.942	61.540			60.005			
4.0	3.7					4.6	5.0	4.9	4.5				3.4			
No	No		No			Yes	Yes	No	Yes	No			No			
Closed	Closed		Closed			Closed	Closed	Closed	Closed	Closed			Closed			
Strong	Strong		Strong			Regular	Regular	Regular	Regular	Strong			Regular			
Rounded	Rounded		Flattened-Rounded			Rounded	Rounded	Rounded	Flattened-Rounded	Rounded			Flattened-Rounded			
Ovate	Ovate		Ovate			Ovate	Ovate	Trochiform	Trochiform	Ovate			Ovate			
No	No		No			No	No	No	No	No			No			
Dextral	Dextral	Dextral	Dextral	Dextral	Dextral	Dextral	Dextral	Dextral	Dextral	Dextral	Dextral	Dextral	Dextral	Dextral	Dextral	Sinistral

0744	InL004b-3	hydB	0.819	0.68	0.256	0.562	0.493	0.324	15.161	64.7	52.568		No	Closed	Strong	Rounded	Ovate	No	Dextral
0745	InL004b-3	viv																	Dextral
0746	InL004b-3	vivB	1.726	1.829	0.542	1.184	0.968	0.955	10.701	70.6	62.021		No	Closed	Strong	Rounded	Trochiform	No	Dextral
0747	InL004b-3	viv																	Dextral
0748	InL004b-3	vivB	0.814	0.931	0.197	0.617	0.457	0.374	7.552	77.6	64.151		Yes	Closed	Strong	Rounded	Trochiform	No	Dextral
0749	InL004b-3	vivB	0.882	0.828	0.19	0.692	0.539	0.416	10.222	92.9	69.209	3.4	Yes	Closed	Regular	Rounded	Trochiform	No	Dextral
0750	InL004b-3	valB	0.85	0.81	0.246	0.604	0.58	0.425	11.146	82.9	64.026	3.5	Yes	Closed	Strong	Rounded	Turbinifor m-Trochiform	No	Dextral
0751	InL004b-3	hydB	0.918	0.606	0.201	0.717	0.451	0.24	10.897	69.8	59.859		No	Closed	Strong	Rounded	Ovate	No	Dextral
0752	InL004b-3	viv																	Dextral
0753	InL004b-3	vivB	0.765	0.707	0.224	0.54	0.426	0.349	13.766	68.2	71.384	3.6	No	Closed	Strong	Rounded	Trochiform	No	Dextral
0754	InL004b-3	viv																	Dextral
0755	InL004b-3	viv																	Dextral
0756	InL004b	viv																	Dextral
0757	InL004b	viv																	Dextral
0758	InL004b	phyB	26.195	13.36	3.004	23.191			9.176	82.4	75.097	3.4	No	Closed	Some	Flattened-Rounded	Fusiform	No	Sinistral
0759	InL004b	lymB	11.609	4.118	3.059	3.549	6.549	2.024	23.110	46.3	77.471	4.9	No	Closed	Regular	Flattened-Rounded	Elongate Conic	No	Dextral
0760	InL096	viv																	Dextral

0777	0776	0775	0774	0773	0772	0771	0770	0769	0768	0767	0766	0765	0764	0763	0762	0761
InL096b	InL096b	InL096b	InL096b	InL096	InL096b	InL096	InL096b	InL096b	InL096b	InL096b	InL096	InL096	InL096	InL096b	InL096	InL096
hydC	styB	vivB	vivB	viv	hydA	lym	viv	vivB	hydB	hydB	vivA	hydB	viv	viv	hydC	viv
2.685	3.518	0.572	0.979		1.131			1.654	1.455	1.749	3.149	5.193			3.413	
1.462	2.106	0.562	1.032		1.111			1.435	1	1.402	2.522	3.512			2.816	
1.252	1.976	0.154	0.248		0.463			0.602	0.502	0.484	0.981	1.764			2.206	
1.433	1.542	0.418	0.731		0.668			1.052	0.954	1.265	2.168	3.429			1.207	
0.975			0.535						0.611	0.739	1.665	2.489				
0.497			0.499						0.567	0.697	1.224	1.972				
10.382	10.850	14.036	12.771		10.574			10.657	11.201	13.912	5.631	8.198		16.101	13.420	
37.8	46.3	89.9	77.4		66			69.7	53.3		61.1	52.4			44.4	
74.600	63.101		71.479		68.199			68.669	77.381	60.164	62.026	64.814				
5.3									4.2	4.0	3.3	4.0				
No	No	No	No		No			No	No	No	No	No		No	No	
Closed	Closed	Closed	Closed		Closed			Closed	Closed	Closed	Closed	Closed		Closed	Closed	
Regular	Regular	Strong	Strong		Strong			Strong	Regular	Strong	Regular	Strong		Regular	Strong	
Rounded	Flattened-Rounded	Rounded	Rounded		Flattened-Rounded			Rounded	Flattened-Rounded	Rounded	Flattened-Rounded	Rounded		Flattened-Rounded	Rounded	
Ovate-Conic	Conic	Trochiform	Trochiform		Trochiform			Trochiform	Ovate	Trochiform	Trochiform	Ovate		Trochiform	Conic	
No	No	No	No		No			No	No	No	No	No		No	No	
Dextral	Dextral	Dextral	Dextral	Dextral	Dextral	Dextral	Dextral	Dextral	Dextral	Dextral	Dextral	Dextral	Dextral	Dextral	Dextral	Dextral

0794	0793	0792	0791	0790	0789	0788	0787	0786	0785	0784	0783	0782	0781	0780	0779	0778
InL096b	InL096b	InL096b	InL096b	InL096b	InL096b	InL096b	InL096b	InL096b	InL096b	InL096b	InL096b	InL096b	InL096b	InL096b	InL096b	InL096b
hydC	viv	vivB	hydC	phyB	lymA	vivB	hydC	valB	hydB	hydC	lymA	hydB	hydB	viv	vivB	hydC
1.207		0.567		1.004	2.078	1.022	1.949	1.197	1.758	2.442	4.063				0.857	1.502
0.926		0.554		0.663	1.554	0.914	1.177	1.184	1.1	1.654	1.962				0.912	1.141
0.411		0.129		0.225	0.353	0.244	0.626	0.371	0.708	1.251	1.621				0.224	0.672
0.797		0.438		0.778	1.725	0.778	1.323	0.827	1.05	1.191	2.442				0.634	0.83
					1.441		0.921	0.74	0.728	0.776					0.49	
					0.853		0.688	0.713	0.575	0.7					0.442	
15.430		13.021	16.063	29.805	8.865	6.483	3.460	13.614	12.688	8.762	24.404	13.195	8.366		9.185	11.768
46.9		78.7	46	76.1	87.8	78.5	44.2	78	57.2	49.3	46	69.4			84	53.1
				88.305	62.535		68.398	81.093	66.140		69.737		69.624		71.980	76.849
					3.2	4.2	4.9	4.1	4.4	5.2	4.4					
No		No	No	No	No	No	No	No	No	No	No	No	No		No	No
Closed		Closed	Closed	Closed	Closed	Closed	Closed	Closed	Closed	Closed	Closed	Closed	Closed		Closed	Closed
Strong		Strong	Strong	Strong	Regular	Strong	Regular	Strong	Strong	Strong	Regular	Regular	Strong		Strong	Strong
Rounded		Rounded	Rounded	Flattened-Rounded	Flattened-Rounded	Rounded	Rounded	Rounded	Rounded	Flattened-Rounded	Flattened-Rounded	Rounded	Rounded		Rounded	Rounded
Ovate-Conic		Trochiform	Ovate-Conic	Fusiform	Elongate Cylindrical	Trochiform	Ovate-Conic	Turbinifor m-Trochiform	Ovate	Ovate-Conic	Elongate Conic	Trochiform			Trochiform	Ovate
No		No	No	No	No	No	No	No	No	No	No	No	No		No	No
Dextral	Dextral	Dextral	Dextral	Sinistral	Dextral	Dextral	Dextral	Dextral	Dextral	Dextral	Dextral	Dextral	Dextral	Dextral	Dextral	Dextral

0811	0810	0809	0808	0807	0806	0805	0804	0803	0802	0801	0800	0799	0798	0797	0796	0795
InL096b	InL096b	InL096b	InL096b	InL096b	InL096b	InL096b	InL096b	InL096b	InL096b	InL096b	InL096b	InL096b	InL096b	InL096b	InL096b	InL096b
viv	viv	viv	hydC	viv	lymA	viv	viv	vivB	vivA	vivB	hyd	lymB		hydB	lymB	hydC
			1.543		2.481			1.178	1.1	1.101		1.706		1.309	3.125	
			0.807		1.604			1.233	0.882	0.966		0.838		0.871	1.488	
			0.573		0.364			0.321	0.535	0.359		0.317		0.416	1.125	
			0.97		2.117			0.857	0.565	0.743		1.389		0.893	2.001	
			0.659		1.574			0.7	0.38	0.564						
			0.529		0.709			0.711	0.479	0.597						
			14.859		6.557			12.615	21.550	13.462		18.733		12.331	21.173	23.565
			35.5		73.5			70.1	53.6	70.2		47.7		69.7	34.8	
			71.194		69.791			74.343	68.254	76.407					72.085	
								2.9	5.2						3.4	
			No		No			No	No	No		No		No	No	No
			Closed		Closed			Closed	Closed	Closed		Closed		Closed	Closed	Closed
			Strong		Regular			Strong	Regular-Strong	Regular-Strong		Strong		Regular	Strong	
			Rounded		Flattened-Rounded			Rounded	Flattened-Rounded	Rounded		Flattened-Rounded		Rounded	Flattened-Rounded	
			Trochiform		Elongate Cylindrical			Trochiform	Trochiform	Trochiform		Elongate Conic		Ovate-Conic	Elongate Conic	Conic
			No		No			No	No	No		No		No	No	No
Dextral	Dextral	Dextral	Dextral	Dextral	Dextral	Dextral	Dextral	Dextral	Dextral	Dextral	Dextral	Dextral		Dextral	Dextral	Dextral

0828	0827	0826	0825	0824	0823	0822	0821	0820	0819	0818	0817	0816	0815	0814	0813	0812
InL096b	InL096b	InL096b	InL096b	InL096b	InL096b	InL096b	InL096b	InL096b	InL096b	InL096b	InL096b	InL096b	InL096b	InL096b	InL096b	InL096b
hydB	viv	phy	hydB	lymB	hyd	styB	hydC	styB	styB	vivB	styC	hyd	lymA	viv	val	viv
2.27		2.004	2.472	3.283		2.682	2.985	3.163	3.749	3.026	3.568		4.104			
1.509		1.611	1.865	1.803		1.154	1.989	1.44	2.2	2.344	1.983		2.243			
0.91		0.009	0.835	0.831		1.337	1.323	1.621	1.947	0.81	2.099		0.899			
1.36		1.905	1.637	2.452		1.345	1.662	1.542	1.802	2.216	1.469		3.204			
0.963		1.995	1.16			1.13	1.396	1.02		1.565	0.98		2.236			
0.647		0.832	0.856			0.59	1.047	0.733		1.222	1.11		1.131			
10.770			9.314	36.491		13.496	19.952	16.015	10.211	9.139	12.653		16.113			
59.8			67.6	34.8		28.1	51.7		39.4	73.5	36.6		63			
73.768			73.034	67.964		75.604	74.438	65.404	69.031	71.135	69.677		68.369			
5.2				3.9		6.4		6.9	5.2	3.9	4.6		3.8			
No		No	No	No		No	No	No	No	No	No		No			
Closed		Closed	Closed	Closed		Closed	Closed	Closed	Closed	Closed	Closed		Closed			
Regular-Strong			Strong	Strong		Strong	Strong	Regular	Regular	Strong	Strong		Regular			
Rounded			Rounded	Flattened-Rounded		Rounded	Rounded	Flattened-Rounded	Flattened-Rounded	Rounded	Rounded		Flattened-Rounded			
Ovate			Ovate	Elongate Conic		Conic	Trochiform	Ovate-Conic	Ovate-Conic	Trochiform	Conic		Elongate Cylindrical			
No		No	No	No		No	No	No	No	No	No		No			
Dextral	Dextral	Sinistral	Dextral	Dextral	Dextral	Dextral	Dextral	Dextral	Dextral	Dextral	Dextral	Dextral	Dextral	Dextral	Dextral	Dextral

0829	InL096b	viv																	Dextral
0830	InL096b	phyA	1.865	1.042	0.314	1.551	1.659	0.638	25.805	55.3	80.954	2.5	No	Closed	Regular	Flattened-Rounded	Elongate Fusiform	No	Sinistral
0831	InL096b	hydC	2.262	1.23	1.062	1.199	0.706	0.579	10.088	47.5	71.740	5.7	No	Closed	Regular	Flattened-Rounded	Ovate-Conic	No	Dextral
0832	InL096b	hydA	2.181	1.587	0.936	1.245	0.888	0.659	8.559	47.2	70.769	3.8	No	Closed	Regular	Flattened-Rounded	Ovate	No	Dextral
0833	InL096b	viv																	Dextral
0834	InL096b	viv																	Dextral
0835	InL096b	valB	1.666	1.612	0.562	1.104	1.025	0.814	12.529	84.8	58.958	3.7	No	Closed	Strong	Rounded	Turbinifor m-Trochiform	No	Dextral
0836	InL096b	hydC	1.837	1.157	0.833	1.005	0.805	0.54	4.160	47.2	62.166	4.6	No	Closed	Strong	Rounded	Ovate-Conic	No	Dextral
0837	InL096b	phyB	2.162	1,524	0.645	1.517			16.928	80.9	77.159	3.8	No	Closed	Strong	Rounded	Fusiform	No	Sinistral
0838	InL096b	viv																	Dextral
0839	InL096b	vivA	2.005	1.665	0.789	1.216	0.953	0.854	10.812	74.5	66.532	4.8	No	Closed	Regular-Strong	Flattened-Rounded	Trochiform	No	Dextral
0840	InL096b	valB	1.415	1.585	0.539	0.876	0.798	0.929	10.008	76.8	67.338	3.1	No	Closed	Strong	Rounded	Turbinifor m-Trochiform	No	Dextral
0841	InL096b	viv																	Dextral
0842	InL096b	viv																	Dextral
0843	InL096b	phy																	Sinistral
0844	InL096b	viv																	Dextral
0845	InL096b	viv																	Dextral

0862	0861	0860	0859	0858	0857	0856	0855	0854	0853	0852	0851	0850	0849	0848	0847	0846
InL096b	InL096b	InL096b	InL096b	InL096b	InL096b	InL096b	InL096b	InL096b	InL096b	InL096b	InL096b	InL096b	InL096b	InL096b	InL096b	InL096b
phyA	viv	hydB	viv	viv	viv	vivB	viv	hydA	viv	lym	phy	lymB	hydB	viv	viv	phy
1.185						1.111		1.498								
0.738						0.89		0.989								
0.163						0.304		0.602								
1.021						0.807		0.896								
0.834						0.569		0.628								
0.437						0.44		0.402								
18.667		22.316				13.504		14.455					8.427			
63.4		45.6				73.6		49.7								
78.551		63.880				70.170		71.147					64.863			
2.6								4.3								
No		No				No		No					No			
Closed		Closed				Closed		Closed					Closed			
Regular		Strong				Regular-Strong		Regular					Regular			
Flattened-Rounded		Rounded				Rounded		Rounded					Flattened-Rounded			
Elongate Fusiform		Ovate				Trochiform		Ovate					Ovate			
No		No				No		No					No			
Sinistral	Dextral	Dextral	Dextral	Dextral	Dextral	Dextral	Dextral	Dextral	Dextral	Dextral	Sinistral	Dextral	Dextral	Dextral	Dextral	Sinistral

0863	InL096b	viv																	Dextral
0864	InL096b	vivB	0.962	0.887	0.277	0.685	0.556	0.535	20.811	70.9	58.050		No	Closed	Strong	Rounded	Trochiform	No	Dextral
0865	InL096b	phy																	Sinistral
0866	InL096b	viv																	Dextral
0867	InL096b	viv																	Dextral
0868	InL096b	vivB	3.043	2.672	0.767	2.276	1.637	1.414	9.462	77.7	71.847		No	Closed	Regular-Strong	Rounded	Trochiform	No	Dextral
0869	InL096b	phy																	Sinistral
0870	InL096b	valA	8.332	8.093	2.723	5.609	4.947	5.161	13.134	77.5	77.983	2.1	No	Open	Strong	Rounded	Turbiniform-Trochiform	Revolving	Dextral
0871	InL096b	lymB	4.556	2.786	0.992	3.564	3.188	1.625	16.248	49.6		3.2	No	Closed	Strong	Flattened-Rounded	Elongate Conic	No	Dextral
0872	InL096b	valB	2.186	3.095	0.706	1.48	1.257	1.213	11.514	93.8		3.1	No	Open	Regular	Flattened-Rounded	Turbiniform	Revolving	Dextral
0873	InL096b	viv																	Dextral
0874	InL096b	hydB	2.613	1.852	0.926	1.687	1.181	1.004	7.539	44.7	68.094		No	Closed	Regular	Flattened-Rounded	Ovate	No	Dextral
0875	InL096b	viv																	Dextral
0876	InL096b	hydC	2.837	1.824	1.173	1.665	1.103	0.925	12.789	61.7	69.918	5.7	No	Closed	Some	Flattened-Rounded	Ovate-Conic	No	Dextral
0877	InL096b	vivB	2.552	2.075	0.565	1.987	1.733	1.158	14.520	76.8	73.160	4.2	No	Closed	Strong	Rounded	Trochiform	No	Dextral
0878	InL096b	styB	3.045	1.524	1.73	1.314	1.026	0.871	12.431	44.1	80.870	6.6	No	Closed	Regular	Flattened-Rounded	Conic	No	Dextral
0879	InL096b	styB	2.835	1.387	1.524	1.31	0.942	0.659	12.724	38.7	53.297	6.2	No	Closed	Regular	Flattened-Rounded	Conic	No	Dextral

0880	InL096b	hydA	2.193	1.933	0.855	1.338	1.26	0.972	10.402	69.2	70.967	3.1	No	Closed	Regular	Rounded	Ovate	No	Dextral
0881	InL096b	hydB	2.375	1.607	0.794	1.581	1.114	0.89	9.806	54.2	63.435	3.8	No	Closed	Strong	Rounded	Ovate	No	Dextral
0882	InL096b	lymB	1.935	1.249	0.595	1.339	1.042	0.605	12.011	54.3	72.525	4.0	No	Closed	Strong	Flattened-Rounded	Elongate Cylindrical	No	Dextral
0883	InL096b	viv																	Dextral
0884	InL096b	styB	2.165	0.63	1.02	1.145	0.738	0.343	25.821		63.587		No	Closed	Regular	Flattened-Rounded	Ovate-Conic	No	Dextral
0885	InL096b	lym																	Dextral
0886	InL096b	hydA	1.598	1.284	0.49	1.108	0.822	0.673	10.054	64.5	71.647		No	Closed	Regular	Rounded	Ovate	No	Dextral
0887	InL096b	hyd																	Dextral
0888	InL096b	viv																	Dextral
0889	InL096b	hydB	1.449	0.926	0.516	0.933			8.476	57.2	75.849	4.4	No	Closed	Strong	Rounded	Ovate	No	Dextral
0890	InL096b	viv																	Dextral
0891	InL096b	viv																	Dextral
0892	InL096b	lym																	Dextral
0893	InL096b	lym																	Dextral
0894	InL096b	hyd																	Dextral
0895	InL096b	hyd																	Dextral
0896	InL096b																		

0897	InL096b	styB	3.09	1.634	1.694	1.396	0.839	0.703	16.365	37.7	72.525		No	Closed	Regular	Flattened-Rounded	Conic	No	Dextral
0898	InL096b	valA	3.737	3.142	1.273	2.464	1.626	1.505	12.848	76.5	75.426	4.7	No	Open	Regular	Flattened-Rounded	Turbiniform-Trochiform	Revolving	Dextral
0899	InL096b	vivA	6.383	6.405	2.238	4.145	3.532	3.466	6.710	79.2	68.405	5.8	No	Closed	Some-Regular	Flattened-Rounded	Turbiniform-Trochiform	No	Dextral
0900	InL096b	valB	2.765	3.81	0.694	2.071			4.677			1.6	No		Regular	Flattened-Rounded	Turbiniform-Trochiform	Revolving	Dextral
0901	InL096b	viv																	Dextral
0902	InL096b	val																	Dextral
0903	InL096b	val																	Dextral
0904	InL096b	val																	Dextral
0905	InL096b	val																	Dextral
0906	InL096b	val																	Dextral
0907	InL096b	hydC	3.918	3.167	2.12	1.799			13.183	67.4			No	Closed	Regular-Strong	Rounded	Ovate	No	Dextral
0908	InL096b	phy																	Sinistral
0909	InL096b	hyd																	Dextral
0910	InL096b	lym																	Dextral
0911	InL096b	phy																	Sinistral
0912	InL096b	valA	3.219	3.137	1.356	1.863	1.73	1.491	6.203	74.7			No	Open	Strong	Rounded	Turbiniform-Trochiform	Revolving	Dextral
0913	InL096b	val																	Dextral

0930	0929	0928	0927	0926	0925	0924	0923	0922	0921	0920	0919	0918	0917	0916	0915	0914
InL096b	InL096b	InL096b	InL096b	InL096b	InL096b	InL096b	InL096b	InL096b	InL096b	InL096b	InL096b	InL096b	InL096b	InL096b	InL096b	InL096b
lymA	lymB	lymB	valB	val	hydB	phy	hyd	viv	viv	hydC	hydC	hyd	val	val	hyd	hyd
2.363	5.342	5.649	2.112							2.343	4.908					
1.986	2.654	2.418	2.639							1.632	2.523					
	2.588	1.535	1.046							1.494	2.428					
	2.754	4.114	1.066							0.849	2.481					
18.597	10.692	17.913	4.028		13.092					11.717	11.868					
56.2	41.7	47	78.8							47.7	63.6					
4.9			3.6													
No	No	No	No		No					No	No					
Closed	Closed	Closed			Closed					Closed	Closed					
Regular	Strong	Strong	Strong		Regular					Strong	Strong					
Flattened-Rounded	Rounded	Flattened-Rounded	Flattened-Rounded		Flattened-Rounded					Rounded	Rounded					
Elongate Conic	Elongate Conic	Elongate Conic	Turbinifor m-Trochiform		Ovate					Ovate-Conic	Conic					
No	No	No	Revolving		No					No	No					
Dextral	Dextral	Dextral	Dextral	Dextral	Dextral	Sinistral	Dextral	Dextral	Dextral	Dextral	Dextral	Dextral	Dextral	Dextral	Dextral	Dextral

0931	InL096b	phy																	Sinistral
0932	InL096b	valB	2.591	2.687	1.114	1.477			9.586	83.5			No		Regular	Flattened-Rounded	Turbinifor m-Trochiform	Revolving	Dextral
0933	InL096b	val																	Dextral
0934	InL096b	viv																	Dextral
0935	InL096b	hyd																	Dextral
0936	InL096b	valB	1.818	1.733	0.711	1.107			8.092	75.9			No		Strong	Flattened-Rounded	Turbinifor m-Trochiform	Revolving	Dextral
0937	InL096b	lymB	3.879	2.509	1.349	2.53	1.72	1.171	21.618	53.3		4.6	No	Closed	Some-Regular	Rounded	Elongate Conic	No	Dextral
0938	InL096b	val																	Dextral
0939	InL096b	styB	1.422	3.44	4.802	2.619			12.695	64.5			No	Closed	Regular	Flattened-Rounded	Conic	No	Dextral
0939b	InL096b	vivA	2.704	2.039	1.24	1.464			6.682	68.1			No	Closed	Strong	Rounded	Trochiform	No	
0940	InL096b	val																	Dextral
0941	InL096b	val											No				Turbinifor m-Trochiform	Revolving	Dextral
0942	InL096b	val																	Dextral
0943	InL096b	val																	Dextral
0944	InL096b	lymB	5.97	2.572	1.997	3.973	2.838	1.369	20.821	34.7	70.259	3.9	No	Closed	Strong	Flattened-Rounded	Elongate Conic	No	Dextral
0945	InL096b	val																	Dextral
0946	InL096b	val																	Dextral

0963	0962	0961	0960	0959	0958	0957	0956	0955	0954	0953	0952	0951	0950	0949	0948	0947
InL096b	InL096b	InL096b	InL096b	InL096b	InL096b	InL096b	InL096b	InL096b	InL096b	InL096b	InL096b	InL096b	InL096b	InL096b	InL096b	InL096b
hydC	hyd	viv	hydC	viv	lymB	hydC	vivB	val	val	valB	valB	valB	valB	valB	lymB	valB
2.875			3.347		5.898	2.601				1.302		3.729	3.914	2.805	8.081	3.797
1.778			2.251		2.966	1.767				1.468		5.593	3.174	3.288	3.44	3.724
1.125			1.458		1.191	1.283				0.571		1.534	1.942	1.323	3.175	1.812
1.749			1.889		4.707	1.318				0.732		2.196	1.972	1.482	4.906	1.984
0.932			1.428		3.431	1.191										
0.832			1.312		1.81	0.926										
3.042			13.257		18.346	18.819	12.366			6.369		11.260	8.542	9.230	11.310	3.003
57.2			39.4		47.2	46.2	69			106.4		101.3	77.9	93.3	45.9	83.1
56.023			68.199		69.376	71.690				78.198		65.807				
			4.0			3.4				3.6	3.2	4.2				4.7
No			No		No	No	No			No	No	No	No	No	No	No
Closed			Closed		Closed	Closed	Closed			Open		Open			Closed	Open
Some			Strong		Regular	Regular-Strong	Strong			Regular		Regular	Regular	Strong	Some-Regular	Strong
Flattened-Rounded			Rounded		Flattened-Rounded	Flattened-Rounded	Rounded			Rounded		Flattened-Rounded	Flattened-Rounded	Rounded	Flattened-Rounded	Flattened-Rounded
Ovate-Conic			Ovate-Conic		Elongate Conic	Ovate-Conic	Turbiniform-Trochiform			Turbiniform		Turbiniform	Turbiniform-Trochiform	Turbiniform-Trochiform	Elongate Conic	Turbiniform-Trochiform
No			No		No	No	No			Revolving	Revolving	Revolving	Revolving	Revolving	No	Revolving
Dextral	Dextral	Dextral	Dextral	Dextral	Dextral	Dextral	Dextral	Dextral	Dextral	Dextral	Dextral	Dextral	Dextral	Dextral	Dextral	Dextral

0980	0979	0978	0977	0976	0975	0974	0973	0972	0971	0970	0969	0968	0967	0966	0965	0964
InL096b	InL096b	InL096b	InL096b	InL096b	InL096b	InL096b	InL096b	InL096b	InL096b	InL096b	InL096b	InL096b	InL096b	InL096b	InL096b	InL096b
phy	hydB	hydC	vivA	hydC	valB	valB	hydC	valA	lym	val	styB	phy	valB	lymB	hydC	lym
	2.956	2.348	3.135	5.364				5.418					1.48	3.049	1.775	
	2.369	1.513	2.506	3.498				4.192					2.348	1.429	1.174	
	0.98	1.414	0.953	3.498				2.694					0.678	0.682	0.783	
	1.976	0.934	2.183	1.866				2.724					0.802	2.367	0.992	
							1.323							1.667		
							1.006							0.876		
	11.101	9.841	1.901	9.357	15.996	10.305	10.877	5.711			11.370		11.929	20.186	11.070	
	75.3	51	74.6	42.8	101.6	91.8	61.1	66.7			41.8		101.3	38.6	45.4	
					62.319			78.050						70.241	67.098	
					3.6	4.1							3.3	3.2	4.3	
	No	No	No	No	No	No	No	No			No		No	No	No	
	Closed	Closed	Closed	Closed		Open	Closed	Open			Closed			Closed	Closed	
	Regular	Strong	Regular	Some	Regular	Regular	Some-Regular	Regular			Strong		Regular	Strong	Regular	
	Rounded	Flattened-Rounded	Rounded	Flattened-Rounded	Flattened-Rounded	Flattened-Rounded	Flattened-Rounded	Flattened-Rounded			Flattened-Rounded		Flattened-Rounded	Flattened-Rounded	Rounded	
	Trochiform	Ovate	Trochiform	Conic	Turbiniform	Turbiniform	Ovate-Conic	Turbiniform-Trochiform			Conic		Turbiniform	Elongate Conic	Ovate-Conic	
	No	No	No	No	Revolving	Revolving	No	Revolving			No		Revolving	No	No	
Sinistral	Dextral	Dextral	Dextral	Dextral	Dextral	Dextral	Dextral	Dextral	Dextral	Dextral	Dextral	Sinistral	Dextral	Dextral	Dextral	Dextral

0981	InL096b	phyB	2.324	1.981	0.637	1.687	1.68	0.971	10.539	83.8	74.859	2.9	No	Closed	Strong	Flattened-Rounded	Fusiform	No	Sinistral
0982	InL096b	lym																	Dextral
0983	InL096b	styB	2.212	0.735	1.3	0.912	0.557	0.311	3.504	20.6	63.249	5.8	No	Closed	Strong	Flattened-Rounded	Ovate-Conic	No	Dextral
0984	InL096b	styB	2.521	1.427	1.199	1.321	1.053	0.667	9.123		70.481	4.3	No	Closed	Some	Flattened-Rounded	Conic	No	Dextral
0985	InL096b	hydC	2.217	1.127	1.06	1.157			20.163		72.443	3.9	No	Closed	Regular	Flattened-Rounded	Conic	No	Dextral
0986	InL096b	lym																	Dextral
0987	InL096b	viv																	Dextral
0988	InL096b	phyB	1.951	1.34	0.579	1.371			23.385	64.4	70.626	3.1	No	Closed	Strong	Flattened-Rounded	Fusiform	No	Sinistral
0989	InL096b	phy																	Sinistral
0990	InL096b	viv																	Dextral
0991	InL096b	viv																	Dextral
0992	InL096b	hydB	1.401	1.001	0.471	0.93			13.591	57.8	68.629	3.3	No	Closed	Strong	Flattened-Rounded	Ovate	No	Dextral
0993	InL096b	viv																	Dextral
0994	InL096b	vivB	0.916	0.81	0.333	0.583	0.473	0.367	10.521	65.7	73.160	3.9	No	Closed	Regular	Rounded	Trochiform	No	Dextral
0995	InL096b	viv																	Dextral
0996	InL096b	viv																	Dextral
0997	InL096b	viv																	Dextral

0998	InL096b	valA	0.686	0.719	0.204	0.482	0.384	0.38	16.504	69.8	68.268	2.8	No	Open	Strong	Rounded	Turbinifor m- Trochiform	Revolving	Dextral
0999	InL096b	viv																	Dextral
1000	InL096b	hydC	2.844	1.825	1.279	1.565			10.860	53.1		6.4	No	Closed	Regular	Flattened- Rounded	Ovate- Conic	No	Dextral
1001	InL096b	viv																	Dextral
1002	InL096b	viv																	Dextral
1003	InL096b	viv																	Dextral
1004	InL096b	val																	Dextral
1005	InL096b	vivA	2.063	1.869	0.819	1.244			10.033	66.2			No	Closed	Strong	Rounded	Trochiform	No	Dextral
1006	InL096b	val																	Dextral
1007	InL096b	viv																	Dextral
1008	InL096b	viv																	Dextral
1009	InL096b	hydC	2.605	1.482	1.11	1.495			13.950		59.697	5.8	No	Closed	Regular	Rounded	Conic	No	Dextral
1010	InL096b	styB	3.286	1.201	1.737	1.549	1.003	0.667	18.232		61.139		No	Closed	Some- Regular	Flattened- Rounded	Conic	No	Dextral
1011	InL096b	styB							12.562		57.995		No	Closed	Some- Regular	Flattened- Rounded	Conic	No	Dextral
1012	InL096b	phyB	5.755	5.077	0.372	5.383	5.765	2.812	16.504		72.553	2.0	No	Closed			Fusiform	No	Sinistral
1013	InL096b	hydB	3.986	2.195	1.579	2.406	1.813	1.038	15.945	39.2	61.830	4.3	No	Closed	Regular	Flattened- Rounded	Ovate	No	Dextral
1014	InL096b	viv																	Dextral

1031	1030	1029	1028	1027	1026	1025	1024	1023	1022	1021	1020	1019	1018	1017	1016	1015
InL096b	InL096b	InL096b	InL096b	InL096b	InL096b	InL096b	InL096b	InL096b	InL096b	InL096b	InL096b	InL096b	InL096b	InL096b	InL096b	InL096b
valB	lym	hydB	hydB	lym	hydB	lymA	hydC	styB	lymA	hyd	hydB	lymA	lymB	viv	hydB	viv
2.318		2.348	3.566		2.588	3.416	2.528		3.561		3.293	2.751	4.134		3.93	
2.198		1.641	2.134		1.856	2.555	1.835		2.266		2.606	2.712	2.006		2.953	
0.783		0.837	1.383		1.118	0.829	1.427		0.937		0.926	0.485	0.805		1.245	
1.535		1.512	2.183		1.47	2.587	1.101		2.624		2.367	2.266	3.329		2.685	
1.179		1.481	1.764		1.097	2.361			2.582		1.648	2.176	2.467		1.836	
1.191		0.695	1.356		0.954	1.741			0.989		1.075	1.541	1.177		1.306	
10.429		7.463	15.945		15.887	11.017	15.716	13.052	19.714		22.126	20.179	16.493		9.819	
62.3		64.5	51.2		48.4	104.2	35.3	50.1	59		54.3		61.2		67.5	
70.190		66.420	68.068		62.536		58.744	63.997			64.231		72.897		70.001	
4.6		3.9	5.6		4.8	4.2			3.4		5.8	4.3	5.5		5.3	
No		No	No		No	No	No	No	No		No	No	No		No	
Open		Closed	Closed		Closed	Closed	Closed	Closed	Closed		Closed	Closed	Closed		Closed	
Strong		Regular	Regular		Regular-Strong	Some-Regular	Some-Regular	Regular	Regular		Regular	Strong	Regular		Regular-Strong	
Rounded		Rounded	Rounded		Rounded	Flattened-Rounded	Flattened-Rounded	Flattened-Rounded	Flattened-Rounded		Flattened-Rounded	Flattened-Rounded	Flattened-Rounded		Flattened-Rounded	
Turbinifor m-Trochiform		Ovate	Ovate		Ovate	Elongate Cylindrical	Ovate-Conic	Conic	Elongate Cylindrical		Ovate	Elongate Cylindrical	Elongate Conic		Ovate	
Revolving		No	No		No	No	No	No	No		No	No	No		No	
Dextral	Dextral	Dextral	Dextral	Dextral	Dextral	Dextral	Dextral	Dextral	Dextral	Dextral	Dextral	Dextral	Dextral	Dextral	Dextral	Dextral

1048	1047	1046	1045	1044	1043	1042	1041	1040	1039	1038	1037	1036	1035	1034	1033	1032
InL096b	InL096b	InL096b	InL096b	InL096b	InL096b	InL096b	InL096b	InL096b	InL096b	InL096b	InL096b	InL096b	InL096b	InL096b	InL096b	InL096b
hydB	sty	hydC	hydC	hyd	hydC	hyd	hydB	hydC	styB	lym	hydB	lymB	lymB	styC	lymA	hyd
1.753		1.861	2.137		1.976			2.734			2.46	2.624	3.278	2.569	2.007	
1.262		1.527	1.177		1.359			1.306			1.503	1.359	1.496	1.582	1.907	
0.706		1.045	1.227		0.816			1.346			1.03	0.654	0.704	1.251	0.524	
1.047		0.816	0.91		1.16			1.388			1.43	1.97	2.574	1.317	1.483	
0.728		0.591	0.639		0.893			0.989			1.006	1.593	2.245	0.917	1.513	
0.78		0.784	0.645		0.72			0.79			0.609	0.66	0.773	0.676	0.963	
13.109	13.046	11.923	12.140		13.742		11.731	21.695	21.092		11.268	13.958	24.274	19.628	4.214	
43.4	37.3	41.4	43.2		49.6		62.9	34.5	33		66	48.3	47	45.3	84.4	
69.409		63.961	70.750		60.524			62.319			64.002	69.984	73.573	65.966	68.749	
4.0			6.4		5.1				6.0			3.1	3.9	5.0		
No	No	No	No		No		No	No	No		No	No	No	No	No	
Closed	Closed	Closed	Closed		Closed		Closed	Closed	Closed		Closed	Closed	Closed	Closed	Closed	
Strong	Regular	Strong	Regular		Regular		Regular	Some-Regular	Regular		Regular-Strong	Strong	Regular	Regular	Regular	
Rounded	Flattened-Rounded	Rounded	Rounded		Flattened-Rounded		Flattened-Rounded	Flattened-Rounded	Flattened-Rounded		Rounded	Flattened-Rounded	Flattened-Rounded	Flattened-Rounded	Flattened-Rounded	
Ovate	Conic	Ovate-Conic	Ovate-Conic		Ovate-Conic		Ovate	Ovate-Conic	Conic		Ovate	Elongate Conic	Elongate Conic	Conic	Elongate Cylindrical	
No	No	No	No		No		No	No	No		No	No	No	No	No	
Dextral	Dextral	Dextral	Dextral	Dextral	Dextral	Dextral	Dextral	Dextral	Dextral	Dextral	Dextral	Dextral	Dextral	Dextral	Dextral	Dextral

1065	1064	1063	1062	1061	1060	1059	1058	1057	1056	1055	1054	1053	1052	1051	1050	1049
InL096b	InL096b	InL096b	InL096b	InL096b	InL096b	InL096b	InL096b	InL096b	InL096b	InL096b	InL096b	InL096b	InL096b	InL096b	InL096b	InL096b
hydC	vivB	vivB	hydB	viv	lymB	phy	hydA	vivB	viv	vivB	valB	viv	viv	phy	hyd	vivB
2.332	0.964	1.14			6.337		1.905	1.788		1.093	1.61					1.224
1.51	0.929	1.075			2.897		1.508	1.549		0.977	1.657					1.211
1.135	0.228	0.275			2.077		0.787	0.608		0.434	0.528					0.256
1.196	0.736	0.865			4.26		1.118	1.18		0.659	1.082					0.967
0.712	0.602	0.649			3.23		0.631	0.976		0.543	0.896					0.789
0.716	0.546	0.566			0.97		0.865	0.732		0.594	0.9					0.685
9.436	8.436	13.069	14.036		16.675		13.988	12.357		17.312	12.995					10.939
42	68.8	61.7	63.8		40.3		49.7	75.9		61.3	78.8					89.9
73.551	73.698	71.381	69.614		69.495		62.526	74.055		63.150	65.659					66.631
6.1	3.5	3.3			3.7			4.0								3.7
No	No	No	No		No		No	No		No	No					No
Closed	Closed	Closed	Closed		Closed		Closed	Closed		Closed	Closed					Closed
Regular	Strong	Strong	Regular		Strong		Regular	Strong		Strong	Strong					Strong
Flattened-Rounded	Rounded	Rounded	Rounded		Flattened-Rounded		Rounded	Rounded		Rounded	Rounded					Rounded
Ovate-Conic	Trochiform	Trochiform	Ovate		Elongate Conic		Ovate	Trochiform		Trochiform	Turbiniform-Trochiform					Trochiform
No	No	No	No		No		No	No		No	No					No
Dextral	Dextral	Dextral	Dextral	Dextral	Dextral	Sinistral	Dextral	Dextral	Dextral	Dextral	Dextral	Dextral	Dextral	Sinistral	Dextral	Dextral

1066	InL096b	lym																	Dextral
1067	InL096b	phyB	19.759	9.596	3.613	16.145	3.622	0.876	24.249		81.321		No	Closed	Strong	Flattened-Rounded	Fusiform	No	Sinistral
1068	InL096b	phyB	9.265	15.19	2.258	7.006			3.406	108.2		4.7	No	Closed	Regular	Flattened-Rounded	Fusiform	No	Sinistral
1069	InL096b	phyB	7.161	8.184	1.447	5.713			4.118	64.5	61.390		No	Closed	Strong	Flattened-Rounded	Fusiform	No	Sinistral
1070	InL096b	val																	Dextral
1071	InL096b	hydC	3.82	2.183	2.078	1.742			13.357	43.7	73.059		No	Closed	Regular	Flattened-Rounded	Ovate-Conic	No	Dextral
1072	InL096b	lym																	Dextral
1073	InL096b	lym																	Dextral
1074	InL096b	lymA	3.42	2.226	0.675	2.744	1.935	1.191	10.359	88.2	71.959	4.0	No	Closed	Some-Regular	Flattened-Rounded	Elongate Cylindrical	No	Dextral
1075	InL096b	valB							8.130			4.1	No		Strong	Rounded	Turbiniform	Revolving	Dextral
1076	InL096b	valA	8.136	9.062	2.993	5.143	4.311	4.366	3.701	93.1	69.228	2.1	No	Open	Regular	Rounded	Turbiniform-Trochiform	Revolving	Dextral
1077	InL096b	phyA	16.925	9.761	1.395	15.531			20.283		83.384		No	Closed	Regular	Flattened-Rounded	Elongate Fusiform	No	Sinistral
1078	InL096b	phyB	21.089	25.19	3.114	17.975	17.707	16.217	11.848		75.897		No	Closed			Fusiform	No	Sinistral
1079	InL096b																		
1080	InL096b	viv																	Dextral
1081	InL096b	viv																	Dextral
1082	InL096b	hydC	3.704	2.381	1.852	1.852			12.462	48.9			No	Closed	Strong	Rounded	Ovate-Conic	No	Dextral

1099	1098	1097	1096	1095	1094	1093	1092	1091	1090	1089	1088	1087	1086	1085	1084	1083
InL096b	InL096b	InL096b	InL096b	InL096b	InL096b	InL096b	InL096b	InL096b	InL096b	InL096b	InL096b	InL096b	InL096b	InL096b	InL096b	InL096b
valA	valA	hyd	styA	hydC	lymA	hydA	lymB	lymB	valB	phyB	lymB	phy	viv		val	viv
6.813	8.415		3.076	3.44	4.022		5.662	4.167	2.696	4.106	2.648					
6.271	6.382		1.508	2.395	2.309		2.183	2.778	3.539	4.999	1.707					
2.209	3.075		1.627	2.203	2.044		1.892	2.567	1.24	1.101	0.965					
4.604	5.34		1.449	1.237	1.978		3.77	1.601	1.455	3.005	1.683					
3.186	3.806		1.042	0.832							2.817					
3.516	3.137		0.766	1.174							1.499					
9.823	14.931		16.909	10.305	13.627	6.829	22.782	19.440	12.051	16.746	22.063					
69	58.6		34.1	48.5	54.1	88.5	33.8	36.9	96.1	63.3	50.7					
72.992	65.511		63.138	60.945												
4.8	5.1		5.5					5.0	3.3	2.9						
No	No		No	No	No	No	No	No	No	No	No					
Open	Open		Closed	Closed	Closed	Closed	Closed	Closed		Closed	Closed					
Strong	Strong		Some-Regular	Regular	Regular	Strong	Strong	Some-Regular	Regular	Regular	Regular					
Rounded	Rounded		Flattened-Rounded	Rounded	Rounded	Flattened-Rounded	Flattened-Rounded	Flattened-Rounded	Flattened-Rounded	Flattened-Rounded	Flattened-Rounded					
Trochiform	Trochiform		Conic	Ovate-Conic	Elongate Conic	Trochiform	Elongate Conic	Elongate Conic	Turbiniform-Trochiform	Fusiform	Elongate Conic					
Revolving	Revolving		No	No	No	No	No	No	Revolving	No	No					
Dextral	Dextral	Dextral	Dextral	Dextral	Dextral	Sinistral	Dextral	Dextral	Dextral	Sinistral	Dextral	Sinistral	Dextral		Dextral	Dextral

1100	InL096b	valA	9.393	8.361	3.069	6.323	4.388	4.785	12.804	77.7	75.407	6.3	No	Open	Strong	Rounded	Trochiform	Revolving	Dextral
1101	InL096b	hydA	2.104	2.047	1.085	1.019			6.754	60.3			No	Closed	Strong	Rounded	Trochiform	No	Dextral
1102	InL096b	lym																	Dextral
1103	InL096b	phy																	Sinistral
1104	InL096b	viv																	Dextral
1105	InL096b	vivB	2.352	2.094	0.619	1.733	1.411	1.134	20.410	85.5	69.384	5.0	No	Closed	Strong	Rounded	Trochiform	No	Dextral
1106	InL096b	viv																	Dextral
1107	InL096b	phy																	Sinistral
1108	InL096b	hyd																	Dextral
1109	InL096b	hydB	1.068	0.838	0.311	0.757	0.413	0.518	11.269	68.6	71.493	3.9	No	Closed	Regular	Rounded	Ovate	No	Dextral
1110	InL096b	lym																	Dextral
1111	InL096b	lym																	Dextral
1112	InL096b	viv																	Dextral
1113	InL096b	viv																	Dextral
1114	InL096b	vivB	1.624	1.806	0.476	1.148	0.886	0.817	9.075	78	69.937	3.0	No	Closed	Strong	Rounded	Trochiform	No	Dextral
1115	InL096b	hyd																	Dextral
1116	InL096b	phy																	Sinistral

1117	InL096b	phy																	Sinistral
1118	InL096b	viv																	Dextral
1119	InL096b	viv																	Dextral
1120	InL096b	vivB	2.057	2.2	0.549	1.508	1.21	1.23	9.545	82.7	70.367		No	Closed	Strong	Rounded	Trochiform	No	Dextral
1121	InL096b	viv																	Dextral
1122	InL096b	hydB	1.457	1.137	0.525	0.932	0.615	0.689	13.401	64.5	76.083		No	Closed	Strong	Rounded	Ovate	No	Dextral
1123	InL096b	phyB	1.654	1.22	0.455	1.199			20.854	90.6	73.202	3.8	No	Closed	Strong	Rounded	Fusiform	No	Sinistral
1124	InL096b	viv																	Dextral
1125	InL096b	hyd																	Dextral
1126	InL096b	viv																	Dextral
1127	InL096b																		
1128	InL096b	lym																	Dextral
1129	InL096b	viv																	Dextral
1130	InL096	lym																	Dextral
1131	InL096	lym																	Dextral
1132	InL096	lym																	Dextral
1133	InL096	phy																	Sinistral

1134	InL096	phy										4.7	No	Closed				No	Sinistral
1135	InL096	phyB	48.816	32.74	1.058	47.757	42.422	25.135	9.682		70.924		No	Closed			Fusiform	No	Sinistral
1136	InL096a-1	phyB	29.859	25.22	6.644	23.214	24.367	12.063	17.526	92.1		6.7	No	Closed	2	Flattened-Rounded	Fusiform	No	Sinistral
1137	InL096a-1	lym																	Dextral
1138	InL096a-1	lym																	Dextral
1139	InL096d	phyB	29.243	20.63	0.779	28.464	22.905	10.031	9.403		76.942		No	Closed			Fusiform	No	
1140	InL096d	valB	4.035	6.853	1.733	2.368			8.691	96.1		3.4	No	Open	Regular	Flattened-Rounded	Turbinifor m- Trochiform	Revolving	Dextral
1141	InL096d	phyA	22.64	10.21	1.312	21.328	18.925	6.133	21.413	109.1	80.538		No	Closed	1	Flattened-Rounded	Elongate Fusiform	No	Sinistral
1142	InL096d	hyd																	Dextral
1143	InL096d	phy																	Sinistral
1144	InL096b	hyd																	Dextral
1145	InL096b	hydC							22.878		65.063		No	Closed	Regular	Rounded	Ovate-Conic	No	Dextral
1146	InL096b	styB							14.036	44.5			No	Closed	Some-Regular	Flattened-Rounded	Conic	No	Dextral
1147	InL096b	phy																	Sinistral
1148	InL096b	lym	9.808	3.89	3.311	6.496			6.503				No	Closed	Regular	Rounded	Elongate Conic	No	Dextral
1149	InL096b	hydC	2.015	1.185	1.089	0.926	0.712	0.796	9.693	40.9	67.203	3.0	No	Closed	Regular	Rounded	Ovate-Conic	No	Dextral
1150	InL096b	styB	3.254	1.3	2.134	1.12			7.716	31.3			No	Closed	Some-Regular	Flattened-Rounded	Conic	No	Dextral

1151	InL096b	hydB	2.593	2.269	1.158	1.435			8.334	61.2		5.2	No	Closed	Strong	Rounded	Trochiform	No	Dextral
1152	InL096b	valA	3.223	3.291	1.699	1.523			5.543	79			No		Strong	Flattened-Rounded	Turbiniform-Trochiform	Revolving	Dextral
1153	InL096b	val																	Dextral
1154	InL096b	val																	Dextral
1155	InL096b	valA							10.784			4.0	No				Turbiniform-Trochiform	Revolving	Dextral
1156	InL096b	valB	2.844	4.075	1.032	1.812			7.719	94.4		2.9	No		Regular	Rounded	Turbiniform-Trochiform	Revolving	Dextral
1157	InL096b	styB	2.471	1.064	1.61	0.861			11.310	31.8	47.203		No	Closed	Strong	Rounded	Conic	No	Dextral
1158	InL096b	valA	8.334	7.938	3.439	4.895			0.121	67.7		3.1	No		Regular	Flattened-Rounded	Trochiform	Revolving	Dextral
1159	InL096b	valB	1.448	1.678	0.509	0.939	0.67	0.794	7.072	79.9	79.783	4.5	No	Open	Strong	Rounded	Turbiniform-Trochiform	Revolving	Dextral
1159a	InL096b	styB	3.792	2.712	1.929	1.863			5.440				No	Closed	Some	Flattened-Rounded	Ovate-Conic	No	
1160	InL004	styB	2.948	1.091	1.364	1.583	1.187	0.475	16.148	32.4	65.391	5.8	No	Closed	Regular	Rounded	Conic	No	Dextral
1161	InL004	hydC	2.334	1.815	1.164	1.17			9.145	49.6		5.1	No	Closed	Some-Regular	Rounded	Ovate-Conic	No	Dextral
1162	InL004	hydB	1.271	1.096	0.583	0.688			8.130	67.8	69.775	4.3	No	Closed	Regular	Flattened-Rounded	Trochiform	No	Dextral
1163	InL004	hydC					0.885	0.755	16.928		75.630		No	Closed	Regular	Rounded		No	Dextral
1164	InL004	phy																	Sinistral
1165	InL004	phy																	Sinistral
1166	InL004	phy																	Sinistral

1167	InL096b	valB	4.349	4.304	1.196	3.153	2.153	2.262	10.804	75	77.164	4.7	No	Open	Regular	Flattened-Rounded	Turbinifor m-Trochiform	Revolving	Dextral
1168	InL096b	hydB	1.484	1.1	0.591	0.893			10.414	70.1	67.659	4.2	No	Closed	Strong	Flattened-Rounded	Ovate	No	Dextral
1169	InL096b	styB	4.245	2.359	2.447	1.797			12.642	35.8	57.139	5.0	No	Closed	Regular	Flattened-Rounded	Conic	No	Dextral
1170	InL096b	lymB	5.771	2.266	2.547	3.225			19.983	27.8			No	Closed	Strong	Flattened-Rounded	Elongate Conic	No	Dextral
1171	InL096b	valB	5.645	7.53	2.282	3.44			11.179	95.4		4.0	No		Strong	Rounded	Turbinifor m-Trochiform	Revolving	Dextral
1172	InL096b	phyB	2.753	2.795	0.562	2.191			5.395	66.4		2.2	No	Closed	Strong	Flattened-Rounded	Fusiform	No	Sinistral
1173	InL096b	viv																	Dextral
1174	InL096b	val																	Dextral
1175	InL096b	val																	Dextral
1176	InL096b	val																	Dextral
1177	InL096b	lym																	Dextral
1178	InL017	phyB		25.07		33.097	25.472	12.951	1.061		73.951		No	Closed			Fusiform	No	Sinistral
1179	InL017	phyB	48.708	30.85	7.205	41.503	35.243	15.369	4.399	79.8	78.100	6.8	No	Closed	Slight	Flattened	Fusiform	No	Sinistral
1180	InL017	phyB	45.706	32.8	2.176	43.529	39.14	19.013	20.697				No	Closed	Slight	Flattened	Fusiform	No	Sinistral
1181	InL017	lymC	4.28	3.474					15.690				No	Closed	Strong	Rounded	Fusiform	No	Dextral
1182	InL017	lymB	7.472	2.801	2.693	4.779	3.896	1.509	16.136	26.8	81.870	3.2	No	Closed	Regular	Rounded	Elongate Conic	No	Dextral
1183	InL017	hydC	3.751	2.017	1.212	2.539	1.277	1.026	10.784		63.128	4.5	No	Closed	Regular	Flattened-Rounded	Ovate-Conic	No	Dextral

1200	1199	1198	1197	1196	1195	1194	1193	1192	1191	1190	1189	1188	1187	1186	1185	1184
InL017	InL017	InL017	InL017	InL017	InL017	InL017	InL017	InL017	InL017	InL017	InL017	InL017	InL017	InL017	InL017	InL017
valA	valB	phy	val	val	viv	viv	viv	phyB	hydB	plant	phy	viv	viv	hydC	viv	vivA
6.743	6.812							7.506	11.023					1.650		2.234
6.363	7.642							8.628	7.325					1.132		2.216
1.798	1.772	4.488						1.256	3.857					0.858		0.65
4.945	5.04							6.251	7.166					0.792		1.583
	4.234								5.225					0.681		1.458
	3.452								4.299					0.544		1.318
15.730	8.438	5.287							15.049					6.299		10.811
86.9	83.4	60.4						104.3	56.8					46.9		86.2
64.885	71.109							79.380	63.701					70.937		56.418
3.4	7.4	5.3						5.5	5.2					6.4		3.5
No	No	No						No	No					No		No
	Open	Closed						Closed	Closed					Closed		Closed
Regular	Some	Regular						Regular	Regular					Strong		Regular
Flattened-Rounded	Flattened	Flattened-Rounded						Flattened	Flattened-Rounded					Rounded		Flattened-Rounded
Turbiniform-Trochiform	Turbiniform							Fusiform	Ovate					Ovate-Conic		Trochiform
No	No	No						No	No					No		No
Dextral	Dextral	Sinistral	Dextral	Dextral	Dextral	Dextral	Dextral	Sinistral	Dextral		Sinistral	Dextral	Dextral	Dextral	Dextral	Dextral

1217	1216	1215	1214	1213	1212	1211	1210	1209	1208	1207	1206	1205	1204	1203	1202	1201
InL017	InL017	InL017	InL017	InL017	InL017	InL017	InL017	InL017	InL017	InL017	InL017	InL017	InL017	InL017	InL017	InL017
phyB	viv	viv	viv	val/viv	viv	valA	valB	phy	valB	vivA		val/viv	viv	valB	valA	viv
1.46						5.222	6.596		6.68	6.166				5.827	7.936	
1.131						5.114	5.68		6.313	5.556				6.743	6.086	
0.224						1.866	1.866		2.007	2.406				1.798	3.026	
1.236						3.357	4.731		4.673	3.76				4.029	4.91	
1.107						2.72	3.471		3.637	3.323				2.182	3.279	
0.613						2.212	2.546		3.583	2.6				2.584	3.062	
13.662						13.349	6.483		10.162	10.521				6.963	9.960	
63.2						86.2	81.2		70.3	73.2				83	60.1	
76.855						68.629	70.408		70.326	70.001				72.719	67.551	
2.7						6.4	5.4		4.3	5.7				6.3	5.4	
No						No	No		No	No				No	No	
Closed						Open	Open		Open	Closed				Open	Open	
Strong						Strong	Regular		Regular	Regular				Regular	Regular	
Rounded						Rounded	Flattened-Rounded		Flattened-Rounded	Flattened-Rounded				Flattened-Rounded	Flattened-Rounded	
Fusiform						Turbinifor m	Turbinifor m		Turbinifor m	Trochiform				Turbinifor m-Trochiform	Turbinifor m-Trochiform	
No						No	No		No	No				No	No	
Sinistral	Dextral	Dextral	Dextral	Dextral	Dextral	Dextral	Dextral	Sinistral	Dextral	Dextral		Dextral	Dextral	Dextral	Dextral	Dextral

1218	InL017	viv															Dextral
1219	InL017	viv															Dextral
1220	InL017	phyB	2.998	2.256	0.513	2.485	2.278	1.158	15.594	94	74.932	4.3	No	Closed	Some	Flattened-Rounded	Fusiform	No	Sinistral
1221	InL017	viv															Dextral
1222	InL017	phy															Sinistral
1223	InL017	phy															Sinistral
1224	InL017	ostracode															Sinistral
1225	InL017	viv															Dextral
1226	InL017	viv															Dextral
1227	InL017	viv															Dextral
1228	InL017	phy															Sinistral
1229	InL017	lymA	4.355	2.143	1.203	3.152			11.782	60	73.940	4.2	No	Closed	Some-Regular	Rounded	Elongate Cylindrical	No	Dextral
1230	InL017	viv															Dextral
1231	InL017	viv															Dextral
1232	InL017	viv															Dextral
1233	InL017	phyB	2.298	1.936	0.519	1.779	1.892	1.012	12.864	78.7	73.051	3.8	No	Closed	Strong	Rounded	Fusiform	No	Sinistral
1234	InL017	viv															Dextral

1235	InL017	viv																	Dextral
1236	InL017	vivB	2.47	2.665	0.803	1.667	1.406	1.516	9.005	78.4	76.178	3.1	No	Closed	Strong	Rounded	Trochiform	No	Dextral
1237	InL017	viv																	Dextral
1238	InL017	val																	Dextral
1239	InL017	lymA	3.547	2.027	1.284	2.264			8.820	54.3	69.366		No	Closed	Strong	Rounded	Elongate Cylindrical	No	Dextral
1240	InL017	lym																	Dextral
1241	InL017	viv																	Dextral
1242	InL017	viv																	Dextral
1243	InL017	viv																	Dextral
1244	InL017	viv																	Dextral
1245	InL017	viv																	Dextral
1246	InL017	viv																	Dextral
1247	InL017	viv																	Dextral
1248	InL017	hydC	2.171	1.368	0.878	1.294	0.99	0.843	12.131	54.2	63.174	4.9	No	Closed	Strong	Rounded	Ovate-Conic	No	Dextral
1249	InL017	viv																	Dextral
1250	InL017	viv																	Dextral
1251	InL017	viv																	Dextral

1252	InL017	phy																	Sinistral
1253	InL017	viv																	Dextral
1254	InL017	lymA	1.637	0.856	0.356	1.282	0.69	0.383	12.115	65.5	73.038	3.3	No	Closed	Strong	Rounded	Elongate Cylindrical	No	Dextral
1255	InL017	viv																	Dextral
1256	InL017	vivB	0.583	0.522	0.082	0.501			14.370	98.2		2.7	No	Closed	Regular	Rounded	Trochiform	No	Dextral
1257	InL017	phy																	Sinistral
1258	InL017	viv																	Dextral
1259	InL017	lym																	Dextral
1260	InL017	valB	0.801	0.96	0.247	0.554	0.545	0.436	11.889	91.8	73.982	3.2	No	Closed	Strong	Rounded	Turbinifor m-Trochiform	No	Dextral
1261	InL017	lymA	2.156	1.278	0.334	1.822	1.554	0.647	14.421	83.9	69.027	2.0	No	Closed	Strong	Rounded	Elongate Cylindrical	No	Dextral
1262	InL017	lym																	Dextral
1263	InL017	viv																	Dextral
1264	InL017																		
1265	InL017	phy																	Sinistral
1266	InL017	viv																	Dextral
1267	InL017	phyB	42.874	34.36	3.78	39.094	34.555	22.013	16.000		86.202		No	Closed			Fusiform	No	Sinistral
1268	InL017	lymC	14.673	4.715	4.979	9.694	7.829	2.323	13.276	34.5	66.007	4.6	No	Closed	Strong	Flattened-Rounded	Elongate Conic	No	Dextral

1285	1284	1283	1282	1281	1280	1279	1278	1277	1276	1275	1274	1273	1272	1271	1270	1269
InL017	InL017	InL017	InL017	InL017	InL017	InL017	InL017	InL017	InL017	InL017	InL017	InL017	InL017	InL017	InL017	InL017
viv	styB	valA	val	phyA	viv	viv	vivA	phy	vivA	phy	viv	viv	viv	val	phyB	phyA
	2.528	8.529		13.456			2.655		7.849						26.08	34.312
	1.522	7.063		6.837			2.865		7.945						18.28	17.57
	0.95	2.382		1.306			1.584		2.911						1,741	5.62
	1.577	6.147		12.15			1.071		4.938						24.339	28.692
	0.97	3.985		11.03					4.069						21.625	24.277
	0.87	3.274		3.572					3.86						9.953	10.543
	15.396	9.611		8.902			9.211		9.881						8.311	13.497
	38.7	54.6		93.6			72		82.8						105.8	52.5
	69.634	65.433		82.980					62.859						79.330	
	3.7	3.6		3.5			4.8		5.5							5.6
	No	No		No			No		No						No	No
	Closed	Open		Closed					Closed						Closed	Closed
	Strong	Regular		Some			Strong		Regular						Slight	Some
	Rounded	Rounded		Flattened			Rounded		Flattened-Rounded						Flattened	Flattened
	Conic	Turbinifor m		Elongate Fusiform			Turbinifor m- Trochiform		Trochiform						Fusiform	Elongate Fusiform
	No	No		No					No						No	No
Dextral	Dextral	Dextral	Dextral	Sinistral	Dextral	Dextral	Dextral	Sinistral	Dextral	Sinistral	Dextral	Dextral	Dextral	Dextral	Sinistral	Sinistral

1286	InL017	lymA	3.756	2.244	0.973	2.783	2.348	1.182	9.340	65.5	69.027	3.2	No	Closed	Strong	Rounded	Elongate Cylindrical	No	Dextral
1287	InL017	viv																	Dextral
1288	InL017	viv																	Dextral
1289	InL017	viv																	Dextral
1290	InL017	viv																	Dextral
1291	InL017	styB	3.858	1.965	2.005	1.853	1.156	0.915	12.216	33	73.740	5.7	No	Closed	Strong	Rounded	Conic	No	Dextral
1292	InL017	lymB	4.166	2.413	1.238	2.928	2.58	1.091	7.292	62.8	70.662	5.1	No	Closed	Regular	Flattened-Rounded	Elongate Cylindrical	No	Dextral
1293	InL017	viv																	Dextral
1294	InL017	viv																	Dextral
1295	InL017	viv																	Dextral
1296	InL017	valB	4.35	4.017	1.079	3.271	2.53	1.778	7.294	70.9	64.864	4.2	No	Open	Regular	Flattened-Rounded	Turbinifor m-Trochiform	No	Dextral
1297	InL017	styB	6.254	3.219	3.387	2.868	2.106	1.717	11.619	33.9	70.602	6.5	No	Closed	Strong	Rounded	Conic	No	Dextral
1298	InL017	lym																	Dextral
1299	InL017	viv																	Dextral
1300	InL017	hydC	1.735	1.108	0.899	0.836			14.273	53.3		4.4	No	Closed	Strong	Rounded	Ovate-Conic	No	Dextral
1301	InL017	phy																	Sinistral
1302	InL017	viv																	Dextral

1303	InL017	viv																	Dextral
1304	InL017	vivB	1.181	1.228	0.264	0.917			11.834	78.6	68.199	3.4	No	Closed	Strong	Rounded	Trochiform	No	Dextral
1305	InL017	vivA	2.154	2.645	0.81	1.343			13.325	71		3.8	No	Closed	Strong	Rounded	Trochiform	No	Dextral
1306	InL017	valB	1.291	1.383	0.336	0.956	0.741	0.834	10.574	94.4	62.999	3.7	No	Open	Strong	Flattened-Rounded	Turbinifor m-Trochiform	No	Dextral
1307	InL017	vivB	3.781	4.103	1.407	2.375	2.324	2.282	10.305	78.9	73.325	5.5	No	Closed	Regular	Rounded	Trochiform	No	Dextral
1308	InL017	lym																	Dextral
1309	InL017	viv																	Dextral
1310	InL017	viv																	Dextral
1311	InL017	viv																	Dextral
1312	InL017	viv																	Dextral
1313	InL017	viv																	Dextral
1314	InL017	lymA	1.62	1.279	0.571	1.048			15.322	54.1	65.906	4.1	No	Closed	Strong	Flattened-Rounded	Elongate Cylindrical	No	Dextral
1315	InL017	viv																	Dextral
1316	InL017	viv																	Dextral
1317	InL017	viv																	Dextral
1318	InL017	viv																	Dextral
1319	InL017	phy																	Sinistral

1320	InL017	viv																	Dextral
1321	InL017	phy																	Sinistral
1322	InL017	lymA	1.656	1.383	0.629	1.027			10.125	68.8		3.8	No	Closed	Strong	Flattened-Rounded	Elongate Cylindrical	No	Dextral
1323	InL017	vivA	1.965	1.709	0.535	1.43	1.05	0.798	8.013	81	64.666	2.9	No	Closed	Strong	Flattened-Rounded	Trochiform	No	Dextral
1324	InL017	viv																	Dextral
1325	InL017	viv																	Dextral
1326	InL017	styB	4.187	2.252	1.668	2.519	1.707	1.229	12.181	28	78.635	3.0	No	Closed	Strong	Rounded	Conic	No	Dextral
1327	InL017	viv																	Dextral
1328	InL017	hydA	3.146	2.475	1.264	1.882			13.686	62.7		5.8	No	Closed	Regular	Rounded	Ovate	No	Dextral
1329	InL017	vivB	2.307	2.176	0.888	1.419	1.129	1.141	10.416	74.2	59.400	4.7	No	Closed	Strong	Rounded	Trochiform	No	Dextral
1330	InL017	viv																	Dextral
1331	InL017	styB	3.406	1.724	1.675	1.731	1.072	0.804	12.915	32.6	73.106	5.4	No	Closed	Strong	Flattened-Rounded	Conic	No	Dextral
1332	InL017	lym																	Dextral
1333	InL017	lymB	3.054	1.249	0.542	2.512	1.765	1.156	20.875	69.8			No	Closed	Some	Flattened-Rounded	Elongate Cylindrical	No	Dextral
1334	InL017	viv																	Dextral
1335	InL017	viv																	Dextral
1336	InL017	viv																	Dextral

1337	InL017	lymB	3.663	1.769	1.323	2.34	2.303	0.888	16.905		82.299	3.7	No	Closed	Strong	Flattened-Rounded	Elongate Cylindrical	No	Dextral
1338	InL017	viv																	Dextral
1339	InL017	vivA	2.466	2.77	0.714	1.752	1.286	1.26	7.958	90.4	63.258	4.2	No	Closed	Regular	Flattened-Rounded	Turbinifor m-Trochiform	No	Dextral
1340	InL017	viv																	Dextral
1341	InL017	phyB	1.788	1.423	0.487	1.302	1.445	0.663	10.252	66.2	74.578	3.4	No	Closed	Strong	Flattened-Rounded	Fusiform	No	Sinistral
1342	InL017	phyA	35.912	12.17	3.826	32.085			19.442	45.4	80.446	5.5	No	Closed	Regular	Flattened-Rounded	Elongate Fusiform	No	Sinistral
1343	InL017	phy																	Sinistral
1344	InL017	viv																	Dextral
1345	InL017	val																	Dextral
1346	InL017	viv																	Dextral
1347	InL017	valB	4.132	4.258	1.297	2.835	2.142	2.175	9.819	82.2	64.470	5.0	No	Open	Regular	Flattened-Rounded	Turbinifor m-Trochiform	No	Dextral
1348	InL017	valA	4.922	4.507	1.448	3.474	2.701	2.183	14.307	82.4	72.671	5.2	No	Open	Strong	Rounded	Trochiform	No	Dextral
1349	InL017	styB	4.851	2.254	2.506	2.346	0.939	0.65	18.861	35.7	66.871	4.1	No	Closed	Strong	Rounded	Conic	No	Dextral
1350	InL017	hydC	3.044	1.41	1.813	1.231	0.937	0.717	10.766	63.6	69.185	7.3	No	Closed	Regular	Rounded	Ovate-Conic	No	Dextral
1351	InL017	hydC	2.498	1.326	1.272	1.226	0.891	~0.752	11.709	44.8	62.354	6.6	No	Closed	Strong	Rounded	Ovate-Conic	No	Dextral
1352	InL017	viv																	Dextral
1353	InL017	viv																	Dextral

1370	1369	1368	1367	1366	1365	1364	1363	1362	1361	1360	1359	1358	1357	1356	1355	1354
InL017	InL017	InL017	InL017	InL017	InL017	InL017	InL017	InL017	InL017	InL017	InL017	InL017	InL017	InL017	InL017	InL017
val	valB	vivA	valB	valB	hydB	phyB	hydC	hydC	phyB	phy	phy	phy	phy	phy	phyA	viv
	1.146	1.466	1.779	2.812	1.261	1.188	1.448	1.874	0.802						11.385	
	1.302	1.964	1.666	2.594	1.062	0.665	1.288	1.316	0.672						7.261	
	0.361	0.576	0.593	0.735	0.485	0.178	0.781	1.194	0.137						2.446	
	0.785	0.89	1.186	2.077	0.776	1.009	0.667	0.68	0.665						8.939	
	0.724		1.06	1.766		0.79		0.84	0.6						7.772	
	0.728		0.934	1.472		0.377		0.716	0.344						4.118	
	7.489	10.353	10.539	17.232	13.745	14.792	0.647	13.041	6.510						13.222	
	86.6	90.8	83	67.5	81.6	72.6	54.4		72						55.5	
	57.381	72.681	62.922	64.404		81.469	75.030	70.560	66.448						83.130	
	2.8	4.4	4.2	2.6		2.9	3.9	4.4							5.5	
	No	No	No	No	No	No	No	No	No						No	
	Open	Closed	Open	Open	Closed	Closed	Closed	Closed	Closed						Closed	
	Strong	Regular	Strong	Strong	Regular	Regular	Regular	Regular	Strong						Regular	
	Flattened-Rounded	Flattened-Rounded	Rounded	Rounded	Rounded	Flattened-Rounded	Rounded	Rounded	Rounded						Flattened-Rounded	
	Turbinifor m-Trochiform	Turbinifor m-Trochiform	Turbinifor m-Trochiform	Turbinifor m-Trochiform	Ovate	Fusiform	Ovate-Conic	Ovate-Conic	Fusiform						Elongate Fusiform	
	No	No	No	No	No	No	No	No	No						No	
Dextral	Dextral	Dextral	Dextral	Dextral	Dextral	Dextral	Dextral	Dextral	Sinistral	Sinistral	Sinistral	Sinistral	Sinistral	Sinistral	Sinistral	Dextral

1387	1386	1385	1384	1383	1382	1381	1380	1379	1378	1377	1376	1375	1374	1373	1372	1371
InL017	InL017	InL017	InL017	InL017	InL017	InL017	InL017	InL017	InL017	InL017	InL017	InL017	InL017	InL017	InL017	InL017
viv	viv	viv	phyA	lym	lym	lym	lym	lymA	lymA	lymA	lymA	lymA	lymC	lymA	phy	val
			32.716					0.852	0.964	0.897	1.48	1.549	2.972	2.573		
			15.28					0.67	0.777	0.813	1.002	1.136	1.47	1.926		
			1.834					0.151	0.165	0.161	0.301	0.381	0.978	0.575		
			30.881					0.701	0.799	0.737	1.179	1.168	2.002	1.998		
			28.472					0.651	0.708		0.939			1.745		
			10.592					0.325	0.351		0.391			0.939		
			8.028					11.802	7.645	6.911	14.121	7.386	11.310	10.008		
								75.8	81.5		62.6	73.6	40.5	78.8		
			83.351					76.079	75.795		70.065	75.964	77.805	67.973		
								2.7	2.6	3.1	3.2	3.6		4.7		
			No					No	No	No	No	No	No	No		
			Closed					Closed	Closed	Closed	Closed	Closed	Closed	Closed		
								Strong	Strong	Regular	Strong	Strong	Regular	Regular		
								Rounded	Rounded	Rounded	Rounded	Flattened-Rounded	Rounded	Flattened-Rounded		
			Elongate Fusiform					Elongate Cylindrical	Elongate Cylindrical	Elongate Cylindrical	Elongate Cylindrical	Elongate Cylindrical	Elongate Conic	Elongate Cylindrical		
			No					No	No	No	No	No	No	No		
Dextral	Dextral	Dextral	Sinistral	Dextral	Dextral	Dextral	Dextral	Dextral	Dextral	Dextral	Dextral	Dextral	Dextral	Dextral	Sinistral	Dextral

1388	InL017	vivB	2.688	2.948	0.82	1.867	2.153	1.482	11.147	79.8	76.149	3.1	No	Closed	Regular	Flattened-Rounded	Trochiform	No	Dextral
1389	InL017	vivA	3.001	2.654	1.187	1.814	1.731	1.53	11.508	69.4	75.858	4.8	No	Closed	Regular	Flattened-Rounded	Trochiform	No	Dextral
1390	InL017	vivA	2.606	2.866	0.97	1.636	1.484	1.513	15.859	93.8	65.143	5.0	No	Closed	Strong	Flattened-Rounded	Turbinifor m-Trochiform	No	Dextral
1391	InL017	viv																	Dextral
1392	InL017	viv																	Dextral
1393	InL017	phy																	Sinistral
1394	InL017	valB	1.946	1.776	0.65	1.296	1.034	0.901	7.202	75.1	72.324	4.5	No	Open	Strong	Flattened-Rounded	Turbinifor m-Trochiform	No	Dextral
1395	InL017	valB	1.428	1.351	0.444	0.984	0.719	0.686	9.689	72	63.954	4.4	No	Open	Strong	Rounded	Turbinifor m-Trochiform	No	Dextral
1396	InL017	viv																	Dextral
1397	InL017	viv	1.221	1.1	0.509	0.712			14.712	75.1	66.652	4.1	No	Closed	Strong	Rounded	Trochiform	No	Dextral
1398	InL017	vivA	1.209	1.544	0.415	0.794	0.827	0.802	7.374	92.1	70.193	3.8	No	Closed	Strong	Flattened-Rounded	Trochiform	No	Dextral
1399	InL017	vivB	1.388	1.516	0.439	0.949	0.78	0.76	8.081	86.3	69.228	4.3	No	Closed	Strong	Rounded	Trochiform	No	Dextral
1400	InL017	viv																	Dextral
1401	InL017	viv																	Dextral
1402	InL017	viv																	Dextral
1403	InL017	viv																	Dextral
1404	InL017	viv																	Dextral

1421	1420	1419	1418	1417	1416	1415	1414	1413	1412	1411	1410	1409	1408	1407	1406	1405
InL017	InL017	InL017	InL017	InL017	InL017	InL017	InL017	InL017	InL017	InL017	InL017	InL017	InL017	InL017	InL017	InL017
viv	viv	viv	viv	viv	viv	viv	viv	viv	viv	viv	viv	viv	viv	viv	viv	viv
Dextral	Dextral	Dextral	Dextral	Dextral	Dextral	Dextral	Dextral	Dextral	Dextral	Dextral	Dextral	Dextral	Dextral	Dextral	Dextral	Dextral

1422	InL017	viv																	Dextral
1423	InL017	viv																	Dextral
1424	InL017	viv																	Dextral
1425	InL017	viv																	Dextral
1426	InL017	viv																	Dextral
1427	InL017	viv																	Dextral
1428	InL017	viv																	Dextral
1429	InL017	viv																	Dextral
1430	InL017	viv																	Dextral
1431	InL017	viv																	Dextral
1432	InL017	viv																	Dextral
1433	InL017	viv																	Dextral
1434	InL017	viv																	Dextral
1435	InL017	viv																	Dextral
1436	InL017	viv																	Dextral
1437	InL017	viv																	Dextral
1438	InL017	viv																	Dextral

1439	InL017	viv																	Dextral
1440	InL017	viv																	Dextral
1441	InL017	viv																	Dextral
1442	InL017	viv																	Dextral
1443	InL017	viv																	Dextral
1444	InL017	viv																	Dextral
1445	InL017	viv																	Dextral
1446	InL017	viv																	Dextral
1447	InL017	viv																	Dextral
1448	InL017	viv																	Dextral
1449	InL017	viv																	Dextral
1450	InL017	viv																	Dextral
1451	InL017	viv																	Dextral
1452	InL017	viv																	Dextral
1453	InL017	viv																	Dextral
1454	InL017	viv																	Dextral
1455	InL017	viv																	Dextral

1456	InL017	viv																	Dextral
1457	InL017	styB	5.073	2.101	3.568	1.505	1.191	1.108	10.697	31.6	76.350	8.1	No	Closed	Regular	Flattened-Rounded	Conic	No	Dextral
1458	InL017	styB	4.748	2.171	3.445	1.303			11.051	38.7	71.095	6.2	No	Closed	Strong	Rounded	Conic	No	Dextral
1459	InL017	valB	1.482	3.047	0.689	0.794			8.171	88.5		4.3	No		Strong	Flattened-Rounded	Turbiniform-Trochiform	No	Dextral
1460	InL017	valA	12.397	9.736	5.206	7.191			8.512	70.7		5.4	No	Closed	Some	Flattened-Rounded	Trochiform	No	Dextral
1461	InL017	styB	3.194	1.592	2.075	1.119			15.322	27.6		5.1	No	Closed	Strong	Rounded	Conic	No	Dextral
1462	InL017	valB	7.938	7.004	1.973	5.965	3.688	2.844	10.260	86	69.161	3.2	No	Open	Regular	Flattened-Rounded	Turbiniform-Trochiform	No	Dextral
1463	InL017	styC	5.298	2.21	3.146	2.152	1.53	1.232	14.149	29.6		5.2	No	Closed	Strong	Rounded	Conic	No	Dextral
1464	InL017	styB	4.936	2.135	3.207	1.729	1.486	1.168	13.696	36.2		6.4	No	Closed	Regular	Rounded	Conic	No	Dextral
1465	InL017	hydC	4.3	2.191	2.166	2.133	1.359	1.017	6.093	47		5.2	No		Regular	Rounded	Ovate-Conic		Dextral
1466	InL017	val																	Dextral
1467	InL017	valB		3.584				1.296				4.6	No					No	Dextral
1468	InL017	valB	7.005	7.354	4.238	2.767	2.815	1.407					No	Open	Regular	Flattened-Rounded	Turbiniform-Trochiform	No	Dextral
1469	InL017	styC	3.243	2.547	1.562	1.681	1.035	1.363	13.900	35.0		6.6	No		Regular	Rounded	Ovate-Conic	No	Dextral
1470	InL017	hydC	10.947	8	6.383	4.564	1.158	1.306	15.010	50.8		6.9	No		Regular	Flattened-Rounded	Ovate	No	Dextral
1471	InL017	valB	7.304	7.255	2.132	5.173	3.318	3.175	5.440	76.9		4.0	No	Open	Regular	Flattened-Rounded	Turbiniform-Trochiform	No	Dextral
1472	InL017	lymC	9.062	2.811	5.655	3.407			24.877	37.7			No	Closed	Regular	Rounded	Elongate Conic	No	Dextral

1489	1488	1487	1486	1485	1484	1483	1482	1481	1480	1479	1478	1477	1476	1475	1474	1473
InL106	InL106	InL106	InL106	InL106	InL106	InL017	InL017	InL017	InL017	InL017	InL017	InL017	InL017	InL017	InL017	InL017
hydB	vivB	lymC	hydD	hydB	styB	viv	viv	lymB	hydC	styB	hydA	valB	lymB	lymC	lymA	lymC
2.114	1.538	6.48	6.631	1.831	6.733			2.683	2.818	3.761	6.995	7.217	2.857	4.399	2.543	7.112
1.532	1.232	1.571	3.522	1.257	2.83			1.683	1.375	1.833	6.714	6.943	1.492	2.729	2.247	2.932
1.26	0.719	3.57	3.192	1.079	4.726			0.715	1.461	2.049	3.969	2.318	1.327	2.034	0.929	3.958
0.854	0.819	2.91	3.44	0.752	2.007			1.968	1.357	1.712	3.026	4.899	1.53	2.365	1.614	3.154
	0.951							1.499	0.878	4.49	4.564					
	0.48							0.874	0.76							
13.656	7.256	51.801	18.153	10.985	19.195			14.744	13.661	15.492	22.104		14.868	13.476	5.677	14.482
50.4	61.9	22.5	30.8	45.6	20.5			65.3	35.2	29.6		96.8	35	39.5	66.5	45.8
								72.306	63.308			73.895				
								4.4				5.4				
No	No	No	No	No	No			No	No	No	No	No	No	No	No	No
Closed	Closed	Closed	Closed	Closed	Closed			Closed	Closed	Closed	Closed		Closed	Closed	Closed	Closed
Regular	Regular	Regular	Strong	Regular	Strong			Strong	Regular	Some	Some	Regular	Strong	Strong	Regular	Regular
Flattened-Rounded	Rounded	Rounded	Rounded	Rounded	Rounded			Flattened-Rounded	Rounded	Flattened-Rounded	Flattened-Rounded	Flattened-Rounded	Rounded	Rounded	Flattened-Rounded	Rounded
Ovate-Trochiform	Trochiform	Elongate Conic	Ovate-Conic	Trochiform	Conic			Elongate Cylindrical	Ovate-Conic	Conic	Trochiform	Turbinifor m-Trochiform	Elongate Conic	Elongate Conic	Elongate Cylindrical	Elongate Conic
No	No	No	No	No	No			No	No	No	No	No	No	No	No	No
Dextral	Dextral	Dextral	Dextral	Dextral	Dextral	Dextral	Dextral	Dextral	Dextral	Dextral	Dextral	Dextral	Dextral	Dextral	Dextral	Dextral

1505	1504	1503	1502	1501b	1501	1500	1499	1498	1497	1496	1495	1494	1493	1492	1491	1490
InL106	InL106	InL106	InL106	InL106	InL106	InL106	InL106	InL106	InL106	InL106	InL106	InL106	InL106	InL106	InL106	InL106
thi	hydA	hydC	hydB	lymB	styB	hydC	hydC	hydA	hydB	hydB	styB	vivB	hydC	viv	hydC	styB
	1.665	1.956	3.522	2.964	6.168	2.726	0.779	1.213	2.365	2.264	2.312	2.573	2.045		1.637	2.166
	1.303	1.166	2.398	1.393	2.249	1.713	0.471	1.021	1.683	1.613	1.138	2.276	1.325		0.879	1.158
	0.945	1.054	2.472	0.55	2.757	1.742	0.442	0.651	1.393	1.303	1.703	0.873	0.899		1.02	1.323
	0.72	0.901	1.05	2.414	3.411	0.984	0.337	0.562	0.972	0.961	0.609	1.7	1.146		0.618	0.843
		0.552		1.567								1.462	1.045			
		0.502		0.562								1.191	0.655			
	11.944	13.788	14.287	23.575	13.948	11.678	13.812	9.228	17.428	9.571	8.823	7.688	15.327		9.250	7.125
	49.8	36	49.5	46.2	27.4	42.9	30.7	65.7	43.6	47.3	43.9	75.4	56		50.3	46.9
	No	No	No	No	No	No	No	No	No	No	No	No	No		No	No
	Closed	Closed	Closed	Closed	Closed	Closed	Closed	Closed	Closed	Closed	Closed	Closed	Closed		Closed	Closed
	Strong	Strong	Strong	Strong	Strong	Strong	Strong	Regular	Strong	Strong	Strong	Strong	Strong		Strong	Strong
	Rounded	Rounded	Rounded	Rounded	Rounded	Rounded	Rounded	Rounded	Rounded	Rounded	Rounded	Rounded	Flattened-Rounded		Rounded	Rounded
	Trochiform	Ovate	Ovate	Elongate Conic	Conic	Ovate-Conic	Ovate	Trochiform	Ovate	Ovate	Conic	Trochiform	Ovate		Ovate-Conic	Conic
	No	No	No	No	No	No	No	No	No	No	No	No	No		No	No
Dextral	Dextral	Dextral	Dextral		Dextral	Dextral	Dextral	Dextral	Dextral	Dextral	Dextral	Dextral	Dextral	Dextral	Dextral	Dextral

1517	1516	1515	1514	1513	1512	1511	1510	1509	1508	1507	1506
InL096b	InL096b	InL096b	InL096b	InL106	InL106	InL106	InL106	InL106	InL106	InL106	InL106
valB	valB	lymB	styC	lym	lym	hydD	viv	hydC	viv	hydC	hydB
8.361	4.608	5.498	5.325			4.862		1.649	0.653	1.997	1.191
4.985	4.487	2.877	3.318			2.96		1.07	0.686	1.294	1.187
3.098	1.984	1.67	3.352			2.538		0.965	0.471	1.162	0.765
5.262	2.624	3.828	1.973			2.323		0.683	0.182	0.835	0.426
4.604	2.321		1.587								
2.805	2.845		1.641								
14.500	18.654	18.360	14.534			12.470		11.236	12.137	8.746	13.314
	71.1	39.4	34.9			32.6		48.1		45.3	
77.339	65.807	74.932	67.051								
3.9	4.4	3.3	6.1								
No	No	No	No			No		No		No	No
Open	Open	Closed	Closed			Closed		Closed		Closed	Closed
Regular	Regular	Strong	Regular			Strong		Strong		Strong	Regular
Flattened-Rounded	Flattened-Rounded	Flattened-Rounded	Flattened-Rounded			Rounded		Rounded		Rounded	Rounded
Turbinifor m-Trochiform	Turbinifor m-Trochiform	Elongate Conic	Conic			Ovate		Ovate		Ovate-Conic	Trochiform
Revolving	Revolving	No	No			No		No		No	No
Dextral	Dextral	Dextral	Dextral	Dextral	Dextral	Dextral	Dextral	Dextral	Dextral	Dextral	Dextral

REFERENCES

Annandale, N., 1918, Records of the Indian Museum, v. 14, p. 159-168.

Annandale, N., 1920, Observations on *Physa prinsepii*, Sowerby and on a clionid sponge that burrowed in its shell: Records of the Geological Survey of India, v. 51, p. 50-66.

Annandale, N., 1921, Indian fossil Viviparidae: Records of the Geological Survey of India, v. 51, p. 362–368.

Basu, A.R., Renne, P.R., DasGupta, D.K., Teichmann, F., and Poreda, R.J., 1993, Early and Late Alkali Igneous Pulses and a High-3He Plume Origin for the Deccan Flood Basalts: Science, v. 261, p. 902-906.

Bates, D., Chambers, J., Dalgaard, P., Falcon, S., Gentleman, R., Hornik, K., Iacus, S., Ihaka, R., Leisch, F., Ligges, U., Lumley, T., Maechler, M., Murdoch, D., Murrell, P., Plummer, M., Ripley, B., Sarkar, D., Temple Lang, D., Tierney, L., and Urbanek, S., 2011, R: A language and environment for statistical computing v. 2.13.0.

Beane, J.E., Turner, C.A., Hooper, P.R., Subbarao, V., and Walsh, J.N., 1986, Stratigraphy, composition and form of the Deccan basalts, Western Ghats, India: Bulletin of Volcanology, v. 48, p. 61–83.

Beck, R.A., Burbank, D.W., Sercombe, W.J., Riley, G.W., Barndt, J.K., Berry, J.R., Afzal, J., Khan, A.M., Jurgen, H., Metje, J., Cheema, A., Shafique, N.A., Lawrence, R.D., and Khan, A, 1995, Stratigraphic evidence for an early collision between northwest India and Asia: Nature, v. 373, p. 55–58.

Blanford, W., 1867, The geology of Taptee and Nerbudda Valleys and some adjoining districts: Memoirs of the Geological Survey of India, v. 6, p. 56–71.

Bouchet, P. and Rocroi, J.P., 2005, Classification and nomenclature of gastropod families: Malacologia: International Journal of Malacology, v. 47, 397 p.

Buffetaut, E., 1987, Archosaurian reptiles with Gondwanan affinities in the Upper Cretaceous of Europe: Terra Nova, v. 1, p. 69–74.

Bunbury, C., 1861, Notes on a collection of fossil plants from Nagpur, central India: Quarterly Journal of the Geological Society, v. 17, p. 325–346.

Burch, J.B., 1989, North American Freshwater Snails: Malacological Publications, Hamburg, Michigan, 365 p.

Calkins, K.G., 2005, Applied statistics: Correlation coefficients: http://www.andrews.edu/~calkins/math/edrm611/edrm05.htm, Andrews University, Berrien Springs, Michigan.

Campbell, I.H. and Griffiths, R.W., 1990, Implications of mantle plume structure for the evolution of flood basalts: Earth and Planetary Science Letters, v. 99, p. 79–93.

Cande, S., Kent, D.V., 1995, Revised calibration of the geomagnetic polarity timescale for the Late Cretaceous and Cenozoic: Journal of Geophysical Research, v. 100, p. 159–190.

Chand, S., Radhakrishna, M., and Subrahmanyam, C., 2001, India–East Antarctica conjugate margins: rift-shear tectonic setting inferred from gravity and bathymetry data: Earth and Planetary Science Letters, v. 185, p. 225–236.

Chenet, A.L., Quidelleur, X., Fluteau, F., Courtillot, V., and Bajpai, S., 2007, $^{40}K/^{40}Ar$ dating of the main Deccan large igneous province: further evidence of KTB age and short duration: Earth and Planetary Science Letters, v. 263, p. 1–15.

Correa, A.C., Escobar, J.S., Durand, P., Renaud, F., David, P., Jarne, P., Pointier, J.P., Hurtrez-Bousses, S., 2010, Bridging gaps in the molecular phylogeny of the Lymnaeidae (Gastropoda: Pulmonata), vectors of Fascioliasis: BMC Evolutionary Biology, v. 10, p. 381.

Courtillot, V., Besse, J., Vandamme, D., Montigny, R., Jaeger, J.J., Cappetta, H., 1986, Deccan flood basalts at the Cretaceous/Tertiary boundary?: Earth and Planetary Science Letters, v. 80, p. 361–374.

Courtillot, V., Féraud, G., Maluski, H., Vandamme, D., Moreau, M.G., Besse, J., 1988, The Deccan flood basalts and the Cretaceous–Tertiary boundary: Nature, v. 333, p. 843–846.

Courtillot, V. and Renne, P.R., 2003, On the ages of flood basalt events: Comptes Rendus Geoscience, v. 335, p. 113–140.

Cripps, J.A., Widdowson, M., Spicer, R.A., and Jolley, D.W., 2005, Coastal ecosystem responses to late stage Deccan Trap volcanism: the post K–T boundary (Danian) palynofacies of Mumbai (Bombay), west India: Palaeogeography, Palaeoclimatology, Palaeoecology, v. 216, p. 303–332.

Davis, G. M, 1967, The systematic relationship of *Pomatiopsis lapidaria* and *Oncomelania hupensis formosana* (Prosobranchia: Hydrobiidae): Malacologia, v.6, p. 1–143.

Davis, G. M., 1979, The origin and evolution of the gastropod family Pomatiopsidae, with emphasis on the Mekong River Triculinae: Monograph of the Academy of Natural Sciences of Philadelphia, v. 20, p. 1–120.

Davis, G. M. and S. Rao., 1997, Discovery of *Erhaia* (Gastropoda: Pomatiopsidae) in northern India with description of a new genus of *Erhaiini* from China: Proceedings of the Academy of Natural Sciences of Philadelphia, v. 148, p. 273–299.

Duncan, R.A., Pyle, D.G., 1988. Rapid eruption of the Deccan flood basalt at the Cretaceous/Tertiary boundary: Nature, v. 333, p. 841–8443.

Fischer, P., 1887, Manuel de conchyliologie et de paleontologie conchyliologique of histoire naturelle des mollusques vivants et fossiles: Paris Librarie F, Savy, p. 507-511.

Fischer, J.C., 1963, Mollusques du Continental intercalaire (Mesozoique) du Sahara central: Societe geologique de France.

Ghosh, P., Bhattacharya, S.K., Sahni, A., Kar, R.K., Mohabey, D.M., and Ambwani, K., 2003, Dinosaur coprolites from the Late Cretaceous (Maastrichtian) Lameta Formation of India: isotopic and other markers suggesting a C3 plant diet: Cretaceous Research, v. 24, p. 743–750.

Gnos, E., Immenhauser, A., Peters, T.J., 1997, Late Cretaceous/early Tertiary convergence between the Indian and Arabian plates recorded in ophiolites and related sediments: Tectonophysics, v. 271, p. 1–19.

Harrison, T., 2011, Paleontology and geology of Laetoli: human evolution in context, Volume 2: Fossil hominins and the associated fauna: ed. Terry Harrison, Springer, New York, New York, 600 p.

Hartman, J.H., Erickson, D.N., and Bakken, A., 2008, Stephen Hislop and his 1860 Cretaceous continental molluscan new species descriptions in Latin from the Deccan Plateau, India: Paleontology, v. 51, p. 1225–1252.

Hislop, S., 1853, Remarks on the geology of the Nagpur state: Journal of the Bombay Natural History Society, v. 5, p. 148-150.

Hislop, S. and Hunter, R., 1854, On the geology of the neighborhood of Nagpur, central India: Proceedings of the Geological Society of London, p. 470–473.

Hislop, S., 1860, On the Tertiary deposits associated with trap-rock in the East Indies – with descriptions of the fossil shells: Quarterly Journal of the Geological Society of London, v. 16, p. 154–182, 188, 189.

Hofmann, C., Féraud, G., Courtillot, v., 2000, 40Ar/39Ar dating of mineral separates and whole rocks from the Western Ghats lava pile: further constraints on duration and age of the Deccan traps. Earth and Planetary Science Letters: v. 180, p. 13–27.

Jaeger, J.J., Courtillot, V., and Tapponnier, P., 1989, Paleontological view of the ages of the Deccan Traps, the Cretaceous/Tertiary boundary, and the India-Asia collision: Geology, v. 17, p. 316–319.

Jain, S.L. and Sahni, A., 1983, Some upper Cretaceous vertebrates from central India and their paleogeographical implications: in Cretaceous of India, ed. Maheswari, H.K., p. 66-83.

Jay, A.E. and Widdowson, M., 2008, Stratigraphy, structure and volcanology of the SE Deccan continental flood basalt province: implications for eruptive extent and volumes: Journal of the Geological Society, v. 165, p. 177–188.

Keller, G., Adatte, T., Gardin, S., Bartolini, A., and Bajpai, S., 2008, Main Deccan volcanism phase ends near the K–T boundary: Evidence from the Krishna–Godavari Basin, SE: Earth and Planetary Science Letters, v. 268, p. 293–311.

Kerney, M.P. and Cameron, R.A.D., 1979, A field guide to the land snails of Britain and northwest Europe: Collins, London, England, 288 p.

Khosla, A., Prasad, G.V.R., Verma, O., Jain, A.K., and Sahni, A., 2004, Discovery of a micromammal-yielding Deccan intertrappean site near Kisalpuri, Dindori District, Madhya Pradesh: Current Science, v. 87, p. 380-383.

Lightfoot, P.C., Hawkesworth, C.J., Sethna, S.F., 1987, Petrogenesis of rhyolites and trachytes from the Deccan Trap: Sr, Nd, and Pb isotopic and trace element evidence: Contributions to Mineralogy and Petrology, v. 95, p. 44–54.

Malcolmson, J.G., 1836, On the fossils of the eastern portion of the Great Basaltic District of India: Transactions of the Geological Society of London, v. 5, p. 96-121.

Malcolmson, J. G., 1840, On the fossils of the eastern portion of the Great Basaltic District of India: Transactions of the Geological Society of London, v. 5, p. 537–575.

Medlicott, J., 1859, On the geological structure of the central portion of the Nerbudda District: Memoirs of the Geological Survey of India, v. 2, p. 217–227.

Mohabey, D.M., Udhoji, S.G., and Verma, K.K., 1993, Palaeontological and sedimentological observations on non-marine Lameta Formation (Upper Cretaceous) of Maharashtra , India : their palaeoecological and palaeoenvironmental significance: Palaeogeography , Palaeoclimatology , Palaeoecology, v. 105, p.83–94.

Mohabey, D.M., 1996, A new oospecies, *Megaloolithus matleyi*, from the Lameta Formation (Upper Cretaceous) of Chandrapur District, Maharashtra, India, and general remarks on the paleoenvironment and nesting behavior of dinosaurs: Cretaceous Research, v. 17, p. 183–196.

Mohabey, D.M. and Udhoji, S.G., 1996, Fauna and flora from Late Cretaceous (Maastrichtian) non marine Lameta Sediments associated with Deccan volcanic episodes, Maharashtra: its relevance to the K/T boundary problem, Palaeoenvironment and palaeoclimate: Gondwana Geological Magazine, Special Publication 2 349–364.

Mohabey, D.M. and Samant, B., 2003, Floral remains from Late Cretaceous fecal mass of Sauropods from central India: implications to their diet and habitat: Gondwana Geological Magazine, Special Publication 6, p. 225–238.

Mohabey, D.M. and Samant, B., 2005. Late Cretaceous non-marine diatom assemblage from Iridium bearing intertrappean sediments of Anjar Kachchh, Gujarat: in Ab XX Colloquium on Micropaleontology and Stratigraphy, Visakhapatnam, p. 18–19.

Mordan, P.B., 1999, A terrestrial pulmonate gastropod from the late Miocene Baynunah Formation, Emirate of Abu Dhabi, United Arab Emirates: in Fossil vertebrates of Arabia: late Miocene faunas, geology, and paleoenvironments of the Emirate of Abu Dhabi, United Arab Emirates, eds. Whybrow, P.J. and Hill, A., Yale University Press, New Haven, Connecticut and London, England, 465 p.

Morgan, W.J., 1981, Hotspot tracks and the opening of the Atlantic and Indian oceans: in The Oceanic Lithosphere, ed. Cesare Emiliani, John Wiley & Sons, Inc., Oxford, England, 1730 p.

Najman, Y., Appel, E., Boudagher-Fadel, M., Bown, P., Carter, A., Garzanti, E., Godin, L., Han, J., Liebke, U., Oliver, G., Parrish, R., and Vezzoli, G., 2010, Timing of India-Asia collision: Geological, biostratigraphic, and palaeomagnetic constraints: Journal of Geophysical Research, v. 115, p. 16–18.

Newton, R.B., 1920, On some freshwater fossils from central South Africa: Annals and Magazine of Natural History, 9th series, p. 241–249.

Pande, K., 2002, Age and duration of the Deccan Trap, India: Constraints from radiometric and Paleomagnetic data: Proceedings of the Indian Academy of Science (Earth and Planetary Science), v. 111, p. 115–123.

Pardo, A. and Keller, G., 2008, Biotic effects of environmental catastrophes at the end of the Cretaceous and early Tertiary: Guembelitria and Heterohelix blooms: Cretaceous Research, v. 29, p. 1058–1073.

Plummer, P.S. and Belle, E.R., 1995, Mesozoic tectono-stratigraphic evolution of the Seychelles microcontinent: Sedimentary Geology, v. 96, p. 73–91.

Prasad, G.V.R. and Sahni, A., 1988, First Cretaceous mammal from India: Nature, v. 332, p. 638–640.

Prasad, G.V.R., Jaeger, J.J., Sahni, A., Gheerbrant, E. and Khajuria, C.K., 1994, Eutherian mammals from the Upper Cretaceous (Maastrichtian) intertrappean beds of Naskal, Andhra Pradesh, India: Journal of Vertebrate Paleontology, v. 14, p. 260–277.

Prashad, B., 1928, Recent and fossil Viviparidae: A study in distribution, evolution, and paleogeography: Memoirs of the Indian Museum, v. 8, p. 153-252.

Rana, R.S., 1984, Microvertebrate paleontology and biostratigraphy of the infra- and intertrappen beds of Nagpur, Maharashtra, PhD thesis, Panjab University, Chandigarh, India, 234 p.

Rana, R.S. and Wilson, G.P., 2003, New Late Cretaceous mammals from the intertrappean beds of Rangapur, India and paleobiogeographic framework: Acta Palaeontologie Poland, v. 48, p. 331–348.

Richards, M.A., Duncan, R.A., and Courtillot, V.E., 1989, Flood basalts and hot-spot tracks: plume heads and tails: Science, v. 246, p. 103–107.

Sahni, A., 1984, Cretaceous-Paleocene terrestrial faunas of India: lack of endemism during drifting of the Indian plate: Science, v. 226, p. 441-443.

Sahni, A., Rana, R.S., and Prasad, G.V.R., 1984a, SEM studies of thin egg shell fragments from the intertrappeans (Cretaceous-Tertiary transition) at Nagpur and Asifabad, peninsular India: Journal of the Paleontological Society of India, v. 29, p. 26-33.

Sahni, A., 1986, Cretaceous-Paleocene microfossil assemblages from the infra- and intertrappeans of peninsular India: implications for the drift of the Indian plate: Bulletin of the Geological, Mining, and Metallurgical Society of India, v. 54, p. 91-100.

Sahni, A., 1987, Faunal assemblage, correlation and paleoecology of Late Cretaceous nonmarine sequences of peninsular India, I GCP 216 Symposium China, Aspects of Nonmarine Cretaceous Geology, p. 94-109.

Sahni, A. and Bajpai, S., 1988, Cretaceous-Tertiary boundary events: the fossil vertebrate, paleomagnetic and radiometric evidence from peninsular India: Journal of the Geological Society of India, v. 32, p. 382-396.

Salil, M.S., Shrivastava, J.P., and Pattanayak, S.K., 1997, Similarities in the mineralogical and geochemical attributes of detrital clays of Maastrichtian Lameta Beds and weathered Deccan basalt, Central India: Chemical Geology, v. 136, p. 25-32.

Samant, B. and Mohabey, D.M., 2009, Palynoflora from Deccan volcano-sedimentary sequence (Cretaceous-Palaeogene transition) of central India: implications for spatio-temporal correlation: Journal of Bioscience, v. 34, p. 811–823.

Sereno, P.C., Dutheil, D.B., Larochene, M., Larsson, H.C.E., Lyon, G.H., Magwene, P.M., Sidor, C.A., Varricchio, D.J. & Wilson, J.A, 1996, Predatory dinosaurs from the Sahara and Late Cretaceous faunal differentiation: Science, v. 272, p. 986-991.

Sereno, P.C., Wilson, J.A., and Conrad, J.L., 2004, New dinosaurs link southern landmasses in the Mid-Cretaceous: Proceedings of the Royal Society: Biological Sciences, v. 271, p. 1325-1330.

Shafique, N.A., 2001, Spatial biostratigraphy of NW Pakistan: PhD dissertation, Miami University, 137 p.

Sharma, N., Kar, R.K., Aggarwal, C., and Ratan, K., 2004, Fungi in dinosaurian (*Isisaurus*) coprolites from the Lameta Formation (Maastrichtian) and its reflection on food habit and environment: Micropaleontology, v. 51, p. 7–82.

Sharma, R., Bajpai, S., and Singh, M.P., 2008, Freshwater Ostracoda from the ?Paleocene-age Deccan intertrappean beds of Lalitpur (Uttar Pradesh), India: Journal of the Paleontological Society of India, v. 53, p. 177–183.

Sheth, H.C., Pande, K., Bhutani, R., 2001a,b, 40Ar/39Ar age of a national geological monument: the gilbert Hill basalt, Deccan Traps, Bombay: Current Science, v. 80, p. 1437–1440.

Sheth, H. C., 2005, Were the Deccan flood basalts derived in part from ancient oceanic crust within the Indian continental lithosphere?: Gondwana Research, v. 8, p. 109–127.

Shrivastava, J.P., Ahmad, M., 2005, Compositional studies on organic matter from iridium enriched Anjar intertrappean sediments: Deccan volcanism and paleoenvironmental implications during the Cretaceous/Tertiary boundary: Journal of Iberian Geology, v. 31, p. 167–177.

Smith, G., 1888, Stephen Hislop – pioneer missionary & naturalist in Central India from 1844 to 1863: ed. John Murray, London, 317 pp.

Sowerby, J. D. C., 1840, Organic remains collected by Mr. [John G.] Malcolmson, and described and engraved by Mr. James de Carle Sowerby: In Plates and maps in illustration of volume V. Transactions of the Geological Society of London, series 2, 5.

Storey, M., Mahoney, J.J., Saunders, A.D., Duncan, R.A., Kelley, S.P., and Coffin, M.F., 1995, Timing of Hot Spot—Related Volcanism and the Breakup of Madagascar and India: Science, v. 267, p. 852-855.

Thiele, J., 1992, Handbook of Systematic Malacology; Part 1-2 (Loricata; Gastropoda: Prosobranchia): Smithsonian Institution Libraries and the National Science Foundation, Washington, District of Colombia, 625 p.

Tyron Jr., G.W., 1884, Structural and systematic conchology: an introduction to study of mollusca, vol. III: Academy of Natural Sciences, Philadelphia, Pennsylvania, 453 p.

Voysey, H.W., 1833a, Geological and mineralogical structure of the hills of Sitabuldi, Nagpur, and its immediate vicinity: Asiatic Researchers or Transactions of the Society instituted in Bengal, v. 18, p. 187-194.

Voysey, H.W., 1833b, Petrified shells found in the Gawilgerh range of hills, in April, 1823: Asiatic Researchers or Transactions of the Society instituted in Bengal, v. 18, p. 123-127.

Wade, C.M., Mordan, P.B., and Clarke, B., 2001, A phylogeny of the land snails (Gastropoda: Pulmonata): Proceedings of the Royal Society of London, v. 268, p. 413-422.

Wenz, W. and Zilch, A., 1959-1960, Gastropoda: Handbook of Paleozoology, v. 6, p. 377-448.

Wilson, G.P., Das Sarma, D.C., and Anantharaman, S., 2007, Late Cretaceous sudamericid gondwanatherians from India with paleobiogeographic considerations of gondwanan mammals: Journal of Vertebrate Paleontology, v. 27, p. 521-531.